A black and white photograph of a charred cross-laminated timber (CLT) wall. The wood is heavily charred, showing a dark, cracked, and textured surface. The vertical and horizontal grain patterns of the timber are visible, though obscured by the charring. The overall appearance is one of significant fire damage.

SELF-EXTINGUISHMENT OF CROSS-LAMINATED TIMBER

Roy Crielaard

Self-extinguishment of Cross-Laminated Timber

Master's Thesis Report

Master of Science in Civil Engineering

by

Roy Crielaard

Faculty of Civil Engineering and Geosciences

Delft University of Technology

March 2015

This master's thesis report has been approved by the graduation committee:

prof.dr.ir. J.W.G. van de Kuilen

Chairman graduation committee - Timber Structures and Wood Technology

T: (+31) (0)15 2782322

E: J.W.G.vandeKuilen@tudelft.nl

dr. ir. K.C. Terwel

Supervisor Delft University of Technology - Building Engineering

T: (+31) (0)15 2781512

E: K.C.Terwel@tudelft.nl

ir. G.J.P. Ravenshorst

Supervisor Delft University of Technology - Timber Structures and Wood Technology

T: (+31) (0)15 2785721

E: G.J.P.Ravenshorst@tudelft.nl

ir. P. Steenbakkens

Supervisor Arup – Fire Safety Engineering

T (+31) (0) 20 3058500

E Pascal.Steenbakkens@arup.com

ir. L.M. Noordijk

Supervisor Efectis – Fire Safety Engineering

T: (+31) (0) 88 3473 752

E: leander.noordijk@efectis.com

This master's thesis report was created by:

R. Crielaard, BSc

Student Civil Engineering – Building Engineering, Structural Design

T: (+31) (0) 642713767

E: roycrielaard@gmail.com

Preface

I first came into contact with tall timber buildings during a summer placement at the London office of engineering firm Arup. During a meeting with Arup employees and fire researchers at Edinburgh University, the topic “fire safety of timber high-rise” was prominently discussed. One of the issues was the fire risk due to the combustible nature of the structure. In that moment my interest in the topic was sparked, largely due to the fact that I could relate it to many of my personal interests and motivations.

My first motivation is that I like buildings and structures. I am fascinated by a well-designed and well-engineered building. Buildings are interesting to me because they provide the context for people to live their life. A building needs to be made to fulfil a function, so people can fulfil theirs.

My second motivation is that I like materials. Materials make something what it is; the look and feel, its strength and stiffness. Wood is a beautiful material that not only looks nice but is also “fun” to work with. It has amazing engineering qualities, is provided to us by nature, and can help us to create sustainable buildings. This thesis was a good opportunity to explore more qualities of wood.

My third motivation is that I am intrigued by fire. Fire engineering it is an increasingly important discipline for the complex buildings of today. Fire provides us with so many benefits, but can also be a devastating force. Fire engineers need to protect society from such harm. This is a rapidly developing field and there are many opportunities to make a contribution.

My fourth motivation is that I wanted to spend time in a lab. A large part of my education was spent behind a desk, but often engineering starts with experiments and I wanted to contribute in such a fundamental way.

Finally, I want to create a better world. This can be achieved in many ways, but in my field of work it is by designing structures that are safe, functional, beautiful, exciting, and do not drain our planet of its resources. With my research, I like to think I contribute to this.

With these motivations in mind, I decided I wanted to further the development of tall timber buildings by creating a better understanding of the fire safety. A better understanding which might, in the end, contribute to the addition of timber to our skylines.

Roy Crielaard
March 2015

Acknowledgements

I would like to acknowledge all the people who made a contribution to this work. I would like to thank:

Jan-Willem van de Kuilen for his support as chairman of my graduation committee. I remember your enthusiasm when I came to you with a couple of proposals for my thesis. Jan-Willem, thank you for allowing me to freely explore and develop the research. Also, thank you for your guidance in creating focus in the work.

Karel Terwel for providing me with invaluable advice and guidance, not only with regards to my research but during my whole Master's. Karel, thank you for your feedback. I hope you will remain a mentor for many years.

Pascal Steenbakkens Pascal, thank you for providing me with opportunities at Arup and its international network. You instilled in me the desire to make the work practically applicable and present it in its context. Thank you for your advice and the insights generated during our discussions.

Leander Noordijk Leander, thank you for your enthusiasm when I first came to the Efectis laboratory with my proposal. The research became much more interesting with the participation of Efectis and our work in the laboratory. Also thank you for your assistance in the design and execution of the experiments.

Geert Ravenshort Geert, thank you for our quick chats on the numerous issues I encountered during my research and your enthusiasm about the results. I would also like to thank you for your guidance on writing and structuring this report.

My colleagues at Arup I would like to thank you for supporting my research and for providing me with an enormous pool of skills and knowledge from which I could draw. In particular I would like to thank Robert Gerard for introducing me to the topic of fire in tall timber buildings. Furthermore I would like to thank Neal Butterworth, Andrew Lawrence, Angus Law, Charlotte Roben, and professor of structures and fire at the University of Edinburgh Luke Bisby for our initial discussions about how my research could contribute to the recent developments.

My colleagues at Efectis I would like thank you for assisting me in the experiments. It was a remarkable experience. In particular I would like to thank Arnoud Breunese for giving me the opportunity to work in the lab. Furthermore, I would like to thank Ad Zwinkels, Arjo Lock, Christoffel Steinhage, and Jos Bienefeld for assisting me and working out the details of the experiments. Without you I would not have been able to perform the experiments successfully. Also a big thanks to Rudolf van Mierlo for sharing his wealth of knowledge of fire and advising me on various issues I ran into during the analysis.

The people at De Groot Vroomshoop I would like to thank you for your support and interest in my work. A special thanks to Bert Brinks for getting me in touch with Stora Enso and providing me with the space and resources to build the samples.

The people at Stora Enso I would also like to thank you for providing the CLT for my research. Big thanks to Andreas Golger, Richard Steindl, and Hermann Kirchmayr for showing a lot of interest in my work. You made it clear I was working on something new and relevant. I hope we can continue to work together on the future of timber high-rises.

The people who aided with creating this report I would like to thank Bastiaan van de Weerd, Liselotte van der A, and Sebastiaan van de Koppel for their textual suggestions, and Robert van de Born for creating a nice cover.

My fellow students Also a big thanks to my fellow students, many of them of the Building Engineering study-association, with whom I went on study tours, organized activities and symposia, or relaxed during the breaks. Thank you for an excellent time at Delft University of Technology.

My Friends Dear friends, thank you for supporting me and listening attentively to my (obviously very interesting) stories about burning wood. Also thank you for understanding that graduation, in combination with my other activities and passions, sometimes prevents me to meet you as often as I would like. I'm sure we will catch up.

My family Mum and Dad, thank you for your support and love, not only this last year, but during my whole time at university. Your support is invaluable. I owe you so much.

Hubertien Without you I would never be able to do what I do. I can always count on your love and thanks to you I can charge up quickly during our moments of free time. Thank you so much for your support.

Table of contents

Preface	I	
Acknowledgements	III	
Table of contents	V	
Summary	IX	
1	Introduction	1
1.1	The interest in tall timber	1
1.2	Cross-laminated timber	2
1.3	Problem description: fire risks of timber	3
1.4	Relevance of the work	4
1.5	Research goals	5
1.6	Research questions	5
1.7	Methodology	6
1.8	Structure of the report	7
1.9	Scope limitations	8
Part 1: Theory	9	
2	Structural fire safety of timber buildings	11
2.1	Introduction	11
2.2	General fire behaviour	11
2.3	Regulatory considerations	12
2.4	Design for structural fire safety of timber structures	17
2.5	Conclusions	20
3	Fire dynamics of burning wood	21
3.1	Introduction	21
3.2	Fundamentals of wood combustion	21
3.3	Flaming combustion	27

3.4	Smouldering combustion	30
3.5	Combustion transitions of wood	35
3.6	Heat release	36
3.7	Heat transfer	38
3.8	Conclusions	38
4	Model of self-extinguishment	39
4.1	Introduction	39
4.2	First indication of self-extinguishment	39
4.3	The influence of delamination	40
4.4	Smouldering under an externally applied heat flux and airflow	40
4.5	The route to self-extinguishment	41
4.7	Hypotheses for the experiments	43
4.8	Conclusions	44
	Part 2: Experiments	45
5	Experiment setup	47
5.1	Introduction	47
5.2	Setup of experiment series 1	47
5.3	Setup of experiment series 2	55
5.4	Conclusions	62
6	Results	63
6.1	Introduction	63
6.2	Results of experiment series 1	63
6.3	Results of experiment series 2	80
7	Analysis	103
7.1	Introduction	103
7.2	Analysis of experiment series 1	103
7.3	Analysis of experiment series 2	110
7.4	Conclusions	117
	Part 3: Exploring consequences	119
8	Design implementation	121
8.1	Introduction	121
8.2	Context and robustness of design implementation	121
8.3	Assessment method	122
8.4	Step 1 - determination of critical lamella thickness	122

8.5	Step 2 - check configuration for potential self-extinguishment	126
8.6	Practical applicable configurations	127
8.7	Relation to previous work	128
8.8	Conclusions	128
9	Regulatory implications	129
9.1	Introduction	129
9.2	Context and robustness of regulatory implications	129
9.3	Compliance with Dutch building code	130
9.4	Fire-safe structure according to Eurocode consequence class 3	130
9.5	Perception and approval	131
9.6	Conclusions	132
10	Conclusions and recommendations	133
10.1	Introduction	133
10.2	Conclusions	134
10.3	Recommendations	134
10.4	Further research	135
	References	137
	Appendices	141
A	Cross-laminated timber	143
B	Existing data	149
C	Post-processing of data in experiment series 1	171
D	Temperature profile prediction experiment series 1	173
E	Design fire experiment series 2	179
F	Results experiment series 1	181
G	Fluctuations experiment series 1	229
H	Charring rates experiment series 1	233
I	Mechanisms experiment series 1	237
J	Charring rates experiment series 2	241
K	Example assessment for self-extinguishment	243
L	Relation to previously conducted research	249

Summary

Cross-laminated timber, or CLT, is currently receiving attention for its potential use in tall building structures. Timber being a combustible material, one of the main challenges for the construction of these buildings is the potential fire risk that results from its use in the structure.

For tall buildings, there is an increased severity of the consequences of structural failure as result of a fire. In order to obtain the desired level of safety, building codes typically require tall buildings to have a high fire resistance rating. The Eurocode recognises the risk associated with failure of the high rise structure and indicates that it is to be designed according to consequences class 3: failure of the structure due to fire is highly undesirable and the structure needs to be reliably safe and robust.

The design of tall buildings in consequence class 3 requires a high degree of insight into their structural fire behaviour. An in-depth investigation is needed of risks associated with the fire behaviour, and the structural fire response. In this research the effect of using the combustible material CLT as the main bearing structure is investigated.

As a combustible material, unprotected CLT can burn along with the fuel load present in a compartment. Irrespective of its fire resistance rating, it is uncertain whether the structure will be totally consumed in the event of a fire. This can result in collapse of the structure.

It is important to understand whether the timber structure continues burning or whether a fire would decay by self-extinguishment, possibly in combination with active fire safety measures such as sprinkler activation or fire-brigade intervention. However, self-extinguishment currently is not part of fire safety considerations for the structural design of tall timber buildings.

This master's thesis aims to increase insight into the fire behaviour of unprotected CLT structures in a compartment burnout, conservatively assuming no active measures. The main research question of this work is: "Under what conditions is there a potential for self-extinguishment of cross-laminated timber?"

A model of self-extinguishment of CLT was created which consists of various phases of a compartment burnout. Under the influence of an initial fire due to burning of room contents, the exposed CLT becomes involved in flaming combustion. Once the room contents have been largely consumed and the initial fire decays, the CLT contribution is expected to decrease as well, transforming from flaming to smouldering combustion. Finally, there will be a transition from smouldering to self-extinguishment. Two series of experiments were conducted to investigate this model and the conditions under which the transitions can take place.

The first series of experiments investigated two conditions at which the CLT can transform from smouldering to self-extinguishment: heat flux on the CLT and the airflow over its surface. This was done by exposing CLT to various heat fluxes and airflows in a cone calorimeter. It was found that smouldering CLT self-extinguishes when the externally applied flux is below 5 to 6 kW/m².

The additional airflow was also found to be of influence. At a heat flux of 6 kW/m², an airspeed of 0,5 m/s resulted in self-extinguishment, while an airspeed of 1,0 m/s resulted sustained smouldering. It can reasonably be assumed that at a heat flux below 6 kW/m², the speed of the airflow should be limited to 0,5 m/s.

The second series of experiments investigated all phases of the model of self-extinguishment. Small compartments with one, two, or three CLT walls were subjected to a propane fire with a decay phase. Delamination was found to be important in the fire behaviour of the CLT. Delamination occurred when the charring front reached the polyurethane adhesive, which then lost bonding. This resulted in fall-off and exposure of new layer of wood to the fire, which could interfere in the transitions from flaming to smouldering and from smouldering to self-extinguishment.

In two experiments, fall-off occurred when temperatures in the compartment were still relatively high. The newly exposed wood contributed rapidly to the fire and flaming was sustained, or smouldering was transformed back to flaming. The CLT in these two experiments continued burning.

In two other experiments, fall-off occurred when temperatures in the compartment were lower. As a result, flaming was not sustained. The CLT smouldered and the heat flux on its surface during was below 5 kW/m²; these compartments extinguished. However, relying on fall-off to occur when the compartment has cooled down might be risky due to its unpredictable nature. Alternatively, delamination and fall-off were prevented in a fifth experiment by applying a thicker top lamella. The charring front seized within the thickness of this lamella before it reached the PU adhesive.

In all five compartments, the exposed CLT increased the heat release rate and total energy released, and extended the duration of a fire. These were further increased when fall-off resulted in prolonged flaming.

Self-extinguishment is currently not part of fire safety considerations for timber high-rises. With further research, self-extinguishment might eventually contribute to a total fire safety concept for tall timber buildings, in addition to active measures. This research extends to translating new insights with regards to self-extinguishment to design and regulatory implications.

A suggestion was made for a method to assess the potential for self-extinguishment of CLT structures. The method is based on the experiments and their specific conditions, e.g. with regards to the fire development, fuel load, ventilation conditions, CLT build-up, type of adhesive, wood species, and compartment configuration and scale. It would require further research and verification before the method could be applied in practice.

The method consists of two steps. First, a thickness is determined, to be applied to the outer lamella of the CLT in order to prevent delamination. This thickness is based on the calculation of a finite charring depth for a parametric natural fire exposure, taking into account the ventilation conditions and the contribution of the CLT to the fuel load.

Second, to allow the transformation to self-extinguishment, the compartment configuration should be such that the heat flux on the CLT surface is limited to 5 kW/m^2 during smouldering. This can be achieved by estimating the temperatures of various surfaces and calculating the heat flux on the CLT with the most unfavourable configuration.

With regards to building regulations and approval, self-extinguishment might contribute in demonstrating compliance of a timber structure with the Dutch building code. Self-extinguishment, as part of an increased insight in the structural fire behaviour, reduces the probability of collapse as a result of the fire. Despite severe consequences of collapse in a high-rise building, this reduction in probability might contribute in achieving a level of risk and safety as intended by the Dutch building code.

Furthermore, an assessment of potential self-extinguishment might be considered in the design of timber buildings according to the Eurocode consequence class 3, which requires a high degree of insight into the structural fire behaviour. Self-extinguishment, as part of an overall fire safety concept, might become part of the risk analysis and the advanced calculations in order to demonstrate the tall timber structure is reliably safe and robust.

Finally, new insight can affect the perception of the material and the way it is treated in building regulations and approval. Due to lack of precedents, limited experience, code limitations, and uncertainties regards the performance in fire, there seems to be reluctance to saying tall timber buildings are sufficiently safe. Timber is perceived as a material less suitable for high-rise buildings. More insight into self-extinguishment, its role in a total fire safety concept for tall timber buildings, and its implications on the structural design, could affect this. A more pragmatic approach might be adopted in which any material poses unique design challenges, but can be applied as long as it contributes to safe buildings. While the combustibility of the timber structure will remain a point of attention, its risk should be managed properly, instead of used to discard the material for high-rise buildings.

Eventually, insight in the structural fire behaviour of timber structures, including potential self-extinguishment, could contribute to making timber available as a material for high-rise buildings.

1.1 The interest in tall timber

Architects and engineers are currently witnessing an increased interest in tall timber construction.

Although wood has been used as a construction material for a long time, it recently received new attention for its potential use in high-rise buildings.

On the one hand, this development has to do with the innovation of new engineered timber products and the potential economic benefits of prefabricated timber. On the other hand, the shift towards a more sustainable architecture makes new applications of timber interesting.

One of the most prominent proponents is Michael Green, a Vancouver based architect. He advocated wooden skyscrapers during the TED 2013 conference and showed the audience the use of timber as a material for high-rise construction. Green explained that wood does not only has aesthetic qualities, but also many favourable material properties for engineering. Furthermore, the renewable nature and low embodied energy make it a sustainable alternative to steel and concrete (Green, 2012).

The idea for wooden skyscrapers was reinforced when a team from Skidmore, Owning & Merrill (SOM), designers of iconic skyscrapers all over the world, presented their “timber tower research project”. They developed a performance-based conceptual design for a 125-metre tall timber and reinforced concrete composite structure that, according to SOM is “marketable, serviceable, economical and sustainable” (SOM, 2013).

More design proposals are known. For example, Van de Kuilen *et al.* (2010, 2011) demonstrated the feasibility of a “wood-concrete skyscraper” for buildings up to 150 meters, made for 80% of timber. The concept uses the advantages of light-weight timber walls, combined with a concrete core and outrigger structure, to obtain a comparable structural performance to that of traditional high-rises.

These proposals have in common that the timber used bears little resemblance to traditional light frame construction. Instead, buildings would be constructed from an engineered wood called cross-laminated timber, which has favourable engineering properties and benefits during construction.

Furthermore, the proponents of timber construction for high-rise buildings consider sustainability a key driver. As a result of population increase, urbanisation and poverty decrease, 3 billion people will need a new home in cities around the world in the next 20 years; many of these in high-rise developments. Since conventional materials such as concrete and steel have a high embodied energy and significantly contribute to the worldwide carbon dioxide emission, this suggests an upcoming clash between world housing and climate change (Green, 2012).

On the other side, wood has a “carbon sink effect”, as it absorbs carbon from the atmosphere. Also, the use of wood instead of other materials adds a “substitution effect” for the energy and carbon saved.

Furthermore, sustainably sourced wood is naturally renewing. Finally, when a building is torn down, prefabricated timber systems allow for disassembly and reuse of the material, or can be burned for energy.

However, before timber high-rise can reach its full potential, a number of issues need to be addressed. There is a gap between what architects and engineers deem possible and what is currently being built. This has to do with concerns regarding fire safety, deforestation, earthquakes, weather, sustainability, durability, longevity, high winds, termites, building codes, market acceptance, and economic considerations. A better understanding of any of these issues through research might allow these concerns to be addressed.

1.2 Cross-laminated timber

Cross-laminated timber, or CLT, is an engineered wood panel product. It currently receives renewed attention for its potential application in high-rise structures. Appendix A provides a brief history and some additional information regarding the manufacturing of CLT.

A CLT panel is composed of a number of layers; each consisting of side-by-side placed solid-sawn timber boards, which are sometimes edge-glued to create single-layer panels. These layers are stacked crosswise, typically at 90 degree angles, and adhesively bonded to create a solid panel, as depicted in figure 1.1. One panel consists typically of an odd number of layers, symmetrical around the mid-layer. Polyurethane (PU), melamine, and phenolic based adhesives are used, with PU being the most popular in Europe.

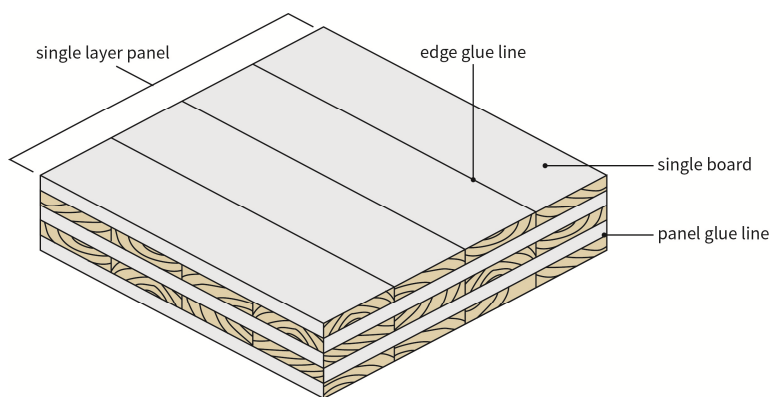


Figure 1.1 Schematic representation of a piece of cross-laminated timber

Due to continuous bonding, a composite action between the layers is achieved and the panel has an improved dimensional stability. Large dimension can be realised and the crosswise orientation of the layers generates favourable mechanical properties, such as high strength and stiffness in- and out-of-plane, and considerable splitting resistance due to a “reinforcement” effect of adjacent layers.

The panels can be relatively long and wide with two-way action capabilities and can be used as load-carrying plates and slabs, as well as linear structural components. Furthermore, CLT allows for a high degree of off-site prefabrication and rapid construction. Other advantages are a good thermal insulation and air tightness. A low damping ratio is one the weaknesses of CLT floors with regards to vibrations.

1.3 Problem description: fire risks of timber

As a combustible material, the potential fire risk resulting from the structure is recognised as one of the main challenges to the construction of tall timber buildings (Gerard *et al.*, 2013). This is reflected in the difference between timber buildings that are realised and which show a clear height limit of 10-14 storeys¹, as opposed to their taller counterparts of 30 plus storeys that exist only in design.

To address the concern of fire, research initiatives and design guidance documents have been developed in recent years. Examples include the “Fire Safety Challenges of Tall Wood Buildings” study by Arup (Gerard *et al.*, 2013), the “Fire safety in timber buildings technical guideline for Europa” by the Technical Research Institute of Sweden (2010), and the “Technical Guide for the Design and Construction of Tall Wood Buildings in Canada” by FPInnovations (2013).

These studies and guidance documents help to gain an understanding of the performance of tall timber buildings in fire. Based on these studies a number of “gaps in knowledge” can be identified. These areas need to be explored in order to better understand the fire performance of timber in tall buildings.

This master’s thesis aims to increase insight of the performance of timber structures by addressing one of the gaps; the behaviour of unprotected CLT in a compartment burnout scenario. Unprotected CLT is considered here, because the aim is to make buildings that actually look and feel like timber.

As a combustible material, unprotected CLT can burn along with the fuel load present in a compartment. In the event of a compartment burnout the fire will burn until all fuel has been consumed. However, the timber can contribute to this fuel. It is uncertain whether the exposed timber structure will be totally consumed. If the structure continues burning, it can be expected to be no longer able to maintain its load-carrying strength or provide acceptable compartmentation.

Alternatively, the timber could self-extinguish. Self-extinguishment occurs if all combustible contents in the compartment have been consumed and the timber structure is still able to maintain its load-carrying strength or provide compartmentation (Gerard *et al.*, 2013). As a result, the structure might be able to survive the fire. In reality, extinguishment could be achieved in combination with active measures, such as sprinkler activation or fire-brigade intervention. However, for the purpose of this research, self-extinguishment is investigated conservatively on its own as passive protection mechanism. The problem description of this research can be summarised as follows.

Problem description

As a combustible material, an exposed CLT structure can be assumed to contribute to a fire along with the compartment contents. It is unclear whether the structure would continue to burn or self-extinguish in a compartment burnout scenario.

¹ Examples include the Forté building in Melbourne, Australia, completed in 2012 and 10 storeys tall; and the Treet building, a 14-storey tall building and going up at the time of writing (2015) in Bergen, Norway.

1.4 Relevance of the work

An investigation of the performance of the timber structure in a compartment burnout, specifically with regards to self-extinguishment, is relevant both from a scientific and a design / regulatory point of view.

1.4.1 Scientific relevance

The topic of self-extinguishment is not investigated fully from a scientific point of view. Previous research has shown timber has the potential to contribute to the combustible fuel load in a compartment. However, it is not clear how much the CLT will contribute to the fire and whether the structure will be completely consumed. This was illustrated for example in previous research by Longhi (2012). In a parametric study with fire simulation and heat transfer software, the contribution of exposed mass timber and the potential to self-extinguish were found difficult to model and quantify.

Fire tests on timber compartments or elements are generally stopped at a pre-determined time, or to prevent damage to the testing facility. As a result, experiments often do not investigate a burnout and the potential for self-extinguishment remains unknown. One example of a test that was stopped is a natural fire test in a light timber frame building, intended to evaluate the potential of fire spread for a duration of 60 minutes (Frangi *et al.*, 2008).

Furthermore, the configurations that have been tested are limited to fully protected, e.g. by a non-combustible plate material, or fully unprotected CLT. For example, experiments have been performed in Canada on fully protected and unprotected CLT rooms by McGregor *et al.* (2012). The results indicated that a fire in an unprotected room can continue to burn at high intensity even after the combustible contents are consumed. Further research in rooms with partially exposed CLT was recommended. Self-extinguishment was not investigated, but its potential was noted.

1.4.2 Design and regulatory relevance

Potential self-extinguishment of CLT would also be relevant in terms of the technical aspects of designing timber structures; and the regulatory aspects of how these building can be demonstrated to be sufficiently safe (Law *et al.*, 2014).

Tall buildings typically require a high fire resistance and a high degree of insight in the structural fire behaviour to ensure the building is reliably safe and robust. The uncertain regarding whether the structure will continue burning in a compartment fire requires an in-depth investigation.

Currently, self-extinguishment is not part of how timber structures are designed. However, should there be a potential for self-extinguishment, it might be incorporated in the total fire safety concept of CLT structures. This might also affect the way timber is treated in building codes with regards to approval. It could contribute to timber buildings that are reliably safe and robust as intended by building codes and tall building design guidance. Furthermore, it could affect the perception of timber as a suitable material for high-rise construction. This master's thesis will pay attention to these design and regulatory implications, in addition to the scientific investigation.

1.5 Research goals

To investigate the problem as described above, research goals are formulated. Both an overarching “meta-goal” and a specific “research goal” are formulated.

The meta-goal illustrates the general wish to contribute to the understanding of the performance of tall timber structures in fire; and to translate this understanding to design and regulatory implications.

Meta-goal

To increase the understanding of the performance of tall timber structures in fire and to translate new insights to design guidance and regulations.

The meta-goal cannot be achieved by this research alone. Nevertheless, it can be concluded that an opportunity is present to address both scientific gaps, and design- and regulatory-related gaps by increasing the understanding regarding if and under what conditions self-extinguishment takes place. This is reflected in the main research goal.

Main research goal

To qualify and quantify the potential self-extinguishment of unprotected cross-laminated timber in building fires.

1.6 Research questions

The main research goal is translated into a main research question.

Main research question

Under what conditions is there a potential for self-extinguishment of unprotected cross-laminated timber in building fires?

To answer the main research question, and address both the meta-goal and the research goal in a structured way, this work is divided in three parts. Each part consists of multiple sub-questions. Table 1.1 provides an overview of these parts and sub-questions.

Table 1.1 Overview of parts and sub-questions

Part 1: Theory

- *What are the fundamentals of structural fire safety of timber high-rise buildings?*
 - *What are the fundamental fire dynamics of burning wood?*
 - *What model describes the process of self-extinguishment of cross-laminated timber?*
-

Part 2: Experiments

- *What series of experiments quantifies the conditions under which self-extinguishment of cross-laminated timber can occur?*
 - *What series of experiments investigates the complete process self-extinguishment of cross-laminated timber?*
 - *How can self-extinguishment of cross-laminated timber be explained in the experiments, and what are the conditions under which it took place?*
-

Part 3: Exploring consequences

- *How can self-extinguishment of cross-laminated timber be taken into account in the design?*
 - *What could be the implications of self-extinguishment on regulations with regards to the fire safety of timber high-rise buildings?*
-

1.7 Methodology

A methodology is defined to answer each sub-question.

1.7.1 Part 1: Literature review

What are the fundamentals of structural fire safety of timber high-rise buildings?

This question is investigated with a literature review to gain an understanding of the principles that govern structural fire safety of timber. This includes a discussion of building regulations and current design methods. The investigation will focus on the Dutch situation. Issues that are to be expected for tall timber buildings are identified. The results will serve as input for the exploration of consequences in part 3.

What are the fundamentals fire dynamics of burning wood?

This question focuses on the mechanisms that govern the burning of wood. This includes a literature review of the fundamentals of combustion, the modes in which wood can burn, and the associated

physical and chemical processes. These topics are reviewed in order to gain an understanding of the burning of wood, which will serve as a basis in creating a model of self-extinguishment.

What model describes the process of self-extinguishment of cross-laminated timber?

A literature review of previously conducted research will be performed to acquire an overview of existing experimental data. This information is combined with the review of fire dynamics and used to create a model of self-extinguishment. This model will serve as a framework upon which two hypotheses are formulated for the experiments in part 2.

1.7.2 Part 2: Experiments

What series of experiments quantifies the conditions under which self-extinguish of cross-laminated timber can occur?

What series of experiments demonstrates the complete process self-extinguishment of cross-laminated timber?

Two series of experiments will be designed, using input from part 1. The experiments aim to generate results that can answer the main research question. The first series aims to quantify the conditions under which CLT can self-extinguish. The second aims to the complete process of self-extinguishment of CLT. For each series the approach, setup, relevant equipment, procedure, and samples are discussed.

How can self-extinguishment of cross-laminated timber be explained in the experiments, and what are the conditions under which it took place?

The results of the experiments are presented and further analysed. The analysis aims to answer the main research question. The conditions under which self-extinguishment takes place, are qualified and quantified. Furthermore, other interesting findings will be presented.

1.7.3 Part 3: Exploring consequences

How can self-extinguishment of cross-laminated timber be taken into account in the design of timber structures?

While the main research question is answered by the experiments and analysis in part 2, the meta-goal of the research extends to translating new insights to design guidance and regulations. This question aims to explore these consequences and formulate a possible assessment method for self-extinguishment.

What could be the effect of self-extinguishment on regulations with regards to the fire safety of timber high-rise buildings?

Finally, the consequences of self-extinguishment with regards to building regulations are explored. This exploration will focus on the Dutch situation, and uses the information gathered in part 1.

1.8 Structure of the report

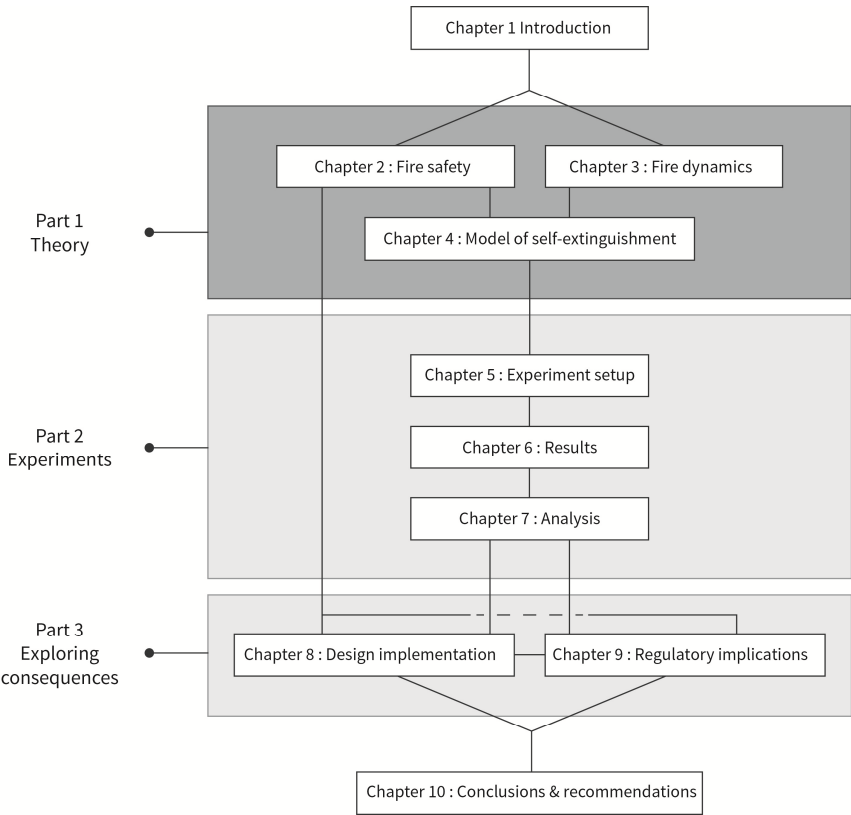
The structure of the report follows the division in three parts as set out above. In each part, the sub-questions are treated one-by-one in various chapters. Multiple chapters make up one part. The current introductory chapter and final chapter on conclusions and recommendations will supplement the three parts. An overview of the structure of the report is added at the start of each part.

1.9 Scope limitations

Fire engineering is a broad and complex field, as is the design and engineering of tall (timber) buildings. Therefore, this work is bounded by some scope limitations that make the research feasible as a graduation thesis.

- This research investigates self-extinguishment as passive protection for an exposed timber structure. It is recognised that in reality, passive protection is only part of the total fire safety strategy, including active measures. However, conservatively, the influence of active measures on the performance of the timber structure in fire is not taken into account.
- Only the post-flashover fire behaviour is considered. This phase is most relevant for structural safety in compartment burnout. The influence of the CLT on pre-flashover conditions is not considered.
- Only exposed and untreated timber is investigated. The influence of fire-protective cladding or intumescent paints is not taken into account.
- Likewise, while fire-retardant treatments may reduce the rate of flame spread of wood surface, it does not improve the fire-resistance of timber when exposed to temperature of a fully-developed fire. Therefore, this is not further investigated in this work.
- The research only considers the most common CLT in Europe, i.e. made from spruce and glued with a polyurethane adhesive. The same type of CLT will be used in all experiments.
- The research does not consider the effects of different types of connections of the exposed timber elements.
- When the research investigates building regulations and design guidance, it will focus on the Dutch building regulations and the Eurocodes.
- The research will investigate fire safety principles, regulations and design guidance, fire dynamics of burning wood, and existing experimental data. However, this work does not aim to be a complete handbook. There is excellent background material readily available and reference will be made to these works.
- In experiments, the effect of loading of elements is not considered. While the potential self-extinguishment will influence the load-bearing capacity during and after a fire, this is not under direct investigation.
- The experiments in this research are carried out under specific conditions; e.g. with regards to the design fire, fire load, ventilation conditions, CLT build-up, adhesive, wood species, compartment configuration, and scale. It is recognised that there are numerous parameters involved in the development of an actual fire. This research will focus on certain parameters that are deemed important in the investigation of self-extinguishment of CLT. If necessary, reasonable assumptions will be made and further research will be recommended.

Part 1: Theory



“The most tangible of all visible mysteries - fire.”

- Leigh Hunt

Structural fire safety of timber buildings

2.1 Introduction

This chapter provides a review of structural fire safety of timber high-rise buildings, both with regards to building regulations and the design. The following research question is answered:

What are the fundamentals of structural fire safety of timber high-rise buildings?

The emphasis in this chapter is on the current situation in the Dutch regulatory system. Issues that are to be expected for tall timber buildings are identified. This is used as input for part 3, where potential consequences of self-extinguishment are discussed.

2.2 General fire behaviour

In order to understand structural fire safety, the “typical” development of a fire needs to be taken into account. Figure 2.1 depicts a typical time-temperature curve of a fire development in an enclosure, assuming no fire suppression takes place. Table 2.1 describes the phases and transitions.

In reality a “typical” fire development does not exist. The development will vary between fires and will depend on the size and location of the ignition source; the type, amount, position, spacing, orientation, and surface area of the fuel packages; the geometry of the enclosure; the size and location of openings; and the properties of the enclosure boundaries. However, a general development as depicted here can be expected to be present in most fires.

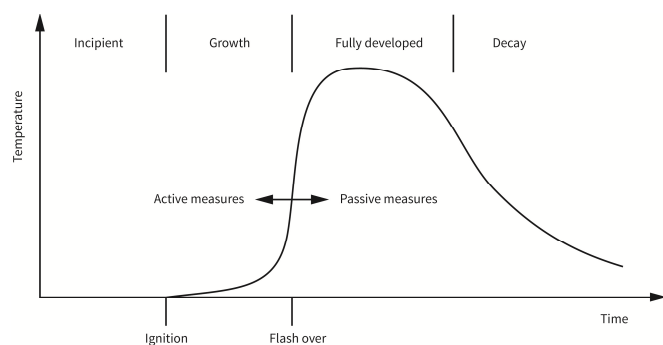


Figure 2.1 Typical time-temperature fire development

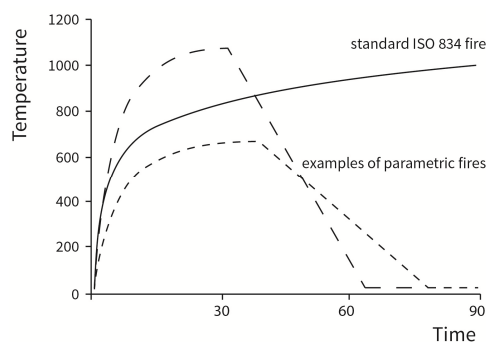


Figure 2.2 Standard fire & parametric fire curves

Table 2.1 Fire development: phases and transitions. Adapted from Karlsson and Quintiere (2000).

Phase / transition	Description
Incipient period	In the incipient period, heating of potential fuel is taking place, e.g. due to a match in a dustbin.
Ignition	Ignition is the start of (flaming) combustion*, marking the transition to the growth phase.
Growth	In the growth phase, a fire may grow at a slow or fast rate. Most building fires spread slowly at first on combustible surfaces from the point of origin, then more rapidly as the fire grows and radiant* feedback is provided from flames and hot gasses to other fuel items. The burning rate* and heat release rate* are generally controlled by the nature of the burning fuel.
Flashover	Flashover is the transition to the fully developed fire, or full room involvement. When upper layer temperatures reach about 500 – 600 °C, the heat flux* received by all surfaces results in a rapid involvement of those surfaces. The burning rate and heat release rate increase rapidly.
Fully developed	In the fully developed phase the temperatures and heat flux within the room are so great that all exposed surfaces are burning. Generally, the burning rate and heat release rate are no longer governed by the nature of the fuel, but by the amount of ventilation (and thus oxygen) available. Average gas temperatures are often high, in the range of 700 – 1200 °C.
Decay	If the fire is left to burn, eventually the fuel is consumed and the compartment burns out. The temperatures, the rate of burning, and the heat release rate again become a function of the fuel. Eventually, the fire extinguishes.

* Note: These terms will be discussed in the chapter on fire dynamics.

In fire safety engineering the periods before and after flashover are different design situations. The pre-flashover phase has the emphasis is on the safety of humans in the compartment. The growth phase of the fire is of most importance. The post-flashover phase has the emphasis on structural safety and safety of firefighters or occupant in other parts of the building. The size of the fully developed fire is of greatest concern. Both phases require different provisions in order to achieve a fire safe building.

When fire-related calculations are made a “design fire” is selected that models its behaviour. A design fire can cover the pre-flashover or post-flashover phase, or both. Figure 2.2 depicts the ISO 834 standard nominal fire curve, which is often used in fire testing and the classification of fire resistance of structures, and examples of natural parametric fire curves, which incorporate the effects of boundaries, ventilation, and fire load in the compartment. Other design fires exist for various engineering purposes.

2.3 Regulatory considerations

This paragraph discusses how structural fire safety is addressed in building regulations and what issues are to be expected for tall timber buildings.

2.3.1 Fire safety objectives

Society expects to be reasonably safe from the effects of unwanted fire. Unfortunately, the experience is that fires can occur in almost any building at any time. As a result, the need arises for fire safety in order to ensure protection from its potentially devastating effects. The primary goals of fire safety are expressed in fire safety objectives. These objectives have been formulated by many countries and fire safety institutions around the world. Table 2.2 provides an overview of the three main fire safety objectives.

Table 2.2 Fire safety objectives. Adapted from Buchanan (2009).

Objective	Description
Life safety	The objective of life safety aims to limit, to acceptable levels, the probability of death or injury in the event of a fire. It provides protection to the occupants of a building and to the people in adjacent buildings or outside the building. Furthermore, this objective requires provisions to be made for the safety of firefighters who enter the building for rescue or fire control purposes.
Property protection Business continuity	This objective aims to limit the probability of loss of property. This includes protection of the building and its contents, but also neighbouring buildings. In some cases this also protects intangible items, such as continuity of business, heritage values, or public image.
Environmental protection	In many countries an additional objective is to limit environmental damage. The primary concern is the protection against the release of hazardous substances, i.e. emissions of gaseous pollutants in smoke, and liquid pollution in firefighting run-off water.

2.3.2 Building regulations

Many countries address fire safety in their regulatory system, which typically encompasses building regulations and building control. Building regulations set minimum quality requirements on safety, health, energy-efficiency, usability, and the environment. Building control approves design proposals. The terms “building regulations” and “building code” are often used interchangeable.

Most building codes today are “performance-based”. These codes do not prescribe in detail how a building is to be designed and constructed, but express the desired outcome. This is achieved with a statement of the legislative objectives and the functional demands on the building. A design is considered to be acceptable in terms of approval if it meets these functional statements and is approved by building control. The means of achieving these functional statements is left up to the designer.

Often, to aid in the design, the functional statements are quantified in a set of performance requirements. When these are achieved, compliance with the functional statements is demonstrated. Alternative solution can be developed, but must demonstrate compliance with the functional statements in another way.

2.3.3 Provisions for fire safety

To achieve the fire safety objectives and the level of fire safety desired by the building code, various provisions are usually taken. These provisions can be categorized as shown in table 2.3.

Table 2.3 Provisions for fire safety. Adapted from Buchanan (2009).

Provision	Description
Detection and warning	Provisions that provide detection of a fire include smoke and heat detectors. Furthermore, automatic sprinklers are activated by heat detecting devices. Once a fire has been detected many types of visual and audio alarm systems can warn occupants and firefighting services.
Active control	Active systems control the fire or its effects by an action taken by a person or automatic device. Typically, these measures are relevant pre-flashover. Well-known is the automatic sprinkler, which can extinguish fires or prevent their growth. Another form of active control is smoke control. Occupants can also extinguish small fires and firefighters can actively control or extinguish a fire.
Passive control	Passive systems control the fire or its effects by means that are built into the fabric of the building. Passive measures are relevant after flashover when a fire has significantly grown. Passive control is provided by structures with fire resistance to prevent collapse and spread of fire. Passive control can also be exerted pre-flashover, when selection of materials can prevent rapid flame spread.

A set of provisions creates a fire safety strategy, often depending on the type of building, its occupancy, size and height. While much can be done to reduce the probability of a large fire through detection, warning, and active measures, it is impossible to prevent all of them. Therefore, the provision of structural fire safety is important. Structural fire safety is often achieved by providing selected members and barriers with a fire resistance to prevent structural collapse and to control the spread of fire (both internally and externally).

2.3.4 Structural fire safety in the Dutch building code

Building structures in The Netherlands have to comply with the requirements of the Dutch building code (in Dutch: “Bouwbesluit”). The Dutch building code sets out requirements for buildings regarding safety, health, usability, energy efficiency, and the environment.

The fire safety objectives of the Dutch building code focus on life safety and protection of adjacent property². Fire safety requirements are provided for building <70 meters. Tall buildings are required an equal level of fire safety as intended by the provisions for buildings <70 meters (article 2.128 of the code).

With regards to structural fire safety, the Dutch building code sets out a functional statement; “a building can be evacuated and searched during a reasonable amount of time in the event of a fire without the danger of collapse” (lid 1, article 2.9 of the Dutch Building code). The code does not state what this reasonable period of time is for building higher than 70 meters.

The Dutch building code then provides a set of performance requirements for various functions and states that “by applying these prescriptions ... compliance with the functional statement is satisfied” (lid 2, article 2.9 of the Dutch Building code)³.

For structural fire safety, these performance requirements are fire resistance requirements for structural members. The required fire resistance is expressed in minutes of increasing levels (30, 60, 90, or 120 minutes) depending on function, height, and fire load of the building. For the determination of the fire resistance of structures the code refers to various Eurocodes (article 2.11 of the Dutch Building code).

It is generally recognised that these levels of increasing fire resistance are related to increased risk in buildings. Risk can be defined as the product of the probability that a hazard will be realised and the consequences of that hazard (CUR, 1997). Consequences can be quantified, for example as the number of fatalities or injuries, or in terms of failure cost.

Terwel (2014) provides a definition of structural safety which incorporates risk. He combines the concept of safety as defined by ISO 8402, art. 2.8, with the concept of structural safety as defined in the NEN-ISO 6707-1:2004 art. 9.3.82. His definition is: “Structural safety can be defined as the absence of unacceptable risk associated with failure of (part of) a structure.”

This definition can be adapted for structural fire safety: “Structural fire safety can be defined as the absence of unacceptable risk associated with failure of (part of) a structure as result of a fire.”

² The balance between fire safety objectives varies between countries. A trend has been for regulations to give more emphasis on life safety and protection of property of third parties. Damage to the building itself is considered a responsibility of the building owner or insurer.

³ An alternative way of compliance with the Dutch code is called “equivalence” (article 1.3 of the Dutch Building Code). Equivalence allows for the prescriptions of the code to be ignored, provided that the same level of safety, health, usability, energy efficiency, and the environmental protection is achieved.

In buildings where more severe consequences due to a fire are to be expected, the code sets higher fire resistance ratings. Often, the fire will not last longer, but the higher rating increases the probability of the structure to withstand its effects. Furthermore the risk to occupants and firefighters is reduced, because they have more time to evacuate and perform search and rescue and firefighting operations. In this context, structural fire resistance is especially important for tall buildings.

The international fire safety community recognises the high complexity of fire safety for tall buildings. It can be argued that for increasingly tall buildings, the severity of the consequences of structural failure as result of a fire increases. These consequences could include loss of life and damage to adjacent property, but also damage to the building itself and loss of business continuity. According to the definition of risk, when the severity of the consequences increases, so does the risk if no measures are taken to lower the probability. This implies a lower - and potentially unacceptable - level of safety.

The Dutch building code specifically requires an equal level of safety for tall buildings as intended for lower buildings. This implies an equal level of risk. With an increasing severity of consequences, an equal risk is achieved by reducing the likelihood of the hazard of structural collapse in a fire.

The current approach seems to increase the fire resistance as to lower the probability of structural failure. Current timber design is able to achieve these levels of fire resistance. However, the probability of structural failure for a timber high-rise cannot be decreased by increasing the fire resistance alone. As a combustible material, the timber structure can continue burning and eventually collapse. Irrespective of the fire resistance rating, the functional statement might not be met. The level of safety intended by the code might only be achieved by further investigating the structural fire behaviour and associated risks.

2.3.5 Eurocode consequence class 3 guidance for tall buildings

To aid in the high complexity of fire safety for tall buildings, additional guidance documents are available in The Netherlands. These documents are not part of the Dutch building regulations, but are created by industry parties to eliminate public and private law issues.

In The Netherlands, the NTA “covenant high-rise buildings” (NEN, 2012) is particular relevant for structural fire safety⁴. The guide aims to translate the objectives, functional statements, and requirements of the Dutch building code into more practical applicable conditions for high-rise, and tie these in with the Eurocode framework. The Eurocode and the NTA suggest increased insight and additional measures are required in order to ensure sufficient structural fire safety for high-rise buildings.

Various reasons are given why these are required. In the previous paragraph it was recognised that for tall buildings the severity of consequences of structural failure as result of a fire increases. This is reinforced by the fact that evacuation by stairs can be slow and simultaneous evacuation of all floors is not always an option, resulting in prolonged occupation. Fire-fighters may need to be inside the building for search and rescue, and fire-fighting operations, after occupants have escaped. Furthermore, the impact on society of collapse in an urban area is large, because the building, its contents, and its surroundings represent great value. As a result, collapse of a high-rise due to fire, even after it has been evacuated and searched, is considered to be highly undesirable. This not an explicit requirement of the Dutch building code, but a

⁴ The NTA guide focuses on building of steel and concrete, but the concepts are applicable for timber as well.

recommendation of these guidance documents. This requires a high degree of insight in the structural fire behaviour and potentially additional measures to ensure sufficient structural fire safety.

The increased insight and additional measures are based on the fact that the Eurocode 1990 and the NTA indicate that “the structural fire design of a high-rise is performed according to the recommendations for a consequence class (CC) 3 building.” The classification is based on the consequences of failure of the structure. Each class is characterised by a reliability index β .

Reliability is defined in Eurocode 1990 as “the ability of a structure or a structural member to fulfil the specified requirements, including the design working life, for which it has been designed. Reliability is usually expressed in probabilistic terms.” The idea is that the resistance of a structure with sufficient reliability should be larger than the effects of the loads. The reliability index is a measure that indicates the failure probability of a structural member. CC 3 is the highest class, with a high reliability and thus a low failure probability. The undesirability of collapse of a high-rise is translated to the high reliability of CC 3.

Furthermore, increase insight and additional measures are due to the required robustness of the structure. The Eurocode 1990 requires a structure to be designed and executed in such a way that it is robust. Robustness is defined in Eurocode 1991-1-7 as “the ability of a structure to withstand events like fire, explosions, impact or the consequences of human error, without being damaged to an extent disproportionate to the original cause.”

However, as a combustible material, the timber structure can continue burning and collapse. The performance of the structure and the fire behaviour are uncertain. The structure might not be reliably safe. Furthermore structural collapse could result in damage disproportionate to the original cause, making it insufficiently robust as well. This would depend on whether the timber continues burning or extinguishes and maintains its function. To obtain a high degree of insight in the structural fire behaviour, an in-depth investigation of the risks associated with the fire behaviour and the structural fire response is needed.

2.3.6 Perception and approval issues

The past decades, building codes have changed from so-called “prescriptive” codes to “performance- or objective-based” codes in response to changing stakeholder needs (Bergeron, 2003; Hadjisophocleous and Bénichou, 2000). A prescriptive code presents a set of rules which set out how a building is to be designed and constructed. These rules lead to a design considered acceptable in terms of approval. This allows for a straightforward evaluation of a design, but can be rigid and result in barriers for innovation. Performance-based codes not prescribe in detail how a building is to be designed and constructed, but express the desired outcome with an explicit statement of the legislative objectives and the functional demands on the building. This offers greater flexibility in design and is more open to innovation.

Compliance with a performance-based code can be demonstrated in two ways. First, these codes are often supported by “acceptable” or “deemed-to-satisfy” solutions that provide a prescriptive way of meeting the functional statements. In the transition from a prescriptive to a performance-based code, old prescriptions would frequently become the first acceptable solutions (Bergeron, 2003). The majority of “standard”

buildings are designed in this way, as it is cost-effective and faster to approve. It could be argued the fire resistance requirements in the Dutch code are part of an “acceptable” solution.

Designs that fall outside this category are called “alternative”, “performance-based”, or “innovative” solutions. These require fire safety engineering as a way of meeting the code objectives. Compliance can be demonstrated by assessing against the code objectives, functional statement, and performance requirements (first principles approach), or by comparing against the acceptable solutions (benchmark approach) (CIBSE, 2010). This allows for solutions that conform to the intent of the code, but do not follow its prescriptions and acceptable solutions. This offers an alternative for non-typical buildings, innovations in design, and objectives beyond those covered by the code to be addressed.

The use of timber in high-rises can be considered an innovative solution. It is not traditionally covered by prescriptive codes and has not made its way in performance-based codes as an acceptable solution. While performance-based codes allow this, a challenge is often the acceptability by the approving authorities. This is particularly the case because there are few precedents and limited experience. Tall timber proposals can expect stringent levels of review. The designer must explicitly demonstrate compliance with the functional statements and objectives of the code. The approval process can be slow and costly.

Furthermore, building regulations of some countries cap the height of structures of combustible materials such as timber. Examples include the United States, Canada, the United Kingdom, and Australia (Gerard *et al.*, 2013). Other countries have no explicit clauses, but for example in The Netherlands more onerous fire resistance requirements are set if the fire load in a compartment exceeds 500 MJ/m^2 , which can be expected when a timber structure contributes to the fire load.

It is reasonable to assume these restrictions are leftover from the transition from a prescriptive to a performance-based code. The prescriptive rules might anticipate light-frame construction with a low level of inherent fire performance. Because these prescriptive rules found their way into the performance based codes, the potential superior performance of mass timber might not be taken into account.

As a result, there seems to be reluctance of designers and regulators to say these timber buildings are sufficiently safe. Timber is perceived as a material less suitable for high-rises. If timber buildings are to be realised, more insight in the fire performance of the material is required.

2.4 Design for structural fire safety of timber structures

Timber structures can be divided into light frame construction and heavy timber construction (Gerard *et al.*, 2013). The primary difference with regards to structural fire safety is the section size.

Light timber frame construction is characterised by walls and floors that are constructed from relatively small sized stud and joist members. These members have a low inherent fire resistance and walls and floors are typically encapsulated within non-combustible boards to ensure a certain fire resistance.

Heavy timber construction is characterised by elements of large section sizes. These can be solid sawn lumber, but engineered timber products, such as CLT, have become increasingly popular. Fire protection can be provided by encapsulation, but also by the inherent fire resistance of the thick elements. The use of large solid panels is also favourable because the risk of fire spread through void cavities is reduced.

2.4.1 Design of unprotected heavy timber exposed to fire

The design of unprotected heavy timber elements according to the Eurocode basically requires verification as expressed in Eurocode 1991-1-2 and in equation 2.1.

$$R_{fi,d,t} \geq E_{fi,d,t} \quad (\text{Eq. 2.1})$$

Where $R_{fi,d,t}$ = the design value of the resistance in the fire situation at time t
 $E_{fi,d,t}$ = the design value of the effect of the loads in the fire situation at time t

The design force results from structural analysis in the fire situation. The load capacity after a certain fire exposure is obtained by calculating the size of a residual cross-section; subtracting charred wood from the original cross-section and taking into account the mechanical properties of wood at elevated temperatures below the char line. This design principle is depicted in figure 2.3 for a 3- and 4-sided exposure.

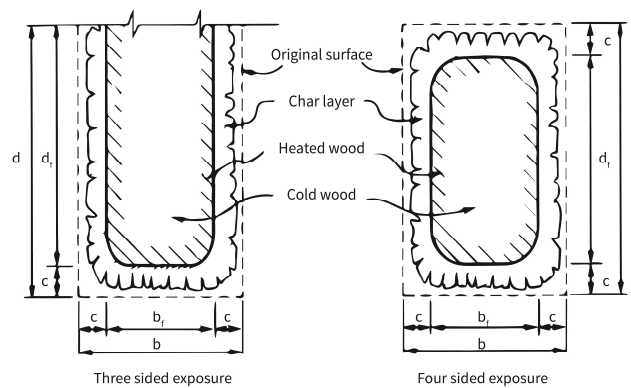


Figure 2.3 Design concept for heavy timber exposed to fire. Adapted from Buchanan (2009).

When wood burns the outer layer becomes char. The char protects and insulates the wood underneath. Due to this protective layer, the wood burns relatively slow and the load capacity is only gradually reduced as the cross-section gets smaller. The speed at which the wood is transformed into char is the charring rate. The original cross-section $b \times d$ is reduced to the residual cross-section $b_f \times d_f$. The charring depth d_{char} (c in figure 2.3) can be calculated according Eurocode 1995-1-2 as expressed in equation 2.1.

$$d_{char} = \beta \cdot t \text{ (mm)} \quad (\text{Eq. 2.1})$$

Where β = rate of charring (mm/min)
 t = time of fire exposure (min)

If the reduced cross-section is still able to carry the load after a certain period of standard fire exposure, the fire resistance is considered to be that many minutes. This concept is adopted by many codes. As a result of the charring behaviour, heavy timber construction has become recognised as having good fire resistance. There are examples of structures surviving fires without collapse and even fit for repair and re-use.

Eurocode standard fire charring

There have been many investigations of charring rates and there are multiple models available. The charring rate has been found dependent on the density and moisture content of the wood (Schaffer, 1967), the level of heat flux (Butler, 1971; Mikola, 1990), as well as the duration of exposure (White, 1988). Some models offer a constant charring rate, while others are non-linear.

This chapter focusses on the Eurocode 1995-1-2, which provides charring rates for the standard ISO-834 exposure and treats charring as a linear phenomenon with a constant charring rate. Table 2.3 presents design charring rates for unprotected timber. If the one-dimensional charring rate β_0 is used, the effect of corner rounding needs to be calculated separately to obtain the actual charred cross-section. Alternatively, an equivalent rectangular residual cross-section can be calculated with the slightly higher notional charring rate β_N , which implicitly includes the effect of corner rounding.

Table 2.3 Eurocode 5 charring rates for standard fire exposure

Design charring rates	β_0 (mm/min)	β_N mm/min)
Softwood and beech		
Glued laminated timber with a characteristic density of $\geq 290 \text{ kg/m}^3$	0,65	0,7
Solid timber with a characteristic density of $\geq 290 \text{ kg/m}^3$	0,65	0,8
Hardwood		
Solid or glued laminated hardwood with a characteristic density of 290 kg/m^3	0,65	0,7
Solid or glued laminated hardwood with a characteristic density of $\geq 450 \text{ kg/m}^3$	0,50	0,55
LVL		
With a characteristic density of $\geq 480 \text{ kg/m}^3$	0,65	0,70
Panels^a		
Wood panelling	0,9	
Plywood	1,0	
Wood-based panels other than plywood	0,9	

^a The values apply to a characteristic density of 450 kg/m^3 and a panel thickness of 20 mm

The use of cross-laminated timber would fall in the category “panels”. However, the panels in the table are of a thickness of 20 mm, while research shows that CLT can behave more like solid or glued laminated wood. As a result, more favourable charring rates can be used, but this has yet to be adopted by the Eurocode (Frangi *et al.*, 2009). Furthermore, Eurocode offers guidance for initially protected elements. Failure of the protection results in a charring rate twice as high due to the fact that no protective char has developed yet. When 25 mm has been charred, the rate is assumed to decrease to the value in the table.

The Eurocode also takes into account the properties of the heated wood below the char line. Two approaches are provided; both do not require a calculation of exact temperature profiles within the wood.

- The effective cross section method uses a cross-section smaller than the residual cross section, assuming a layer of zero strength wood below the char line, but otherwise unaffected material properties in the inner part. The thickness of the zero-strength wood layer is 7 mm.

- The reduced properties method uses the whole residual cross section beneath the char line but with an average reduction in the material properties by means of a strength reduction factor.

Note that the Eurocode approach of charring under a standard fire exposure as presented above does not take into account any potential self-extinguishment.

Eurocode alternative for parametric fires

The Eurocode offers an alternative in natural parametric fires. Parametric fires depend on input regarding ventilation openings, wall lining materials (boundaries), and fuel load. Examples are depicted in figure 2.2. The parametric charring rate β_{par} also depends on these conditions, and a whole range of parametric charring rates can be found, based on the input. Because a parametric fire, in contrast with the standard fire, has a decay phase, the charring rate is assumed to eventually drop to zero.

As a result of the charring rate dropping to zero, the total charring depth is finite. This seems to allow a structure to survive a burnout. However, this would imply the timber extinguishes. While this is not stated explicitly in the Eurocode 5, it is recognised by Buchanan (2009). However, he also indicates that it has been observed that charring often continues, even though the fire in the compartment has extinguished.

2.5 Conclusions

This chapter has provided a review of structural fire safety of timber high-rise buildings, both with regards to building regulations and their design. Various issues were identified for tall timber buildings.

For tall buildings, there is an increased severity of the consequences of structural failure as result of a fire. In order to obtain the desired level of safety, building codes typically require tall buildings to have a high fire resistance rating. However, as a combustible material, the timber structure can continue to burn and eventually collapse. Irrespective of the fire resistance rating, the level of safety intended by the code might not be achieved. A further investigating of the structural fire behaviour is required.

The Eurocode also recognises the risk associated with failure of the structure and suggests it to be designed according to consequences class 3: failure of the structure due to fire is highly undesirable and the structure needs to be reliably safe and robust. The design of tall buildings in consequence class 3 requires a high degree of insight into the structural fire behaviour and potentially additional measures. An in-depth investigation of the fire behaviour and the structural fire response is needed.

As an innovative concept with few precedents and limited experience of designers and regulators, tall timber face challenges in approval. Furthermore, some building codes cap the height of structures made from combustible materials. There seems to be reluctance of designers and regulators to say timber buildings are sufficiently safe and timber is perceived as a material less suitable for high-rise buildings.

Based on these issues, it seems more insight in the fire behaviour of the exposed timber structure is required. It is important to understand whether the timber would continue burning or whether it would decay by self-extinguishment; potentially in combination with active fire safety measures. However, self-extinguishment is currently not part of fire safety considerations for the structural design of timber buildings.

Fire dynamics of burning wood

3.1 Introduction

The burning of wood is a familiar phenomenon to many people. However, scientifically it is quite a complex process. These complexities are associated with the so-called “fire dynamics” involved. This chapter provides a review of the fire dynamics of burning wood and provides an answer to the question:

What are the fundamental fire dynamics of burning wood?

Fire dynamics can be defined as the study of the fire behaviour, including its ignition, development, and the fully grown phase. Within fire dynamics, the sciences of chemistry, physics, fluid mechanics, and heat transfer all play their part (Lilley, 2012).

This definition indicates fire dynamics covers a range of topics. Fire is both a physical and a chemical phenomenon and is highly interactive by nature. The flames, the fuel, and the surroundings, all have relations to each other. These relations are often non-linear and a quantitative estimation of the processes involved is complex. Fire safety engineering typically bypasses this complicity by relying on the results of tests to provide relatively simple data for the assessment of fire hazards and design calculations. However, if one wishes to advance the state of art, a good understanding of the fire dynamics involved is required.

In this chapter, the fundamentals of wood combustion are discussed first. This is followed by a review of the modes in which wood can burn, i.e. flaming combustion and smouldering combustion, and how the fire transforms between these modes. Finally, the topics of heat release and heat transfer are discussed.

3.2 Fundamentals of wood combustion

A piece of wood is defined by its chemical nature. However, as a material wood can burn in various ways. The mode of burning may depend more on the physical state, the distribution of the fuel, and the environment, than on the chemical composition. For example, when creating a campfire, a single log is difficult to ignite with just a match, but thin sticks can be ignited easily and will burn well if piled together.

While wood can burn in various ways, there are some fundamentals of combustion that will play a role in any mode of burning. These fundamentals are the chemical and physical structure of wood, the combustion reaction, the thermal decomposition of the material, and the charring behaviour. This paragraph will discuss these fundamentals.

3.2.1 Chemical and physical structure of wood

In order to understand the burning of wood, it is important to first understand its chemical structure. Wood is a mixture of natural polymers of high molecular weight. Polymers are individual molecules that consist of long chains of repeated units, which in turn are derived from simpler molecules known as monomers (Stevens, 1999).

In wood the most important polymers are cellulose (~45%), hemicellulose (~25%), and lignin (~25%) (Madorsky, 1964). Furthermore, wood contains minor amounts of extraneous materials (<10%), mostly in the form of organic extractives and inorganic minerals. As indicated by Miller (1999), these proportions vary from species to species.

The main constituent, cellulose, is a polymer made up out of many monosaccharide monomers, called D-glucose, a type of sugar. D-glucose and cellulose are depicted in figures 3.1 and 3.2 respectively. Cellulose adopts a linear structure and this linear structure allows the molecules to align themselves into bundles or “micro-fibrils”. These micro-fibrils are strong and thread-like macromolecules and provide the structural strength to the cell wall (Drysdale, 2012).

Compared to cellulose, lignin has a much more complex 3D-structure. The lignin acts as an encrusting material in the cell wall and is much more brittle. The third major constituent, hemicellulose, is much smaller and has a heavily branched or “cross-linked” structure. Hemicellulose is thought to help link the lignin and cellulose into a unified whole in each layer of the cell wall (Wiedenhoef, 2010).

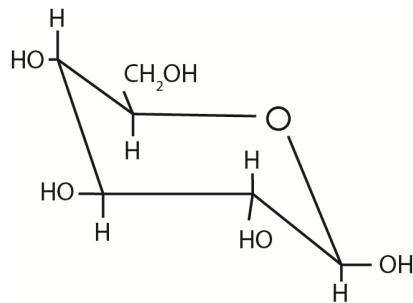


Figure 3.1 β -D-Glucopyranose, the stable configuration of D-glucose. From Drysdale (2012).

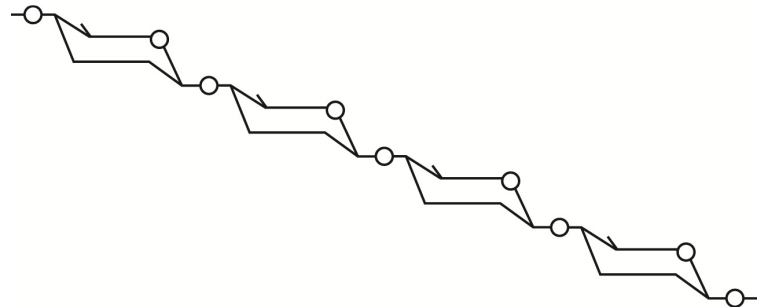


Figure 3.2 Part of a cellulose molecule, consisting of four monomers. H and OH groups have been omitted for clarity. From Drysdale (2012).

Next to these constituents, wood normally contains absorbed moisture. Some of this moisture will be bound by hydrogen bonds to the hydroxyl or OH-groups of the main constituents. However, if the relative humidity is high enough, some water will be held as free water by capillary forces in the natural voids within the wood.

Not only does wood have a typical chemical structure, the physical structure is of importance to the burning behaviour as well. Wood is an inhomogeneous and non-isotropic material. This means many of its properties vary with the direction in which the measurement is made. For example the thermal conductivity parallel to the grain is about twice that perpendicular to the grain. There is an even greater difference in gas permeability, in the order of 10^3 (Drysdale, 2012).

3.2.2 Combustion reaction

The occurrence of a fire is basically the manifestation of a particular type of chemical reaction: the combustion reaction. The combustion reaction is discussed in detail by Drysdale (2002, 2012) and Karlsson and Quintiere (2000) and this paragraph is mainly based on their work.

Most products in building fires, including wood, are carbon based. These products act as fuel during a fire and react with oxygen from the air once ignited by a heat source and under appropriate conditions. This phenomenon indicates the classical “fire triangle” as the simple model for understanding the necessary ingredients for igniting a fire, as depicted in figure 3.3.

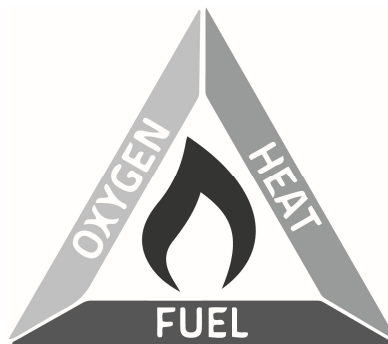
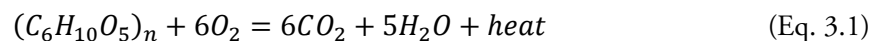


Figure 3.3 The fire triangle with the three ingredients required for igniting a fire.

Once the fire is established, combustion products are generated and heat is released. This reaction is called “oxidation” and is exothermic, i.e. the reaction is accompanied by the release of energy or heat. An example of a combustion reaction is the oxidation of cellulose in equation 3.1.



Equation 3.1 shows the initial and final state of the reaction in balance. This balanced chemical equation defines the “stoichiometry” of the reaction. The stoichiometry indicates the exact proportions of the reactants for complete conversion to the products. In reality the oxidation process is far more complex than suggested in equation 3.1, because the reaction mechanism involves a set of intermediate steps.

The reaction described above is called complete combustion, because the reactants are oxidised completely to yield stable end products. No residual fuel is left and all available combustion energy is released. This type of reaction can occur in ideal conditions with abundance of oxygen, well-mixed fuel and air, and under high pressure. The amount of energy released when a unit mass is oxidised completely to yield stable end products is called the complete heat of combustion. The complete heat of combustion is denoted by ΔH_c and is typically given in kJ/kg.

In real fires, combustion does not take place under ideal conditions: fuel and oxygen are not well-mixed, there is no high pressure, the available oxygen is limited, and temperatures are not ideal. The burning

occurs only in those regions where there is enough fuel and oxidant and the temperature is sufficiently high. The combustion process is less efficient and is referred to as incomplete combustion.

Furthermore, often only a part of a material is converted into actual fuel. As a result some residue is left behind, e.g. in the form of a carbon rich char or a glassy layer of inorganic material. It is also possible that not all of the converted fuel is combusted, leaving some carbon monoxide CO, carbonaceous particles or soot, and unburnt fuel in the products of combustion.

When combustion is incomplete, not all potential energy is released. The amount of energy released when a unit mass combusts in incomplete combustion is called the effective heat of combustion. The effective heat of combustion is denoted by ΔH_{eff} and is typically given in kJ/kg.

The ratio between the effective and the complete heat of combustion indicates the efficiency with which combustion is taking place. The combustion efficiency is denoted by χ and given in a dimensionless number. The combustion efficiency can range from 0,3 - 0,4 for heavily fire-retarded materials, to 0,6 - 0,7 for fuels such as oil that produce sooty flames, to 0,9 or higher in the case of oxygen-containing products and gaseous fuels that burn with a flame that is hardly visible and produce very little soot. The combustion efficiency will also drop if the supply of air is restricted, e.g. in a space with limited ventilation.

3.2.3 Thermal decomposition

Thermal decomposition plays an important role in the combustion reaction. It is the process that transforms a material from its original state into gaseous fuel vapours or “volatiles” and other components under the influence of heat. The volatiles can escape or burn above the solid in the right concentration when mixed with oxygen. This paragraph is mainly based on the work of Drysdale (2012), Karlsson and Quintiere (2000), and Beyler and Hirschler (2002) who discuss thermal decomposition in detail.

Thermal decomposition is also called “gasification”, “pyrolysis”, or “depolymerisation”. It must not be confused with thermal degradation; the process whereby the action of heat causes a loss of physical, mechanical, or electrical property.

During thermal decomposition, both chemical and physical changes occur. The chemical processes are responsible for the generation of flammable volatiles. The physical changes, such as melting, charring, or simple phase transitions, can alter the decomposition and burning characteristics of the material. These chemical and physical changes interact, making decomposition a “physicochemical” process.

For most liquids, the decomposition process is simple evaporation at the surface. However, due to their chemical nature, almost all solids have a more complex chemical decomposition process. In the case of polymeric solids, such as wood, the original material itself is essentially “involatile”. The large polymer molecule chains need to be broken down into smaller molecules of sufficiently low molecular weight, so that they can vaporise from the surface. This process involves various chemical mechanisms that alter the polymer chain, such as scission at the end or random along the chain, stripping of the chain, and cross-linking. During this decomposition process the smaller and lighter molecular fragments will vaporise immediately upon their creation. Other heavier molecules will remain in a condensed phase, i.e. solid or liquid, and may undergo further decomposition to lighter fragments which are more easily vaporised.

When looking specifically at the thermal degradation of wood, it is important to take its chemical structure into account. The constituents of wood decompose to release volatiles at different temperatures, as observed by Roberts (1970) and Browne and Brenden (1964) with “thermogravimetric” analysis, i.e. analysis in which changes in physical and chemical properties are measured as function of temperature. Results and typical values are depicted in figure 3.4.

Furthermore, in cellulosic materials there is an important semi-physical change that occurs on heating: desorption of adsorbed water. The water is both physically and chemically adsorbed and desorption will start at temperatures somewhat lower than the boiling point of water of $\sim 100^\circ\text{C}$.

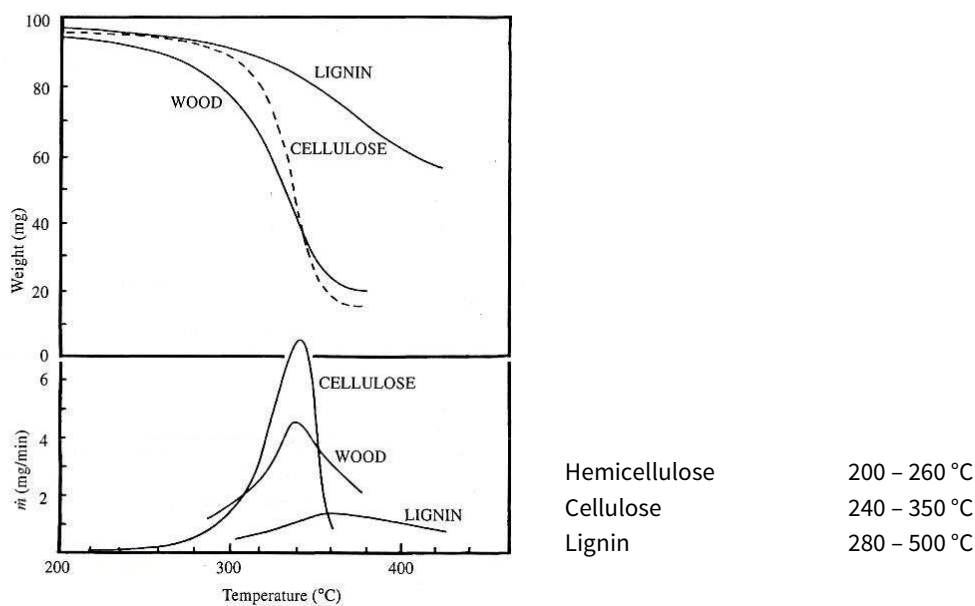


Figure 3.4 Results of thermogravimetric analysis of 90-100 mg samples of Ponderosa pine, cellulose powder and lignin, expressed in weight and as mass loss rate. From Browne and Brendon (1964).

Thermal decomposition occurs under the influence of heat. Because materials in building fires typically do not decompose at ambient temperature, heat must first be supplied in order to get it to a temperature where this will actually occur. Once at the required elevated temperature, the actual thermal decomposition process may either be exothermic or endothermic.

The total energy required to decompose and gasify a unit mass of liquid or solid at an initial temperature (typically 0°C or 25°C) is called the heat of gasification. This includes the temperature elevation required to start the process of thermal decomposing. The heat of gasification indicates a change of enthalpy and is denoted ΔH_g or L_V and typically given in kJ/kg .

For liquids, the heat of gasification is simply the latent heat of evaporation. For solids the heat of gasification is considerably greater as mechanisms that alter the polymer chain are involved. For example, the value of $1,82 \text{ kJ/g}$ for Douglas fir can be compared with the value of $0,49 \text{ kJ/g}$ for liquid benzene, as found by Tewarson and Pion (1976).

3.2.4 Charring

As was discussed, combustion is often not complete. While some polymers break down completely during thermal decomposition, more often not all material becomes fuel vapour and a residue is left behind. For wood this residue is a carbon-rich porous solid called char. As it builds up, the physical structure of this char strongly affects the way the wood burns.

This paragraph is based on the work of Drysdale (2012) and Beyler and Hirschler (2002), who provide a good overview of charring.

When wood burns in ambient air, about 15-25 % of the original mass remains as char. Much of this char is coming from the lignin content of the wood. Lignin has a complex structure and is highly cross-linked. This cross-linked structure enhances charring. If lignin is heated to temperature above 400- 450 °C only ~50 % volatilises (see also figure 3.4).

Considering the importance of the lignin content with regards to the char formation, a difference can be expected between wood species. For softwoods, lignin constitutes about 23-33 % of the wood substance, while the range for hardwoods is about 16-25 % (Miller, 1999). As a consequence softwoods tend to give higher char yields than hardwoods, as discussed by Di Blasi (2009).

The yield of char also depends on the temperature at which the conversion takes place and the rate of heating. Low rates of heating, or relatively low temperatures, appear to favour the char-forming mechanism, as reported by Madorsky (1964) and Di Blasi (2009). As a consequence the charring behaviour will vary with the fire.

As the top layer of the burning material transforms in a residual char, the material underneath still undergoes pyrolysis. As charring progresses, small cracks appear in the char layer because the physical structure begins to break down. This permits volatiles to escape easily through the charred layer from the pyrolysis zone underneath. The cracks gradually widen as the depth of char increases, leading to a characteristic pattern, often referred to as “crocodiling” or “alligatoring”. A cross-section of a burning and charred piece of wood is depicted in figure 3.5.

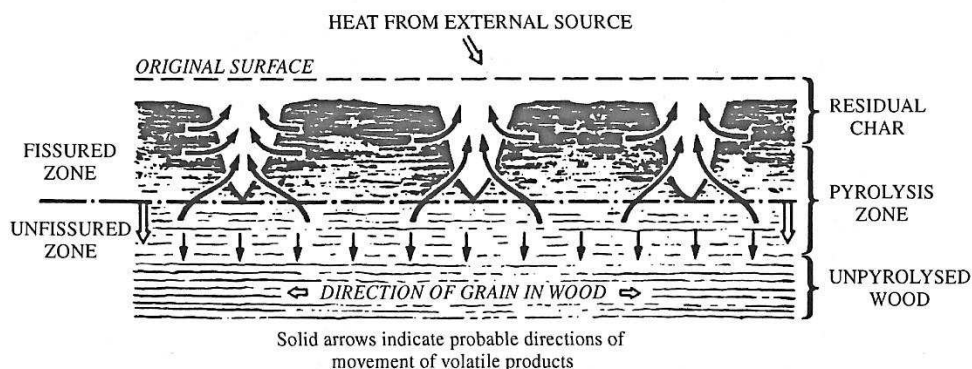


Figure 3.5 – Schematic representation of a cross-section through a slab of burning wood, including a charred, pyrolysis, and unaffected zone. From Roberts (1971).

Char has an important influence on the thermal decomposition of wood. While the formation of the char as described above is a chemical process, the real significance on thermal decomposition is due to its physical properties.

First of all, if any of the material is left in the solid phase as involatile char, less flammable gas is given off during decomposition. This effectively reduces the potential supply of gaseous fuel to a flame and reduces the combustion efficiency.

Furthermore, as the char accumulates, it forms a barrier between the flame and the unaffected material. Char typically has a low density and a high porosity. As a result the char acts as a good thermal insulator and inhibits the flow of heat to the unaffected material, which slows down the thermal decomposition process. This mechanism can vary with time; the flow of heat to the parent material is reduced as the char layer thickens.

Many flame retardants make use of the char formation process and the properties of char to improve the response of wood to fire. By adding inorganic impurities to wood, such as salts, the char rate can be increased, resulting in a better performance in fire.

When char forms a barrier between the flame and the unaffected material, the material is assumed to be in “flaming” combustion. However, char plays a role in a second mode of burning called “smouldering” combustion. These two types of combustion, flaming and smouldering, will be discussed in the following two paragraphs.

3.3 Flaming combustion

Flaming combustion is the combustion that occurs when the fuel is in the gas phase. The flame which is seen is the visible portion of the volume within which oxidation of the volatiles takes place. It often has the characteristic yellow luminosity arising from incandescent carbonaceous particles.

Drysdale (2012) and Karlsson and Quintiere (2000) explain the principles of flaming combustion. This paragraph is largely based on their work.

3.3.1 Flaming combustion mechanism

There are two distinct regimes in which gaseous fuels may burn: premixed or diffuse. Premixed flames occur when the fuel is intimately mixed with oxygen or air before burning. The rate at which combustion takes place is typically high and is determined by the chemical kinetics of oxidation, i.e. the reaction speed. On the other hand, diffuse flames occur when the fuel and the oxygen or air are initially separate but burn in the region where they mix. The rate at which combustion takes place is not determined by the speed of reaction, but by the mixing driven by buoyance. Buildings fires typically yield diffuse flames. The fuel and the oxygen are not initially mixed and the mixing of volatiles and air is an integral part of the fire.

The mechanism of flaming combustion of solids with diffuse flames can be best explained with the “burning rate”. The burning rate is the rate at which mass of a solid or liquid fuel is vaporised and burned. It is denoted by \dot{m} and expressed as mass flow per unit time, typically in kg/s. It can also be expressed as mass flux or mass burning rate per unit area, which is denoted by \dot{m}'' and given in kg/(m² s).

Another often used term is the “mass loss rate”. Strictly speaking, a distinction should be made between burning rate and mass loss rate. When there is insufficient oxygen available, not all of the fuel supplied may be burned. However, most textbooks assume the terms to be identical.

The burning rate is dependent on the rate of supply of volatiles from the fuel surface. This supply of volatiles is in its turn directly linked to the heat transfer from the flame to the fuel, minus any losses. The rate of burning per unit area \dot{m}'' for flaming combustion of solids and liquids with diffuse flames can be expressed quite generally as shown in equation 3.2 (Drysdale, 2012).

$$\dot{m}'' = \frac{\dot{Q}_F'' - \dot{Q}_L''}{L_V} \quad (\text{Eq. 3.2})$$

Where

- \dot{m}'' = burning rate or mass loss rate per unit area (kg/m²s)
- \dot{Q}_F'' = heat flux from the flame to the fuel (kW/m²)
- \dot{Q}_L'' = losses through fuel surface, expressed as heat flux (kW/m²)
- L_V = heat of gasification (kJ/kg)

The heat flux from the flame to the fuel \dot{Q}_F'' is related to the rate of energy release within the flame and the mechanisms of heat transfer to the surface (e.g. radiation from the flame to the surface). Heat losses through the surface \dot{Q}_L'' occur (e.g. convective losses from the surface to the air and conductive losses to cool deeper layers) and are also expressed as a heat flux.

Subsequently, the net heat flux $\dot{Q}_F'' - \dot{Q}_L''$ is used to volatilise the solid fuel. The burning rate \dot{m}'' is found by dividing the net heat flux by the heat of gasification L_V , which represents the heat required to volatilise a unit mass of the solid or liquid. A schematic representation of this process is depicted in figure 3.6.

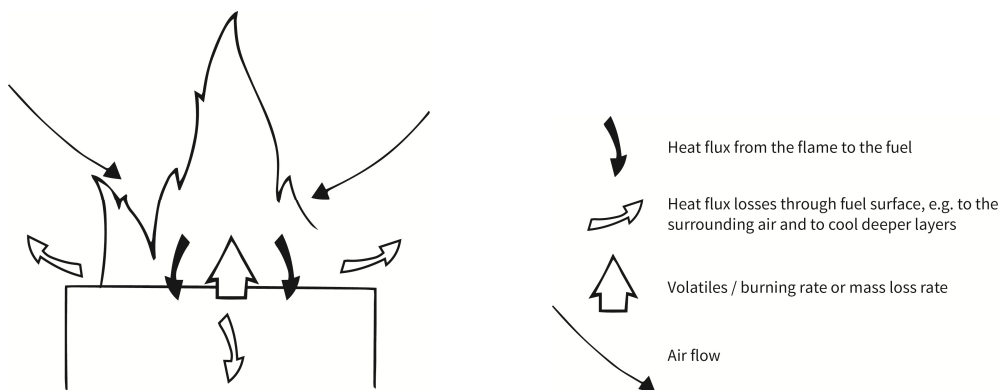


Figure 3.6 Schematic representation of the burning process of flaming combustion.

Flaming combustion as depicted here can be self-sustaining if the thermal feed-back process allows it. In order for the combusting reaction to be self-sustaining, it is necessary for the burning gases to feedback sufficient heat to the material to continue the production of sufficient volatiles (Beyler and Hirschler, 2002).

Equation 3.2 represents steady state burning. However, fires are often changing and thus the terms are transient. For example, for many solids, surface temperatures tend to be high during burning, typically $>350\text{ }^{\circ}\text{C}$, and as a result heat losses from the surface are significant. These heat losses include conductive losses through the solid, which will gradually diminish with time as the solid heats up. Also, in reality it is difficult to quantitatively determine the net heat flux to the fuel surface. Therefore, equation 3.2 is not often used in practice. Instead, the burning rate can be measured directly by weighing the fuel package as it burns.

In order for flaming combustion to occur, ignition has to take place first. Two types of ignition can be distinguished: piloted ignition and spontaneous ignition.

Piloted ignition occurs when combustion is initiated in a flammable mixture by a “pilot”, such as an electrical spark or an independent flame. Under the application of heat, volatiles escape from the solid and mix with air. Close to the surface the minimum conditions are met in which the vapour-air mix is susceptible to ignition. An independent pilot can then produce a flash of flame.

If an independent pilot remains absent, spontaneous ignition can occur. Spontaneous ignition occurs when combustion is initiated on its own under the application of a sufficiently high heat flux. This type of ignition requires a higher heat flux than piloted ignition because a higher surface temperature is required to produce a flow of volatiles that is hot enough for it to ignite.

3.3.2 Flaming combustion of wood

In comparison with many other (especially synthetic) solids, the flaming combustion of wood is a complex process, in part due to the charring behaviour. As the char layer builds up with time it will start to influence the terms in the equation 3.2.

For example, while the char is a residue, it can be further oxidised, which will release some additional heat (Kashiwagi *et al.*, 1987). More importantly, the build-up of char shields the unaffected wood from the flame and thus influences the thermal feedback process. As was discussed in paragraph 3.2.4, char acts as a good thermal insulator due to its low density and high porosity. The amount of heat transferred from the flame to the wood \dot{Q}_F'' is decreased. This slows down thermal decomposition. As a result, higher surface temperatures are required to provide the necessary heat flow to produce volatiles. However, these high surface temperatures will also result in greater heat losses \dot{Q}_L'' .

As a result, for wood the net heat flux is unable to self-sustain flaming combustion. It is common experience that a thick slab of wood will not burn unless supported by heat transferred from another source. For example, in a campfire multiple tick logs close together are able to sustain flaming combustion due to their cross-radiation. However, when one log is separated, it no longer receives this “externally” applied heat flux. Radiative and convective heat losses overwhelm the heat produced by the log burning on its own and the thermal feedback loop is broken.

One might wonder why a thick slab of wood apparently cannot burn in isolation, while thin pieces of wood, such as match sticks, can be ignited easily and will continue to burn. This can be explained by looking at the heat losses. In thin samples the rate of heat loss from the surface into deeper layers will be minimal once ignition has occurred and flaming has been established on all sides.

Apparently, an externally applied heat flux is required to supplement the heat generated by the burning of a thick piece of wood itself. Flaming combustion of wood under the application of an external heat flux has been investigated by Tewarson and Pion (1976) and Petrella (1980). They used a model that adapted equation 3.2 to incorporate the influence of an applied flux. With a test apparatus that can impose a flux on a specimen various properties and quantities were determined for a range of materials, including wood. Reference is made to a more detailed explanation of their work in appendix B.

The results of Tewarson and Pion reinforce the common experience that a thick slab of wood will not burn unless supported by an externally applied heat flux. They observed that for Douglas fir the heat transfer from the flame to the material is theoretically just sufficient to match the heat losses, i.e. $\dot{Q}_F'' \approx \dot{Q}_L''$. Results obtained by Petrella with a similar test-setup indicated that generally losses even are slightly higher for ten species of wood, i.e. $\dot{Q}_F'' < \dot{Q}_L''$.

Apparently, the ability of wood to sustain flaming combustion depends on the presence of an externally imposed heat flux. In a real fire this flux would be provided by mutual cross-radiation between the wooden surfaces and other hot objects or flames, similar as illustrated in the campfire example above.

An example that reflects the complexity of flaming combustion of wood is the lack of consensus in literature regarding the value for the heat of gasification for wood. Values range from of 1,8 kJ/g to 7,0 kJ/g, as reported by Thomas (1967), Tewarson and Pion (1976), and Petrella (1979). This lack of consensus is partly due to the variation in chemical composition and structure between hard- and softwoods and various species (Hadvig and Paulsen, 1976). Furthermore, the heat of gasification can vary with the depth of the char (Janssen 1993). Differences can also be expected due to complexities during thermal degradation when exothermic (e.g. the char formation) and endothermic (e.g. the production of volatiles) reactions compete. Finally, there is sensitivity to experimental conditions and the orientation of the samples due to the inhomogeneous and non-isotropic nature of the wood (Rath *et al.*, 2003).

3.4 Smouldering combustion

A second mode of burning of wood is called smouldering combustion. Smouldering combustion is a slow, low-temperature and flameless form of combustion. The fundamental difference between smouldering and flaming combustion is that smouldering combustion occurs when the oxygen reacts directly on the surface of the condensed fuel rather than in the gas phase (Rein, 2009).

Smouldering combustion has not been studied to the extent as flaming combustion. A definitive theoretical description is lacking. Therefore, this paragraph is restricted to examining experimentally determined behaviour and general qualitative statements. A good overview is given by Ohlemiller (2002) and Drysdale (2012), on whose work this paragraph is largely based.

Most experimental data and theory on smouldering covers materials build up out of particles, fibres, or of a cellular structure. Due to their build-up, these materials have a high permeability with regards to oxygen. While wood is not such a material, its char residue is. As a result “wood” is able to smoulder and theory based on these other materials does have a qualitative application for the problem of smouldering of wood.

3.4.1 Smouldering combustion mechanism

Materials that are able to smoulder are typically porous and form a solid carbonaceous char. Especially loosely packed and finely divided aggregates of these charring materials are prone to smouldering (Ohlemiller, 1990a). Examples include materials of vegetable origin, such as paper, peat, cellulosic insulation, sawdust, fibreboard, latex rubber, and coal; as well as thermosetting plastics in expanded form, such as polyurethane foam.

The mechanism that drives smouldering combustion is different from flaming combustion. Research on cylindrical cellulosic elements by Moussa *et al.* (1977) has shown that smouldering combustion propagates as a “wave” through a material with three distinct zones. These three zones seem to be common to all self-sustained smoulder processes. The smouldering zones are depicted in figure 3.7 and can be described as;

- Zone 1 - a pyrolysis or thermal degradation zone with a steep rise of temperature and an outflow of airborne products from the parent material.
- Zone 2 - a charred zone in which a reaction zone is located and with a maximum in temperature. No visible combustion products are present, but glowing occurs.
- Zone 3 - a zone of porous residual char and ash which is no longer glowing and of which the temperature is falling slowly.

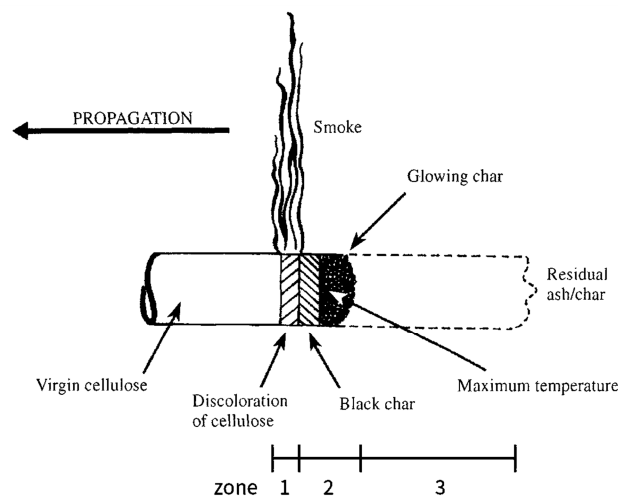


Figure 3.7 –Schematic representation of steady smouldering combustion along a horizontal cellulose cylinder. Adapted from Moussa *et al.* (1977).

The oxidation of char in zone 2 is the principal heat source and driver of most self-sustained smoulder processes. It occurs at ~ 600 °C and is visible as the distinct “glowing” of a smouldering material. The char is an excellent fuel, as it is susceptible to rapid oxygen attack at moderate temperatures of >400 °C and has a high heat of oxidation. Furthermore, the char has a large surface area that permits the reaction of the solid with oxygen. A substantial amount of ~ 30 % of the total heat of combustion of wood is associated with the char. The part of the charred zone where the smouldering occurs is referred to as the reaction zone.

Heat is conducted from the charred zone 2 in the direction of propagation to the thermal degradation zone 1. There it causes thermal decomposition of the parent material. Temperatures of >250-300 °C are required for most materials. Decomposition yields volatiles and the char residue. The volatiles are not oxidised significantly and can escape the material. This is in contrast with flaming combustion where the volatiles would burn as a flame above the fuel.

For some materials a second heat source is located in zone 1. Thermal decomposition can be enhanced by the presence of oxygen, as found by Kashiwagi and Ohlemiller (1982). In some cases, particular for cellulosic materials, thermal degradation in the presence of oxygen is exothermic and this heat can be sufficient to drive the smoulder wave even without char oxidation, as indicated by Ohlemiller and Lucca (1983). However, participation of thermal degradation in driving the smoulder process requires oxygen to have free access to the thermal degradation region (Ohlemiller, 1990a).

If no oxygen is present in the pyrolysis zone, the process is solely driven by the char oxidation in zone 2. The continued propagation of the zones is dependent on heat transfer from the oxidation in zone 2 to the pyrolysis zone 1. In that case, as Dosanjh and Pagni (1987) indicate, smouldering will stop if the heat generated by the char oxidation is insufficient to drive the pyrolysis that precedes char formation.

While zones 1 and 2 propagate through the material, a third zone of porous char and ash is left. This zone acts as an effective thermal insulator that minimises heat losses. This is important because smouldering is characterised by a low heat release. Despite the low heat release, low losses permit sustained smouldering. Many materials require a minimum thickness of char to insulate the reaction zone sufficiently. Note that, while figure 3.7 suggest a linear smoulder propagation, it can in fact occur on or along the surface of a material, inwards into the material, or both in complex 3D patterns.

The mechanism as described above has been modelled in various ways. The simplest models were based on the idea that the smoulder process and propagation were governed by heat transfer. However, these models were found flawed. Alternatively, Moussa *et al.* (1977) found that the rate of oxygen transport to the reaction zone governs the rate of smoulder propagation.

Because smouldering materials (and their residual char) are porous, oxygen is able to reach the reaction zone by convection and diffusion. The oxygen supply rate controls the smouldering because the heat evolved raises the temperature locally. This high local temperature increases the local reaction rate until all oxygen in proximity is consumed. The reaction continues to consume oxygen as fast as it reaches the reaction zone, resulting in a low oxygen level locally, which limits the reaction rate. Based on this idea, more sophisticated models have been developed, e.g. by Ohlemiller (1985) and Dosanjh *et al.* (1987).

Considering the role of the oxygen supply rate in controlling the smoulder process, the presence of an imposed airflow will influence the smouldering. Without an imposed flow, the flow induced by the buoyant plume rising from the material assures a constant supply of oxygen (Ohlemiller, 1990a). However, the process can accelerate in response to an increased oxygen supply due to an imposed air flow through the material or over its surface. An increased flow accelerates the rate of oxygen transfer to the reaction zone. This increases the oxidation rate, the local heat release, the local temperature, and rate of

heat transfer from the reaction zone to the pyrolysis zone. As a result, the smouldering will propagate faster or be sustained longer.

Furthermore, the relative direction of the flow influences the smouldering process. If the oxygen moves through the unburned fuel, it goes opposite to the direction of smoulder propagation; this is called reverse smouldering. Alternatively, oxygen can reach the reaction zone through the char, going in the direction of the movement of the smouldering front; this is called forward smouldering.

There are significant differences between the two modes, for example in speed of propagation and sensitivity to air flow velocity (Ohlemiller and Lucca, 1983). These differences occur due to whether or not the various smouldering zones encounter the airflow hot or cool, with or without a full complement of oxygen, and with or without products of combustion.

Like flaming, smouldering combustion needs to be ignited. There have been few studies of the initiation of smouldering combustion. While the smouldering itself is controlled by the oxygen supply rate, its initiation is governed by the reaction kinetics. It is known that smouldering can be initiated by heat sources too weak to produce a flame. The basic requirement is the provision of a source of heat that will produce some char and initiate its oxidation. Furthermore, smouldering often requires a critical depth of char that will insulate the reaction front and minimise losses.

3.4.2 Smouldering combustion of wood

Most research regarding self-sustained smouldering has been conducted on materials that are porous, such as layers of saw-dust or cellulosic-dust (Palmer, 1957; Ohlemiller and Luca, 1987), cellulosic strips or boards (Moussa *et al.*, 1977), cigarettes (Egerton *et al.*, 1963; Baker, 1977), and cellulosic or synthetic foams (Ohlemiller and Rogers, 1978; Ohlemiller, 1990a and 1990b). These materials have a high permeability with regards to oxygen.

Solid wood differs from these materials because the parent material is not porous and has low air permeability. However, thermal degradation of wood, e.g. during flaming combustion, leaves char. This char can continue to smoulder after cessation of the flames, provided that sufficiently high temperatures are maintained. The basic requirements for smouldering, i.e. the provision of a source of heat that will produce some char and initiate its oxidation, have been satisfied by the preceding flames.

Ohlemiller (1988, 1991) conducted research specifically on smouldering of solid wood and explain the principle differences with porous materials. The low air permeability of the parent material wood influences the smoulder behaviour in various ways.

First of all, air can reach the reaction zone solely through the porous char layer, and access of oxygen to the thermal degradation zone 1 is prevented. This inhibits the participation of thermal degradation in the presence of oxygen as a driving force of the smoulder process. The process must be driven solely by the heat generated by char oxidation in zone 2. Furthermore, the low permeability forces the reaction zone out towards the fuel exterior surface. Here it is subject to substantial heat losses, while a well-insulated reaction zone is a key factor in a self-sustaining smoulder process.

As a consequence, similar to what was found for flaming combustion, a slab of wood will not smoulder unless the reaction heat is supplemented by an external source. Apparently, the heat transferred from the

oxidation in zone 2 to the thermal degradation zone 1 is insufficient to match the heat losses. In other words, the relation $\dot{Q}_G'' < \dot{Q}_L''$ is valid here as well⁵.

This can be illustrated with a heap of glowing charcoal that is opened to expose the burning surfaces. The cross-radiation between the coals is eliminated and the radiative and convective heat losses overwhelm the rate of heat production if the individual pieces are large enough and have not become uniformly heated. The burning surfaces will cool and the smouldering will self-extinguish (Drysdale, 2012).

This experience is reinforced by experiments performed by Ohlemiller (1988, 1991), who examined smoulder propagation on red pine and white oak along the interior surface of a U-shaped channel. These tests focussed on smouldering on the surface of the wood, not inward into the material. Nevertheless, the observations qualitatively indicate certain aspects of the smouldering of wood in general. Reference is made to a more detailed explanation of the work in the appendix B.

The research implied a central role for radiative heat transfer between the smouldering surfaces in sustaining the process. An externally applied flux of $\sim 10 \text{ kW/m}^2$ was required to compensate for heat losses and supplement the heat of oxidation in order to keep the smouldering going. In the test setup this additional flux was provided by cross-radiation due to the concave U-shaped channel.

The airflow over the surface was also found important. An essentially linear increase in smoulder velocity, surface temperature, rate of heat release, and products released was observed with an increased forced air flow rate; especially for forward smouldering. This behaviour was contributed to the increased oxygen supply to the reaction zone. Furthermore, it was found that conduction had a minor role in the heat transfer between the zones. This indicates smouldering is independent of properties such as density.

The requirement of an externally applied heat flux is further reinforced by Beyler *et al.* (2006) and Swann *et al.* (2008), as well as various sources of literature they refer to in their research. They investigated the smouldering ignition of wood and found that a radiative flux of $\sim 8 \text{ kW/m}^2$ was required for the onset of “glowing” at the surface of plywood. This glowing was not sustained in the absence of the flux. Reference is made to a more detailed explanation of the work of Swann *et al.* in the appendix B.

The work of Ohlemiller, Beyler, and Swann suggest that an externally applied flux is required to sustain smouldering of wood. Absence of this flux could result in self-extinguishment. This behaviour is similar to what was found for flaming combustion by Tewarson and Pion (1976) and Petrella (1980). Furthermore, the results of Ohlemiller indicate that airflow over the material influences the smouldering behaviour as well.

The research mentioned above focussed on smouldering on and along the surface of the material and on smoulder initiation. When investigating self-extinguishment of CLT elements in a compartment fire, it is smouldering inward into the material and seizing it that is relevant. Nevertheless, it can reasonably be expected that the requirement of an externally applied flux and the influence of an additional air flow are valid for seizing smouldering inward into the material as well.

⁵ Note that subscript G is used instead of F, as it is not the flame (as was the case for flaming combustion) but the glowing char that produces the heat.

3.5 Combustion transitions of wood

In the previous chapters, the fundamentals of both flaming and smouldering combustion of wood have been discussed. In a real fire, these phenomena do not occur exclusively; transitions occur. This paragraph discusses these transitions, and is based on the work of Ohlemiller (2002) and Drysdale (2012).

3.5.1 Flaming to smouldering

Smouldering combustion can follow flaming combustion in many cellulosic materials if the flame is extinguished without cooling the fuel. The basic requirement is the provision of a source of heat that will produce some char and initiate its oxidation. In wood these requirements can be met after flaming combustion has left some char as a residue. This char can continue to smoulder, provided that sufficiently high temperatures are maintained.

A recent example in which this behaviour was observed is the research conducted by McGregor (2012) on CLT rooms in protected and unprotected configurations. An initial fire load, excluding the CLT, was ignited. It was observed that the CLT in unprotected configurations quickly became involved in flaming combustion. Once the initial fire load entered a phase of decay, the CLT was observed to decay as well. In one test the CLT changed from flaming to smouldering combustion after cessation of the flames. Reference is made to a more detailed explanation of the work in the appendix B.

It is important to note that it is unlikely that both smouldering combustion and significant flaming combustion can occur simultaneously at the same location. The flow of volatiles through the char will tend to exclude air from direct contact with the char. As a result solid-phase char oxidation tends to occur only after volatilization has largely ended (Beyler and Hirschler, 2002).

3.5.2 Smouldering to flaming

Smouldering combustion can transform into flaming as well. Flaming combustion can only be established if the flow of volatiles exceeds a certain critical value and is ignited by pilot or spontaneously. Even though some volatiles are released during smouldering; the application of a small flame to these products rising from the surface is unlikely to lead to flaming because the critical flow is not reached.

However, factors that either enhance the rate of heat generation or decrease the rate of heat loss, will move the smouldering material towards flaming. The temperature in the reaction zone will increase, and so will the rate of pyrolysis gas generated in the thermal degradation zone. As a result, the material is brought closer to flaming. Factors that can enhance the rate of heat release or decrease losses include an enhanced oxygen supply and an increase in scale due to less surface heat losses per unit volume.

For example, Ohlemiller (1990b) observed that a smouldering fuel responds to an increased oxygen supply by becoming hotter until flames erupt. Similar results were obtained in the experiments on the smouldering U-shaped wooden channels. An increased air flow over the surface increased the oxygen supply rate to the reaction zone and eventually resulted in flaming at sufficiently high airspeeds.

In the tests performed by McGregor (2012) on CLT rooms the transition from smouldering to flaming combustion was also observed. In two tests the polyurethane adhesive between a completely charred layer and the unaffected layer underneath lost bonding, resulting in “delamination” and fall-off of the top layer. As a result, a new layer of uncharred wood was exposed. In one test the fire then transformed from smouldering back to flaming combustion. In another test flaming combustion was simply sustained. Reference is made to a more detailed explanation of the work McGregor in appendix B.

Whether the observed transition in these tests is an actual transition from smouldering combustion to flaming combustion is questionable. It was the newly exposed timber that became involved in flaming combustion, not the smouldering char. Nevertheless, the notion that delamination and fall-off can influence in the transitions between flaming and smouldering combustion has to be taken into account when investigating self-extinguishment of CLT.

3.6 Heat release

An important concept that was missing up until now is a measure that characterises the severity of a fire in terms of the amount of energy or heat released. This paragraph discusses the concept of heat release and is mainly based on the work of Drysdale (2012), Karlsson and Quintiere (2000).

When an object burns, it releases energy. The stoichiometry of the combustion reaction provides the total amount of energy released in terms of the heat of combustion, as was discussed in paragraph 3.2.2.

However, generally the rate at which heat is released is more important than the total amount in characterising the behaviour of a fire (Babrauskas and Peacock, 1992).

The amount of energy a burning object releases per unit of time is called the energy release rate, often called heat release rate (HRR). Strictly speaking, the term energy release rate is more appropriate, because heat is energy transported due to a temperature difference. However, in literature these terms are often used synonymously. The heat release rate is often denoted by \dot{Q} and typically given in kW or kJ/s.

The heat release rate is the characteristic that describes quantitatively “how big the fire is”. Information on the rate of heat release as it varies in time is often required in engineering calculations; for example in the estimation of flame height, the production of smoke, the temperatures in a compartment, or the flashover potential of a room. For design purposes the heat release rate is often in the range of 50 kW for a burning paper wastepaper basket, to 2,5 MW for a burning 1 m² pool of gasoline, to 250 MW for a burning petrol tanker with fuel spills.

It is important to note that the rate at which energy is released in a fire depends mainly on the type and quantity of the fuel, but also on the geometrical factors, such as the orientation of fuel and the effects that an enclosure may have.

The heat release rate can be determined in various ways. One way is by looking at the combustion reaction. Techniques offered by thermochemistry, i.e. the study of the energy and heat associated with chemical reaction and physical transformations, provide information about the amount of heat liberated during a complete combustion process. In principle a correction can be made if the reaction is incomplete. However, in real fires the large number of incomplete combustion products makes this approach

cumbersome and effectively unworkable. Alternatively, the heat release rate can be expressed in terms of the burning rate, in the form of equation 3.3.

$$\dot{Q} = \chi \cdot \dot{m}'' \cdot A_f \cdot \Delta H_c \quad (\text{Eq. 3.3})$$

Where	\dot{Q}	= heat release rate (kW)
	χ	= combustion efficiency (-)
	\dot{m}''	= burning rate or mass loss rate per unit area (kg/m ² s)
	A_f	= fuel surface area (m ²)
	ΔH_c	= complete heat of combustion (kJ/kg)

This method was common practice until recently. However, in real fires a large number of materials burn simultaneously. These different sources all contribute depending on various and often unknown factors, e.g. the combustion efficiency, fuel surface, heat of combustion, and burning rate (which also depends on many factors). This makes use of equation 3.3 problematic for most engineering and research purposes.

Fortunately, it is now possible to determine the rate of heat release experimentally using the method of oxygen consumption. This method is based on the principle originally proposed by Thornton (1917), that for most gases, liquids, and solids, more or less the same amount of energy or heat is released for the amount of oxygen consumed.

In tests conducted by Huggett (1980), it was found that the amount of energy released in a fire involving conventional organic materials is 13,1 kJ per gram of oxygen consumed. This value is considered to be accurate with few exceptions to about $\pm 5\%$ for many hydrocarbon materials. Consequently, if the rate of oxygen consumption can be measured, the rate of heat release can be estimated directly. The relationship for heat release rate based on oxygen consumption is presented in equation 3.4.

$$\dot{Q} = E (\dot{m}_{O_2}^o - \dot{m}_{O_2}) \quad (\text{Eq. 3.4})$$

Where	E	= 13,1 \pm 5 % (kJ/g)
	$\dot{m}_{O_2}^o$	= mass flow rate of O ₂ of the incoming air (kg/s)
	\dot{m}_{O_2}	= mass flow rate of O ₂ in the exhaust air (kg/s)

The determination of the heat release rate by measurement of a single parameter, oxygen, is particularly useful in tests where multiple items are involved in the fire. However, in large scale tests, it can be difficult to control the incoming air. Janssens (1991) proposed a series of equations for fire tests where it is not possible to measure the air flow rate into the system. The basic requirement for his equations is that the combustion products are collected and measured downstream in an exhaust duct at a sufficient distance for adequate mixing. The oxygen is measured, but the accuracy can be increased by also measuring CO, CO₂ and H₂O to account for incomplete combustion. This measuring device is called an oxygen consumption calorimeter, and it is now widely used both in fire research and in routine testing.

3.7 Heat transfer

There are three basic mechanisms of heat transfer: conduction, convection, and radiation. While all three contribute in every fire, often one predominates at a given stage or at a given location. Heat transfer is often expressed as a heat flux, denoted by \dot{q}'' and is typically given in W/m^2 . This paragraph is based on the work of Drysdale (2012), who also provides heat transfer equations and refers to various textbooks.

Conduction typically determines the rate of heat flow in and through solids. An example in the context of this chapter is the heat transfer from the reaction zone to the pyrolysis zone during smouldering.

Convection is associated with the exchange of heat between a gas or liquid and a solid and involves movement of the fluid medium. It occurs in all stages of a fire but is particularly important early, when the thermal radiation levels are low. An example in the context of this chapter is the convective cooling of the char layer of the wood during smouldering due to a flow of cooler air over the surface.

Unlike conduction and convection, radiative heat transfer requires no intervening medium. The transfer of energy occurs by electromagnetic waves of all parts of the electromagnetic spectrum. As a result, any opaque object placed in its way will cast a “shadow”. Radiation is the dominant mode of heat typically when the fuel bed diameter increases beyond 0,3 m. A substantial amount of heat release in flames is transmitted by radiation to the surroundings. Most of this radiation is emitted by small solid particles of soot which are formed in almost all diffusion flames. An example in the context of this chapter is the radiation between the hot surfaces, flames, and CLT, both during flaming and smouldering combustion.

3.8 Conclusions

This chapter provided a review of the fire dynamics of burning wood. The burning of wood is basically the manifestation of the combustion reaction. This reaction is called oxidation. Once ignited by a source, fuel and oxygen react to generate combustion products and heat.

Thermal decomposition is the process that transforms the wood from its original state into volatiles and a carbon-rich porous residue called char under the influence of heat. These volatiles can act as fuel and burn in flaming combustion above the wood when mixed with oxygen. The residual char that builds up with time creates a protective barrier between the flame and the unaffected material. However, char is also part of a second mode of burning called smouldering combustion.

Smouldering combustion is flameless and occurs when the oxygen reacts directly on the surface of the char, while the volatiles escape. The process is controlled by the transport of oxygen to the reaction zone through the porous char.

A fire can transform between these modes under certain conditions. For wood, both modes of combustion are generally not self-sustaining. The flaming or smouldering does not provide sufficient heat back to the material to continue thermal degradation. An externally applied heat flux is required to sustain combustion. Absence of this heat flux would result in self-extinguishment because heat losses overcome the heat generated. Furthermore, considering the role of oxygen, a forced oxygen supply due to airflow can influence whether or not combustion is sustained.

Model of self-extinguishment

4.1 Introduction

This chapter presents a model of self-extinguishment of cross-laminated timber, based on literature, fundamentals of fire dynamics, and existing experiment data. The following question is answered:

What model describes the process of self-extinguishment of cross-laminated timber?

This chapter first presents the theory on which the model is based, followed by the actual model. Subsequently, hypotheses are formulated that will be investigated in two series of experiments.

4.2 First indication of self-extinguishment

McGregor (2012) conducted five tests on CLT rooms in protected and unprotected configurations and subjected to propane and furniture fires. In these tests indications were present that self-extinguishment might occur under certain conditions.

In two tests with unprotected CLT, the CLT quickly became involved in flaming combustion and contributed significantly to the fire. In the test with a propane fire, the CLT contribution was observed to diminish when the propane fire decayed. The CLT changed from flaming to smouldering and the heat release rate dropped. The CLT did not delaminate and the smouldering faded until the experiment was stopped and the CLT was extinguished with water. However, in the test with a furniture fire the CLT delaminated and pieces fell off; this exposed new layers of wood. The fire did not transform to smouldering, but flaming was sustained. The test was extinguished with water.

Three other tests were conducted with gypsum protected CLT. In two tests with a furniture fire the CLT did not become involved in the fire. However, in the test with a propane fire, the gypsum failed locally and the CLT burned. It contributed significantly to the fire, but was observed to decay along with the propane. The CLT entered a phase of smouldering and the heat release rate dropped. However, the CLT delaminated and was transformed back to flaming. The test was extinguished with water.

These observations suggest that the contribution of exposed CLT to the fire, in terms of the heat release rate, is most significant during flaming combustion. Furthermore, the CLT can be expected to decay along with the “initial” propane or furniture fire. When delamination did not occur, the CLT transformed from flaming to smouldering combustion. This smouldering faded, which could indicate self-extinguishment. However, self-extinguishment was not observed because the tests were terminated. In the tests where

delamination did occur, the fire was observed to remain in flaming combustion or transform back to it. This suggests that if a potential for self-extinguishment exists, it will likely be reached when the CLT does not delaminate and the fire can enter a smoulder phase.

4.3 The influence of delamination

Considering the influence of delamination on the burning behaviour of CLT, research by Frangi *et al.* (2009) provides important considerations. Reference is made to the work in appendix B. The burning behaviour was found dependent on the performance of the adhesive. Loss of bonding under elevated temperatures resulted in delamination. If the delaminated layer falls off, the next uncharred layer is exposed, resulting in a sudden increase of the burning and charring rate.

It was found that CLT with melamine urea formaldehyde (MUF) adhesive does not delaminate in an unfavourable horizontal configuration with standard fire exposure from below. However, MUF is not a common adhesive for CLT in Europe due to health consideration with regards to formaldehyde emission. The most common alternative is polyurethane (PU). This adhesive was found prone to delamination in this unfavourable configuration. Fall-off occurred after a layer was completely charred, i.e. when the 300 °C isotherm (a measure for the charring front) reached the adhesive.

The influence of the lamella thickness on the burning behaviour was also investigated. It was found that less lamella but greater thickness decreases the amount of layers that can delaminate, while increasing the time before it occurs. As a result, the frequency of delamination is reduced.

These observations suggest that PU-based CLT is prone to delamination and can fall-off in a horizontal configuration with exposure from below. Fall-off in a vertical orientation might be less likely, but was not investigated. When this is combined with the observations of McGregor, it seems that self-extinguishment might be difficult to achieve for PU-based CLT. However, an increased lamella thickness results in more time before delamination. It seems reasonable to assume that by applying an increased thickness, the fire can transform from flaming to smouldering to self-extinguishment within the thickness of a single lamella.

4.4 Smouldering under an externally applied heat flux and airflow

The experiments by McGregor suggest that if a potential for self-extinguishment exists, it will be when the CLT transforms from flaming to smouldering, and subsequently extinguishes. Ohlemiller (1988, 1991, 2002) investigated smouldering wood and found that wood does not smoulder along its surface unless supplemented by a radiant flux of $\sim 10 \text{ kW/m}^2$. Furthermore, the smoulder process is controlled by the diffusion of oxygen to the reaction zone, not as much by the oxygen available in the ambient air. As a result a forced oxygen supply due to an imposed airflow over the surface increased smouldering.

Beyler *et al.* (2006) and Swann *et al.* (2008) also conducted research on smouldering. They found that a radiative flux of $\sim 8 \text{ kW/m}^2$ was required for the onset of glowing at the surface of plywood. Glowing was not sustained in absence of the flux.

The results of Ohlemiller, Beyler, and Swann suggest that an externally applied flux is required to sustain smouldering on the surface of wood. It can be expected that absence of this flux results in extinguishment.

Furthermore, it can be assumed that smouldering is more like to be sustained with a forced oxygen supply. While these observations were done for smouldering on and along the surface, it seems reasonable to assume similar relations are valid for smouldering inward into the wood, which would be relevant for self-extinguishment in a compartment fire.

The idea that wood is not able to self-sustain combustion is supported by the experience that a thick slab of wood will not burn in flaming combustion unless supported by heat from another source. Tewarson and Pion (1976) observed that the heat transfer from the flame to the wood is theoretically just sufficient to match the heat losses. Results obtained by Petrella (1980) indicate that losses even are slightly higher.

It seems an externally applied heat flux would be required to sustain smouldering. In a real compartment fire, this heat flux would be provided by mutual cross-radiation, depending on the amount, geometry, and orientation between the CLT surfaces and other hot objects or flames. If this flux drops below a certain threshold value, the CLT can be expected to transform from smouldering to self-extinguishment.

This scenario seems feasible; once the initial fire due to burning of the compartment contents has decayed, the heat release rate and temperatures can be expected to drop. The CLT transforms to smouldering combustion, and - assuming delamination does not interfere and airflow conditions are favourable - the relative low temperatures in the compartment might result in a sufficiently low heat flux on the CLT.

4.5 The route to self-extinguishment

Based on the review above, a model can be formulated that describes the route to self-extinguishment. The model is based on a set of assumptions and can be depicted in a flowchart, as shown in figures 5.1 to 5.4.

- In a compartment fire, an exposed CLT structure will become involved in flaming combustion along with the initial fire due to burning of the compartment contents.
- In a compartment burnout, the initial fire will decay at a certain moment. This results in a decrease of the CLT contribution as well, and the transformation from flaming to smouldering.
- If a potential for self-extinguishment is present, it is when it follows smouldering combustion.
- Smouldering inward in to the CLT must seize for self-extinguishment to occur.

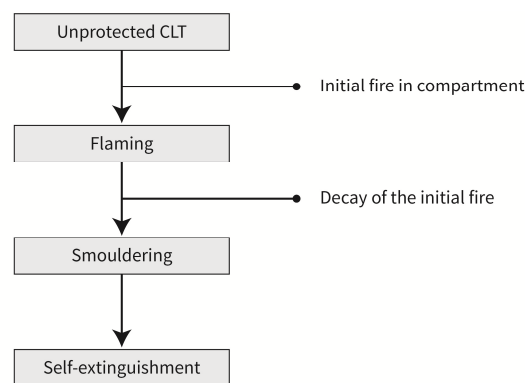


Figure 5.1 The involvement of the CLT in flaming combustion and the transformation from flaming to smouldering take place under influence of an initial fire in the compartment.

To make the transition from smouldering to self-extinguishment, two conditions need to be satisfied regarding the heat flux on the CLT and the air flow over the CLT surface.

- Smouldering combustion ceases at a sufficiently low externally applied flux on the CLT.
- Air flow over the CLT surface might sustain inward smouldering combustion. The air flow needs to be “favourable” for self-extinguishment to occur.

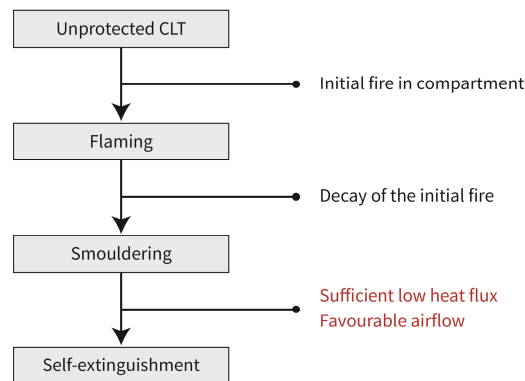


Figure 5.2 Two conditions need to be satisfied to make the transition from smouldering to self-extinguishment; a sufficiently low heat flux and a favourable airflow.

If these conditions are not satisfied, the fire will remain in smouldering combustion. Furthermore, delamination and fall-off can interfere in the transitions from flaming to smouldering and from smouldering to self-extinguishment.

- Delamination and fall-off of the CLT can interfere in the process by sustaining flaming combustion or transforming smouldering combustion back to flaming.
- If flaming combustion is sustained due to delamination and fall-off, or if smouldering is sustained due to a too high heat flux and/or an unfavourable airflow, the CLT will not reach a potential to self-extinguish; the CLT will continue burning.

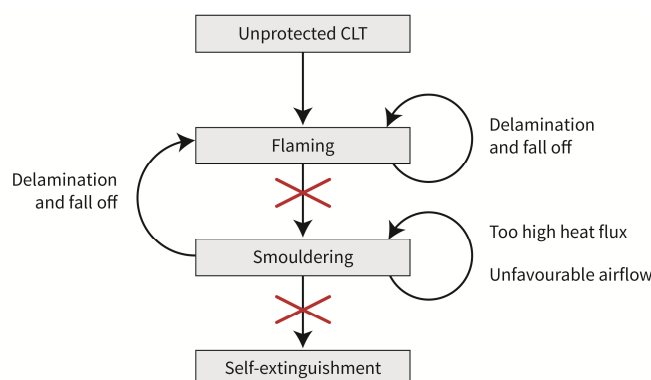


Figure 5.3 Too high heat flux, unfavourable airflow, and delamination and fall-off can interfere in the transitions from flaming to smouldering and from smouldering to self-extinguishment.

It was suggested that sufficiently thick lamellas can delay delamination and assist in self-extinguishment.

- Delamination and fall-off can be prevented for a period of time if the lamella is sufficiently thick.
- As a result, it can be prevented long enough for the transformations from flaming to smouldering and from smouldering to self-extinguishment to occur within the thickness of a single lamella.

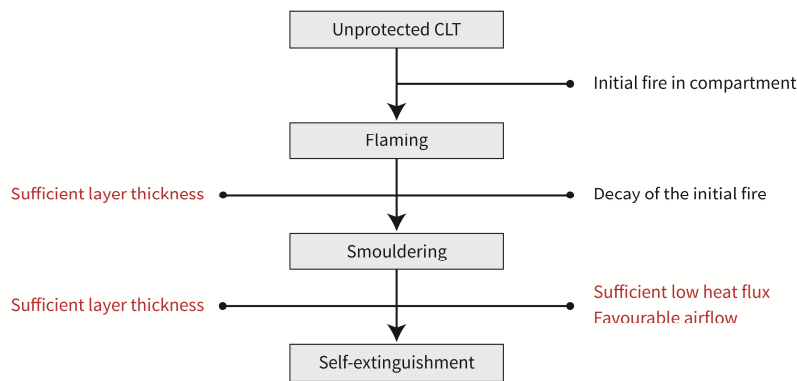


Figure 5.4 The route to self-extinguishment. A sufficient layer thickness could ensure that delamination does not interfere in the transitions.

Charring is implicitly incorporated in the model, as it occurs during flaming and smouldering. As explained in chapter 2, charring is central to the design of exposed timber in fire. The model investigates whether charring will stop or continue to reduce the cross-section until structural failure is imminent. Furthermore, the charring rate is important in determining whether delamination will occur.

4.6 Hypotheses for the experiments

Based on the model, two hypotheses are formulated that will be investigated in two series of experiments. These hypotheses investigate the marked areas of the model, as shown in figure 5.5.

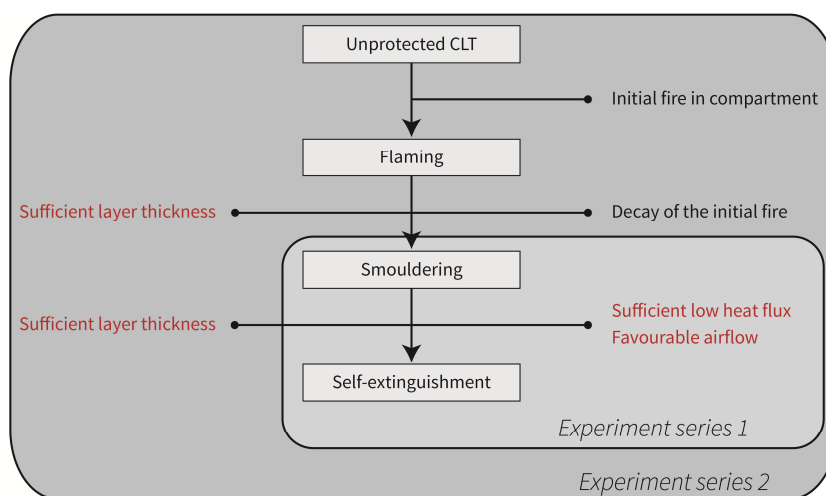


Figure 5.5 Two series of experiments investigate different portions of the model of self-extinguishment.

The first series of experiments investigates and quantifies the heat flux and air flow conditions under which the transition from smouldering to self-extinguishment can take place.

Hypothesis 1

“Small scale cross-laminated timber samples, exposed to a heat flux representative of a compartment fire, will transform from smouldering combustion to self-extinguishment at a sufficiently low externally applied flux and at a favourable airflow over the surface.”

The second series investigates the complete route to self-extinguishment, from an initial fire, to flaming combustion of the CLT, to smouldering combustion, to self-extinguishment. In this complete process the influence of delamination and fall-off and their relation to the layer thickness are investigated as well.

Hypothesis 2

“Medium-scale cross-laminated timber compartments exposed to a compartment fire will become involved in flaming combustion, transform from flaming to smouldering combustion upon decay of the initial fire, and subsequently self-extinguish; if a sufficiently low externally applied heat flux, favourable airflow, and sufficient layer thickness are present.”

4.7 Conclusions

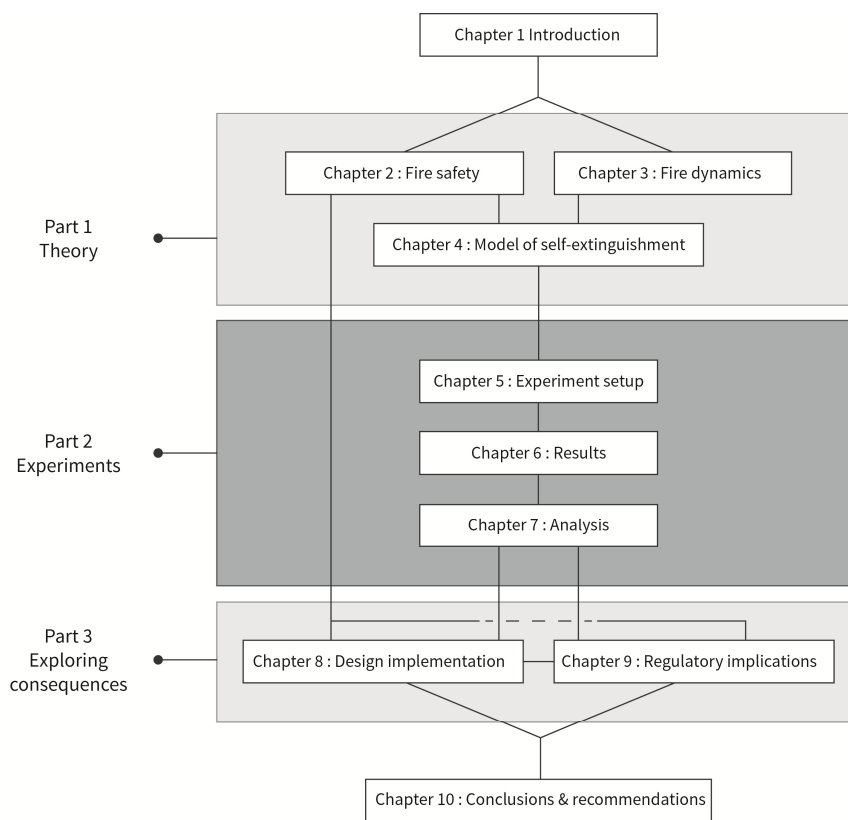
This chapter presented a model of self-extinguishment of cross-laminated timber, based on literature, the fundamental of fire dynamics, and existing experimental data.

Under influence of an “initial” fire due to burning of compartment contents, an exposed CLT structure can be expected to become involved in flaming combustion. In a compartment burnout scenario, the initial fire will decay at a certain moment, resulting in a decrease of the CLT contribution as well, and its transformation from flaming to smouldering combustion.

Subsequently, the CLT can transform from smouldering to self-extinguishment if a sufficiently low heat flux is present and if the airflow over the surface is favourable. However, delamination and fall-off can interfere in these transitions by sustaining flaming or transforming smouldering back to flaming. As a result, the CLT might not self-extinguish. Delamination might be prevented if the lamellas are sufficiently thick. As a result, the charring front does not reach the PU-adhesive layer and the transformations might occur within the thickness of the first lamella.

Based on this model two hypotheses were formulated for two series of experiments. The first series of experiments investigates and quantifies the conditions of heat flux and airflow under which the transition from smouldering combustion to self-extinguishment can take place. The second series investigates the complete route to self-extinguishment, including the influence of delamination and fall-off.

Part 2: Experiments



“To poke a wood fire is more solid enjoyment than almost anything else in the world.”

- Charles Dudley Warner

5.1 Introduction

This chapter presents the setup of two series of experiments that investigate self-extinguishment of cross-laminated timber. Two research questions are answered:

What series of experiments quantifies the conditions under which self-extinguishment of cross-laminated timber can occur?

What series of experiments investigates the complete process self-extinguishment of cross-laminated timber?

The experiments are based on the model of self-extinguishment; and each experiment investigates a hypothesis associated with this model, as presented in part 1 of this work.

For each series of experiments, an approach is formulated first. This is followed by discussion of the equipment, sample preparation, and experiment procedure. Furthermore an overview of all experiments is given and some predictions of the results are presented.

5.2 Setup of experiment series 1

This paragraph describes the setup of the first series of experiments.

5.2.1 Approach

The model of self-extinguishment suggests that in order for self-extinguishment to occur, the fire must first transform from flaming to smouldering combustion, and then extinguish. The heat flux and air flow conditions at which the transformation from smouldering to self-extinguishment takes place are investigated in this first series of experiments.

The chosen approach is to subject small samples of CLT to a two-step heat flux, as depicted in figure 5.1. This two-step exposure represents the exposure the unprotected CLT will receive in a room fire when no delamination occurs, based on the results of McGregor (2012).

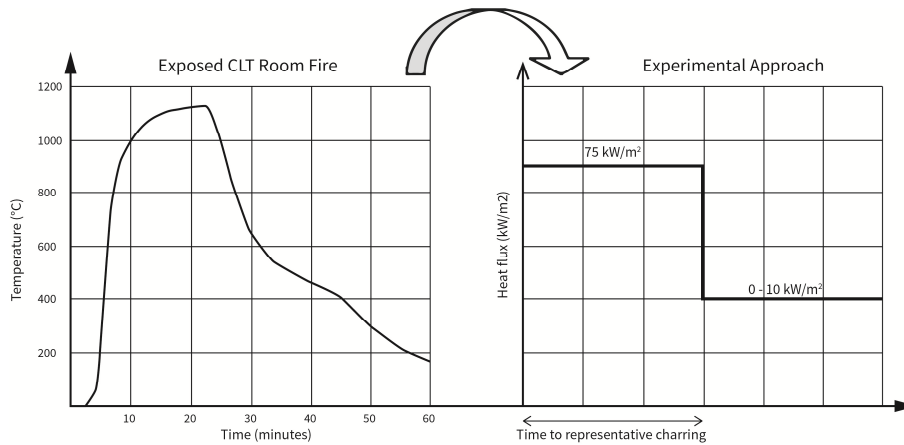


Figure 5.1 Temperature development of an exposed CLT room fire without delamination based on McGregor (2012) (left) translated into a two-step small scale experiment approach (right).

The first heat flux exposure of 75 kW/m^2 will simulate the effect of the fully developed fire on the CLT⁶. Flaming combustion of the CLT is expected to occur and the samples will char. Furthermore, the samples are expected to release a significant amount of heat that would contribute to the total heat release in a real fire.

When the samples have been charring to a representative degree, they are exposed to a second flux of 10 kW/m^2 or lower⁷. This step to a second lower flux simulates the decay of the fire of the room contents, i.e. the burning of the initial fire load excluding the CLT. It is expected the CLT will transform from flaming to smouldering combustion after lowering the flux.

The second lower heat flux will then simulate the effect of cross-radiation between hot surfaces and the smouldering CLT. The samples are expected to self-extinguish when the applied heat flux drops below a certain value. This level of externally applied flux is an important condition in the model of self-extinguishment and is the main variable which this first series of experiments aims to quantify. Another important condition is expected to be the airflow over the sample surface. Therefore, in some experiments, an additional air flow will be forced over the samples during smouldering. However, this variable will be investigated to a limited degree only.

This first series of experiments does not investigate the influence of possible delamination of the CLT, but focuses on the heat flux and air flow conditions required to make the transformation from smouldering combustion to self-extinguishment. The use of a PU-based adhesive in the experiments will make the samples prone to delamination, but on the other hand will greatly enhance the applicability of the results. To avoid the possible disturbing influence of delamination, a favourable horizontal configuration with exposure from above is used. This configuration avoids fall-off of layers. However, it is important to be aware of the limitations this configuration brings to the first series of experiments.

⁶ A heat flux exposure 75 kW/m^2 corresponds to the flux emitted by a charred surface with emissivity of 0,8 and a temperature of approximately $860 \text{ }^\circ\text{C}$, based on formulas by Drysdale (2012).

⁷ A heat flux exposure 10 kW/m^2 corresponds to the flux emitted by a charred surface with emissivity of 0,8 and a temperature of approximately $410 \text{ }^\circ\text{C}$, based on formulas by Drysdale (2012).

5.2.2 Equipment

The equipment consists of a cone calorimeter, a separate cone with a scale, thermocouples, and some auxiliary equipment. The complete setup is depicted in figure 5.2.

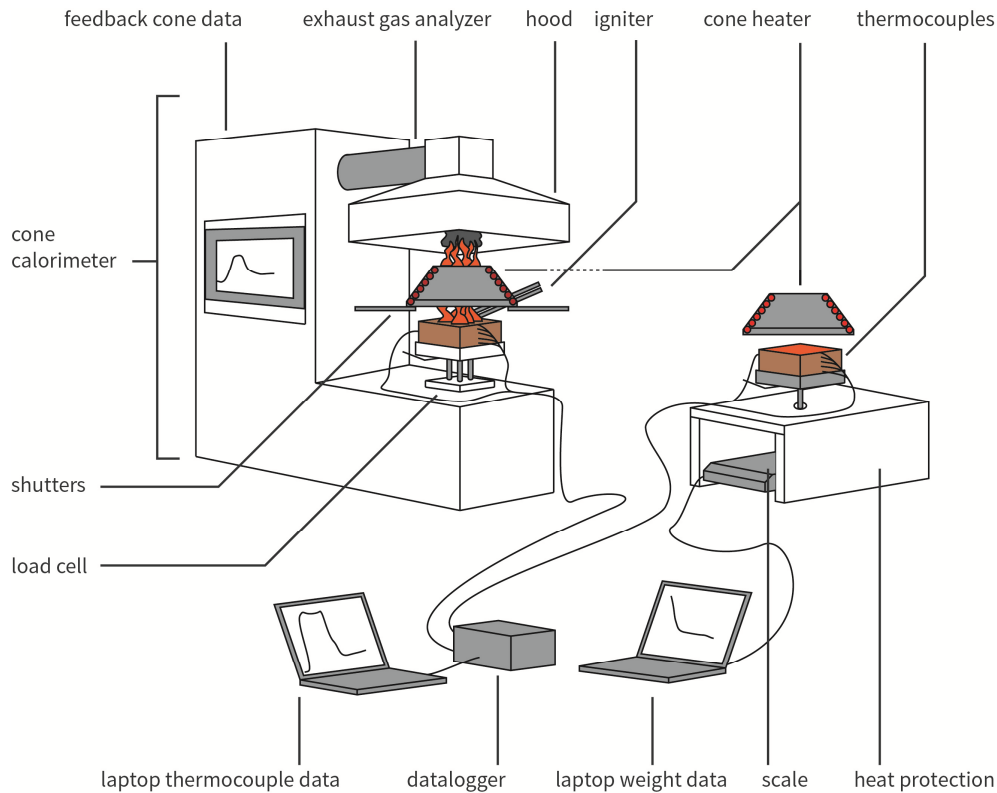


Figure 5.2 The complete setup for the first series of experiments; the cone calorimeter for the first exposure (left) and the separate cone heater with scale for the second exposure (right).

Cone calorimeter

A cone calorimeter is well-suited for the investigation of CLT samples under an externally applied flux. The cone calorimeter is a radiant ignition apparatus, originally developed as a test for measuring the heat release rate of small-scale samples exposed to a uniform heat flux (Babrauskas, 2002). Nowadays, the cone is the most common apparatus for measuring the radiant ignitability of materials. It is also used for the investigation of material properties, such as the mass loss rate, heat release rate, and smoke and toxic gas production.

At the Efectis test facility an ISO 5660-1 certified cone calorimeter is present⁸. This specific cone calorimeter is an “industrial” version of the original apparatus, i.e. much of the calibration and processing is performed by a computer and results are shown in real time.

In the apparatus, samples are tested in room air conditions. A radiant heater can impose up to 100 kW/m^2 upon the face of a rectangular specimen of 100 mm by 100 mm. Samples are up to 50 mm thick and oriented horizontally to prevent disintegration under the influence of gravity. Before the experiment starts,

⁸ The ISO 5660-1 standard specifies a method for assessing the HRR of a specimen using the cone calorimeter.

samples are protected by shutters. Piloted ignition is established by means of an automatic igniter that creates sparks.

During a test, the sample mass and the mass loss rate are measured by a load cell. Exhausted gasses are gathered and analysed and the heat release rate is determined using the oxygen consumption method. Furthermore, the effective heat of combustion is determined, based on the mass loss rate and the heat release rate.

Cone heater and scale

A single cone calorimeter would not be able to accommodate a fast switch from a high heat flux to a low heat flux, as required by the experimental approach. Another cone heater is required for this second flux in the two-step exposure.

A separate cone heater is available at the Efectis test facility. However, just a cone heater does not provide mass and heat release measurements. Instead, the samples can be placed on a separate scale. This setup allows for measurements of the sample weight during the second exposure. This data can be used to obtain the mass loss rate, which can indicate self-extinguishment during the second exposure.

Thermocouples

Thermocouples are installed at various depths in the samples to provide temperature data. A thermocouple consists of two wires made from different metals. The wires are welded together at one end where the temperature is measured. When this end experiences a change in temperature, a voltage is created, which is translated to a temperature.

The experiment will be carried out with type K mantle thermocouples of 1 mm diameter⁹. The temperature can give an indication, in addition to the mass loss rate, on whether a sample has self-extinguished. Furthermore, the temperature data can be used to determine the location the 300 °C isotherm, which is a measure for the location of the charring front.

Auxiliary equipment

Next to the main equipment, the experiments require some auxiliary equipment. A data logger and laptop with measuring software is connected to the thermocouples for acquiring temperature data. Another laptop with measuring software is connected to the scale for acquiring weight data. A heat flux sensor is used to calibrate the separate cone, while the industrial cone includes its own heat flux sensor and other calibration devices.

Furthermore, some experiments require an additional air flow over the samples. A domestic fan was found suitable for imposing this required airflow. The imposed air speed will be measured beforehand with a portable airspeed measuring device.

⁹ Type K thermocouples have a Nickel-Chromium/Nickel-Alumel wire pair. This is a common type of thermocouple. A steel mantle is added to protect the wires and is isolated from the wires with magnesia powder.

5.2.3 Samples

The samples are cut from CLT elements, build-up out of 5 layers / lamellas, and each 20 mm thick. Adjacent layers are orientated cross-wise and are bonded by a PU-based adhesive. Samples are cut to cone calorimeter sample size: 100 x 100 mm, and 50 mm thick. As a result, each sample is 2,5 lamellas thick, as can be seen in figure 5.3. More information on the CLT used for these experiments can be found in appendix A.

The samples are conditioned to the EN 13238 standard at a relative humidity of 50 % and a temperature of 23 °C¹⁰. Samples are conditioned approximately 2 weeks. After that period a constant mass is achieved, indicating the samples are sufficiently conditioned.

After conditioning, 1,6 mm diameter canals are drilled from the sides of the samples at a distance of 10, 20, 30 and 40 mm from the top surface to accommodate thermocouples. This distribution allows for an indication of the temperatures through the sample profile. To improve accuracy and to account for a possible asymmetric charring front, two thermocouples are installed at each depth. In total, 8 canals are drilled per sample. The canals are 33 mm deep to reduce the influence of edge effects. Figure 5.4 indicates the location of the thermocouples in a CLT sample. Note that two couples are installed at the surface, in line with the rows inside the samples.

After drilling the canals, the samples are weighed and the edges wrapped in aluminium foil to reduce the effect of sideward heating. Finally, the thermocouples are fitted through the foil into the canals. Attention was paid to ensure that the tip made contact with the end of the canal.

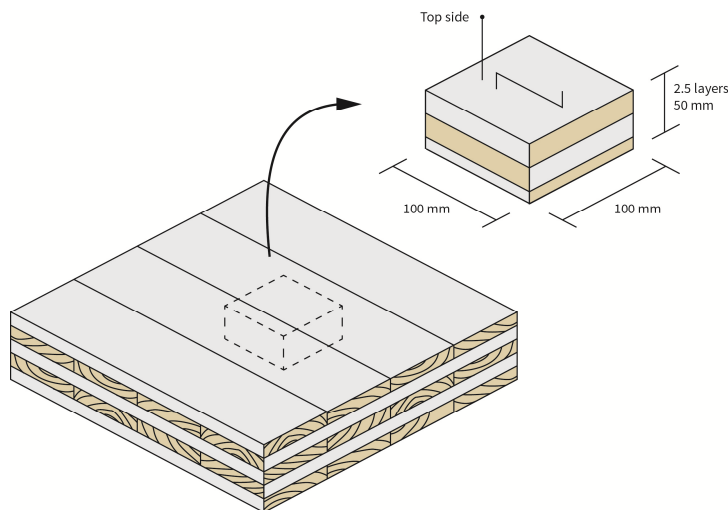


Figure 5.3 The samples are cut from CLT elements to cone calorimeter sizes. As a result, sample are 2.5 layers thick

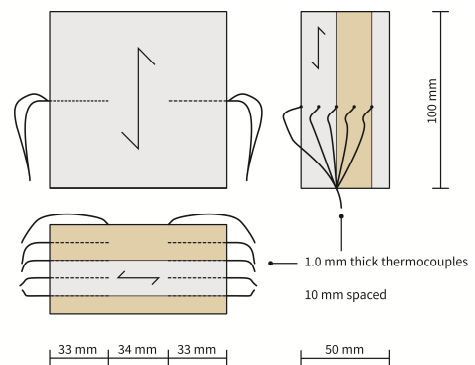


Figure 5.4 Thermocouples are embedded from two sides.

¹⁰ The EN 13238 standard (Reaction to fire tests for building products - Conditioning procedures and general rules for selection of substrates) describes the condition procedures for tests specimens which will be tested according to the European standards for reaction to fire.

5.2.4 procedure

The procedure presented in table 5.1 is followed in each individual experiment. Various devices gather measurements during these steps. These “direct” measurements are shown in the final column.

Table 5.1 Procedure and output of the first series experiments

Step	Description	Direct measurements
1	At the start of an experiment, the cone calorimeter and the separate cone are calibrated with heat flux sensors located 25 mm from the bottom of the heaters. Calibration of the exhaust gas analyser is done by the cone computer. In the experiments with an additional airflow, an air speed measurement device was used to calibrate the air speed at the location of the specimen.	-
2	A CLT sample is placed on the cone calorimeter load cell with the top surface 25 mm below the cone heater. At the start of the experiment the shutters open, exposing the sample to a 75 kW/m ² heat flux. The automatic igniter provides piloted ignition. The cone calorimeter measures the sample mass and analyses the exhaust gases and smoke. The thermocouples gather temperature data.	Cone calorimeter - the sample weight in [g] - mass loss rate in [g/s] - concentrations of exhaust gases
3	After a certain time 20 mm of the CLT will be charred. A char layer of 20 mm is assumed to represent a steady thickness that can be expected to develop in a fully developed fire, while leaving sufficient material uncharred in the specimen to disregard disturbances and edge effects.	Thermocouples - temperatures at 10 locations in the sample, in [°C]
4	When both thermocouples at 20 mm depth exceed 300 °C the charring front is considered to have penetrated this depth. The sample is removed from the cone calorimeter and placed on the scale under the separate cone. This switch takes 10 to 20 seconds, but yields a break in the experiment nevertheless.	-
5	The sample is then exposed to the second heat flux between 0 and 10 kW/m ² . In some experiments an additional airflow is led over the sample surface. The cone calorimeter measurements are stopped, but the separate scale starts measuring the sample weight. The thermocouples continue to gather data.	Separate scale - the sample weight in [g] Thermocouples
6	The experiment is stopped if the sample is considered to be extinguished or burned through. The following criteria are used to determine if these conditions are achieved: Extinguished: the sample is considered to be extinguished when the 300 °C isotherm no longer propagates through the CLT and when the thermocouple temperatures are all near or below 200 °C. The latter indicates no volatiles are produced and no wood is decomposed into char. Another indication is the seizing of mass loss, i.e. a stabilizing mass and a zero mass loss rate. Burned through: the sample is considered to be burned through if the 300 °C isotherm has reached both thermocouples at 40 mm depth. At that moment there is only 10 mm of uncharred CLT left. Any further testing is no longer representative. Another indication is the continuation of mass loss, i.e. a mass which does not stabilize at a certain value and a non-zero mass loss rate.	- temperatures at 10 locations in the sample, in [°C]
7	Once an experiment is done, data from various devices is post-processed in order to make it presentable and suitable for discussion. These 3 data sets (cone data, thermocouple data, and scale data) need to be combined as a post-processing step. Combining of the sets is achieved by making use of 3 “events” that occur during the experiments and that are reflected in these data sets. Appendix C provides additional information.	-

Next to the direct measurements, the cone calorimeter provides indirect measurements: the heat release rate, derived from the oxygen consumption calculation, in kW/m², and the effective heat of combustion, derived from the heat release and mass loss rate, in kJ/kg.

5.2.5 Overview of experiments

An overview of all experiments that were performed is provided in table 5.2.

Table 5.2 Overview of the first series experiments

Experiment	Initial flux[kW/m ²]	Second flux [kW/m ²]	Remark
1	75	0	-
2	75	0	-
3	75	5	-
4	75	5	-
5	75	10	-
6	75	10	-
7	75	8	-
8	75	8	-
9	75	6	-
10	75	6	-
11	75	6	Additional air flow (0,5 m/s) during second exposure
12	75	6	Additional air flow (1,0 m/s) during second exposure
13	75	75	Samples are not switched
14	75	75	Samples are not switched
15	75	75	Samples are not switched / No thermocouples
16	75	75	Samples are not switched / No thermocouples

Experiments 1 to 10 aim to quantify the threshold value at which self-extinguishment takes places. Each level of second flux is tested twice to increase confidence in the results.

Experiments 11 and 12 investigate the possible influence of an additional air flow over the smouldering CLT surface during the second exposure.

Experiments 13 to 16 involve complete burning of the CLT, i.e. there is no second flux, but the 75 kW/m² exposure is continued. These experiments were conducted to investigate the performance of the CLT samples at a constant high heat flux. Furthermore, in experiments 15 and 16 the thermocouples are omitted to investigate their possible influence on the results.

5.2.6 Predictions

Several predictions were made for the first series of experiments, which were checked with the results.

Self-extinguishment

Based on the theory discussed in part 1, and the existing data that was reviewed, it can be expected self-extinguishment occurs at a heat flux below 8–10 kW/m². Furthermore, it can be expected that the air flow over the samples will be of influence, but no quantitative predictions were made.

Delamination

Delamination is expected to occur the moment the 300 °C isotherm reaches the PU glue layer. However, delamination is not expected to result in fall-off, due to the horizontal orientation of the samples.

Charring rate

The Eurocode 1995-1-2 charring rate for solid timber with a characteristic density of ≥ 290 kg/m³ would be appropriate for CLT slabs, not affected by fall-off due to delamination (Frangi *et al.*2009). A charring rate of 0,65 mm/min can be expected. However, this rate is determined in a standard fire exposure. Considering the setup of these experiments, a higher charring rate is expected early due to the absence of the protective char layer, but possibly lower at the end due to rising temperatures in a standard fire.

An alternative method, based on the imposed radiant flux, is provided by Butler (1971) in equation 5.1. This formula cannot be applied for a radiant heat flux < 8 kW/m². Predictions are given in table 5.3.

$$R_w = 2,2 \times 10^{-2} I \quad (\text{Eq. 5.1})$$

Where R_w = charring rate (mm/min)
 I = imposed radiant heat flux (kW/m²)

Table 5.3 Charring rate predictions based on Butler (1971).

Radiant heat flux [kW/m ²]	75	0	5	6	8	10
charring rate [mm/min]	1,65	-	-	-	0,18	0,22

Effective heat of combustion

The effective heat of combustion for timber according to Eurocode 1991-1-2 is 17,5 MJ/kg.

Temperature profiles

Temperature profiles inside the CLT specimen were predicted using a finite difference method and Eurocode wood properties at elevated temperatures. The prediction is added in appendix D.

5.3 Setup of experiment series 2

This paragraph describes the setup of the second series of experiments.

5.3.1 Approach

This second series of experiments investigates the complete model of self-extinguishment, as discussed in chapter 4. The route from flaming of the exposed CLT due to the initial fire, to smouldering combustion, to potential extinguishment is simulated, also taking into account the influence of delamination.

The chosen approach is to subject square compartments with 0,5 x 0,5 x 0,5 m internal dimensions, partially made from CLT and with a single opening, to a simple design fire with a constant HRR of 41 kW and a decay phase. The design fire simulates the burning of an initial fire load in a compartment, excluding the contribution of the CLT. More information regarding this design fire is provided in appendix E.

It is expected the CLT will become involved in flaming combustion. When the samples are charred to a representative degree of 20 mm, the initial fire will be stopped. This represents the depletion of the initial fire load. It is expected the CLT will then either transform from flaming combustion to smouldering combustion, or remain in flaming combustion as a result of delamination and fall-off.

If the fire transform from flaming to smouldering combustion, the CLT is expected to either transform back to flaming combustion as a result of delamination and fall-off, continue smouldering if heat flux and air flow conditions are unfavourable, or extinguish if those condition are favourable. This approach is depicted in figure 5.5.

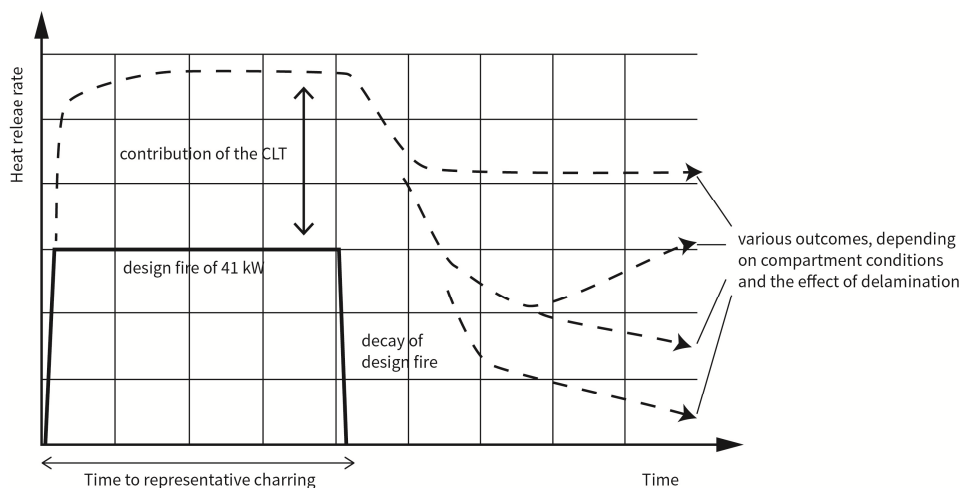


Figure 5.5 A design fire inside the CLT compartments will involve the CLT in flaming combustions. After decay of this initial fire, depending on the conditions in the compartment and the influence of delamination, the compartments can extinguish or continue burning.

The heat flux condition in the compartment is provided by mutual cross-radiation between CLT surfaces and other hot objects or flames. Its severity will depend on the temperatures, amount, geometry, and orientation of smouldering surfaces and other hot surfaces.

To create various heat fluxes in the different experiments, the amount of exposed CLT will vary. More exposed CLT, opposed to non-combustible surfaces, is expected to result in a higher degree of cross-radiation. This is one of the variables in this series of experiments.

A second condition is the airflow over the sample surface. In this second series of experiments, no additional airflow will be present. The burning will occur with only buoyancy due to the fire itself.

In the approach it is recognized that delamination and fall-off can interfere in the transitions from flaming to smouldering and from smouldering to self-extinguishment. In the compartments the CLT is applied in a vertical orientation. In this orientation fall-off can occur if the PU-based CLT delaminates. The influence of delamination on the transitions in the model of self-extinguishment is another condition investigated in this second series of experiments.

In chapter 4 it suggested that the use of sufficient lamella thickness might assist in achieving self-extinguishment, despite the fact that the PU-based CLT is prone to delamination. In that case, self-extinguishment might be achieved within the thickness of a single lamella. Therefore, the lamella thickness will be increased in one of the experiments to investigate this idea.

5.3.2 Equipment

The equipment for the experiments consists of a burner bed with propane supply and mass flow controller, oxygen consumption calorimeter, thermocouples and heat flux sensor, and some auxiliary equipment. The complete setup for the experiments is depicted in figure 5.6.

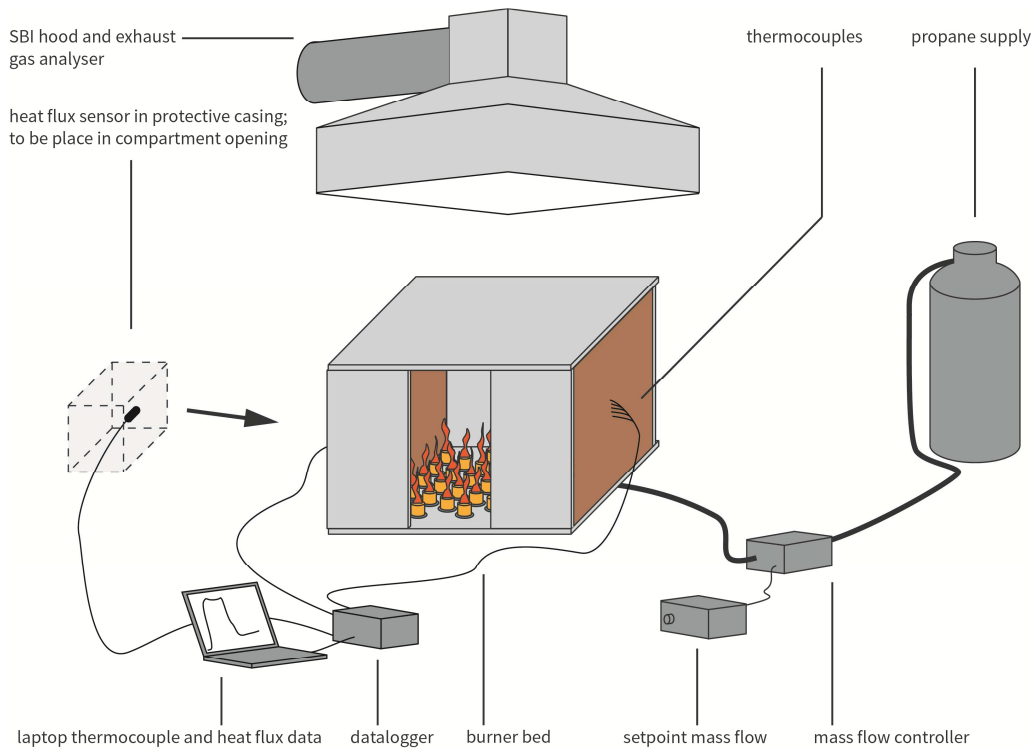


Figure 5.6 The complete setup for the second series of experiments

Burner bed with propane supply and mass flow controller

The design fire is created with a burner bed of 7 rows of 5 power burners, each with a 26 kW maximum capacity. These burners form a 40 cm by 40 cm square and are mounted in a steel frame. The compartment is placed on top of this frame in such a way that the burners are level with the compartment floor. This requires perforation of the floor corresponding to the burner pattern. The burners are fuelled with a 70 kg propane bottle. A mass flow controller is connected to the supply to control the flow at a particular range of flow rates. The mass flow controller can be given a set point from 0 to 100% of its full scale range. Before the experiments, the desired HRR of the design fire was correlated to a flow rate.

Oxygen consumption calorimeter

In order to evaluate the severity of the fire and determine if the fire self-extinguished, the heat release rate needs to be determined. At the Efectis test facility an oxygen consumption calorimeter is present as part of a NEN-EN 13823 certified SBI test setup¹¹. The SBI test normally simulates a single burning item in a corner of a room. However, only the oxygen consumption calorimeter is used for these experiments. The compartments are placed underneath the hood for gas extraction and analysis.

Thermocouples

Similar to the first series of experiments, thermocouples are installed at various depths in the CLT walls of the samples to provide temperature data. The experiment will be carried out with type K mantle thermocouples of 1,6 mm diameter. The temperatures can give an indication, in addition to the heat release rate, whether the samples have self-extinguished. Furthermore, this data can be used to determine the location of the 300 °C isotherm, a measure for the location of the charring front. In addition, 2 couples are installed in the middle of the compartment at 40 and 20 cm height, to obtain room temperatures.

Heat flux sensor

A heat flux sensor is placed in the middle of the ventilation opening to obtain a measurement of the heat flux. As a result, no obstructive devices need to be placed in front of the CLT walls. However, in this way the heat flux on the walls is not measured directly. Alternatively, estimation will be made of the heat flux on the walls, based on the heat flux measured in the opening and the configuration factors inside the compartment, as part of the analysis.

Auxiliary equipment

Next to the main equipment, some auxiliary equipment was used. A data logger and laptop with measuring software is connected to the thermocouples and the heat flux sensor for acquiring temperature and heat flux data. Furthermore, a propane torch is used for ignition of the burner bed. The compartments are weighted on a scale both before and after testing.

¹¹ NEN-EN 13823:2010+A1 specifies a method of test for determining the reaction to fire performance of construction products excluding floorings when exposed to thermal attack by a single burning item (SBI).

5.3.3 Samples

The samples in this series of experiments are small square compartments with 0,5 x 0,5 x 0,5 m internal dimensions. The compartments are partially made from CLT and have a single opening. The single opening was 0,18 m wide, and 0,5 m high, resulting in an opening factor of 0,042 m^{1/2}, corresponding to those of other experiments performed on CLT compartments, such as those by McGregor (2012), but also Hakkaraine (2002).

The compartments vary in the amount of exposed CLT. The CLT is the same as in the first series of experiments and is build up out of 5 cross-wise oriented and PU bonded layers/lamella, each 20 mm thick. An exception was one experiment in which similar CLT was used, but with an increased thickness of the top layer lamella (40 mm instead of 20 mm). More information on the CLT can be found in the appendix A. Non-CLT surfaces were constructed from a 20 mm thick non-combustible plate material¹².

In each compartment, the floor, the ceiling, and the front side with the opening were made from the non-combustible plates. The back wall and side walls were either CLT or also non-combustible plate. An overview of all configurations is presented in figure 5.7.

Similar to the first series of experiments, the compartments are conditioned to the EN 13238 standard at a relative humidity of 50 % and a temperature of 23 °C for approximately 2 weeks. After conditioning, 50 mm holes are drilled in the floor to fit the 40 mm diameter burners. These holes align with the configuration of burners.

To accommodate the thermocouples, 2 mm diameter canals are drilled from the cold-side surface to a depth at 20, 30, 40, 50, and 60 mm from the fire-side surface. These 5 canals are closely spaced to provide an indication of the temperatures through the sample profile at a certain location of the CLT. The location of such a “bundle” of thermocouples was typically located in the middle of the CLT wall elements, or in the middle of the corner connecting two CLT walls.

After drilling the canals, the thermocouples are fitted. Attention was paid to ensure the tip of the couples made contact with the end of the drilled channel. The holes were closed off with a non-combustible and fire-resistant glue based on aluminium silicates and sodium silicates. All connections and gaps in the compartments are also sealed with this glue. Finally, the samples are weighed.

¹² PROMATECT-H is a non-combustible material, made from calcium silicates, cement, and aggregates and has a density of approximately 870 kg/m³

5.3.4 Procedure

The procedure in table 5.4 is followed in each individual experiment. Various devices gather measurements during these steps. These “direct” measurements are shown in the final column.

Table 5.4 Procedure and output of the second series experiments

Step	Description	Direct measurements
1	At the start of the experiment the flow of gas was slightly opened and the propane burners were ignited with a torch. The heat flux sensor was placed in the opening of the compartment. The gas flow was increased to the desired flow, resulting in a premeasured heat release rate for the initial fire.	
2	The propane fire in the compartment burns and the CLT will become in flaming combustion as well, contributing to the total fire.	
3	After a certain time 20 mm of the CLT will be charred. A char layer of 20 mm is assumed to represent a steady thickness that can be expected to develop in a fully developed fire, while leaving sufficient material uncharred in the specimen to disregard disturbances and edge effects.	SBI oxygen consumption calorimeter
4	When all thermocouples at 20 mm depth exceed 300 °C the charring front is considered to have penetrated this depth. Subsequently, the propane flow is reduced to 0 % and the initial fire decays.	- concentrations of exhaust gases, for oxygen consumption calculation
5	Without the initial fire, depending on the conditions in the compartment, the CLT will remain in flaming combustion, transform to smouldering combustion, or transform first to smouldering combustion but back again to flaming combustion.	Thermocouples - temperatures at various depths in the sample, and at two locations in the room, in [°C]
6	The experiment is stopped if the sample is considered to be extinguished or burned through. The following criteria are used to determine if these conditions are achieved: Extinguished: the CLT walls are considered to be extinguished when the 300 °C isotherm no longer propagates and when the thermocouple temperatures are all near or below 200 °C, i.e. no volatiles are produced and no wood is decomposed into char. Another indication is the heat release rate, which should be, or be near, 0 kW when the CLT has extinguished. Burned through: the sample is considered to be burned through if the 300 °C isotherm has reached all thermocouples at 60 mm from the fire-side surface. At that moment the charring front has already progressed 60 % of the CLT; more than half of the structural section is consumed and structure failure can be expected. Another indication is the heat release rate, which remain positive when the CLT continues to burn.	Heat flux sensor - the sample weight in [g]
7	Once an experiment is done, data from various devices is post-processed in order to make it presentable and suitable for discussion. These 2 data sets (SBI oxygen consumption calorimeter and thermocouple data) need to be combined as a post-processing step. Both data sets are started at the same time, so combining these is relatively easy.	

Next to the direct measurements, the SBI provides an indirect measurement: the heat release rate, derived from the oxygen consumption calculation.

5.3.5 Overview of experiments

An overview of the experiments is provided in table 5.5.

Table 5.5 Overview of the second series experiments

Experiment	CLT elements	Remark
1	Back wall	-
2	Back wall and both side walls	-
3	Both side walls	-
4	Both side walls	Repetition of experiment 3
5	Both side walls	Top layer

Experiments 1 to 3 provide configurations with varying degrees of exposed CLT. It was decided that experiment 3 should be repeated in experiment 4, to verify its results. Finally, experiment 5 is also a repetition, but with a thicker lamella in the top layer of the CLT (40 mm instead of 20 mm). Figure 5.7 depicts the various compartment configurations.

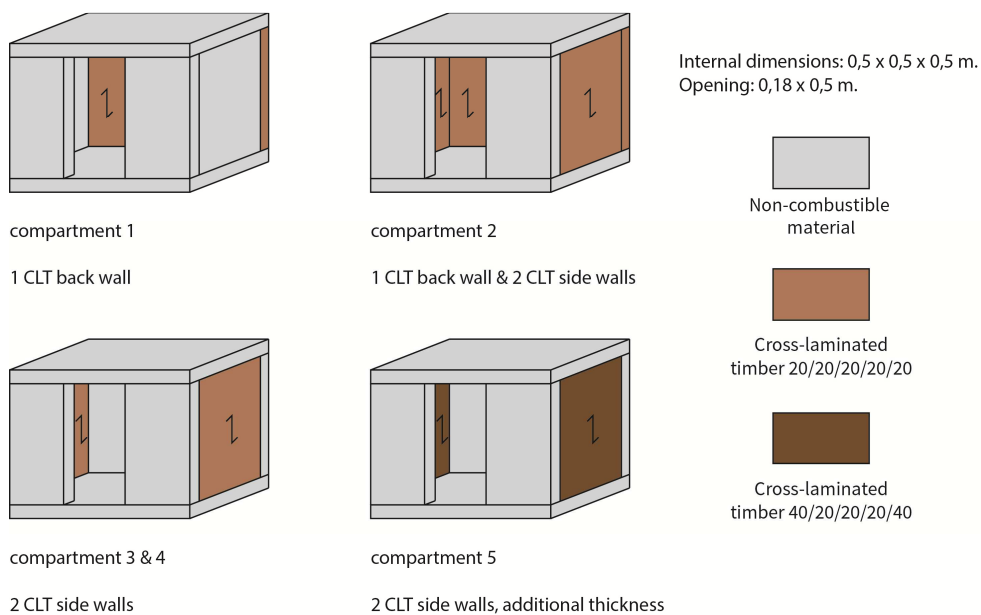


Figure 5.7 Compartment configurations for the second series of experiments.

5.3.6 Predictions

Several predictions were made for the second series of experiments, which were checked with the results.

Self-extinguishment

Assuming the compartments reach a smouldering phase, the heat flux on the CLT can be calculated by making use of equation 5.1. Reference is made to chapter 8, where this formula is discussed in more detail, including how to determine configurations factors.

$$E = \varphi \cdot \varepsilon \cdot \sigma \cdot T^4 \quad (\text{Eq. 5.1})$$

Where	φ	= configuration factor (-)
	ε	= emissivity (-)
	σ	= Stefan-Boltzmann constant ($5,67 \times 10^{-8} \text{ W/m}^2\text{K}^4$)
	T	= temperature (K)

A CLT surface temperature of 400 °C can be used based on the analysis of the results of series 1. The emissivity can be taken as 0,8, as suggested by Eurocode 1995-1-2 for wood surfaces. In reality other hot surfaces would also have to be taken into account, but the calculation here is limited to the contribution of the smouldering CLT walls.

A heat flux of 2,2 kW/m² on the CLT is expected for the compartments with two CLT walls. This is lower than the threshold flux of 5-6 kW/m². These compartments are expected to self-extinguish.

The compartment with one CLT wall is also expected to self-extinguish, because the received heat flux is low; there are no other smouldering CLT walls presents.

The compartment with three CLT walls is also expected to extinguish, because the heat flux on the middle of the back wall would be 3,5 kW/m² and on the side walls 4,0 kW/m². These values are lower than the threshold flux of 5-6 kW/m².

Delamination

Delamination and fall-off might result in the compartment not reaching a smouldering phase. The CLT walls will char 20 mm before the initial fire is stopped. As a result, delamination and fall-off can occur and might influence the fire by sustain flaming combustion or transforming smouldering back to flaming.

Delamination and fall-off might be prevented by the application of a sufficiently thick top lamella. One experiment will be conducted with an increased thickness, and it is expected the CLT will not delaminate.

Charring rate

The Eurocode 1995-1-2 charring rate for solid timber with a characteristic density of $\geq 290 \text{ kg/m}^3$ would be appropriate for the CLT walls. A charring rate of 0,65 mm/min can be expected. However, delamination and fall-off might affect the charring rate (Frangi *et al.*, 2009). Furthermore, the Eurocode charring rate is based on the standard fire and the fire in the compartment will deviate from this fire.

5.4 Conclusions

Based on the theory and the model of self-extinguishment in part 1, two series of experiments were designed. The experiments are performed on CLT samples made with a PU based adhesive.

The first series of experiments investigates the heat flux and air flow conditions at which the CLT can transform from smouldering to self-extinguishment. This is achieved by subjecting CLT samples to a two-step heat flux in a cone calorimeter. The first heat flux exposure of 75 kW/m^2 will simulate the effect of the fully developed fire. After 20 mm charring, the samples are switched to a lower exposure of $\leq 10 \text{ kW/m}^2$. This lower heat flux simulates the effect of cross-radiation in the smoulder phase between hot surfaces and the smouldering CLT.

The samples are expected to self-extinguish when the applied heat flux drops below a certain threshold value. Furthermore an investigation is done to the possible influence of airflow over the sample surface. Temperatures in the CLT, the heat release rate, and the mass are monitored during the experiments.

The second series of experiments investigates the complete route to self-extinguishment, including the possible influence of delamination. This is done by creating an initial propane fire inside small compartments made partially from CLT. Configurations with a varying degree of exposed CLT are investigated. As a result of the initial fire, the CLT will become involved in flaming combustion. The initial fire will be made to decay when the CLT is charred 20 mm. As a result, the CLT is expected to transform from flaming to smouldering combustion.

Subsequently, the transition from smouldering to self-extinguishment can be made, depending on the heat flux and air flow in the compartment. The heat flux depends on the amount of exposed CLT and other hot surfaces and the configuration of the compartment.

Delamination and fall-off can interfere in this process by sustaining flaming combustion or by transforming smouldering back to flaming. As a result, the CLT might not reach a smouldering phase, or potentially self-extinguish. The idea that thicker lamella can assist in achieving self-extinguishment, despite the CLT being prone to delamination, is also investigated. Temperatures in the CLT, the heat release rate, and the heat flux are monitored during the experiments.

6.1 Introduction

This chapter presents the results of the two series of experiments that investigate the self-extinguishment of cross-laminated timber. These results will be further analysed in the next chapter in order to answer the main research question of this research.

6.2 Results of experiment series 1

This paragraph presents the results of the first series of experiments. These experiments took place between 18 June and 10 September 2014.

Considering the amount of experiments and devices that gather data, this series of experiments has resulted in a large amount of output. Presenting all this data would decrease the clarity of this report. Therefore, this paragraph presents only an overview of the results and is limited to representative values and trends. Important deviations are mentioned to avoid omitting any relevant information. Appendix F presents the complete set of results, separately for each experiment.

The results are combined and grouped in 5 categories; visual observations, mass loss, heat release and heat of combustion, temperatures, and charring. Within each category, a distinction is made between the initial exposure of 75 kW/m^2 (similar in each experiment); and the second exposure (varying across the series).

Experiments 13 t/m 17 were different in their approach and had no second exposure. The results of these experiments are presented separately at the end of this paragraph.

6.2.1 Visual observations

This paragraph presents noteworthy visual observations.

Initial exposure of 75 kW/m^2

At the start of the experiments the shutters of the cone calorimeter opened, exposing the samples to a 75 kW/m^2 heat flux. The top surface of the samples discoloured within seconds, turning it black. Gasses were observed leaving the samples.

In each experiment piloted ignition was established within 5 to 10 seconds by the automatic igniter (figure 6.1). Ignition resulted in immediate and fully engulfment of the top surface in flame (figure 6.2). Flaming was intense during the first couple of minutes, but then reduced in intensity, followed by a steady burning (figure 6.3).

Cracks were observed to form on the top surface within 1 minute after ignition. These cracks were located both along the grain and perpendicular to the grain of the top layer, and yielded a typical “alligator” pattern with rectangular patches of char. These cracks grew to several millimetres wide within 3 minutes. Flaming occurred predominantly along these cracks and at the samples edges (figure 6.4).

The thermocouple data indicated when the temperatures at 20 mm depth exceeded 300 °C, i.e. the moment when the samples were to be switched to the separate cone heater. On average the temperatures at 20 mm depth exceeded 300 °C at 1240 seconds (20 minutes 40 seconds), but values ranging from 1150 seconds to 1400 seconds were observed.

Subsequently, the flaming samples were removed from the cone calorimeter and placed on the scale underneath the separate cone heater. The samples were now exposed to the appropriate second heat flux.

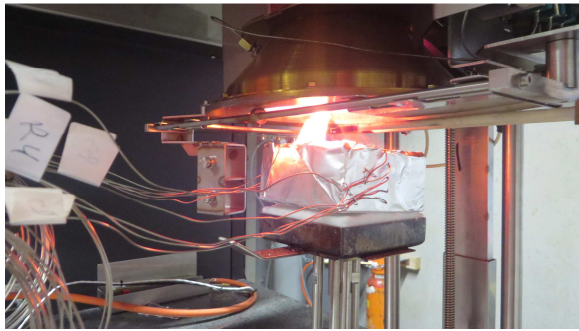


Figure 6.1 Ignition took place under the 75 kW/m² exposure with use of a spark from the cone calorimeter igniter.

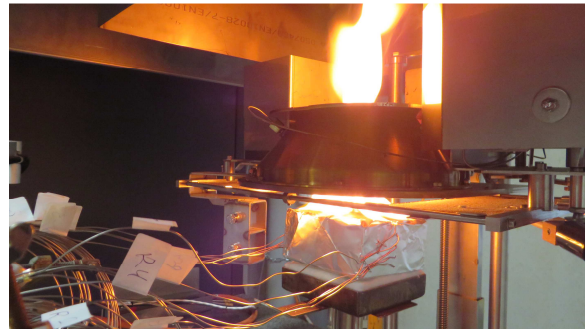


Figure 6.2 Intense flaming took place during the first minutes. The top surface of the sample was fully engulfed in flames.

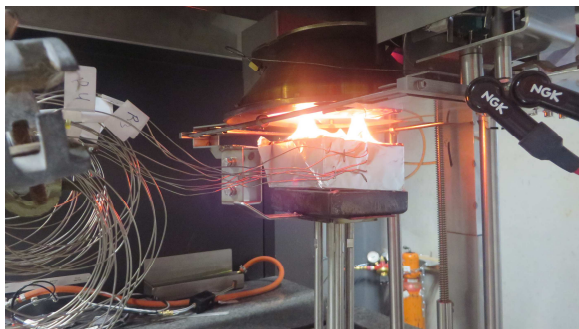


Figure 6.3 The intensity of the flames dropped after a couple of minutes and a more steady burning commenced.



Figure 6.4 Flaming occurred along cracks in the char and along the sample edges. Cracks formed in a typical “alligator” pattern.

Second exposure

After switching the samples to the second exposure, flaming seized within 1 minute in all experiments. The observations for the remainder of the experiments varied.

In experiments 1 and 2 with 0 kW/m² flux, no glowing of the char was observed after flaming seized. No events were observed for the remainder of both experiments. The experiments were stopped at 72 and 79 minutes respectively, because the samples were considered to be extinguished.

In experiments 3 with 5 kW/m² flux no glowing was observed. In experiment 4 however, the char was observed to be glowing. This glowing diminished in intensity and reduced in size to a couple of small spots. 15 minutes after switching glowing was no longer observed. No events were observed for the remainder of both experiments. The experiments were stopped at 89 minutes and 104 minutes respectively, because the samples were considered to be extinguished.

In experiments 5 and 6 with a 10 kW/m² heat flux the char was observed to be glowing after switching⁸. Contrary to previous experiments, glowing was sustained. Glowing diminished in intensity and reduced in size to some patches along a particular wide crack in the char. This crack was located parallel to grain, halfway along the width of the sample. Glowing increased in intensity again 25 minutes after switching and the crack gradually widened into more of cone shape. Glowing was sustained until the experiments were stopped because samples were considered to be burned through. Experiment 5 was stopped at 135 minutes and experiment 6 at 147 minutes.

Glowing was also observed in experiments 7 and 8 with 8 kW/m² flux and occurred predominantly along the cracks in the char. In both experiments glowing diminished in intensity and reduced in size to a couple of patches along a wide crack in the char, similar to the one discussed above. The samples continued glowing at small points in the char along the large crack. The crack gradually widened into more of cone shape. The experiments were stopped at 170 minutes and 162 minutes respectively, because the samples were considered to be burned through.

Glowing was also observed in the experiments 9 and 10 with 6 kW/m² flux. The glowing occurred predominantly along the cracks in the char and sample edges (figure 6.5). Approximately 5 minutes after switching, glowing gradually diminished in intensity to only 1 small area along a large crack. In both experiments, approximately 40 minutes after switching, glowing increased again. This glowing occurred in the middle of the crack (figure 6.6). Glowing decreased in intensity again to only 1 small area near the sample centre 1 hour after switching (figure 6.7). Glowing stopped 2 hours after switching (figure 6.8). No events were observed for the remainder of the experiments and these were stopped because samples were considered to be extinguished. Experiment 9 was stopped at 315 minutes and experiment 10 at 311 minutes.

⁸ In experiment 5, approximately 3 minutes after switching, it was discovered the sample had an increased distance to the cone heater, due to the absence of a sample holder. The sample holder was quickly added, but as a result, it received a heat flux slightly lower than 10 kW/m² for approximately 3 minutes.

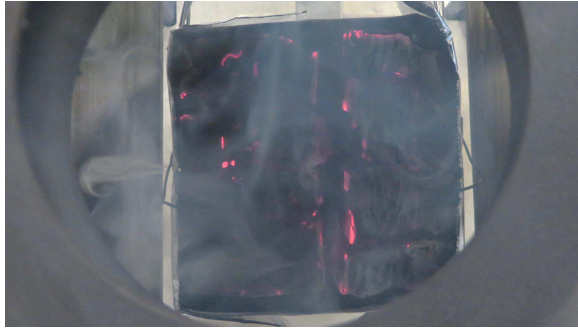


Figure 6.5 Glowing and smoke production at 6 kW/m^2 exposure, just after switching. Glowing occurred predominantly along the cracks and the edges.



Figure 6.6 After an initial decrease, glowing and smoke increased again in a wide central crack, 40 minutes after switching at 6 kW/m^2 exposure.



Figure 6.7 1 hour after switching, glowing reduced to only one area and continued to diminish in intensity at 6 kW/m^2 exposure.



Figure 6.8 2 hours after switching, glowing and smoke production are no longer observed. The sample has extinguished under 6 kW/m^2 exposure.

In experiment 11 with 6 kW/m^2 flux and an additional airflow with speed $0,5 \text{ m/s}$ glowing of the char was also observed. Glowing took place in small points, which were distributed over the complete top surface (figure 6.9). However, glowing diminished in intensity within 5 minutes. Approximately 20 minutes after switching glowing increased along the sample edge from where the air flow was coming. Glowing was quite intense (figure 6.10) but then diminished and seized approximately 50 minutes after switching. No events were observed for the remainder of the experiment and it was stopped at 209 minutes because the sample was considered to be extinguished.

In experiment 12 with 6 kW/m^2 flux and an additional airflow with speed $1,0 \text{ m/s}$ intense glowing of the char was observed after switching (figure 6.11). The intense glowing occurred along all the cracks in the surface and especially along the edge from which the airflow was coming. Glowing did not diminish in intensity and the smouldering was observed to progress rapidly through the sample. Approximately 15 minutes after switching, glowing occurred fairly uniform over the sample surface (figure 6.12). Smouldering continued for the remainder of the experiment, which was stopped at 93 minutes because the sample was considered to be burned through.

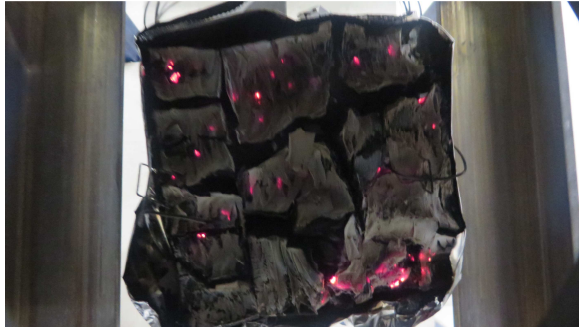


Figure 6.9 1 minute after switching, glowing took place in small points all over the top surface at 6 kW/m² exposure and additional airflow of 0,5 m/s.



Figure 6.10 30 minutes after switching, glowing increased along the sample edge at 6 kW/m² exposure and additional airflow of 0,5 m/s.



Figure 6.11 1 minute after switching, intense glowing and smoke production were observed, at 6 kW/m² exposure and additional airflow of 1,0 m/s.



Figure 6.12 15 minutes after switching, intense glowing occurred fairly uniform over the surface, at 6 kW/m² exposure and additional airflow of 1,0 m/s.

After the experiments, the samples were inspected. The samples in which smouldering / glowing continued for some time after switching, showed an layer of ash on top of the sample (figure 6.13 and 6.14). Furthermore, the cone shaped pattern in which smouldering took place was clearly visible. The samples in which smouldering did not occur, showed only a char layer on top.

Delamination of the CLT was observed in all samples. Delamination occurred typically as the char layer reached the adhesive layer. Figure 6.15 and 6.16 show delamination in experiment 3 with a 0 kW/m² second exposure. In this experiment the char front did not progress much further in the material than 20 mm, because the samples extinguished quickly. This depth coincided with a lamella interface, i.e. the location of a layer of PU adhesive. Delamination did not result in the falling off due to the horizontal orientation of the samples.



Figure 6.13 An ash layer on top of the char is clearly visible after burn-through at a 10 kW/m² exposure.

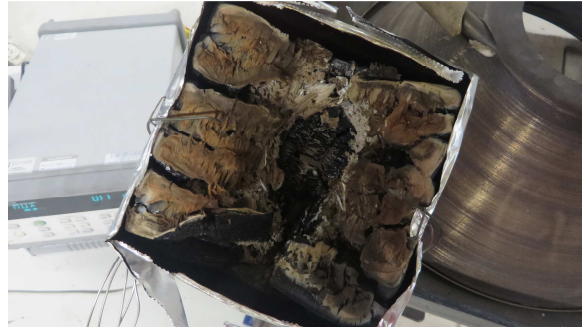


Figure 6.14 An ash layer on top of the char and a cone-shaped pattern are clearly visible after burn-through at an 8 kW/m² exposure.



Figure 6.15 Delamination of the sample in experiment 3 with a 0 kW/m² exposure. Left the delaminated 20 mm thick top layer, right the remaining sample.

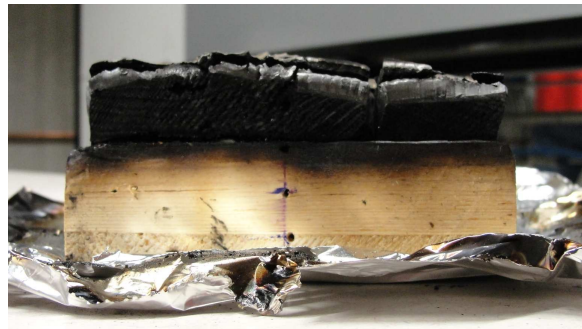


Figure 6.16 The char front has progressed just over 20 mm through the sample in experiment 3 with a 0 kW/m² exposure.

6.2.2 Temperatures

This paragraph presents the results with regards to the temperature in the samples. Unless stated otherwise, the temperatures mentioned in this paragraph are average temperatures at the specified depth. This means the presented values are an average of two thermocouples temperatures at the same depth.

Initial exposure of 75 kW/m²

Similar results were obtained for each experiment during the initial 75 kW/m² heat flux exposure. In each experiment, the average temperature at the surface increased rapidly to approximately 700 – 750 °C, as can be seen in figure 6.17. This rapid increase was typically followed by a more gradually increase to values in the range of 770 – 880 °C, but peak values of over 900 °C were reached by individual thermocouples.

Temperatures in deeper layers also increased upon exposing the sample, although less rapid and typically reaching lower peak values. Significant differences could be observed between temperatures in subsequent layers. This phenomenon indicated a steep temperature gradient as the heat propagated through the material.

Second exposure

The results depended on the level of the second flux and whether an additional air flow was present. Representative temperature developments are shown by the graphs. Figure 6.18 depicts the temperatures in experiment 2 with a 5 kW/m^2 flux.

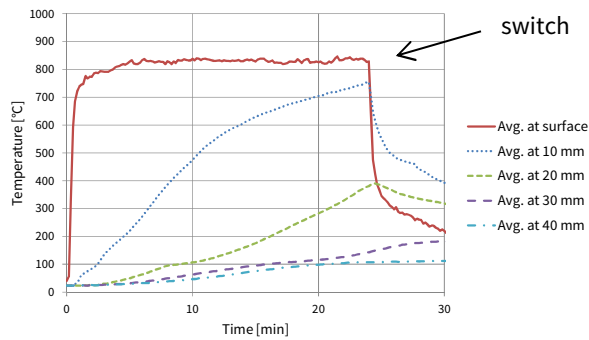


Figure 6.17 Temperatures during the 75 kW/m^2 exposure in experiment 9.

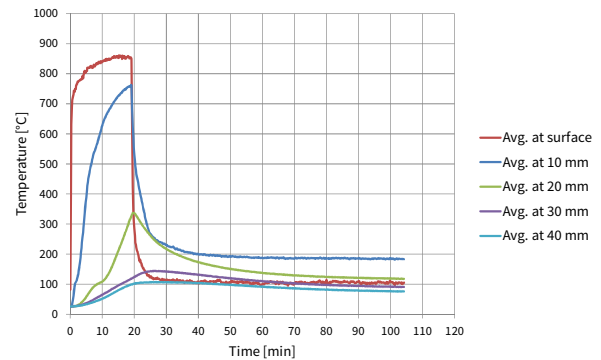


Figure 6.18 Temperatures in experiment 2 during the 75 kW/m^2 and 5 kW/m^2 exposure.

In the experiments with 0 kW/m^2 the temperatures in all layers were found to drop after switching. The surface temperature dropped rapidly and right after removal. Deeper layers dropped less rapidly and after a short of delay. Temperatures of all thermocouples were then observed to converge towards ambient, dropping below 200 °C at approximately 30 minutes from the start of experiments.

The experiments with a 5 kW/m^2 flux showed a similar behaviour, as shown in figure 6.18. The surface temperature dropped rapidly and right after removal, while deeper layers dropped less rapid and after a delay. The thermocouples converged to temperatures in the range of 70 °C to 190 °C . All temperatures dropped below 200 °C at approximately 46 minutes in experiment 3 and at 54 minutes in experiment 4.

Figure 6.19 shows the temperatures in experiment 6 with a 10 kW/m^2 flux. Figure 6.20 shows the temperatures in experiments 8 with an 8 kW/m^2 flux.

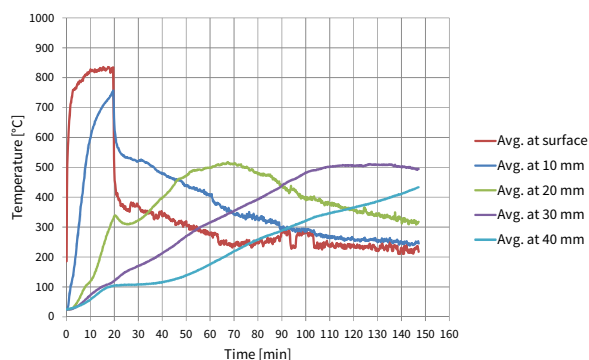


Figure 6.19 Temperatures in experiment 6 during the 75 kW/m^2 and 10 kW/m^2 exposure.

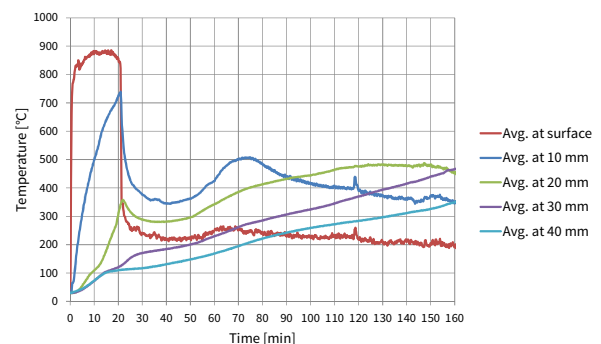


Figure 6.20 Temperatures in experiment 8 during the 75 kW/m^2 and 8 kW/m^2 exposure.

In the experiments with a 10 kW/m^2 exposure the temperatures at the surface, 10 mm, and 20 mm depth, dropped after switching. Surfaces temperature and temperature at 10 mm depth continued to decrease towards $250 \text{ }^\circ\text{C}$, but temperatures at 20 mm depth rose again to approximately $500 \text{ }^\circ\text{C}$ ⁹. After sustaining this temperature for about 15 – 20 minutes temperatures slowly decreased again. When temperature decreased below approximately $400 \text{ }^\circ\text{C}$, they showed an increase in fluctuation, possible because these thermocouples became exposed after the smouldering zones had passed.

Temperatures at 30 and 40 mm depth continued to rise after switching. In both experiments, the temperatures at these depths exceeded $300 \text{ }^\circ\text{C}$ before the experiments were stopped.

The experiments with an 8 kW/m^2 exposure showed a similar behaviour to those with a 10 kW/m^2 exposure, although temperatures increased slower, at a later moment, and reached lower peaks. The temperatures at the surface, 10 mm, and 20 mm depth, dropped after switching. Surfaces temperature continued to decrease towards $200 \text{ }^\circ\text{C}$, but temperatures at 10 mm and 20 mm depth rose again to $450 - 500 \text{ }^\circ\text{C}$. After sustaining these temperatures for up to 30 minutes, they decreased again. When temperature decreased below approximately $400 \text{ }^\circ\text{C}$, they showed an increase in fluctuation.

Temperatures at 30 and 40 mm depth continued to rise after switching. In both experiments, the temperatures at these depths exceeded $300 \text{ }^\circ\text{C}$ before the experiments were stopped.

Figure 6.21 and 6.22 show temperatures in experiment 9 with a 6 kW/m^2 flux and no additional air flow, and in experiment 11 with a 6 kW/m^2 flux and an additional air flow with speed $0,5 \text{ m/s}$, respectively.

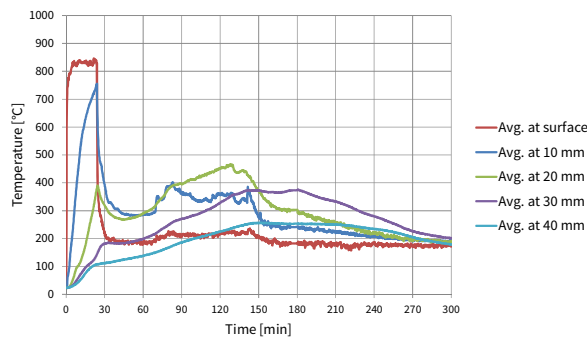


Figure 6.21 Temperatures in experiment 9 during the 75 kW/m^2 and 6 kW/m^2 exposure.

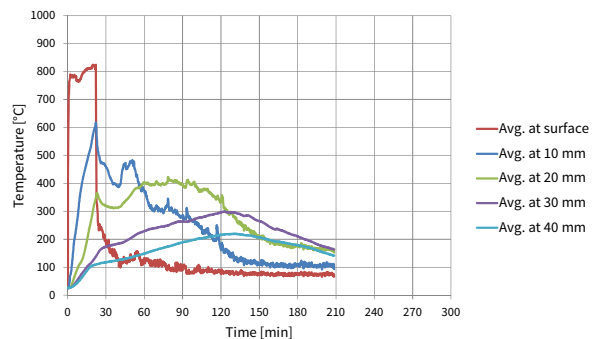


Figure 6.22 Temperatures in experiment 11 during the 75 kW/m^2 and 6 kW/m^2 exposure and an additional airflow with speed $0,5 \text{ m/s}$.

In the experiments with 6 kW/m^2 and no additional air flow, the temperatures at the surface and at 10 and 20 mm depth dropped immediately after switching. Subsequently, in experiment 9, the temperatures at 10 and 20 mm increased again to $350 - 450 \text{ }^\circ\text{C}$. After sustaining these temperatures for 60 – 90 minutes, these temperatures decreased and eventually dropped to below $200 \text{ }^\circ\text{C}$. In test 10, temperatures at these depths were not found to increase temporarily, with the exception of one thermocouple at 20 mm depth.

⁹ Temperatures in experiment 5 rose later, supposable due to absence of the sample holder and the lower flux the first minutes after switching.

Temperatures in deeper layers continued to rise after switching, but subsequently decreased and eventually dropped below 200 °C. In both experiments, the temperature at 40 mm depth never exceeded 300 °C.

Temperatures in experiment 11 with 6 kW/m² and additional air flow with speed 0,5 m/s were similar to those with 6 kW/m² without additional air flow. At various depths temperatures were found to rise, but subsequently drop. However, lower peak values were reached and sustained for a shorter period of time. Furthermore, temperatures did drop towards 200 °C, but 100 °C. The temperatures at 40 mm depth never exceeded 300 °C.

Figure 6.23 shows temperatures in experiment 12 with a 6 kW/m² flux and an air flow of speed 1,0 m/s.

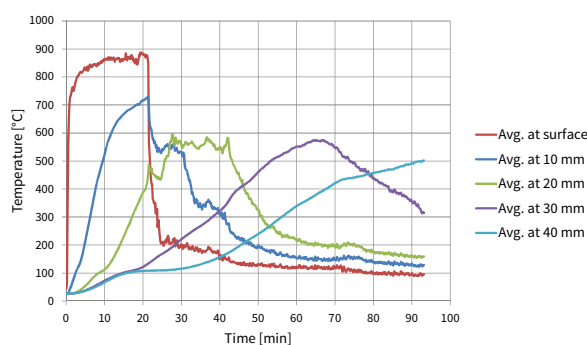


Figure 6.23 Temperatures in experiment 12 during the 75 kW/m² and 6 kW/m² exposure and an additional airflow with speed 1,0 m/s.

In experiment 12 with 6 kW/m² and additional air flow with speed 1,0 m/s temperatures at the surface and at 10 mm depth were found to drop rapidly after switching. At 20 mm, 30 mm and 40 mm depth, temperatures rose relatively fast compared to the other experiments and reached relative high peak values over 500 °C. These peak values were sustained for approximately 20 minutes before they dropped again towards 100 – 150 °C. When temperature decreased below approximately 300 – 400 °C, they showed an increase in fluctuation.

In some experiments a significant difference was observed between the two thermocouples at the same depth, e.g. the two couples at 10 mm depth. Usually, this difference was small, i.e. below 50 °C, but occasionally this difference increased over 100 °C or even to a rare 450 °C.

6.2.3 Mass loss

This paragraph presents the results with regards to the mass loss; expressed in terms of the development of mass as a percentage from the original weight and in terms of the mass loss rate. Expressing the mass loss as a percentage of the original weight allows for a comparison between samples of different mass.

Initial exposure of 75 kW/m²

During the initial exposure of 75 kW/m² heat flux, the samples in all experiments reduced in mass. This mass loss is depicted in figure 6.24 for 6 representative experiments. Figure 6.25 depicts the MLR of a representative experiment during the initial 75 kW/m² heat flux exposure.

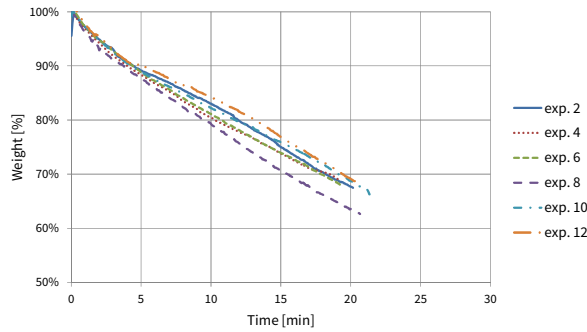


Figure 6.24 Sample weight during the 75 kW/m² exposure in 6 representative experiments, expressed as a percentage from the starting sample weight.

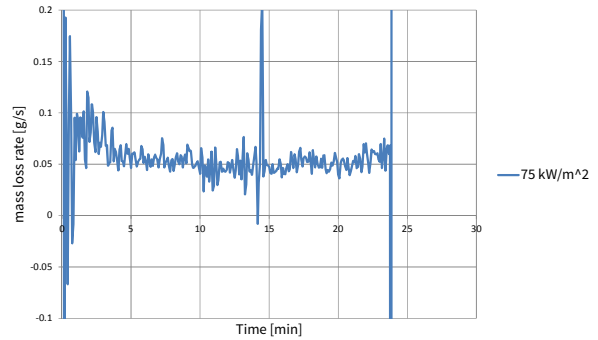


Figure 6.25 Mass loss rate during the 75 kW/m² exposure in experiment 9.

The samples lost mass in a fairly linear way under the 75 kW/m² exposure. However, the mass loss typically appeared to slow down or increase in speed at certain moments during the exposure. To quantify these changes in speed of mass loss, we look at the mass loss rate (MLR).

After some initial fluctuations due to placement of the sample on the cone calorimeter load cell, the mass loss rate was observed to peak early in each experiment at approximately 20 seconds. After this early peak, the mass loss rate showed a decreasing trend. The mass loss rate then stabilized and remained fairly constant between 5 to 19 minutes. A slight increase in MLR was observed in some experiments, just before switching. In most experiments occasional positive or negative spikes were observed.

Values for the peak MLR and average MLR between 5 to 19 minutes are presented in table 6.3.

Table 6.3 Mass loss rate during the 75 kW/m² exposure.

MLR [g/s]	1	2	3	4	5	6	7	8	9	10	11	12	Avg.
Peak value	0,158	0,260	0,153	0,189	0,171	0,182	0,165	0,181	0,193	0,138	0,209	0,214	0,184
Avg. 5-19 min	0,065	0,054	0,051	0,054	0,045	0,054	0,056	0,056	0,052	0,049	0,052	0,057	0,054

On average the peak mass loss rate at 20 seconds was 0,184 g/s, but values ranging from 0,138 to 0,260 g/s were measured. The mass loss rate then fluctuated fairly constant in the period of 5 to 19 minutes around values of 0,045 to 0,065 g/s. On average the mass loss rate was 0,054 g/s during this period.

Second exposure

The mass loss during the second exposure was dependent the level of the second flux and whether an additional air flow was present. The mass loss is depicted in figure 6.26 for 5 representative experiments, and in figure 6.27 for all experiments with a 6 kW/m² exposure, with or without air flow.

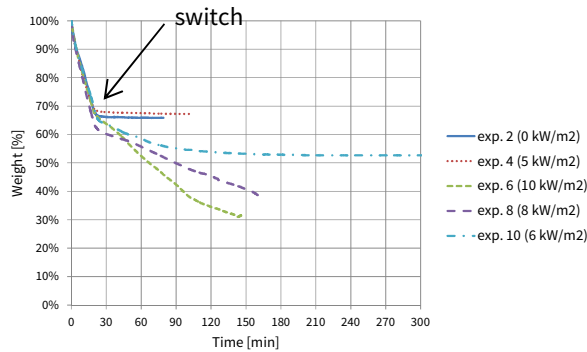


Figure 6.26 Sample weight during the 75 kW/m² and the subsequent lower exposure in 5 representative experiments, expressed as a percentage from the starting sample weight.

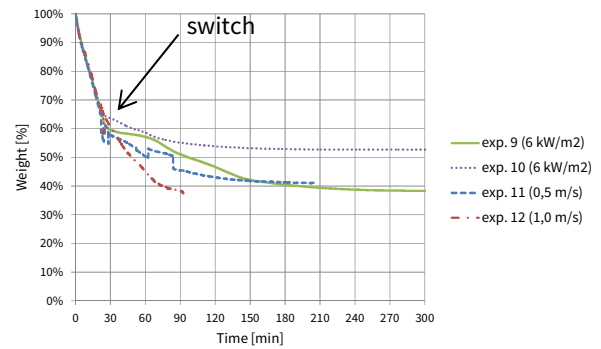


Figure 6.27 Sample weight during the 75 kW/m² and the subsequent 6 kW/m² exposure in experiments 9 to 12, expressed as a percentage from the starting sample weight.

As can be observed from the figures, the samples either continued to lose mass, albeit significantly slower, or converged slowly to a stable value, depending on the level of the second flux and whether an additional air flow was present.

This behaviour was also reflected in the MLR, which either remained positive or converged to 0 g/s.

Examples are given in figures 6.28 and 6.29.

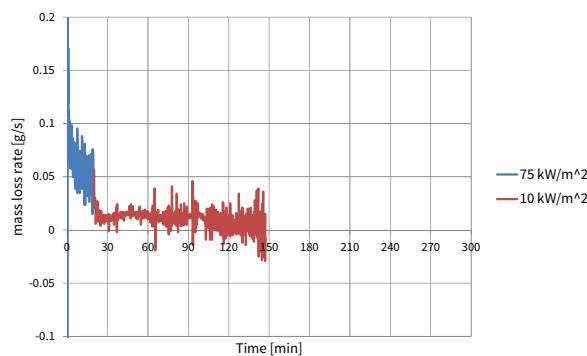


Figure 6.28 Mass loss rate in experiment 6 during the 75 kW/m² and 10 kW/m² exposure.

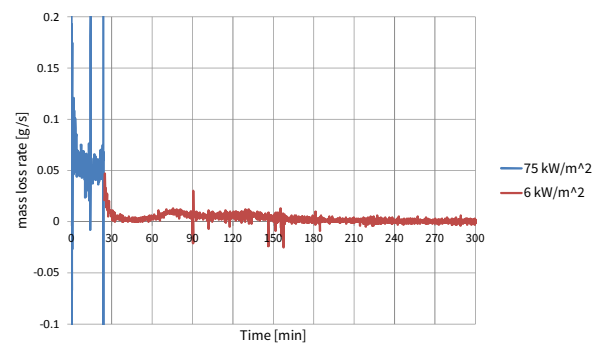


Figure 6.29 Mass loss rate in experiment 9 during the 75 kW/m² and 6 kW/m² exposure.

Values for the average MLR during the second exposure, taken from 25 minutes onwards to exclude the aftermath of the initial exposure of 75 kW/m², are presented in table 6.4. The table also indicates if the MLR converged to 0 g/s.

Table 6.4 Mass loss rate during the various second exposures

MLR [g/s]	0 kW/m ²		5 kW/m ²		10 kW/m ²		8 kW/m ²		6 kW/m ²		6 kW/m ²	
	1	2	3	4	5	6	7	8	9	10	0,5 m/s	1,0 m/s
25+ m	0,000	0,000	0,000	0,000	0,009	0,010	0,006	0,006	0,003	0,002	0,003	0,016
→ 0	yes	yes	yes	yes	no	no	no	no	yes	yes	yes	no

In the experiments with 0 or 5 kW/m² flux, the mass initially continued to decrease after switching the sample to the second setup, but quickly stabilized and remained constant. This was reflected in the MLR, which dropped rapidly, followed by a gradual decline to 0,000 g/s.

In the experiments with 10 kW/m² flux the mass did not stabilize, but continued a slow decline. This was reflected by the MLR which did not converge to 0 g/s, as can be seen in figure 6.28. Instead average MLRs from 25 minutes onwards of 0,009-0,010 g/s were obtained.

The mass in experiments with 8 kW/m² flux also did not stabilize, but continued to decrease. The MLR in both experiments dropped to values of ~ 0,006 g/s, where it remained until the end of the experiments.

The experiments with 6 kW/m² flux initially showed a continuation of mass loss. Both samples decreased in weight with various speeds, occasionally slowing down or losing mass more rapidly. This was reflected in the MLR with values ranging from 0,002 g/s to 0,010 g/s, as can be seen in the figure 6.29. However, in both experiments the mass eventually stabilized and the MLR decreased to 0,000 g/s.

During the experiment with a 6 kW/m² flux and additional air flow with speed 0,5 m/s the sample initially remained losing mass, but then stabilized. The MLR dropped to values around 0,015 g/s but gradually decreased to 0,000 g/s. This stabilization of the mass occurred sooner than in the experiments without an additional airflow.

In the experiment with 6 kW/m² flux and additional air flow with speed 1,0 m/s the mass did not stabilize, but continued to decrease. This was reflected in an average MLR from 25 minutes onwards of 0,016 g/s, i.e. the highest MLR obtained in all second exposures.

The MLR constantly fluctuated with $\pm 0,002$ g/s in the experiments, as be observed in figures 6.28 and 6.29. In some cases, these fluctuations were larger; up to $\pm 0,005$ g/s. The experiments with additional air flow fluctuated even more, up to $\pm 0,050$ g/s, possible due to the disturbing influence of the wind on the sensitive mass loss measurements.

In addition to these fluctuations, in most experiments, some positive and negative “spikes” were observed in the MLR. These spikes occurred typically at the start of the test and at the moment of switching when the samples were removed from the load cell and placed on the scale, as a result, these devices experiment an impulse. Furthermore due to the sensitive nature of the load cell and the scale, some other spikes were observed. These fluctuations and spikes are discussed and explained in more detail in the analysis and in appendix G.

6.2.4 Heat release rate and heat of combustion

This paragraph presents the results with regards to the heat release rate and effective heat of combustion.

Initial exposure of 75 kW/m²

During the initial exposure the samples released heat. Figure 6.30 shows the heat release rate (HRR) for one experiment during the 75 kW/m² exposure. The effective heat of combustion (EHC) was determined during the 75 kW/m² exposure, based on the MLR and HRR. Figure 6.31 depicts the EHC for one of the experiments.

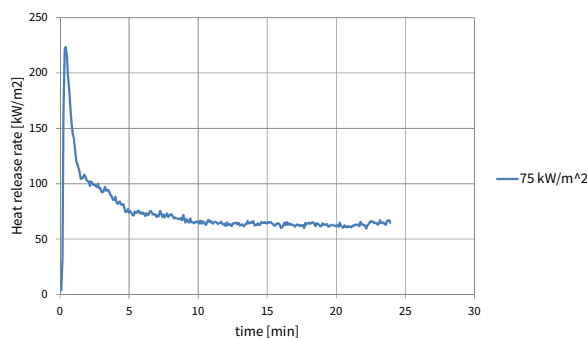


Figure 6.30 Heat release rate in experiment 9 during the 75 kW/m² exposure.

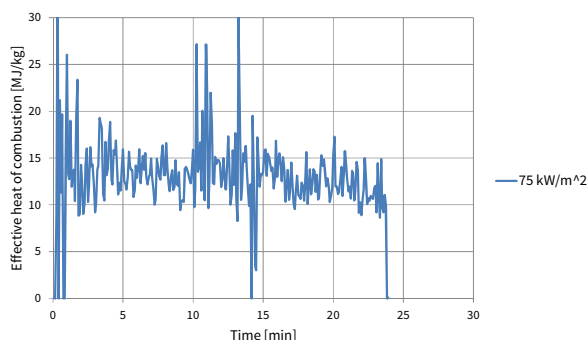


Figure 6.31 Effective heat of combustion in experiment 9 during the 75 kW/m² exposure.

As can be observed from the figure, the HRR increased rapidly once ignition had taken place. A peak was obtained in each test after 10–25 seconds. After this peak, the HRR decreased, stabilized and remained constant between 5–19 minutes. A slight increase was observed in some experiments prior to switching.

Values of the peak heat release rate, the average between 5 to 19 minutes, and average during the total 75 kW/m² exposure, are presented in table 6.5.

Table 6.5 Heat loss rates during the 75 kW/m² exposure.

HRR [kW/m ²]	1	2	3	4	5	6	7	8	9	10	11	12	average
peak	214	232	224	253	202	261	220	235	224	242	275	281	239
Avg. 5-19 m	75	68	66	71	62	76	83	77	66	67	80	83	73
Avg.	81	77	74	80	72	88	89	86	74	77	91	90	82

The initial peak HRR was on average 239 kW/m², with values ranging from 202 – 281 kW/m². The HRR between 5 to 19 minutes was on average 73 kW/m², with values ranging from 66 – 83 kW/m². The HRR over the total 75 kW/m² exposure was on average 82 kW/m², with values ranging from 72 – 91 kW/m².

Average values of the EHC are presented in table 6.6. The standard deviation provides an indication of the degree of fluctuation in each test.

Table 6.6 Effective heat of combustion during the 75 kW/m² exposure.

EHC [MJ/kg]	1	2	3	4	5	6	7	8	9	10	average
Avg.	11,3	13,7	13,8	13,3	15,0	14,4	14,1	16,1	13,0	15,5	14,0
st. dev.	2,5	6,4	5,8	4,7	7,7	4,4	4,7	11,8	4,2	9,5	6,2

The degree of fluctuation was found to vary significantly between experiments. In some cases, the EHC fluctuated between 8 and 18 MJ/kg. Occasionally positive spikes or zeros were present, e.g. in figure 6.31. In extreme cases, such as the experiments with an additional air flow, values ranged from 0 to well over 30 MJ/kg. These fluctuations are discussed in more detail in the analysis and appendix G. Despite the variation in fluctuation, the average EHC ranged from 11,3 to 16,1 MJ/kg; an average of 14,0 MJ/kg.

Second exposure

The HRR was not measured during the second exposure. However, by combining the MLR data of the second exposure with the average EHC of the 75 kW/m² exposure; graphs for the HRR could be obtained. As a result of this method, the HRR followed the behaviour of the MLR during the second exposure; i.e. it remained positive or converged to 0 g/s. Examples are given in figures 6.32 and 6.33.

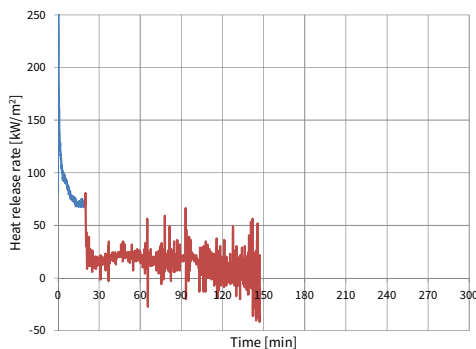


Figure 6.32 Heat release rate during the 75 kW/m² and 10 kW/m² exposure in experiment 6.

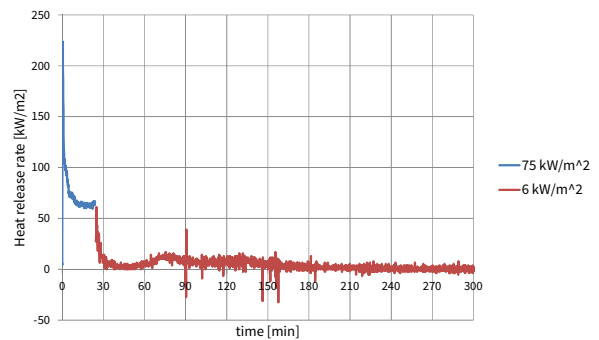


Figure 6.33 Heat release rate during the 75 kW/m² and 6 kW/m² exposure in experiment 9.

Values for the average HRR during the second exposure, taken from 25 minutes onwards to exclude the aftermath of the initial exposure of 75 kW/m², are presented in table 6.7. The table also indicates whether the heat release rate converged to 0 g/s.

Table 6.7 Heat release rates during the various second exposures

HRR [kW/m ²]	0 kW/m ²		5 kW/m ²		10 kW/m ²		8 kW/m ²		6 kW/m ²		6 kW/m ²	
	1	2	3	4	5	6	7	8	9	10	0,5 m/s	1,0 m/s
Avg. 25 + min	0	1	0	1	14	15	9	9	4	2	4	23
→ 0	yes	yes	yes	yes	no	no	no	no	yes	yes	yes	no

In the experiments with 0 or 5 kW/m² exposure the samples seized producing energy quickly. The HRR dropped fast followed by a gradual decline to 0 kW/m². Average HRRs of 0 kW/m² were obtained. In the experiments with 10 or 8 kW/m² flux the samples continued to release energy. The HRR did not decline to 0 kW/m², as can be seen in figure 6.32. Average HRRs om 25 minutes onwards of 15 kW/m² and 9 kW/m² were obtained respectively.

In the experiments with 6 kW/m² flux the samples initially continued to release energy, but then seized. The HRR ranged from 3 to 12 kW/m², but eventually decreased to 0 kW/m², as can be seen in the figure 6.33. This was reflected in low average HRRs, which eventually converged to 0 kW/m². The experiment with 6 kW/m² flux and additional air flow of speed 0,5 m/s showed similar results. The HRR dropped to values around 20 kW/m² and gradually decreased to 0 kW/m². This was reflected in a low average HRR, which converged to 0 kW/m². In the experiment with 6 kW/m² flux and additional air flow of speed 1,0 m/s the sample continued to release energy. An average HRR of 23 kW/m² was found.

Because the HRR graphs of the second exposure are based on the MLR data, the fluctuations and spikes in the MLR can also be found in the HRR. The HRR was observed in most experiments to fluctuate with ± 3 kW/m². In some experiments, fluctuations were larger; up to ± 10 kW/m². The experiments with additional air flow fluctuated heavily; up to ± 100 kW/m². Furthermore, due to the fluctuation in the MLR negative values for the HRR are obtained.

6.2.5 Results experiments 13 to 16 - continuation of the 75 kW/m² exposure

This paragraph presents the results of experiments 13 – 16, which investigate the CLT under a constant 75 kW/m² heat flux exposure, yielding different results from approximately 20 minutes onwards (the focus of this paragraph). Furthermore, experiments 15 and 16 investigate the samples without thermocouples.

Visual observations

Under the 75 kW/m² exposure, the samples continued burning in flaming combustion. At approximately 40 to 50 minutes burning was observed along the sample edges, indicating the sample became completely involved in flaming, instead of just the top side. The top lamella was observed to bow upwards and detached itself from the second lamella (figure 3.34).



Figure 6.34 Bowing upwards of the top charred lamella of the sample in experiment 15.



Figure 3.35 Brown-coloured ash after burning through in experiment 13.

Tests 13 to 16 were stopped at approximately 50 minutes because samples were burned through and because edge effects were increasing showing in the results. The top of the char layer had transformed into a brown-coloured ash (figure 3.35). After the experiments, the samples were observed to have been reduced to only a thin layer of wood and char, covered in a thick layer of ash.

Temperatures and mass loss

Figure 6.36 depicts the temperatures for one experiment. The mass loss is depicted in figure 6.37.

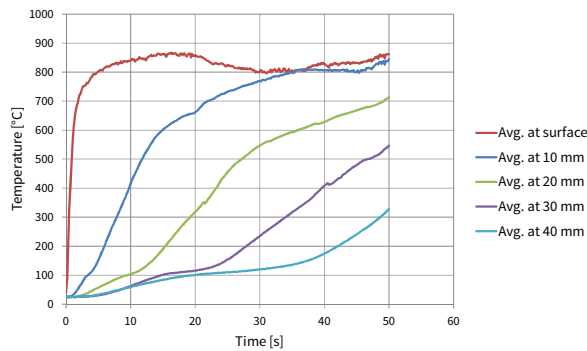


Figure 6.36 Temperatures during the 75 kW/m² exposure in experiment 13.

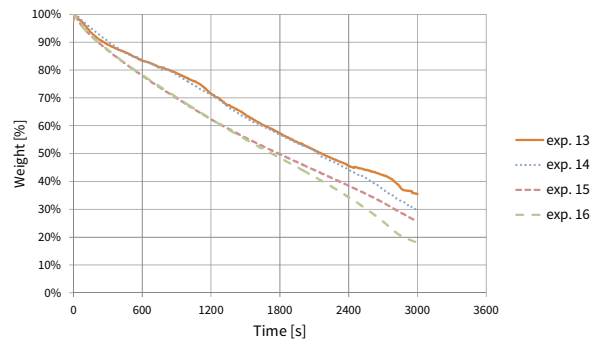


Figure 6.37 Sample weight, expressed as a percentage from the starting sample weight.

The temperatures in all layers continued rising during the 75 kW/m² exposure. The 300 °C isotherm progressed through each layer. The samples remained losing mass in a fairly linear way. However, the samples without thermocouples lost more mass than the samples with thermocouples. This difference was established during the first 5 to 15 minutes of testing. This is discussed in more detail in the analysis and appendix G. Figures 6.38 and 6.39 depict the MLR for an experiment with and without thermocouples.

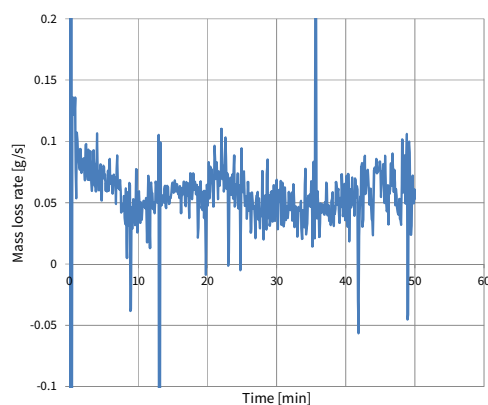


Figure 6.38 Mass loss rate during the 75 kW/m² exposure in experiment 14.

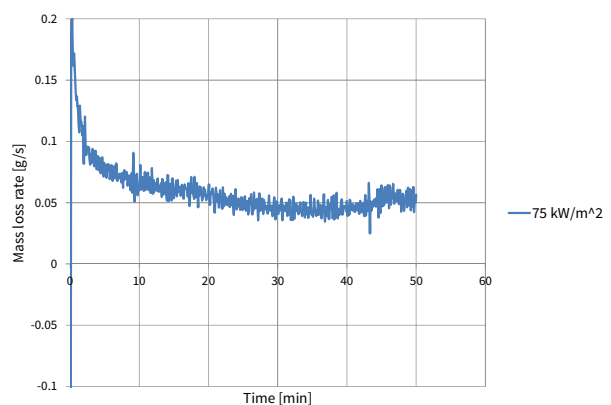


Figure 6.39 Mass loss rate during the 75 kW/m² exposure in experiment 15.

Similar to the experiments 1 to 12, these experiments with constant 75 kW/m² flux showed some initial fluctuations, an early peak, and fairly constant mass loss for the remainder of the experiments. The MLR

typically decreased slightly to values < 0.050 g/s. However, all 4 experiments showed an increase in mass loss rate after 40 minutes. Furthermore, a difference was observed in the amount of fluctuation between the tests with and without thermocouples. This is discussed in more detail in the analysis and appendix G.

Heat release rate and heat of combustion

Figure 6.40 depicts the HRR for an experiment.

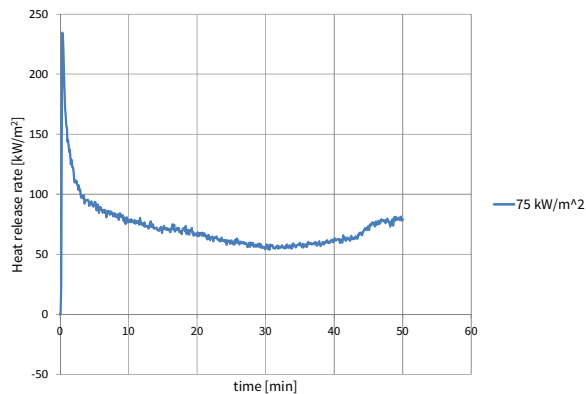


Figure 6.40 Heat release rate in experiment 15 during the 75 kW/m^2 exposure.

The HRR decreased slightly to values typically $< 70 \text{ kW/m}^2$ during continuation of the 75 kW/m^2 exposure. However, all 4 experiments showed an increase in the HRR at approximately 40 minutes testing, which dropped again toward the end of the tests. Figures 6.41 and 6.42 depict the effective heat of combustion for an experiment with and without thermocouples.

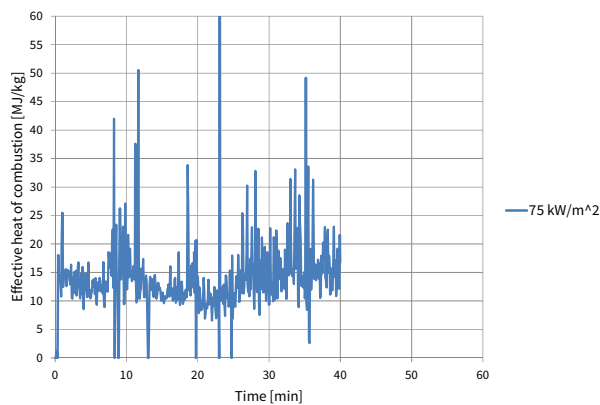


Figure 6.41 Effective heat of combustion in experiment 14 during the 75 kW/m^2 exposure.

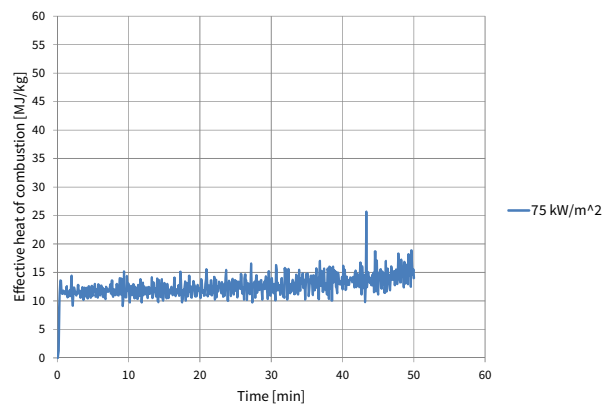


Figure 6.42 Effective heat of combustion in experiment 15 during the 75 kW/m^2 exposure.

A significant difference was observed in the amount of fluctuation between the tests with and without thermocouples. However, average values (18,2; 14,3; 12,6; and 13,47 MJ/kg), were consistent with the range of values found of experiments 1-12. Exception was experiment 13 with a fairly high effective heat of combustion of 18 MJ/kg, but this might be due to a natural variation in the material.

6.3 Results of experiment series 2

This paragraph presents the results of the second series of experiments. These experiments took place between 22 October and 7 November 2014. The results are presented per experiment in 5 categories; visual observations, temperatures, mass loss, heat release, and radiation.

6.3.1 Compartment 1 – CLT back wall

The first experiment was conducted using a compartment with a CLT back wall only.

Visual observations

At the start of the experiment the burners were ignited with a torch (figure 6.43). After ignition of all burners the heat flux sensor was placed in the opening of the compartment. Subsequently, the gas flow was increased to 15 % of maximum capacity, i.e. a HRR of 63 kW (figure 6.44). As a result of the propane fire, the CLT back wall started to discolour and emit gasses. Within 2 minutes the CLT was completely involved in flaming combustion. Flaming was observed outside the compartment (figure 6.45).



Figure 6.43 At the start of the experiment, all propane burners were ignited with a torch. The burner bed HRR was increased to 63 kW.



Figure 6.44 After ignition of the burners, the heat flux sensor and its protective encasing were placed inside the opening. The CLT discoloured.

After 12 minutes, the decision was made to reduce the flow rate of propane to 10 % of maximum capacity, i.e. 41 kW. At this level most combustion was contained within the compartment (figure 6.46). At 41 minutes, the thermocouple data indicated the temperatures at 20 mm depth exceeded 300 °C. The propane flow was reduced to 0 %.

The intensity of flaming decreased within 1 minute. Initially, flaming was still observed over the charred CLT surface (figure 6.47), but quickly seized after 5 minutes. Subsequently, the char smouldered (figure 6.48). Delaminated pieces of CLT were observed on the floor, as well as some pieces missing in the wall. The smouldering quickly decreased in intensity. At approximately 50 minutes, i.e. 9 minutes after decay of the propane fire, glowing was only observed of the delaminated pieces on the floor and along edges of the areas where CLT had fallen off. At approximately 58 minutes a large piece delaminated but this did not influence the fire. The single spots where smouldering still occurred, kept decreasing in intensity. The experiment was stopped at 85 minutes because the sample was considered to be extinguished.



Figure 6.45 The compartment became completely involved in flaming combustion. External flaming was observed



Figure 6.46 After reduction of the burner bed HRR to 41 kW, flaming was largely contained within the compartment.



Figure 6.47 Once the propane fire was stopped, flaming quickly decreased and could be observed over the charred CLT surfaces.



Figure 6.48 Flaming quickly seized and the char glowed. Glow could be clearly observed along the edges where pieces of CLT had fallen off.



Figure 6.49 Some charred pieces of the first layer are visible, as the charred boards of the second layer.

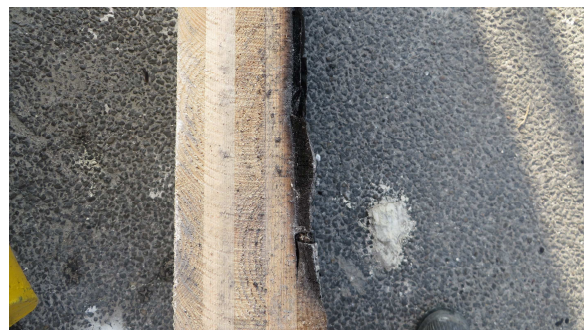


Figure 6.50 Top view of the sample. The char front has progressed through the first layer of CLT and into the second layer.

Inspection of the char showed the char front had progressed through the first layer of 20 mm CLT and several millimetres into the second layer. Several pieces of CLT had fallen off of the first layer. As a result, the boards of the second layer of CLT were visible (figure 6.49 and 6.50). In the figure more CLT has fallen off than during the experiment, due to handling of the samples after testing.

Temperatures

Figure 6.51 shows temperatures in the middle of the compartment. Figure 6.52 depicts the temperatures in the middle of the CLT back wall at certain depths, expressed as the distance from the fire-side surface.

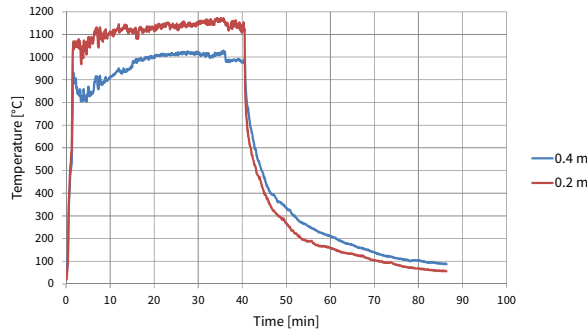


Figure 6.51 Room temperatures in compartment 1

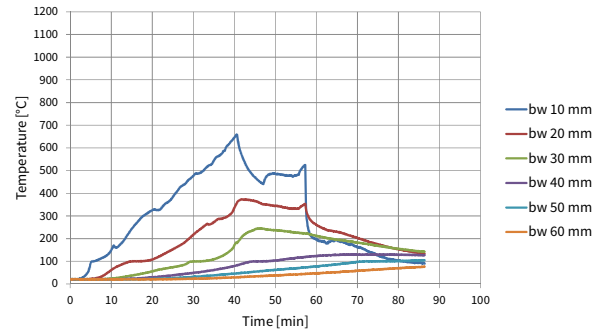


Figure 5.52 CLT temperatures in middle of the back wall

When the propane burners were ignited, room temperatures quickly increased to approximately 900 °C at 0,4 m and 1050 °C at 0,2 m. Room temperatures dropped momentarily, followed by an increase to 1000 °C and 1150 °C respectively over a 20 minute period. Room temperatures stabilized and did not seem affected by the decrease in HRR of the propane fire at 12 minutes.

After decay of the propane fire, room temperatures plummeted. The temperature at 0,2 m was found to drop faster. Within 1 minute, temperatures dropped to 750 °C at 0,4 m and 650 °C at 0,2 m.

Temperatures continue to decrease and dropped below 200 °C at approximately 1 hour.

The temperatures in all layers of the CLT were found to increase after the start of the experiment in a fairly linear way. Temperatures typically stabilized shortly at 100 °C, as energy was used to vaporize the water in the wood. Significant temperature differences could be observed between adjacent layers, indicating a steep temperature gradient as the heat propagated through the material. At 41 minutes, the thermocouple data indicated the temperatures at 20 mm depth exceeded 300 °C.

After decay of the propane fire, the temperature at 10 mm depth decreased; deeper layers (i.e. 20 and 30 mm) dropped less rapidly and after a short delay. The layers at 40, 50 and 60 mm depth continued to increase in temperatures, although very slowly as the heat dissipated through the wood.

Approximately 5 minutes after decay of the propane fire, the temperature at 10 mm depth rose again. At approximately 58 minutes, when a large piece of CLT delaminated and fell off, the thermocouples in the first layer of CLT (i.e. 10 and 20 mm) became exposed and their temperature dropped to approximately room conditions. At 71 minutes, all temperatures in the CLT were below 200 °C

Mass loss

Before the experiment, the conditioned sample weighed 50.6 kg. After the experiment, the sample weighed 43.5 kg; a loss of 7.1 kg.

Heat release rate and heat flux

Figure 5.53 depicts the HRR during the experiment. Figure 6.54 depicts the heat flux measured in the middle of the opening in the compartment.

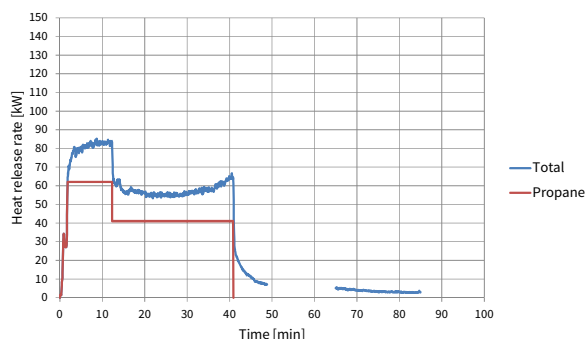


Figure 5.53 HRR in compartment 1 - due to a software malfunction, a part of the graph is missing. A second measurement was started with at 16 minute delay.

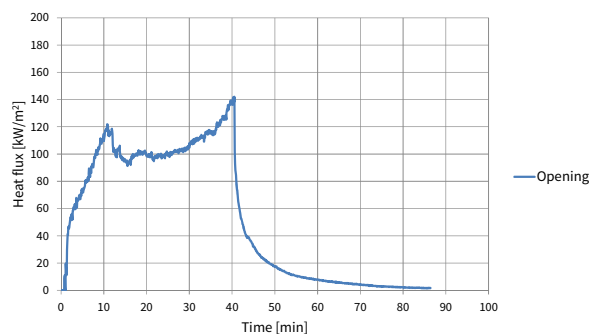


Figure 6.54 heat flux measured in the middle of the opening in compartment 1.

Upon igniting the burners, the total HRR rose to approximately 30 kW. The burners were then increased to the desired output of 62 kW and the HRR measurement followed this. Subsequently, when the CLT became involved in flaming combustion, the HRR increased further to 82 kW.

At 12 minutes the HRR dropped 20 kW to 62 kW when the propane fire was reduced to 42 kW. This drop was followed by slow decrease to 55 kW. Then, flaming in the compartment increased again and the HRR rose to 65 kW just before the propane fire was stopped.

After the propane fire was decayed, the total HRR dropped to 22 kW. This drop was followed by an increasingly slower descent to 7 kW at 49 minutes during smouldering of the CLT. The HRR continued to decrease until the experiment was stopped. At that moment values of $<3\text{ kW}</math> were measured. The effect of the delamination at 58 minutes on the HRR is unknown. However, all observations suggest nothing but to assume a continuation of the decrease between the two HRR data sets.$

After ignition of the burner bed and subsequently flaming of the CLT, the heat flux increased to 50 kW/m² at 2 minutes. This rapid increase was followed by a more gradual increase to 120 kW/m², which was reached at 11 minutes.

At 12 minutes the heat flux dropped to 100 kW/m² when the propane fire was reduced. This drop was followed by a slower decrease to 95 kW/m². However, when flaming in the compartment increased again, the heat flux was found to rise to 140 kW/m² just before the propane fire was seized.

After the propane fire was stopped, the heat flux decreased rapidly to 100 kW/m². This drop was followed by an increasingly slower descent towards 0 kW/m² during smouldering and subsequent extinguishment of the CLT. Delamination and fall-off of the CLT at 58 minutes was not observed to influence the heat flux measurements.

6.3.2 Compartment 2 – CLT back wall and side walls

The second experiment was conducted using a compartment with a CLT back wall and two side walls.

Visual observations

Ignition went similar as described for the previous experiment. The propane fire was set to a HRR of 41 kW from the beginning. The CLT walls became involved in flaming combustion within 2 minutes. Flaming was observed outside the compartment (figure 6.55). At approximately 16 minutes, delamination occurred and pieces of timber fell on the compartment floor. At 33 minutes, the thermocouple data indicated the temperatures at 20 mm depth in the walls and corner exceeded 300 °C. The propane flow was reduced to 0 %.

After decay of the propane fire, the intensity of flaming decreased. However, external flaming remained visible (figure 6.56). Some delaminated pieces of CLT could be observed on the floor (figure 6.57). At 50 minutes, multiple large pieces of CLT fell off and flaming increased in severity. After a period of 10 minutes the fire reduced in intensity again, but some external flaming remained visible. Delamination and fall-off occurred multiple times during the remainder of the experiment, for example at 72 minutes and 94 minutes. As a result, the compartment remained in flaming combustion (figure 6.58). The experiment was stopped at 111 minutes because the CLT was considered to be burned through. Flaming was observed to penetrate the walls (figure 6.59 and 6.60).



Figure 6.55 After ignition, the compartment became completely involved in flaming combustion.



Figure 6.56 After seizing the propane fire, the intensity of flaming reduced.



Figure 6.57 Delaminated pieces of CLT had fallen off and were visible on the compartment floor.



Figure 6.58 External flaming increased in severity after delamination and fall-off of large pieces.



Figure 6.59 Removal of the heat flux sensor revealed the compartment in flaming combustion.



Figure 6.60 Flames were observed to penetrate the left-hand side CLT at the end of the experiment.



Figure 6.61 Various depths to which the charring front progressed and at which delamination and fall-off occurred.



Figure 6.62 Various depths to which the charring front progressed and at which delamination and fall-off occurred.



Figure 6.63 In the corners up to 4 layers of CLT were still in place. Beneath the charred out layer, unaffected wood was still present.



Figure 6.64 Up to 5 different levels of charring and delamination can be observed. In the top left 4 layers remains. Adjacent, 3 layers, then 2 layers, and surrounding the gap only 1 layer.

Inspection of the char showed a large portion of the CLT had charred and fallen off or was reduced to ash. The pattern of the remaining char showed how delamination and fall-off in the various layers of CLT had occurred (figure 6.61 to 6.64).

In the corners where walls connected, 4 layers were still present. The top layer was completely charred but unaffected wood was still visible underneath. This indicates the char front had progressed through 2 layers of 20 mm CLT at these locations. In large areas of the back wall and along the edges of the side walls, 3

layers of CLT remained; again the innermost layer again completely charred. This indicates the char front had progressed at least through 3 layers of 20 mm CLT at these locations.

The middle areas of the side walls had usually only 1 of 2 charred layers of CLT still remaining. At these locations the char front had almost progressed through the complete sample. Finally, at some locations, the CLT was completely burned through, resulting in holes.

Temperatures

Figure 6.65 depicts room temperatures in the middle of the compartment at various heights. Figures 6.66 to 6.68 depict the temperatures in the middle of the CLT back wall (bw), middle of the left side wall (sw), and middle of the right side wall at the corner with the back wall (swc). Temperatures are measured at various depths expressed as a distance from the fire-side surface.

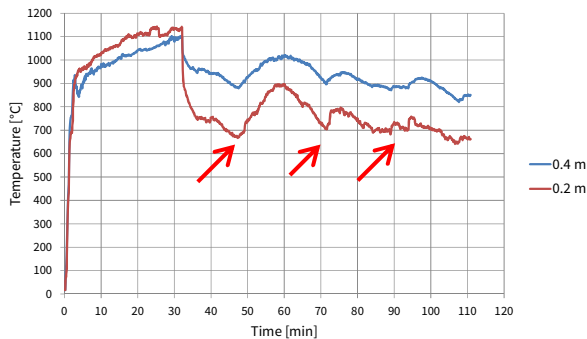


Figure 6.65 Room temperatures in compartment 2. Significant delamination is indicated by the arrows.

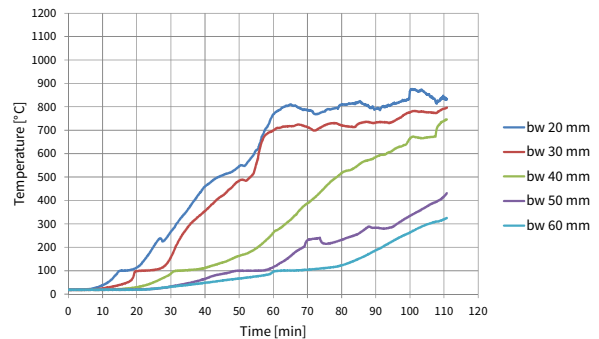


Figure 6.66 CLT temperatures in middle of the back wall

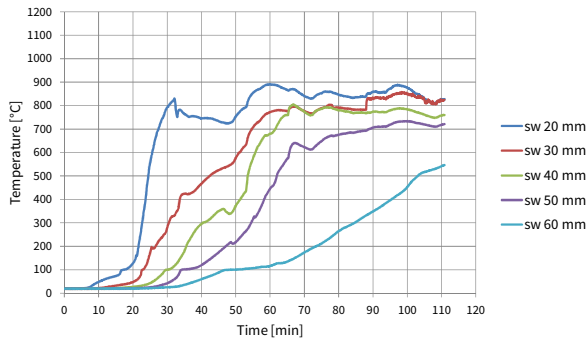


Figure 6.67 CLT temperatures in middle of left side wall

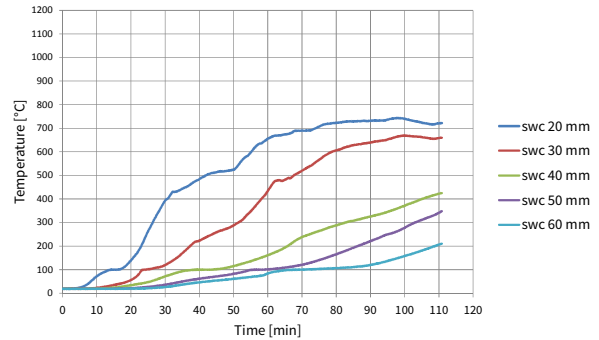


Figure 6.68 CLT temperatures in middle of right side wall corner

Room temperatures quickly increased to approximately 900 °C when the propane burners were ignited and the CLT became involved in flaming combustion. After a momentary drop of the thermocouple at 0,4 meters, temperatures then slowly increased during the following 30 minutes. Temperatures of 1100 °C at 0,4 m and 1140 °C at 0,2 m were measured just before the propane fire was seized. Delamination at 16 minutes was not observed to influence the temperatures.

After decay of the propane fire, the room temperatures dropped. The temperature at 0,2 m was found to drop faster. Within 1 minute, temperatures dropped to 1000 °C at 0,4 m and 850 °C at 0,2 m. Room

temperatures continued to decrease during flaming combustion to 880 °C and 670 °C respectively, before rising again when flaming increased in severity due to CLT fall-off. Temperatures of 1020°C and 890 °C respectively were reached, before both decreased again.

Room temperatures increased and decreased twice more; at 72 minutes and 94 minutes, the moments when increased flaming due to delamination and fall-off occurred. When the experiment was stopped, room temperatures still exceeded 650 °C and 850 °C respectively.

The temperatures in all layers of the CLT side wall, back wall, and corner of the side wall increased at the start of the experiment. The temperatures in the side wall were found to increase more rapidly.

Temperature increases were typically found to slow down temporarily at 100 °C. Significant differences could be observed between temperatures in adjacent layers, indicating a steep temperature gradient as the heat propagated through the material. At 33 minutes, the thermocouple data indicated the temperatures at 20 mm depth at all 3 locations exceeded 300 °C. The temperature in the back wall reached this value the last.

After decay of the propane fire all temperatures in the CLT continued to rise. An exception was the thermocouple at 20 mm depth in the side wall. When significant delamination occurred from 50 minutes onwards, the thermocouples in the layers at 20, 30, 40 mm depth of the side- and back walls became exposed one by one. As a result, these thermocouples measured room temperatures. As a result, the final part of the graphs seems consistent with the those of the room temperatures. The thermocouples in the corner were not exposed. Towards the end of the experiment temperatures in the CLT were still high and without any sign of decreasing.

Mass loss

Before the experiment, the conditioned sample weighed 65.2 kg. After the experiment, the sample weighed 37.3 kg; resulting in a loss of 27.9 kg.

Heat release rate and heat flux

Figure 6.69 depicts the heat release rate during the experiment. Figure 6.70 depicts the heat flux measured in the middle of the opening in the compartment.

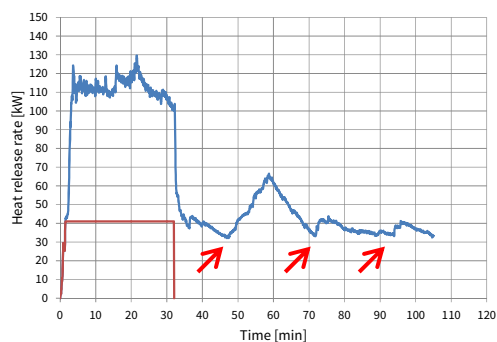


Figure 5.69 HRR in compartment 2. Significant delamination is indicated by the arrows.

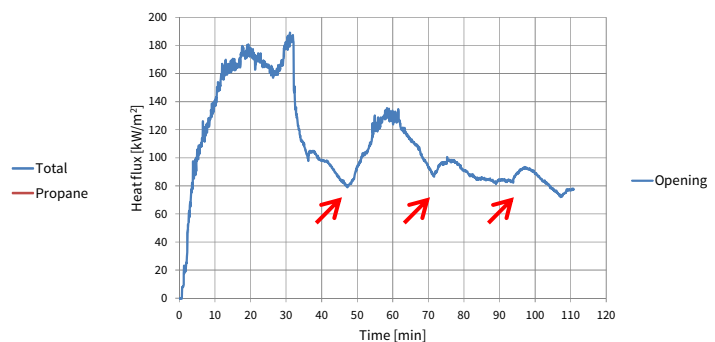


Figure 6.70 heat flux measured in the middle of the opening in 2.

Upon igniting the burners, the HRR increased to approximately 30 kW. The burners were set to the desired output of 41 kW and the HRR measurement followed this. Subsequently, when the CLT became involved in flaming combustion, the HRR increased to values over 120 kW within minutes and then stabilized just above 110 kW.

At approximately 16 minutes, when some delamination occurred, the HRR increased to 120 kW. Another increase to 130 kW occurred at 22 minutes. The HRR then decreased slowly to 100 kW.

After the propane fire was stopped, the total HRR was dropped to 55 kW, followed by a slower descent to approximately 32 kW at 47 minutes. When significant delamination occurred and flaming increased, the HRR rose again to 65 kW over a 10 minutes period, followed by a decrease back to 33 kW.

For the remainder of the experiment, when various pieces delaminated and fell off, the HRR remained in the range of 33 to 43 kW.

At the start of the experiment, the heat flux increased to 90 kW/m² in 4 minutes. This rapid increase was followed by a more gradual increase to 180 kW/m² at 17 minutes, just after some delamination occurred. It dropped to approximately 160 kW/m², followed by another increase to 190 kW/m² just before the propane fire decayed.

After the propane fire was stopped, the heat flux decreased to 100 kW/m² within 4 minutes. This was followed by a slower descent to 80 kW/m². The heat flux increased to 130 kW/m² when flaming increased due to delamination and fall-off, before dropping back to 90 kW/m². For the remainder of the experiment, when various pieces delaminated and fell off, the heat flux remained in the range of 70 to 100 kW.

6.3.3 Compartment 3 – CLT side walls (1)

The third experiment was conducted using a compartment with two CLT side walls to each other.

Visual observations

Ignition went similar as described in previous experiments. The propane flow was increased to a heat release rate of 41 kW and the CLT became involved in flaming combustion within 2 minutes. Flaming was observed outside the compartment (figure 6.71).

At approximately 15 minutes, some delamination occurred and pieces of timber fell on the compartment floor. At approximately 24 minutes, the thermocouple data indicated the temperatures at 20 mm depth in both side walls exceeded 300 °C. The propane flow was reduced to 0 %.

After the propane fire decayed, the intensity of flaming decreased. Nevertheless, external flaming remained present. At 27 minutes more CLT delaminated (figure 6.72).

However, within 10 minutes of reducing the propane flow, external flaming was no longer observed (figure 6.73). At 40 minutes flaming combustion was almost completely absent and was only visible on certain areas of the char (figure 6.74).

At 50 minutes, flaming had seized inside the compartment. The char smouldered. This smouldering slowly decreased in intensity (figure 6.75).



Figure 6.71 After ignition, the compartment became completely involved in flaming combustion. External flaming was observed.



Figure 6.72 Delaminated and fallen pieces of CLT lie on the compartment floor. The CLT wall is in flaming combustion.



Figure 6.73 Within 10 minutes of reducing the propane flow, external flaming was no longer observed.



Figure 6.74 Flaming reduced in intensity, but remained visible on certain areas of the char.

However, at 65 minutes, a large piece of CLT fell off at the right-hand side of the compartment (figure 6.76). Some local flaming occurred at that location (figure 6.787) but seized after 10 minutes. The fire transformed back to smouldering. Significant delamination also occurred at 75 minutes on the left-hand side and was followed by momentary local flaming. This sequence of events was repeated multiple times over a 1 hour period.

At 120 minutes, a layer of CLT delaminated on the left-hand side. However, this piece did not fall-off. Behind the piece, flaming developed, but seized again and smouldering continued (figure 6.78).



Figure 6.75 After flaming had seized, the char smouldered.



Figure 6.76 At 65 minutes, a large piece of CLT delaminated and fell off from the right- side wall.



Figure 6.77 Local flaming occurred at the location where the CLT had fallen off.



Figure 6.78 At 120 minutes, a piece delaminated on the left side. Flaming occurred behind it.



Figure 6.79 At 140 minutes, delamination and fall-off occurred on both side walls. Both walls again entered a phase of flaming combustion.



Figure 6.80 Flaming combustion increased in intensity and the complete compartment became involved in flaming again.

At 140 minutes, delamination occurred both left and right. The smouldering transformed to flaming on both walls (figure 6.79). This flaming increased in intensity and the complete compartment was burning again (figure 6.80), resulting in a second flash-over. The experiment was stopped at approximately 155 minutes because the sample was considered to be burned through.

Inspection of the char showed a large portion of the CLT was charred and had fallen off or was reduced to ash. The pattern of the remaining char showed how delamination and fall-off of the various layers of CLT had occurred (figure 6.81 to 6.84).

In the corners of the side walls, some small patches were still present where 4 layers were still held in place. The top layer was completely charred, but unaffected wood was still visible underneath, indicating the charring front had progressed through 2 layers of 20 mm CLT.

Along the edges of the walls, 3 layers remained, the top layer of which was also completely charred. This indicates the charring front had progressed through 3 layer of 20 CLT at these locations. The middle areas of the side walls had only 1 or 2 layers remaining.



Figure 6.81 Various depths to which the charring front progressed and at which delamination and fall-off occurred.



Figure 6.82 Along this edge, up to 3 layers of CLT remain. The inner most layer is almost completely charred.



Figure 6.83 Various depths to which the charring front progressed and at which delamination and fall-off occurred.

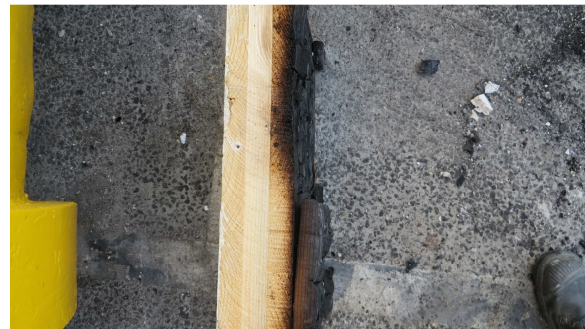


Figure 6.84 Along this edge, up to 3 layers of CLT remain. At the bottom of the picture, a fourth charred layer is still attached to the corner

Temperatures

Figure 6.85 depicts room temperatures in the middle of the compartment at various heights.

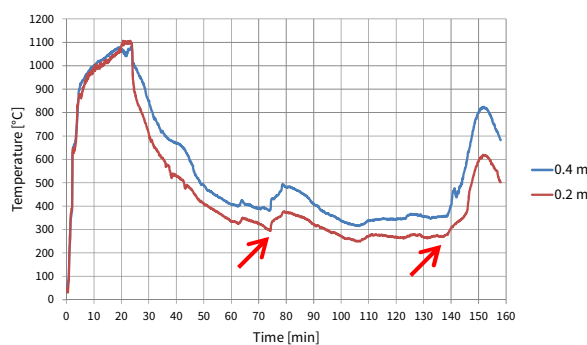


Figure 6.85 Room temperatures in compartment 3. Significant delamination is indicated by the arrows.

When the propane fire was ignited and the CLT became involved in flaming combustion, room temperatures rapidly increased to approximately 900 °C. Temperatures increased more slowly during the next 20 minutes to values of 1070 °C at 0,4 m. and 1100 °C at 0,2 m. Delamination at 15 minutes was not observed to influence the temperatures.

After decay of the propane fire, room temperatures dropped. Temperatures at 0,2 meters were found to drop faster. Within 1 minute, temperatures dropped to 990 °C at 0,4 m and 880 °C at 0,2 m, and then continued to decrease during the subsequent flaming and smouldering of the CLT to values around 380 °C and 300 °C respectively. At 75 minutes, temperatures increased again to 500 °C and 380 °C respectively, when significant flaming due to delamination and fall-off occurred.

Over a 60 minutes period, when smouldering and local flaming alternated, temperatures did not drop below 250 °C. Near the end of the experiment, they increased once more due the second flash-over.

Figure 6.86 and 6.87 depict the temperatures in the CLT side wall on the right (swr) and on the left (swl). Temperatures are measured at various depths expressed as a distance from the fire-side surface.

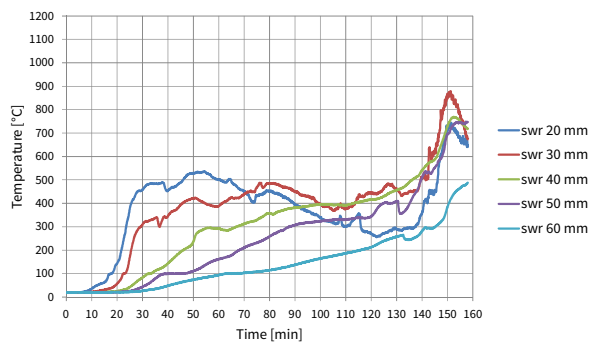


Figure 6.86 CLT temperatures in middle of the right side wall

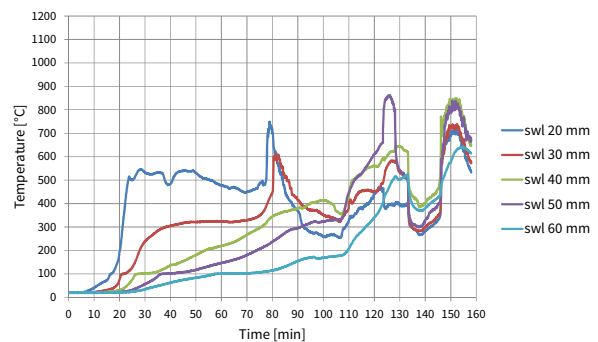


Figure 6.87 CLT temperatures in middle of the left side wall

The temperatures in all layers of both CLT walls increased after the start of the experiment. Temperatures slowed down at 100 °C and large differences could be observed between temperatures in the adjacent layers. At 24 minutes, the thermocouple data indicated the temperatures at 20 mm depth in both side walls exceeded 300 °C. The right side wall reached this temperature last.

After decay of the propane fire, temperatures at 20 mm depth stabilized at approximately 500 °C.

Temperatures in deeper layers continued to increase, although less rapid.

On the left-hand side, at 20 and 30 mm depth, and at 40 and 50 mm depth, temperatures were found to increase rapidly and then decrease again at 75 and 120 minutes respectively. This was attributed to the short periods of local flaming due to delamination that occurred there. From 140 minutes onwards, due to further delamination, the thermocouples at the left side became exposed and measured room temperature.

On the right-hand side, temperatures at 40, 50 and 60 mm depth continued to increase slowly.

Temperatures at 20 and 30 mm depth decreased and subsequently followed room temperatures when they became exposed due to delaminating at approximately 65 minutes. In a similar fashion, the layers at 40 and 50 mm depth also started to follow the room temperatures from 140 minutes onwards.

Mass loss

Before the experiment, the conditioned sample weighted 53.8 kg. After the experiment, the sample weighted 37.6 kg; a loss of 16.2 kg.

Heat release rate and heat flux

Figure 6.88 depicts the heat release rate during the experiment. Figure 6.89 depicts the heat flux measured in the middle of the opening in the compartment.

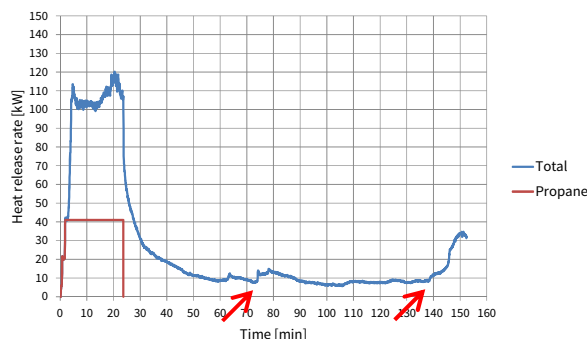


Figure 6.88 HRR in compartment 3. Significant delamination is indicated by the arrows.

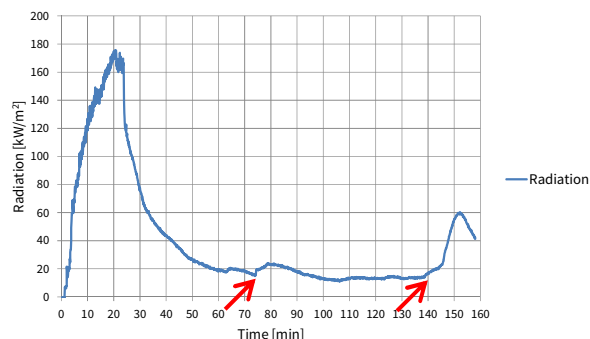


Figure 6.89 heat flux measured in the middle of the opening in 3.

When the CLT became involved in flaming combustion, the HRR increased rapidly to 110 kW and stabilized just above 100 kW. The HRR increased again to approximately 120 kW, before dropping back to 110 kW.

After the propane fire was stopped, the total HRR was dropped immediately to 75 kW, followed by an increasingly slower descent to values round 10 kW from 50 minutes onwards.

The HRR increased slightly on various occasions, for example at 65 minutes and 75 minutes when local flaming due to delamination occurred. Near the end of the experiment, when significant flaming occurred again, the HRR increased to values over 30 kW just before the experiment was stopped.

After ignition and flaming of the CLT, the heat flux increased to 60 kW/m² at 4 minutes. This rapid increase was followed by a more gradual increase to 170 kW/m² at 20 minutes. Some fluctuation could be observed at 15 minutes when some delamination occurred. The heat flux dropped slightly to 165 kW/m² before the propane fire was stopped.

After the propane fire was stopped, the heat flux dropped instantly to 130 kW/m², followed by a slower descent to 20 kW/m² during a 35 minute period of time. Similar to the HRR, small increases were observed when delamination occurred at 65 and 75 minutes. The heat flux then decreased to approximately 13 kW/m², where it remained fairly constant. At 140 minutes, when significant flaming occurred due to delamination at both sides, the heat flux increased again to values of approximately 60 kW/m².

6.3.4 Compartment 4 – CLT side walls (2)

Identical to the third experiment, the fourth experiment used a compartment with two CLT side walls.

Visual observations

After ignition was established and the propane flow was increased to a heat release rate of 41 kW, the CLT sidewalls became involved in flaming combustion within 2 minutes. Flaming was observed outside the compartment (figure 6.90). Similar to the other experiment with 2 CLT sidewalls, at approximately 15 minutes a piece of CLT delaminated and fell off. This occurred a second time at approximately 25 minutes (figure 6.91). At 27 minutes the thermocouple data indicated the temperatures at 20 mm depth in both sidewalls exceeded 300 °C. The propane flow was reduced to 0 %.



Figure 6.90 After ignition, the compartment became completely involved in flaming combustion.



Figure 6.91 Several pieces of CLT delaminated and fell off during the first 25 minutes of the experiment.



Figure 6.92 After seizing the propane fire, the intensity of flaming reduced.



Figure 6.93 At 40 minutes, flaming had almost completely seized and the char was glowing.

After seizing the propane fire, the intensity of flaming reduced (figure 6.92). At 32 minutes, no external flaming was observed, though flaming still occurred inside the compartment. Similar to the previous experiment with two side walls, flaming combustion was almost completely absent at 40 minutes. The char was glowing (figure 6.93), but quickly decreased in intensity (figure 6.94).

At approximately 67 minutes, some local flaming was observed on the left-hand side where a piece of CLT was delaminated but did not fall-off. Flaming occurred behind the layer, but seized again after a couple of minutes. Glowing was still observed at some spots in the char.

At approximately 83 minutes, glowing increased on the right-hand side and 10 minutes later delamination and fall-off occurred at that location. This resulted in some local flaming for a couple of minutes (figure 6.95). More delamination occurred at that location at approximately 102 minutes, but this did not result in flaming combustion.

At 115 minutes, some single spots were still smouldering, but decreased in intensity. The experiment was stopped at approximately 150 minutes because the sample was considered to be extinguished.



Figure 6.94 At 50 minutes, glowing had decreased in intensity.



Figure 6.95 After increased glowing, delamination and fall-off, some flaming occurred on the right side.

Inspection of the char showed the charring front had progressed through the first layer of CLT and through the second layer and into the third layer, depending on the location (figure 6.96 to 6.99). Along the edges of the CLT walls, the char front had stopped in the second layer (left side wall), or at the interface between the second and third layer (right side wall). The charred first layer had fallen off and removal of the charred second layer revealed the unaffected wood of the third layer underneath. In the middle areas of the walls, the char front had progressed to the interface between the second and third layer (left side wall) or even into the third layer (right side wall). At the left side, the charred first layer had fallen off and removal of the charred second layer revealed unaffected wood underneath. At the right side, both the first and the second layer had fallen off, revealing the partially charred third layer.



Figure 6.96 In the middle of the left side wall, the 1st layer has fallen off. Removal of the charred 2nd layer revealed the char front stopped at the interface between 2nd and the 3rd layer. Discoloured but otherwise unaffected wood of the 3rd layer is visible

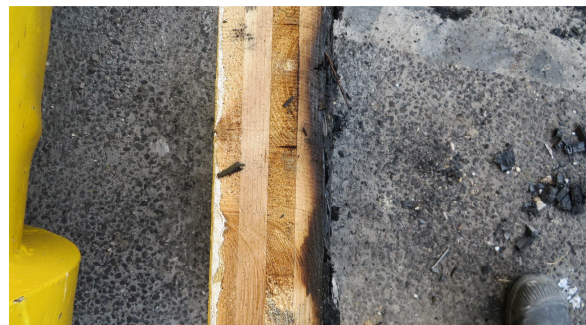


Figure 6.97 Along the edges of the left side wall, the char front progressed into the 2nd layer. The 1st layer has fallen off, but the second layer is still partially unaffected and attached to the wall.



Figure 6.98 In the middle of the right side wall, the char front has progressed into the third layer. Both the 1st and 2nd layer had fallen off.



Figure 6.99 Along this edge of the right side wall, the char front progressed to the interface between the 2nd and 3rd layer. The 1st layer has fallen off and the 2nd layer was removed to reveal unaffected wood.

Temperatures

Figure 6.100 depicts room temperatures in the middle of the compartment at various heights.

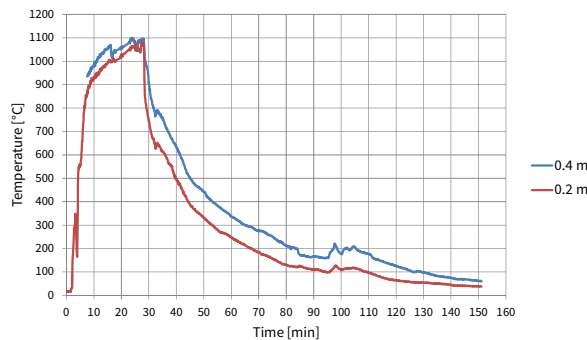


Figure 6.100 Room temperatures in compartment 4. Significant delamination is indicated by the arrows.

8 minutes of data were lost due to a failing connection of the couple at 0,4 m. Temperatures increased rapidly to approximately 900 °C, and then more slowly during the following 20 minutes to 1090 °C at 0,4 m. and 1080 °C at 0,2 m, just before the propane fire was stopped.

After decay of the propane fire, the temperatures dropped to 980 °C at 0,4 m and 800 °C at 0,2 m. within one minute. Temperatures then continued to decrease during the subsequent flaming and smouldering of the CLT to 160 °C and 100 °C respectively at 95 minutes. Local Flaming due to delamination at 67 minutes was not observed to influence the room temperatures.

At 95 minutes, temperatures increased when flaming due to delamination and fall-off occurred on the right side. Temperatures then fluctuated for 15 minutes around 200 °C and 115 °C respectively, before decreasing again. At the end of the experiment, room temperatures were below 100 °C.

Figure 6.101 and 6.102 depict the temperatures in the CLT side wall on the right (swr) and on the left (swl), at various depths and measured from the fire-side surface.

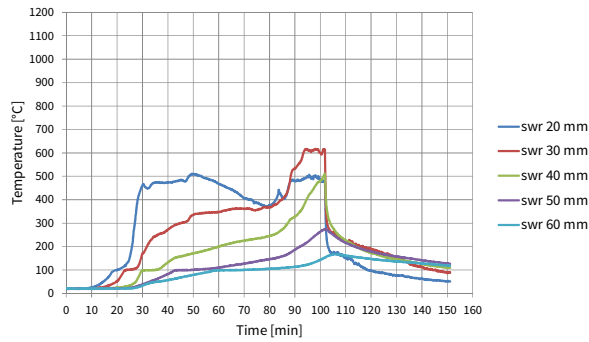


Figure 6.101 CLT temperatures in middle of right wall

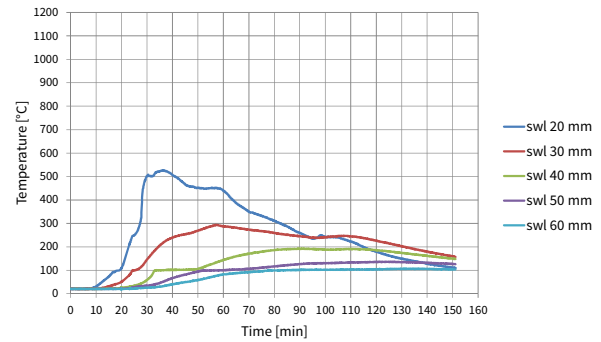


Figure 6.102 CLT temperatures in middle of left wall

The temperatures in the CLT increased. At 27 minutes, the thermocouple data indicated the temperatures at 20 mm depth in both side walls exceeded 300 °C; both walls reached this value within 1 minute of each other.

After decay of the propane fire, temperatures at 20 mm depth stabilized at 500 °C. Temperatures in deeper layers continued to increase slowly. From 50 minutes, temperatures at 20 mm depth decreased at both sides. Despite delamination, the thermocouples were not exposed. Local flaming due to delamination on the left side at 67 minutes did not result in an increase of temperatures. From 83 minutes and onwards, when local flaming due to delamination occurred on the right side, temperatures rose at that side. Then, at 102 minutes, when further delamination and fall-off occurred, the thermocouples in the top layers became exposed and measured room conditions. Subsequently, temperatures of all layers on the right-hand side were decreasing. In the meantime, temperatures at left-hand side had stabilized, or were decreasing slowly. Towards the end of the experiment, all temperatures in the CLT were below 200 °C and decreasing.

Mass loss

Before the experiment, the conditioned sample weighted 53.0 kg. After the experiment, the sample weighted 41.2 kg; a loss of 11.8 kg.

Heat release rate and heat flux

Figure 6.103 depicts the heat release rate during the experiment. Figure 6.104 depicts the heat flux as measured in the middle of the opening in the compartment.

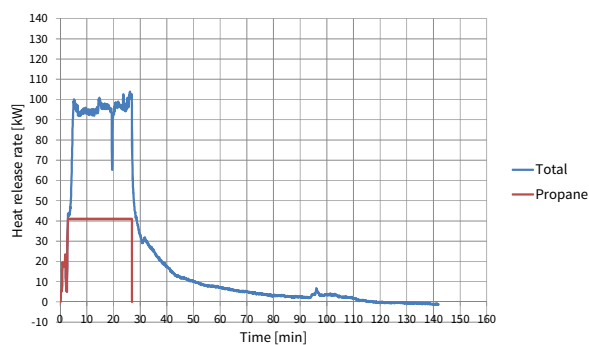


Figure 6.103 HRR in compartment 4.

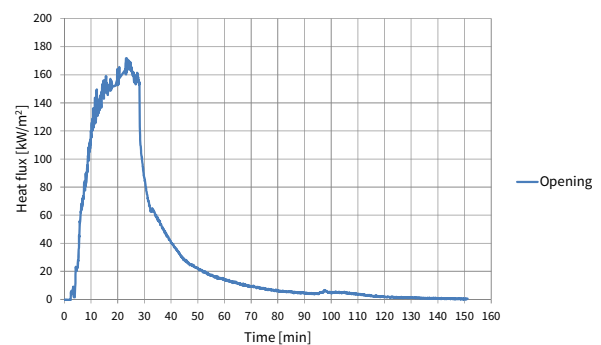


Figure 6.104 heat flux measured in the middle of the opening in 4.

When the CLT became involved in flaming combustion, the HRR increased to 100 kW at 5 minutes and stabilized at approximately 95kW. At 15 minutes, the HRR increased slightly after some CLT delaminated and fell off. Furthermore, a sudden and momentary drop in HRR was observed at 19 minutes. Just before the propane fire was seized, the HRR increased again after some fall-off. After the propane fire was stopped, the total HRR was dropped rapidly to 60 kW, followed by a slow descent to values < 10 kW at 50 minutes. At approximately 32 minutes, a small momentary increase was measured. The HRR was observed to increase slightly at 95 minutes just after some local flaming due to delamination and fall-off occurred on the right side. Towards the end of the experiment, the HRR was close to 0 and even became negative, possible due to a small drift in the measurements.

After ignition and flaming of the CLT had been established, the heat flux increased to 60 kW/m² over a 4 minute period. This rapid increase was followed by a more gradual increase to 170 kW/m² at 25 minutes. The heat flux dropped to 155 kW/m² just before the propane fire was stopped. Delamination and fall-off during this phase of the experiment did not seem to affect the heat flux measurement significantly. After the propane fire was stopped, the heat flux decreased rapidly to 120 kW/m², followed by a slower descent to values < 5 kW/m² at 87 minutes and onwards. Exception was a small momentary increase, at approximately 32 minutes. At 95 minutes, just after local flaming due to delamination and fall-off occurred on the right hand side, the heat flux then increased slightly. Towards the end of the experiment, the heat flux became very small; values of < 0.5 kW/m² were measured.

6.3.5 Compartment 5 – CLT side walls with 40 mm thick outer lamella

Similar to the third and fourth experiment, the fifth experiment used a compartment with two CLT side walls. The outside lamellas of the CLT were 40 mm thick, instead of 20 mm.

Visual observations

After ignition was established, the propane flow to the burners was increased to a HRR of 41 kW. The CLT sidewalls became involved in flaming combustion within 2 minutes and flaming was observed outside the compartment (figure 6.105).

At approximately 26 minutes, the thermocouple data indicated the temperatures at 20 mm depth in both sidewalls exceeded 300 °C. The propane flow was reduced to 0 %. Contrary to previous experiments, no fall-off of the CLT was observed and the CLT walls were able to retain the char layer (figure 6.106).

After the propane fire was stopped, the intensity of flaming reduced within 1 minute (figure 6.107). The CLT transformed from flaming to smouldering combustion at approximately 30 minutes. The glowing surfaces did not show any sign of delamination or fall-off (figure 6.108 and 6.109). The smouldering of the CLT quickly decreased in intensity and at 38 minutes, smouldering was observed only at some spots in the char. These single spots kept decreasing in intensity until no glowing was observed anymore (figure 6.110). The experiment was stopped at 70 minutes because the sample was considered to be extinguished.



Figure 6.105 After ignition, the compartment became completely involved in flaming combustion.



Figure 6.106 No fall-off of char was observed during the initial fire and flaming combustion of the CLT.



Figure 6.107 After seizing the propane fire, the intensity of flaming reduced. The CLT was in flaming combustion. No pieces of char had fallen off.



Figure 6.108 The CLT transformed from flaming combustion to smouldering combustion at 30 minutes.



Figure 6.109 The glowing surfaces did not show any sign of delamination or fall-off.



Figure 6.110 The smouldering of the CLT quickly decreased in intensity until no glowing was observed.

Inspection of the sample revealed no pieces of CLT had fallen off. The charred portion of the CLT was still attached to the wood underneath (figures 6.111 to 6.114). Furthermore, it became clear that the charring front had progressed approximately 20 mm, i.e. half way the first layer of 40 mm thick CLT. Because no char had fallen off, the surfaces were “clean” and the alligator pattern could be observed. Furthermore, the boards which make up the CLT layer were visible in the char pattern.

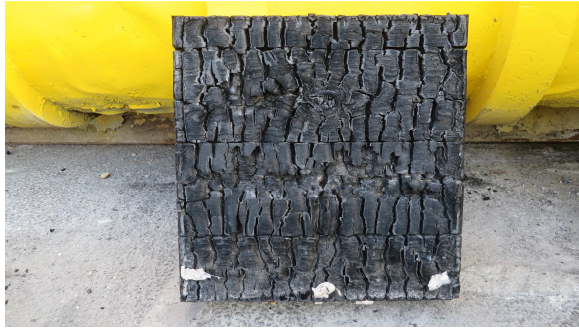


Figure 6.111 No pieces of charred CLT had fallen off.



Figure 6.112 The char front progressed approximately 20 mm into the first layer of 40 mm thick CLT.



Figure 6.113 The charred surface had an alligator pattern. The boards are clearly visible.



Figure 6.114 Along this edge, the char front progressed 20 mm into the first layer of 40 mm CLT.

Temperatures

Figure 6.115 depicts room temperatures in the middle of the compartment at various heights.

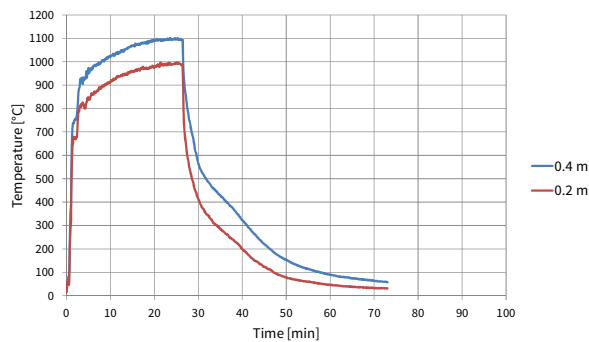


Figure 6.115 Room temperatures in compartment 5.

At the start of the experiment, room temperatures quickly increased to approximately 750 °C at 0,4 m. and 670 °C at 0,2 m. These then increased gradually during 25 minutes to approximately 1090 °C and 990 °C respectively, just before the propane fire was stopped.

After the propane fire was stopped, room temperatures decreased rapidly. Within 1 minute, these dropped to 810 °C and 610 °C respectively. Room temperatures continued to decrease for the remainder of the experiment and both were below 200 °C at approximately 46 minutes.

Figure 6.116 and 6.117 depict the temperatures in the CLT side wall on the right (swr) and on the left (swl), at various depths and measured from the fire-side surface.

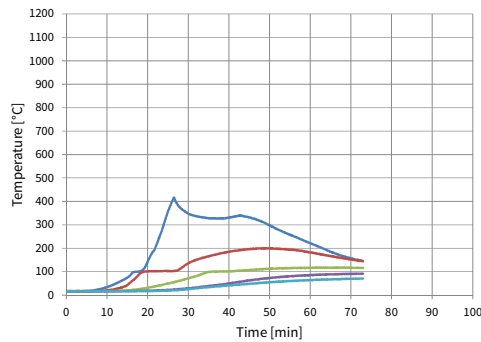


Figure 6.116 CLT temperatures in middle of the right side wall.

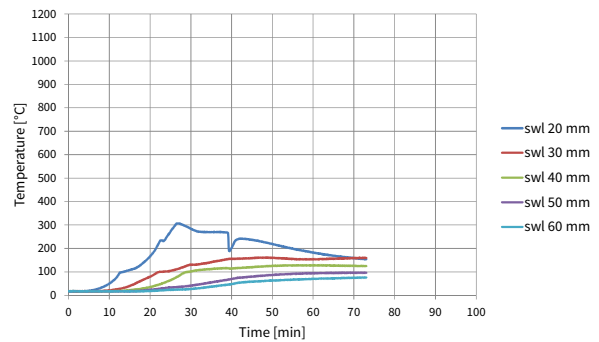


Figure 6.117 CLT temperatures in middle of the left side wall.

The temperatures in all layers the CLT walls increased after the start of the experiment. Similar to previous experiments, temperatures slowed down at 100 °C and large differences were observed between temperatures in the adjacent layers. At 27 minutes, the thermocouple data indicated the temperatures at 20 mm depth in both side walls exceeded 300 °C. The right side wall reached this temperature approximately 2 minutes earlier.

After decay of the propane fire, temperatures at 20 mm depth of both walls decreased. During smouldering combustion these temperatures stabilized at approximately 330 °C on the right and 270 °C on the left. In the meantime, deeper layers kept increasing in temperature, although very slowly. The left side thermocouple at 20 mm depth experienced a momentary dip at 40 minutes, possible due to loss of contact with the CLT.

From approximately 42 minutes, when smouldering increasingly diminished in intensity, temperatures at 20 mm depth started to decrease further. From approximately 50 minutes, deeper layers also seized their slow increase and stabilized. Towards the end of the experiment all temperatures in the CLT were below 200 °C.

Mass loss

Before the experiment, the conditioned sample weighted 67.2 kg. After the experiment, the sample weighted 59.7 kg; a loss of 7.5 kg.

Heat release rate and heat flux

Figure 6.118 depicts the heat release rate during the experiment. Figure 6.119 depicts the heat flux measured in the middle of the opening in the compartment.

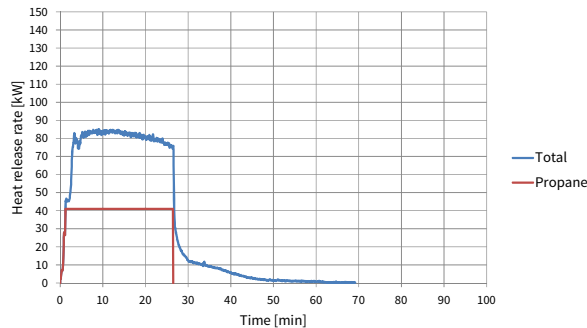


Figure 6.118 HRR in compartment 5.

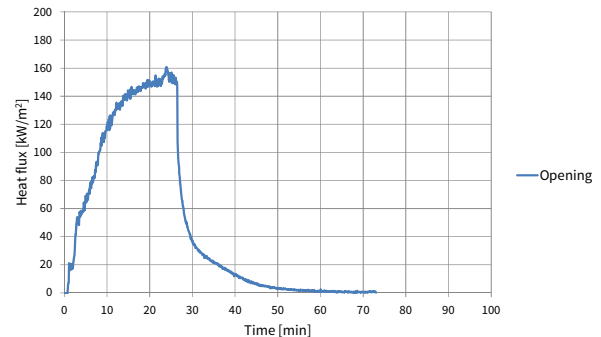


Figure 6.119 heat flux measured in the middle of the opening in 5.

When the CLT became involved in flaming combustion, the HRR increased to 80 kW at 4 minutes. The HRR gradually rose to 84 kW, before slowly decreasing to 75 kW, just before the propane fire was seized. After the propane fire was stopped, the total HRR dropped almost instantaneously to 30 kW. This was followed by a descent to 15 kW at 30 minutes, the moment the fire transformed to smouldering. During smouldering the HRR decreased further. At the end of the experiments the HRR was 0 kW.

After ignition and flaming of the CLT, the heat flux increased to 50 kW/m² at 3 minutes. This rapid increase was followed by a more gradual increase to 160 kW/m² at 24 minutes. The heat flux dropped to 150 kW/m² just before the propane fire was stopped.

After decay of the propane fire, the heat flux dropped to 110 kW/m². This drop was followed by an increasingly slower descent to 0 kW/m² during smouldering and subsequent extinguishment of the CLT.

7.1 Introduction

In this chapter, the results from the experiments are analysed and the following question is answered:

How can self-extinguishment of cross-laminated timber be explained in the experiments, and what are the conditions under which it took place?

Due to the large amount of data of both series of experiments, the possibilities for analysis are numerous. This chapter is limited to those areas most interesting for answering the main research question. Other analyses could certainly provide more understanding of the burning of CLT as part of follow-up research.

7.2 Analysis of experiment series 1

In this paragraph the results from experiment series 1 are analysed. The focus of the first series is the transformation from smouldering combustion to self-extinguishment, and the conditions at which this takes place. The analysis will focus on these conditions with regards to heat flux and air flow. However, other analyses, including a derivation of charring rates, an explanation of mechanisms involved, and a comparison with prediction and Eurocode guidance are added.

7.2.1 Flaming combustion during the 75 kW/m² exposure

During the initial 75 kW/m² exposure, all investigated CLT samples became involved in flaming combustion within 10 seconds. Without a protective char layer, temperatures in the wood rose rapidly, typically to 700 - 750 °C, followed by a more gradually increase to 770 - 880 °C. Temperatures in deeper layers also increased, although less rapid and typically reached lower peak values. Significant differences between temperatures in various layers indicated a steep temperature gradient as the heat propagated through the material. This behaviour reinforces the idea of wood as an insulator of heat.

As a result of the increased temperatures, thermal degradation of the wood took place; volatile were released and could be observed leaving the surface. As a result, the samples lost mass. These volatiles were quickly ignited and heat was generated. Both mass loss rates and heat release rates peaked early at approximately 20 seconds; for all 16 experiments on average 0,18 g/s (values ranging from 0,12 to 0.26 g/s) and 237 kW/m² (values ranging from 202 to 281 kW/m²) respectively. This early peak can be attributed to the absence of a protective char layer at the start of the experiments.

As a result of the continued thermal degradation of the wood, a char layer developed. This char protected the wood underneath, which was reflected in mass loss rates and heat release rates decreasing after the initial peak. This suggests the char layer decreased the flow of heat to the thermal degradation zone, which slows down the production of volatiles and thus the mass loss and heat release rates. Typically, the MLR and HRR stabilized at 5 minutes. From 5 minutes onwards to 19 minutes, i.e. just prior to switching, the average mass loss and heat release rates were 0,05 g/s and 73 kW/m² for all 16 experiments.

Continuation of the 75 kW/m² exposure

In experiments 13 to 16, the samples were not switched to a second and lower flux. The samples continued burning in flaming combustion under the 75 kW/m² exposure. The MLR and HRR typically decreased slightly during continuation of the 75 kW/m² exposure to < 0.050 g/s and < 70 kW/m². This decrease could be attributed to the continued build-up of a protective char and ash layer.

All 4 experiments showed an increase in the MLR and HRR at approximately 40 minutes, which dropped again toward the end of the experiments at 50 minutes. During this period, burning was observed along the sample edges, which could indicate the samples had become thin and all sides became involved in flaming. This would temporary increase the MLR and HRR, until almost all fuel was consumed.

Two of these experiments were conducted without thermocouples to investigate the influence of these on the measurements. Reference is made to appendix G, which contains a general discussion of various fluctuations and spikes in measurements.

Effective heat of combustion

During the 75 kW/m² heat flux exposure the effective heat of combustion was determined using the quotient of the HRR and the MLR. The average EHC over all experiments was found to be 14,2 MJ/kg.

Between the experiments, a high variation in the degree of fluctuation was found. Despite this variation in fluctuation, values for the average EHC ranged only from 11,3 to 18,1 MJ/kg. This suggested that even though individual momentary measurements of the EHC were found to vary, the average over a longer period was fairly constant. The reasons for the high variation in fluctuation are discussed in appendix G.

It is interesting to compare the EHC of 14,2 MJ/kg to the value provided by Eurocode 1995-1-2 table E.3 of 17,5 MJ/kg. The Eurocode value seems to be higher than the value obtained for specifically this type of CLT. It is likely the Eurocode uses a high percentile value.

7.2.2 Transformation from flaming to smouldering combustion

In experiment 1 to 12, the samples were switched to a second lower flux in the range of 0-10 kW/m². This switch simulated the transition from flaming to smouldering combustion in a CLT compartment. Once the samples were switched, flaming seized within 1 minute and the CLT started smouldering. Depending on the conditions, i.e. the level of heat flux and the airflow over the material, this smouldering was sustained and the sample burned-through, or the smouldering seized and the sample self-extinguished.

7.2.3 Self-extinguishment / burn-through during smouldering combustion

Prior to testing, criteria were set to determine if a sample was burned-through or had self-extinguished. These criteria were based on the propagation of the 300 °C isotherm, the 200 °C threshold of producing volatiles, and the continuation of loss of mass. Table 7.1 presents an overview of extinguishment and burning-through, based on a comparison of the results with these criteria.

Table 7.1 Self-extinguishment and burning-through in the experiments.

Experiment	0 kW/m ²		5 kW/m ²		10 kW/m ²		8 kW/m ²		6 kW/m ²		6 kW/m ²	
											0,5 m/s	1,0 m/s
	1	2	3	4	5	6	7	8	9	10	11	12
extinguished	yes	yes	yes	yes	-	-	-	-	yes	yes	yes	-
burned-through	-	-	-	-	yes	yes	yes	yes	-	-	-	yes

Based on these results, the conditions at which self-extinguishment took place, can be determined. A distinction is made between the condition of heat flux and of air flow.

Heat flux as a condition for self-extinguishment

When no additional airflow was present, the sample extinguished quickly at a heat flux of 0 or 5 kW/m². A flux of 5 kW/m² can be taken as a lower bound for the threshold flux at which self-extinguishment takes place. At fluxes of 8 and 10 kW/m² the samples continued smouldering and burned-through.

In the samples exposed to a 6 kW/m² heat flux, the 300 °C isotherm penetrated to 30 mm, temperatures continued rising, and the sample weight reduced. These samples were smouldering. However, as these experiments progressed, the 300 °C isotherm did not reach 40 mm depth. All temperatures were observed to drop below 200 °C and the weight stabilized. The samples had extinguished after some initial smouldering.

The fact that these samples initially smouldered, but then extinguished, can be explained by a slowly increasing distance between the sample and the cone heater during smouldering. This is due to the reduction of volume when char is formed and further transformed to ash. As result of this increased distance, the flux on the sample would decrease.

Therefore, 6 kW/m² can be considered to be an upper bound for the threshold flux at which self-extinguishment takes place. Based on this analyse, the following condition with regards to heat flux can be formulated.

The threshold flux at which self-extinguishment occurs is in the range of 5 to 6 kW/m².

Air flow as a condition for self-extinguishment

The second condition which was investigated was the air flow. This condition was investigated to a limited degree; only in combination with a 6 kW/m^2 heat flux exposure and at speeds of $0,5 \text{ m/s}$ and $1,0 \text{ m/s}$. An additional airflow of speed $0,5 \text{ m/s}$ resulted in self-extinguishment more quickly than without it. The addition of an additional airflow with speed $1,0 \text{ m/s}$ resulted in quick burn-through.


These results illustrate the importance of the air flow conditions. Based on this limited amount of data, it can be expected that additional airflow with a speed of $1,0 \text{ m/s}$ results in less favourable conditions for self-extinguishment, while an additional airflow with a speed of $0,5 \text{ m/s}$ results in more favourable conditions. Considering the results that were obtained in the investigation of the heat flux condition, it can reasonably be assumed that at heat fluxes below 6 kW/m^2 , an airflow with a speed limited to $0,5 \text{ m/s}$ results in self-extinguishment. It would be recommended to investigate more air speeds in combination with other heat fluxes in order to obtain a better understanding of the influence of the air flow.

At heat fluxes below 6 kW/m^2 , the air flow should be limited to $0,5 \text{ m/s}$ in order to self-extinguishment to occur.

Overview of conditions for self-extinguishment

An overview is presented in table 7.2 that indicates the potential for self-extinguishment, based on the heat flux and air flow conditions. The dark areas in this table show the results based on this series of experiments. The light areas need further investigation.

Table 7.2 Conditions for self-extinguishment and burning-through.

Heat flux Add. air flow	$\leq 5 \text{ kW/m}^2$	6 kW/m^2	$\geq 6 \text{ kW/m}^2$	
none	Self-extinguishes	Self-extinguishes after some smouldering	Burns-through	
$0,5 \text{ m/s}$	Expected to self-extinguish	Self-extinguishes	Unknown	
$1,0 \text{ m/s}$	Unknown	Burns through	Expected to burn through	

It is expected that the airflow with speed $0,5 \text{ m/s}$, (which was found favourable with regards to self-extinguishment at a heat flux of 6 kW/m^2) will also result in self-extinguishment at lower fluxes. Furthermore it is expected that the airflow with speed $1,0 \text{ m/s}$ (unfavourable with regards to self-extinguishment at 6 kW/m^2) will also result in burning-through at higher fluxes.

Comparison with predictions based on literature

Based on the theory and the existing data discussed in part 1, it was expected self-extinguishment occurs at a heat flux below 8–10 kW/m². These values were threshold values at which smouldering ignition occurred on wood, and which was required to sustain smouldering along a wooden surface respectively. The threshold for self-extinguishment that was found was somewhat lower: 5-6 kW/m². It seems that a slightly higher flux is required for the onset of glowing than is required to sustain it, and that smouldering inward into wood requires less heat than smouldering along the surface.

Furthermore, it was expected air flow over the samples would be of influence, based on experiments of smouldering along wooden surfaces. This was indeed found to be of importance for smouldering inward as well.

7.2.4 Charring rates

Charring rates are obtained for both the 75 kW/m² and the various second lower exposures using the location of the 300 °C isotherm. The location of the 300 °C isotherm was determined with the average of the two thermocouple temperatures at a certain depth (0, 10, 20, 30, and 40 mm from the CLT surface).

Appendix H presents charring rates during the initial exposure of 75 kW/m² of experiments 1–12, during the various lower second exposures of these experiments, and for experiments 13 and 14 in which the 75 kW/m² exposure was continued. Furthermore, these charring rates are compared to the predicted values and those provided by Eurocode 5. Charring rates obtained for the various lower exposures, and for the initial 75 kW/m² exposure, corresponded well with the predictions based on the work of Butler (1971), Charring rates for the prolonged 75 kW/m² exposure corresponded well with Eurocode guidance.

7.2.5 Delamination

Inspection of the samples revealed delamination had occurred. Delamination occurred typically as the char layer, indicated by the 300 °C isotherm, reached a PU adhesive layer.

This became clear in the experiments with a 0 kW/m² second exposure. The samples extinguished quickly after the 300 °C isotherm had penetrated to 20 mm depth, i.e. the location of the first PU glue layer. In these samples the top layer had delaminated, while the second layer wasn't charred. This observation is in line with the predictions based on the observations made by Frangi *et al.* (2009).

Delamination did not result in the fall-off of layers due to the horizontal orientation of the samples. As a result, delamination had almost no influence on the burning behaviour of the CLT.

In some experiments, a slight increase in MLR and HRR was observed just before the samples were switched, i.e. the moment the 300 °C isotherm penetrated to 20 mm depth and thus the PU adhesive layer. This might be a result of delamination and a subsequent minor increase of the burning as the two layers slightly come apart. However, this was not further investigated, because the influence was small and because delamination will be investigated to a more significant degree in the second series of experiments.

7.2.6 Mechanism of self-extinguishment, burn-through, and additional airflow

The distribution of temperatures and their propagation through the CLT samples offers an explanation of the mechanisms during self-extinguishment and burn-through, as well as the effect of additional airflow.

In appendix I, temperatures profiles are given for two experiments with a 10 and 6 kW/m² exposure. Based on these temperature profiles, the various zones of the smouldering mechanism, as discussed in chapter 3, can be observed propagating through the material in the experiment with a 10 kW/m² exposure. Furthermore, it was observed that energy is generated by the smoulder reaction zone. In the experiment with 6 kW/m² it can be observed that initially the smouldering reaction was established and generated heat, but, when losses overcame the heat generated by the smouldering and supplemented by the 6 kW/m² applied flux, the reaction was not able to sustain itself and temperatures dropped.

Appendix I also investigates the effect of the additional airflow. It was found reasonable to assume two mechanisms occur; additional surface cooling and additional heat generated due to an increased reaction speed as a result of forced oxygen supply.

These mechanisms might compete in slowing down or speeding up the smoulder reaction. Both effects of the additional air flow were also recognized in the experiments carried out by Ohlemiller (1985, 1988), as discussed in the appendix B. The net result might be dependent on the speed of the additional airflow and possible on the level of the externally applied heat flux. More research on this would be recommended.

Finally, appendix I investigates the cone shape in which burn-through typically occurred.

7.2.7 Comparison of temperatures with predictions and Eurocode guidance

The temperatures obtained for the experiments can be compared to those predicted using a finite difference method and the Eurocode wood properties at elevated temperatures. Figures 7.1 and 7.2 compare the experimental results with the predictions.

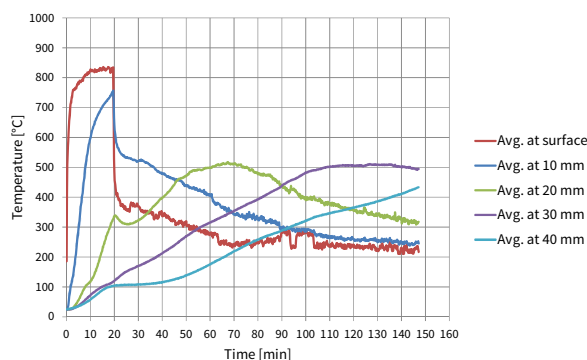


Figure 7.1 Temperatures in experiment 6 during the 75 kW/m² and 10 kW/m² exposure.

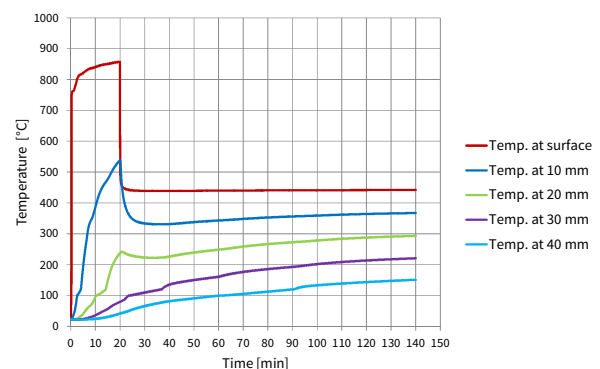


Figure 7.2 Temperatures as predicted for a 75 kW/m² and 10 kW/m² exposure.

Despite the fact that the prediction makes use of a gas temperature (taken as the cone heater temperature) instead of a pure radiative heat flux exposure, surface temperatures corresponded well with the experiments during the initial exposure. This suggests the gas temperature was chosen correctly.

However, deeper layers rose much quicker in the experiments. This could be attributed to the fact that the Eurocode properties do not incorporate a higher heat penetration due to cracks in the char. However, other reasons might be the cause and further research would be recommended.

The important difference however is the lack of the smoulder process in the predictions. The increases and decreases in the temperatures of adjacent layers in the experiment data indicate the smoulder zones propagate through the material. This is not incorporated in the Eurocode properties at all. It would be recommended to investigate how this could be incorporated.

7.2.8 CLT surface temperature

In the experiments, a stable heat flux was generated with a cone heater. In reality, this flux is provided by mutual cross-radiation between smouldering CLT surfaces and other hot objects or flames. The actual value will depend on the temperatures, and on the amount, geometry, and orientation of these surfaces and objects. While the latter are building specifics, the CLT surface temperature during smouldering can be estimated based on the results.

During smouldering, the highest temperatures were located in the reaction zone where oxidation of the char took place, as explained in appendix I. This layer is covered by the residual ash and char layer with a lower temperature. It would be this residual layer that would radiate to other surfaces.

In the experiments where burn-through occurred, maximum temperatures in the reaction zone were 500 - 600 °C. This corresponds well with the theory from chapter 3 where it is observed that char is susceptible to rapid oxygen attack at temperatures of > 400 °C.

Once the reaction zone progressed further, these zones became residual ash and char, typically with temperatures of 400 °C or lower. When temperatures decreased below 400 °C they showed an increase in fluctuation. This could be due to the fact that these thermocouples became exposed.

In the experiments where the samples just extinguished, maximum char temperatures were 400-500 °C. Then, as these samples extinguished, surface temperature of < 400 °C were observed.

Based on these observations, a reasonable estimation for the surface temperature of the CLT during charring would be 400 °C. Using this temperature and the geometry of a compartment, the heat flux on the CLT can be estimated. This will be discussed in more detail in chapter 8 on design implementation.

7.2.9 Repeatability

The experiments that were carried out twice showed a high degree of repeatability. Furthermore, results obtained during the 75 kW/m² exposure (which was present in each test) also showed a high degree of repeatability. This increases the confidence in the results, particularly with regards to the value of the threshold flux at which self-extinguishment occurs.

7.3 Analysis of experiment series 2

In this paragraph the results from experiment series 2 are analysed. The analysis will focus on the transitions of the CLT fire and the conditions at which these occur, as described in the model of self-extinguishment. However, other analyses, including a derivation of charring rates, the contribution of the CLT to the fire in terms of energy released, and a comparison with predictions and Eurocode guidance are added.

7.3.1 Flaming combustion during the initial fire

After ignition of the initial fire, the CLT walls became involved in flaming combustion within 2 minutes. The total HRR rose rapidly and exceeded the propane HRR due to the involvement of the CLT. Table 7.3 presents values for the HRR of the propane fire, the average total HRR during the fully developed fire, and the contribution of the CLT. Values per m² floor area or per m² CLT surface are given in parentheses.

Table 7.3 Heat release rates during burning of the propane fire

Experiment	Configuration	propane [kW]/(m ² floor)	Avg. total * [kW]/(m ² floor)	CLT contribution [kW]/(m ² CLT)	increase
1	1 back wall	62 (248) [^]	78 (312)	16 (64)	26 - 39 %
1		41 (164)	57 (228)	16 (64)	
2	1 back-, 2 side walls	41 (164)	110 (440)	69 (92)	168 %
3	2 side walls	41(164)	102 (408)	61 (122)	149 %
4	2 side walls	41(164)	95 (380)	54 (108)	132 %
5	2 side walls +	41(164)	79 (316)	38 (76)	93 %

* Average within the period from flashover (room temperatures > 600 °C) until start of decay of initial fire

[^] During the first 12 minutes of experiment 1, the initial fire burned with HRR 62 kW, but was adjusted.

The HRR of the propane fire was 164 kW/m² floor and the average total HRR was 354 kW/m². This total HRR is higher than 250 kW/m² recommended by Eurocode 1991-1-2 table E.5 as a maximum HRR for determining design fires for fires in dwellings and offices.

On average, the CLT contributed 90 kW/m² CLT to the total HRR during burning of the propane fire, but values up to 122 kW/m² were observed. Compared to the propane HRR, the relatively largest contribution of the CLT was in experiment 2 with 3 CLT walls. The HRR was increased with an additional 168 %.

Contrary to the first series of experiments, where the HRR and MLR were found to peak significantly within the first minute of testing, this did not occur in these experiments. It is reasonable to assume this is due to the fact that the CLT was not instantly exposed to a high heat flux, as occurred in the first series after opening the shutters, but more gradually due to the initial propane fire.

Temperatures in the compartments typically rose fast to approximately 900 °C, followed by a more gradual increase to 1000-1170 °C. Table 7.4 provides average and maximum room temperatures during burning of the propane fire.

Table 7.4 Room temperatures during burning of the propane fire

Experiment	Setup	Avg. at 0,4 m* [°C]	Max. at 0,4 m [°C]	Avg. at 0,2 m* [°C]	Max. at 0,2 m [°C]
1	1 back wall	965	1029	1121	1173
2	1 back-, 2 side walls	1001	1102	1054	1143
3	2 side walls	989	1081	979	1107
4	2 side walls	1045	1100	982	1085
5	2 side walls +	1025	1100	919	996

* Average within the period from flashover (room temperatures > 600 °C) until start of decay of initial fire

Temperatures in the CLT also increased during flaming combustion. Temperature typically stabilized shortly at 100 °C, because energy was used to vaporize the water. Significant temperature differences could be observed between adjacent layers, indicating a steep temperature gradient as the heat propagated through the material. Depending on the moment when the 300 °C isotherm reached the thermocouples at 20 mm depth in the various measurement locations in the CLT walls, the samples were switched.

The heat flux was measured in the middle of the compartment opening. It is expected this total heat flux during the initial fire was made up of radiation of various hot surfaces and the flames, as well as convection due to the flames touching the heat flux sensor. This heat flux increased slower than the room temperatures, because surfaces first heated up. Table 7.5 provides average and maximum heat flux values during burning of the propane fire.

Table 7.5 Heat flux in middle of compartment opening during burning of the propane fire

Experiment	Setup	Avg. in opening [kW/m ²]	Max. in opening [kW/m ²]
1	1 back wall	101	142
2	1 back-, 2 side walls	147	189
3	2 side walls	126	176
4	2 side walls	146	172
5	2 side walls +	118	161

* Average within the period from flashover (room temperatures > 600 °C) until start of decay of initial fire

The heat flux measured in the opening of the compartment can be converted to an estimation of the radiative emission by the CLT walls, based on configurations factors. However, considering the fact that the heat flux sensor is hit directly by the flames, the effect of radiation between the walls cannot be singled out. However, it can be expected the CLT wall received a similar heat flux to those measured in the opening, because these walls were hit by the flames as well.

During the propane fire, some fall-off occurred in experiments 2, 3 and 4. This occurred typically around 15 – 16 minutes, but in experiment 4 also at 25 minutes. At these moments the 300 °C isotherm had not yet reached the PU adhesive. This suggests these pieces had not actually delaminated, but were pieces of char breaking off. Furthermore, the amount of fall-off in this stage was relatively few compared to what occurred after the charring front had progressed further into the material.

Fall-off in this stage of the fire typically resulted in a slight increase in HRR, but hardly affected temperatures in the compartment. An exception was experiment 4, in which small drops in temperature were observed when delamination occurred. This might be due to the fact that some energy was used to heat up the newly exposed wood.

When the thermocouple data indicated the temperatures at 20 mm depth exceeded 300 °C, the propane flow was reduced to 0 %. Experiments 3, 4, and 5 with a similar configuration, reached this moment approximately at the same time; at 24, 27, and 26 minutes respectively.

In experiment 1, this moment occurred later, possible due to the fact that only 1 CLT wall contributed to the fire. In experiment 2, this moment also occurred later, after 33 minutes. This was possible due to the fact that the propane fire was reduced only when all temperatures at 20 mm depth exceeded 300 °C. The 300 °C isotherm propagated relatively slow through the back wall, possibly due to its lower configuration factor with regards to the other CLT surfaces.

7.3.2 Transformation from flaming to smouldering to extinguished

Once the propane flow was reduced to 0 %, the initial fire decayed. The results for the remainder of the experiments were quite different. The performance of the compartments, in terms of the “route” in the model of self-extinguishment, is shown in the figure 7.3.

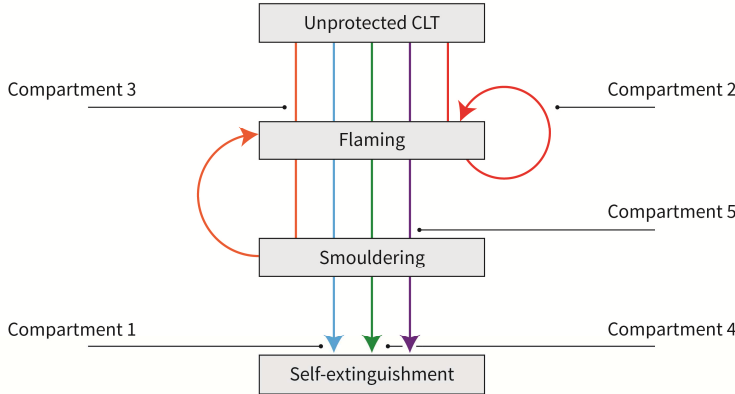


Figure 7.3 Compartments 1 -5 and their relation to the model of self-extinguishment.

Compartments 1, 4 and 5 self-extinguished, while compartment 2 and 3 burned through in flaming combustion. Delamination and fall-off was observed to play a major role in whether the various transformations between phases were made. Table 7.6 presents an overview of the transformations, the influence of delamination and fall-off, and the conditions at which these occurred.

Table 7.6 Overview of transformations, the influence of delamination and fall-off, and the conditions at which these occurred, in the 5 compartments.

	Transform. Flaming → smoulder	Conditions during transformation	Delamination and fall-off	Conditions during delamination	Transform. Smoulder → extinguished
1	Yes, 5 min after decay*	HRR: 10 kW Room T: 400 °C Flux: 30 kW/m ²	Yes, during smoulder; 17 min after decay However, this did not result in (local) flaming	HRR: 6 kW Room T: < 225 °C Flux [^] : 9 kW/m ²	Yes
2	No	N.a.	Yes, multiple times during flaming; e.g. 17, 39, 61 min after decay As a result, the fire remained in flaming	HRR: >32 kW Room T: >650 °C Flux: >70 kW/m ²	No
3	Yes, 26 min after decay	HRR: 10 kW Room T: 400 – 500 °C Flux: 30 kW/m ²	Yes, multiple times during smouldering As a result, the fire transformed back to flaming eventually	HRR: 10 kW Room T: 250 – 500 °C Flux: 13 – 23 kW/m ²	No
4	Yes, 13 min after decay	HRR: 15 kW Room T: 450 – 600 °C Flux: 30 kW/m ²	Yes, multiple times during smouldering , e.g. 40, 56, 102 min after decay Did not result in transform. back to flaming	HRR: <5 kW Room T: <250 °C Flux: <10 kW/m ²	Yes
5	Yes, 5 min after decay	HRR: 10 kW Room T: 400 – 550 °C Flux: 30 kW/m ²	No delamination or fall-off during flaming and smouldering	n.a.	Yes

*decay = decay of propane fire

[^]this heat flux is measured in the opening of the compartment and will be translated into an estimation of the flux on the CLT.

Compartments that burned-through

In compartment 2 with three walls, delamination resulted in sustained flaming combustion. A smouldering phase was never reached. It can be expected flaming was sustained because new wood became exposed when the temperatures in the compartment were still high, > 650 °C, and a high heat flux was present, 70 kW/m². This heat flux can be translated into an estimation of 49 kW/m² on the middle of side walls and 43 kW/m² on the middle of the back wall¹⁰.

¹⁰ Assuming pure radiative heat transfer, based on the heat flux in the opening and the configuration factors of the compartment, a CLT surface temperature can be estimated. This information can then be used to estimate the heat flux on the various walls. An emissivity of 0,8 is assumed, based on Eurocode 1995-1-2 for wood surfaces.

In compartment 3 with two side walls, the fire transformed from flaming to smouldering, when room temperatures were 400–500 °C and the estimated heat flux on the middle of the side walls was 12 kW/m². Subsequently, delamination resulted in local flaming and eventually to a transformation from smouldering back to flaming in a “second flash-over”.

Right before this transition occurred, room temperatures were 250–350 °C and the heat flux on the middle of the side walls was estimated to be 8 kW/m². These conditions are lower than during the transformation from flaming to smouldering. This might be explained by the fact that delamination and local flaming on multiple locations resulted in higher temperatures and heat fluxes. When even more pieces delaminated, this resulted in a “chain reaction” and eventually a second flash over.

Compartments that extinguished

In compartment 1 with only a CLT back wall, the fire was able to transform from flaming to smouldering, when room temperatures were 400 °C and the estimated heat flux on the middle of the side walls was 12 kW/m². Delamination and fall-off occurred when room temperatures were < 225 °C and when the estimated heat flux on the middle of the side wall was < 3,5 kW/m². This did not result in a transformation from smouldering back to flaming. Subsequently, the fire extinguished.

In compartment 4 with an equal configuration as compartment 3, the fire was able to transform from flaming to smouldering when room temperatures were 450–600 °C and the estimated heat flux on the middle of the side walls was 12 kW/m². Delamination and fall-off occurred when room temperatures were < 250 °C and when the estimated heat flux on the middle of the side wall was < 4 kW/m². Some local flaming occurred, but this did not result in a transformation from smouldering back to flaming. Contrary to compartment 3 which continued burning a second flash-over, compartment 4 extinguished.

In compartment 5, with two CLT side walls and a 40 mm layer thickness of the top lamella, the fire was also able to transform from flaming to smouldering. This occurred when room temperatures were 400–550 °C and the estimated heat flux on the middle of the side walls was 12 kW/m². No delamination and fall-off were observed. The CLT extinguished shortly after the propane fire was stopped. Self-extinguishment occurred when the charring front was approximately halfway within the thickness of the first lamella.

Delamination and lamella thickness as conditions for self-extinguishment

As was predicted, the experiments illustrate delamination can either sustain flaming combustion, or a transformation smouldering back to flaming. The char front reaches the polyurethane adhesive layer between two CLT layers. The adhesive fails and delamination occurs; this can result in fall-off. Due to the vertical orientation of the walls, fall-off was not entirely predictable, as was the case in the experiments of Frangi *et al.* (2009), where horizontal configurations were exposed from below. However, there were moments when delamination occurred in multiple experiments, e.g. at 17 and 40 minutes after decay of the propane fire.

Fall-off exposed the new layers of wood, which rapidly contributed combustible gases if compartment conditions were sufficiently “hot”. This was the case in compartments 2 and 4, in which flaming was sustained or smouldering was transformed back to flaming after fall-off.

In these experiments, the “hot” conditions were found to be room temperatures of $> 250\text{ °C}$ and heat flux on the middle of the walls of $> 8\text{ kW/m}^2$. Subsequently, the HRR and temperatures rose and other CLT surfaces were exposed to a higher heat flux. This made delamination of these other CLT surfaces more likely, which could result in a “chain reaction”.

However, in compartments 1 and 4 delamination did not result in sustained flaming. Compartment conditions were sufficiently “cooled-down” by the time delamination occurred. Unsufficient combustible gases were released when uncharred wood became exposed (compartment 1); or some local flaming occurred, but insufficiently to result in a transformation back to flaming (compartment 4). The conditions at which delamination was “safe” were found to be room temperatures of $< 250\text{ °C}$ and an estimated heat flux on the wall of $< 4\text{ kW/m}^2$.

Relying on compartment conditions to sufficiently cool down to allow for safe delamination seems risky, considering its unpredictable nature. This was illustrated by compartments 3 and 4, which had equal configurations, but showed a big difference in the results; one burned through, while the other extinguished. This indicates that even at equal conditions there is a range of possible outcomes. This is seems partly due to the unpredictable nature of delamination and fall-off. Further research would be recommended to verify conclusions.

Finally, in compartment 5, an increased thickness of the lamella (40 mm instead of 20 mm) prevented delamination. As a result, the fire transformed from flaming to smouldering. The increased thickness ensured the charring front seized propagating within the thickness of the top lamella. This was recognized as a possible solution to prevent delamination by the model of self-extinguishment. The following conditions can be formulated with regard to preventing delamination.

A sufficiently thick top lamella can prevent delamination and fall-off, when the charring front seizes within the thickness of this lamella.

The application of a sufficiently thick lamella as to prevent delamination and fall-off was observed in only one experiment. Further research would be required to increase confidence in this approach. Nevertheless, its potential is noted in the performance of compartment 5, where no fall-off was observed at all.

When delamination is prevented in this way, its disturbing influence in the model of self-extinguishment is prevented. As a result, the fire can make the transition from flaming to smouldering. Subsequently, the conditions of heat flux and air flow become important again.

Heat flux and air flow as conditions for self-extinguishment

The compartments that smouldered had such configurations, that (as long as delamination and fall-off did not interfere) the heat flux received by the CLT led was below the threshold value. This is in line with what was predicted before the experiments.

7.3.3 Total energy released by the CLT

The contribution of the CLT to the fire can be expressed in terms of the fire load / total energy released. Table 7.7 depicts the total energy released during the experiment, by the propane fire, and by the CLT.

Table 7.7 Energy released during the experiments

Experiment	Setup	Propane [MJ] (/m ² floor)	Total [MJ] (/m ² floor)	CLT contribution [MJ] (/m ² CLT)	increase
1	1 back wall	112 (448)	169 (676)	57 (228)	51%
2	1 back-, 2 side walls	77 (308)	386 (1544)	309 (412)	401%
3	2 side walls	55 (220)	240 (960)	185 (370)	336%
4	2 side walls	62 (248)	183 (732)	121 (242)	195%
5	2 side walls +	63 (252)	134 (536)	71 (142)	113%

In the experiments where the compartments did not self-extinguish, the CLT contributed significantly to the fire; up to 412 MJ/m² CLT, an increase of up to 401 % of the fire load. In the experiment where the CLT did extinguish, the contribution of the CLT remained limited to up to 242 MJ/m². The lowest contribution was in compartment 5 where no delamination occurred; 142 MJ/m². Note these values are obtained under specific conditions of the experiments, with a lot of CLT compared to floor area.

Figure 7.4 illustrate the contribution of the CLT to the fire in experiments with two CLT walls where burn-through (compartment 3) and self-extinguishment (compartment 5) occurred.

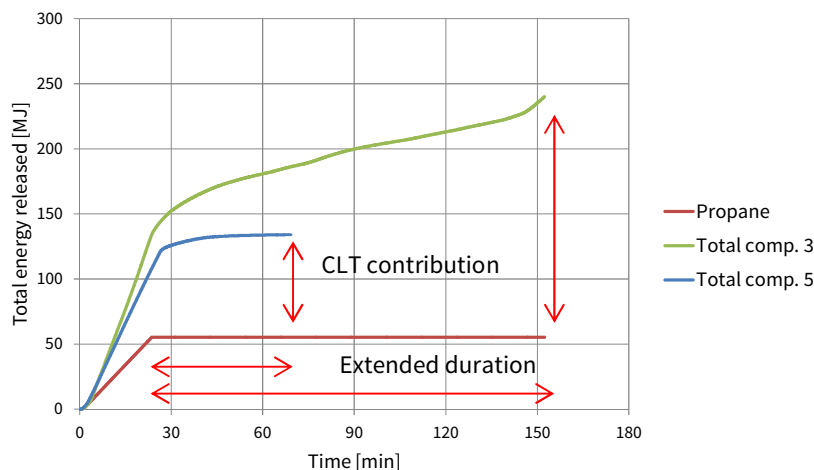


Figure 7.4 Total energy released and propane fire energy released for compartments 3 and 5.

The exposed CLT can significantly increase the fire load and total energy released in a compartment, as well as extend the duration of the fire. The total energy released and the duration of the fire increase even further when delamination and fall-off result in prolonged flaming. It would be recommended to investigate how this influences the severity and development of the fire - compared to the standard fire - and the fire resistance of members. The standard fire might not be conservative.

7.3.4 Charring rates and temperatures

Appendix J investigates the charring rates based on the temperatures in the CLT and compares these to the predicted values and those provided by Eurocode 5. Charring rates were typically higher than provided by the Eurocode 5, possible due to the relative severe propane fire compared to the standard fire in the beginning of the experiments, the contribution of the CLT to the fire, and the fact that delamination increases the overall charring rate.

Furthermore, the temperatures also show that the smouldering zones that were clearly visible in the first series of experiments were not really observed in this second series of experiments. This can be explained by the fact that steady smouldering of the CLT did not occur in these compartments. The compartments either burned through in flaming combustion, or smouldered and extinguished. Burn-through by means of sustained smouldering, as was observed in the first series of experiments, did not occur.

7.4 Conclusions

Two series of experiments were conducted to investigate the transitions from flaming combustion to smouldering combustion and from smouldering combustion to self-extinguishment, and the conditions at which these take place.

The first series of experiments investigated the heat flux and air flow conditions at which the CLT can transform from smouldering to self-extinguishment by exposing small CLT samples to heat fluxes in a cone calorimeter. It was found an externally applied heat flux is required to sustain smouldering. Absence of this flux resulted in extinguishment. The threshold flux at which self-extinguishment occurs is in the range of 5 to 6 kW/m². The experiments on which this value is based showed a good repeatability, increasing the confidence in this result.

Furthermore, an additional airflow over the samples was found to be of influence. At a heat flux of 6 kW/m², an airflow with speed 0,5 m/s resulted in quick self-extinguishment, while an airflow with speed 1,0 m/s resulted in quick burn-through. Based on these results, it can reasonably be assumed that at heat fluxes ≤ 6 kW/m², an airflow with a speed of $\leq 0,5$ m/s results in self-extinguishment. Air flow was investigated to a limited degree, and it would be recommended to further investigate a range of airspeeds in combination with various heat flux exposures.

The second series of experiments investigated the complete model of self-extinguishment by subjecting medium-scale compartments to a propane fire. Configurations with one, two, or three CLT walls were investigated. The fire and performance of the CLT depended heavily on delamination.

Delamination occurred when the charring front reached the polyurethane (PU) adhesive, which then lost bonding. This resulted in fall-off, exposing new layer of wood to the fire. This could interfere in the transitions from flaming to smouldering to extinguishment.

In one compartment with three CLT walls fall-off occurred when the compartment was still in flaming combustion. New layers of wood contributed rapidly to the fire, and as a result flaming was sustained. In another compartment with two CLT walls, the CLT initially transformed from flaming to smouldering. However, delamination and fall-off transformed it back to flaming in a “second flash-over”.

In these two compartments fall-off occurred when compartment conditions were still sufficiently “hot”, with room temperatures of $> 250\text{ }^{\circ}\text{C}$ and an estimated heat flux on the CLT of $> 8\text{ kW/m}^2$. These conditions were lower than during the transformation from flaming to smouldering, which might be explained by the fact that delamination and local flaming on multiple locations can result in a “chain reaction”. As a result, flaming was sustained and the CLT continued burning.

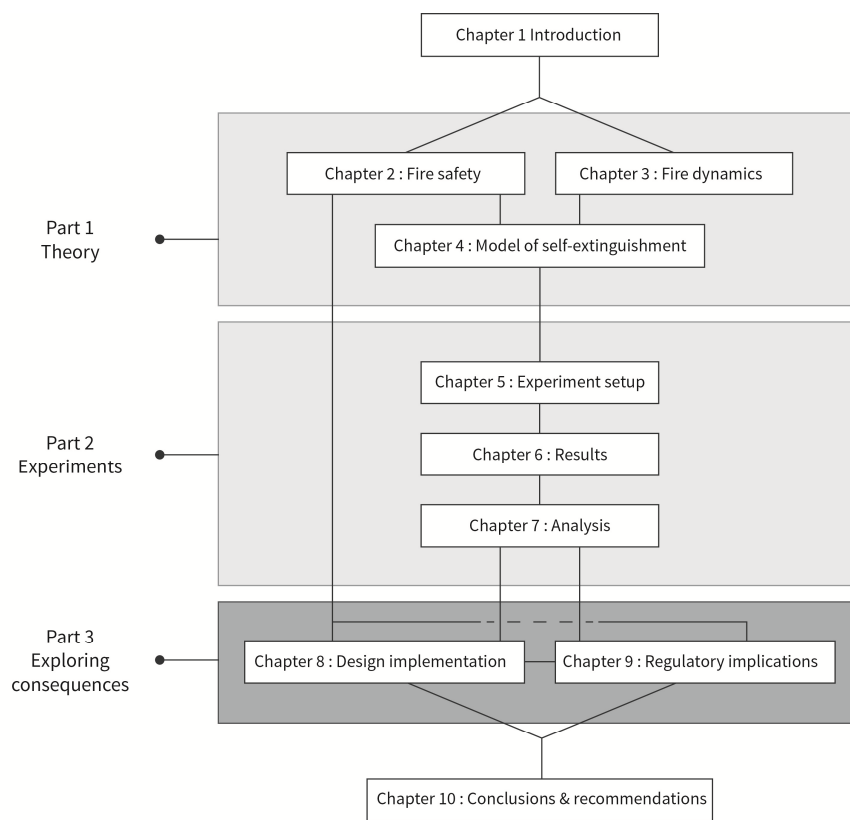
In two other compartments, with one and two CLT walls respectively, delamination and fall-off occurred when conditions were sufficiently “cooled-down”, with room temperatures of $< 250\text{ }^{\circ}\text{C}$ and an estimated heat flux on the CLT of $< 4\text{ kW/m}^2$. As a result, fall-off did not sustain flaming. However, relying on delamination to occur when the compartment has cooled down was found risky, due to its unpredictable nature. Even at equal conditions (2 CLT walls) there were multiple possible outcomes. This is seems partly due to the unpredictable nature of delamination and fall-off and further research would be recommended in general to verify conclusions.

Delamination and fall-off were avoided in a fifth compartment with two CLT walls. This was achieved by applying a thicker top lamella. As a result the charring front did not reach the PU adhesive. It was found that a sufficiently thick top lamella can potentially prevent delamination and fall-off, when the charring front seizes within the thickness of this lamella. This was observed in one experiment and further investigation is recommended to increase confidence in this approach.

These three compartments smouldered and had such configurations that the heat flux on CLT (depending on the amount of exposed CLT, its temperature, other hot surfaces, and the compartment configuration) during smouldering was below 5 kW/m^2 . No additional airflow was present and the CLT extinguished.

In all five compartments, when compared to the propane fire, the CLT walls significantly increased the heat release rate and the total energy released, and extended the duration of the fire. These were even further increased when delamination and fall-off result in prolonged flaming.

Part 3: Exploring consequences



“One can enjoy a wood fire worthily only when he warms his thoughts by it as well as his hands and feet”

- Odell Shepard

Design implementation

8.1 Introduction

While the main research goal focusses on the conditions for self-extinguishment, the “meta-goal” extends to translating new insights to design guidance. This chapter aims to answer the research question:

How can self-extinguishment of cross-laminated timber be taken into account in the design?

In chapter 2 it was concluded that the structural fire safety design of exposed timber structures currently does not take self-extinguishment into account. Based the results of the experiments, a potential assessment method is formulated that does incorporate self-extinguishment.

8.2 Context and robustness of design implementation

It must be stressed that the method presented here is a first suggestion. First of all, it is based on results from limited amount of experiments. These experiments were performed under specific conditions, e.g. with regards to the fire development, fuel load, ventilation conditions, CLT build-up, type of adhesive, wood species, and compartment configuration. In reality, a large number of parameters can influence the fire development and the structural response.

Furthermore, the experiments showed that even with equal conditions, results can vary. This was especially the case for delamination and fall-off. Two identical compartments (3 and 4) showed different results due to the unpredictable nature of delamination and fall-off. In this context it must also be noted that the first series of experiments did show a good repeatability. The threshold value for self-extinguishment of 5-6 kW/m² is assumed to be reasonably likely.

Another issue is the scale of the experiments. At this stage, it remains unclear how applicable the results are for full sized compartments. Furthermore, the assessment method will assume a certain fire development, which might not be accurate.

It should also be noted that while the method presents self-extinguishment as a single measure, in reality it might be achieved as part of a complete concept of fire safety provisions, in combination with active measures such as sprinkler activation and fire-brigade intervention.

Considering these points, extrapolation of the results and the assessment method should only be done with extreme care. This chapter should be viewed in that context. The assessment method would require more research and validation before it could be applied in practice.

8.3 Assessment method

The assessment method consists of two steps, as depicted in figure 8.1. The first step is to ensure the CLT can transform from flaming to smouldering combustion, by preventing delamination by means of sufficiently thick lamellas. The second step is to ensure the smouldering CLT is able to make the transition to self-extinguishment, depending on the conditions of heat flux and airflow. Based on these steps, this chapter also investigates the implications with regards to actual compartment configurations.

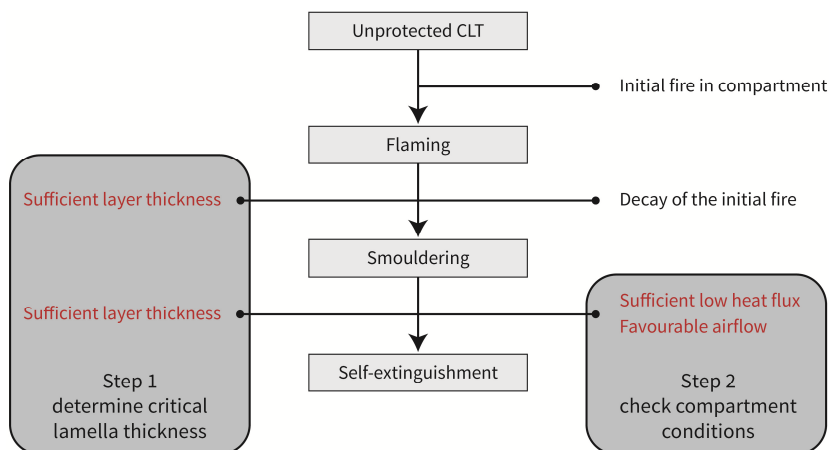


Figure 8.1 Proposal for an assessment method for self-extinguishment of CLT structures.

8.4 Step 1 - determination of critical lamella thickness

Delamination can interfere in achieving self-extinguishment. The first step is to ensure the CLT does not delaminate by applying a “critical lamella thickness” to the outer layer. The experiments showed a sufficiently thick top lamella can prevent delamination and fall-off, and ensure the fire can transform from flaming to smouldering by preventing the charring front from reaching the PU adhesive¹¹.

To determine the critical lamella thickness, a total charring depth should be calculated. This requires a design fire with a decay phase, because a finite charring depth needs to be obtained. Furthermore, this design fire needs to take into account the contribution of the CLT to the fire.

The standard fire does not meet these requirements. Alternatively, the parametric natural fire can be used. This design fire, as described in Eurocode 1992-1-2, decays and is dependent on input regarding the fire load, ventilation conditions, and boundary conditions of the compartment.

Guidance is available for the calculation of the charring behaviour of timber exposed to a parametric fire in Eurocode 1995-1-2 annex A. This method is based on the research of Hadvig (1981) and confirmed by Olesen and Hansen (1992), Olesen and König (1992), and König and Walleij (1999). The formulas from the original research will be used here. The approach of step 1 is depicted in the figure 8.2.

¹¹ It could be possible to achieve self-extinguishment in the 2nd or 3rd layer, after delamination of the 1st. However, this seems risky. It is difficult to control when delamination occurs and how it affects the fire. This was illustrated by compartment 3 and 4. These were identical and both delaminated during the experiments. However, compartment 3 continued burning, while 4 self-extinguished in the 2nd and 3rd layer. Preventing delamination seems more reliable.

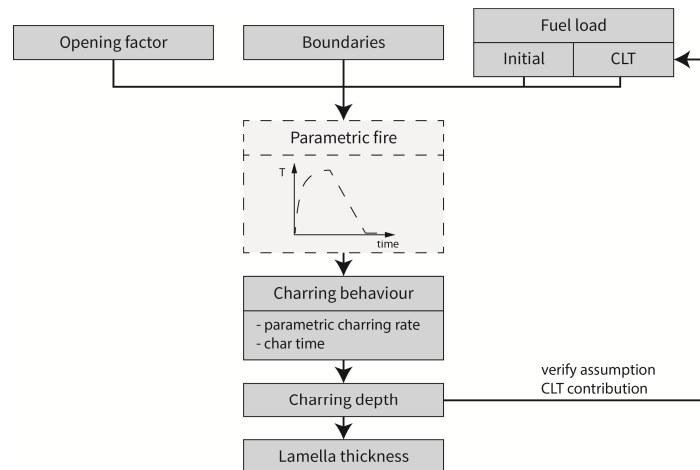


Figure 8.2 Step 1 - Determination of a lamella thickness based on the parametric charring behaviour.

8.4.1 Input

The approach does not require the calculation of the exact parametric fire curve, but determines the charring behaviour directly from the input.

Opening factor

The parametric fire takes into account the opening factor O in the compartment, which represents the ventilation conditions. The opening factor can be calculated according to equation 8.1.

$$O = \frac{A_v}{A_t} \cdot \sqrt{h_{eq}} \quad (\text{m}^{1/2}) \quad (\text{Eq. 8.1})$$

Where

- A_v = total area of all openings in vertical boundaries (m^2)
- A_t = total area of floors, walls, and ceilings, including the openings (m^2)
- h_{eq} = weighted average of heights of all vertical openings (m)

Boundaries

The Eurocode parametric fire also takes into account the thermal adsorption of the boundaries. However, the method presented here is based on the original research, which does take the boundaries into account.

Fuel load

The parametric fire takes into account the total fuel load in the compartment. This should include the CLT contribution in addition to the “initial” fuel of the compartment contents. For the initial fuel load of the room contents, Eurocode 1991-1-2 appendix E offers values for various functions. A fuel load for the CLT needs to be assumed and would depend on the development and duration of the initial fire as well as the CLT contribution itself. For a high fuel load of the initial fire, the contribution of the CLT should also be assumed high. Values in the range of 80 - 400 MJ/m^2 of the CLT surface seem reasonable¹².

¹² These values are based on charring depths of 15 to 60 mm, an EHC of 14,2 MJ/kg, and a density of 450 kg/m^3 of the CLT. Furthermore, this range is consistent with the results, as well as the experiments by McGregor (2012).

8.4.2 Charring behaviour

Based on the opening factor and fuel load, the parametric charring rate is calculated, as expressed in equation 8.2.

$$\beta_{par} = k_p \cdot \beta_n \text{ (mm/min)} \quad (\text{Eq. 8.2})$$

Where

- β_{par} = parametric charring rate (mm/min)
- k_p = parametric char factor (-)
- β_n = notional charring rate (mm/min)

The char factor depends on the opening factor and is given in equation 8.3 and depicted in figure 8.3. If the Eurocode approach is adopted, this formula changes to incorporate the effect of the boundaries.

$$k_p = 1,5 \cdot (5 \cdot O - 0,04) / (4 \cdot O + 0,08) \quad (\text{Eq. 8.3})$$

Due to the decay phase of the parametric fire, the charring rate is assumed to slow down after an initial period t_0 and linearly decrease to zero over a period of $2t_0$, as depicted in figure 8.4.

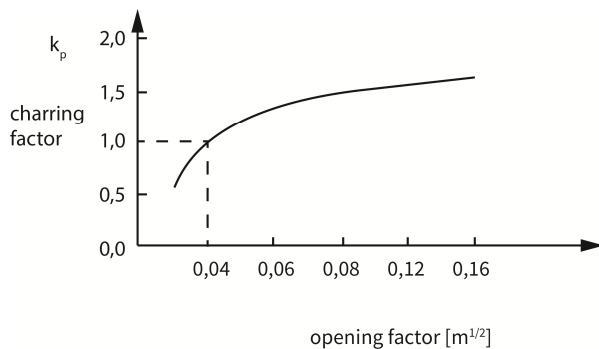


Figure 8.3 The parametric char factor as ratio of the notional charring rate. From Buchanan (2009).

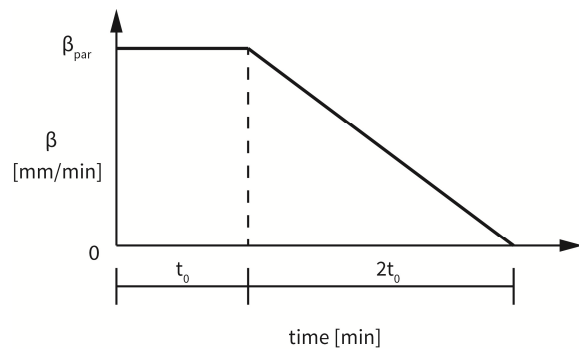


Figure 8.4 The relationship between parametric charring rate and time. From Eurocode 1995-1-2.

The initial char time t_0 is dependent on the fire load density and is obtained from equation 8.4. If the Eurocode approach is adopted, the factor 0,006 changes to 0,009.

$$t_0 = 0,006 \cdot \frac{q_{t;d}}{O} \quad (\text{Eq. 8.4})$$

Where

- t_0 = initial char time (min)
- $q_{t;d}$ = design fire load density related to the total area of floor, walls and ceilings which encloses the compartment (MJ/m^2)

8.4.3 Charring depth

The parametric charring rate and the charring time have now been calculated. Because the charring rate decreases to zero, a finite charring depth can be determined with equation 8.5.

$$d_{char} = 2 \cdot \beta_{par} \cdot t_0 \quad (\text{Eq. 8.5})$$

Where d_{char} = final charring depth (mm)

Based on the charring depth, the total amount of burned CLT in kg can be estimated. This can be multiplied with the effective heat of combustion and checked against the assumption of CLT contribution to the fuel load. After a couple of iterations, a final charring depth is achieved.

8.4.4 Lamella thickness

The lamella thickness of the first layer of CLT should be larger than the calculated charring depth, in order to prevent delamination. For example, it seems reasonable to add 5 mm additional thickness for safety and then round up to the nearest commercially available lamella thickness.

The charring rate can also be used to calculate the residual cross-section. Corner rounding is taken into account, because the notional charring rate is used. To allow for the reduced strength of the residual cross-section, the load capacity should be calculated using a reduction factor k_f , given in equation 8.6.

$$k_f = 1,0 - 3,2 \cdot \frac{d_{char}}{d} \quad (\text{Eq. 8.6})$$

Where d = original dimension of the cross-section (mm)

8.4.5 Remarks step 1

The Eurocode approach and the approach of the original research differ. In the original research, the charring factor depends on the ventilation conditions. The Eurocode also takes into account the thermal adsorption of the boundaries, based on the density, specific heat capacity, and thermal conductivity of the materials. Furthermore, the Eurocode applies a factor 1,5 to the initial char time.

The reasons for the changes made by Eurocode 1995-1-2 are unclear. It might be reasonable to assume these changes were the result of a wish to incorporate the boundary conditions, introduce additional safety, and make approach more in line with wishes from various countries involved in the process of creating the Eurocode.

The original approach was developed based on (full-scale) testing. Furthermore, it was applied to compartment 5 of the second series of experiments, and was found to provide an accurate prediction. The Eurocode approach resulted in a significantly higher final charring depth. This difference might be due to wrong assumptions regarding the boundaries, as well as additional safety provided by the Eurocode. Reference is made to the appendix K where the calculation is provided for both approaches.

In this assessment method, the original approach was used, because it corresponded well with experimental data. The Eurocode approach might result in a more conservative lamella thickness, although sections sizes might become uneconomical. Further research would be recommended to explore differences between the methods and potentially bring the Eurocode approach more in line with the experimental results.

A final remark is that the Eurocode 1991-1-2 limits the use of the parametric fire to relative small compartments of $\leq 500 \text{ m}^2$ and $\leq 4 \text{ m}$ in height. Expansion of this model for larger compartment would be recommended. Alternatively, another model might be developed for fires in larger compartments.

8.5 Step 2 - check configuration for potential self-extinguishment

Assuming delamination is prevented and the CLT reaches a smouldering phase, the second step in the assessment method is to ensure the smouldering CLT can make the final transition to self-extinguishment. To make the transition to self-extinguishment, the heat flux and airflow conditions must be checked during smouldering. The design approach of step 2 is depicted in the figure 8.5, using compartment 5 from experiment series 2 as an example.

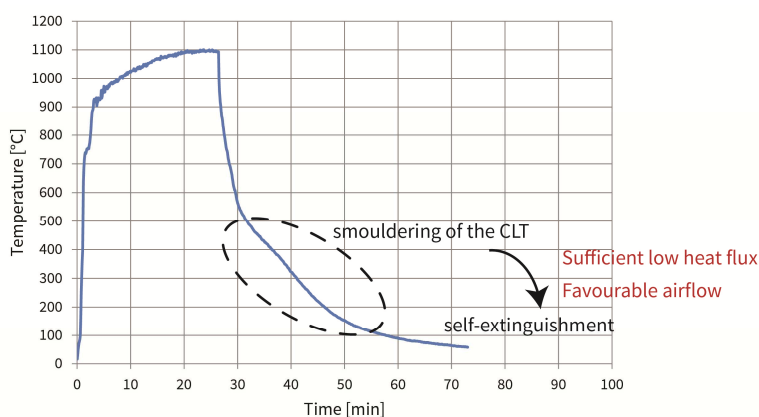


Figure 8.5 Step 2 - Checking airflow and heat flux conditions during smouldering.

8.5.1 Check airflow condition

The airflow was found to have influence on the smouldering of the CLT and the potential to self-extinguish. However the investigation of the air flow was limited to two air speeds at a 6 kW/m^2 exposure. An additional air flow of $0,5 \text{ m/s}$ resulted in quick self-extinguishment, while an additional air flow of $1,0 \text{ m/s}$ resulted in a quick burn-through.

It is recommended to investigate more speeds and combinations with fluxes and relate these to real compartments. For now, the condition of air flow is not taken into account in this assessment method.

8.5.2 Check heat flux condition

Based on the geometry and orientation of the compartment, the heat flux on the CLT during smouldering can be calculated. This flux will predominantly be (cross-) radiation between the smouldering CLT and other hot surfaces. The energy emitted to a receiver can be calculated with equation 8.7.

$$E = \varphi \cdot \varepsilon \cdot \sigma \cdot T^4 \quad (\text{Eq. 8.7})$$

Where	E	= energy emitted (kW/m ²)
	φ	= configuration factor (-)
	ε	= emissivity (-)
	σ	= Stefan-Boltzmann constant (5,67 x 10 ⁻⁸ W/m ² K ⁴)
	T	= temperature (K)

The energy emitted by the smouldering CLT can be based on the estimation of the CLT surface temperature of 400 °C, as found in experiment series 1. The emissivity of char can be taken as 0,8, as suggested by Eurocode 1995-1-2 for wood surfaces.

The configuration factor takes into account the geometrical relationship between the emitter and the receiver. It is important to consider the CLT with the most unfavourable configuration with regards to other hot objects and smouldering surfaces. Drysdale (2012) and Eurocode 1991-1-2 appendix G provide calculation methods for the configuration factor, and refer to values for common shapes and geometries in literature. Other hot objects and surfaces have to be taken into account in a similar way.

By adding up the energy emitted by various sources, the radiative heat flux on the CLT with the most unfavourable configuration can be calculated and compared to the threshold flux. This flux was found to be 5 – 6 kW/m². A conservative approach would be to ensure the resulting heat flux on the CLT is limited to ≤ 5 kW/m². The heat flux check is performed as an example for compartment 5 in the appendix K.

8.5.3 Remark step 2

A “steady state” heat flux check on the CLT with the most unfavourable configuration, as suggested above, might be too conservative, because it does not account for the interactive nature of smouldering surfaces in the compartment.

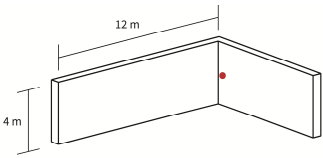
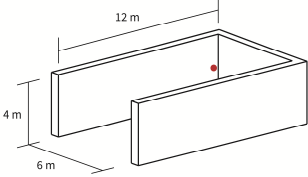
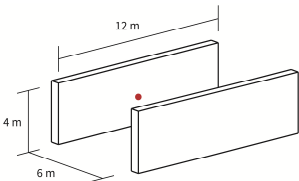
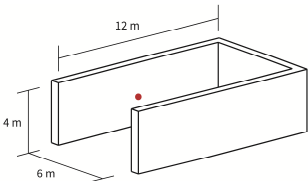
For example, it might be possible for one area of CLT to receive a heat flux of 10 kW/m² and keep smouldering, while another receives 5 kW/m² and self-extinguishes. Because sustained smouldering is dependent on the externally applied heat flux, the extinguishment of the latter section will influence the heat flux on the first section. The flux on the first section might drop from 10 kW/m² to 5 kW/m², which would result in self-extinguishment as well.

These interactions make it difficult to assess a compartment solely in a steady state. Further research would be recommended on this interactive nature and the implications on the assessment method. For now, it is not taken into account and most unfavourable configuration is checked in a steady state.

8.6 Practical applicable configurations

Some examples of “real” compartment configurations and the resulting heat flux on the CLT are provided in table 8.1. The configurations are limited to CLT walls. Other hot objects are not taken into account, nor is the interactive nature of the smouldering. The flux is calculated assuming a char emissivity of 0,8 and a CLT temperature of 400 °C. These configurations are provided for illustrative purposes; extrapolation to real compartments should be done with care, as discussed at the beginning of this chapter.

Table 8.1 Possible CLT wall configurations and the resulting heat flux at the location of the dot.

Configuration	Factor	kW/m ²	Configuration	Factor	kW/m ²
<p>Configuration 1</p> 	0,49	4,56	<p>Configuration 3</p> 	0,65	5,96
<p>Configuration 2</p> 	0,26	2,42		0,31	2,88

In configurations 1 and 2 the heat flux on the CLT remains below 5 kW/m². In configuration 3 the heat flux in the corner is just above 5 kW/m², but at most other locations below 5 kW/m².

8.7 Relation to previous work

The assessment method and the findings of this work were viewed in relation to previous work by Longhi (2012) in appendix L. Based on his work, it would be recommended to further investigate the influence of the fire load on self-extinguishment and tie this in the results of this work. Furthermore, it would be recommended to compare the method used by Longhi (based on natural fire modelling and finite element heat transfer software) with the method proposed in this work and investigate differences and similarities.

8.8 Conclusions

This chapter presented a potential assessment method that incorporates self-extinguishment. This method corresponded well with the results from the experiments, but is a first suggestion and extrapolation to real compartments should be done with care. The method would require more research and validation before it could be applied in practice. Furthermore, it could be further enhanced by incorporating the condition of airflow and taking account for the interactive nature during smouldering combustion.

The method consists of two steps. First, a critical lamella thickness is determined to be applied to the first layer of CLT in order to prevent delamination and ensure the CLT can transform from flaming to smouldering. This method is based on the calculation of a total finite charring depth for a parametric natural fire exposure. The method takes into account the ventilation conditions and the fuel load in the compartment, including an estimation of the contribution of the CLT. It is suggested that the lamella thickness of the first layer of CLT exceeds the calculated charring depth by a margin.

Secondly, assuming delamination is prevented and the CLT reaches a smouldering phase, the smouldering CLT needs to be able to make the transition to self-extinguishment. To ensure this transition, the heat flux on the CLT with the most unfavourable configuration should be ≤ 5 kW/m². This can be achieved by estimating the temperatures of various surfaces and calculating the heat flux on the CLT.

Regulatory implications

9.1 Introduction

In chapter 2, various regulatory issues were identified for tall timber buildings. It was concluded that more insight into the fire behaviour of the exposed timber structure, including self-extinguishment, is required.

Currently, self-extinguishment is not part of the fire safety considerations for the structural design of tall timber buildings. Chapter 8 presented a potential assessment method that incorporates self-extinguishment in the design of unprotected timber structures, specifically for CLT. With further research, self-extinguishment might eventually become part of a total fire safety concept for tall timber buildings, including the effects of active measures, such as sprinkler activation and fire-brigade intervention. This chapter explores the implications on the regulatory issues identified in chapter 2 when self-extinguishment would be taken into account and aims to answer the research question:

What could be the implications of self-extinguishment on regulations with regards to the fire safety of timber high-rise buildings?

A focus will be on the Dutch situation. However, these implications might be applied to regulations of other countries as well. Three areas were defined in which consequences can be expected:

- Demonstrating compliance with the Dutch building regulations.
- Designing a fire-safe structure according to the Eurocode “consequence class 3” approach.
- Issues regarding perception and approval.

9.2 Context and robustness of regulatory implications

Similar to what was stated at the beginning of the chapter 8, it must be stressed that the implications presented here are a first suggestion. They assume self-extinguishment is used as part of a complete concept of fire safety for tall timber buildings.

However, this will not be realised solely based on this work. The limitations that were mentioned in paragraph 8.2 need to be taken into account. The implications that are addressed in this chapter should be seen in this context. Before self-extinguishment could actually influence these regulatory issues, it would require more research and validation.

9.3 Compliance with Dutch building code

In chapter 2 it was observed that the Dutch building code provides fire safety requirements for building of < 70 meters. Tall buildings are required a level of fire safety equal as intended by the provisions for buildings of < 70 meters.

For increasingly tall buildings, the severity of the consequences of structural failure as result of a fire increases. It was discussed in chapter 2 (by looking at the concept of risk) that the building code typically requires a higher fire resistance rating for tall buildings in order to obtain the desired level of safety. However, as a combustible material, the timber structure can continue burning and eventually collapse. Irrespective of the fire resistance rating, the level of safety intended by the code may not be achieved. A further investigating of the structural fire behaviour was suggested.

Based on the results of this work, there seems to be a potential for self-extinguishment, as part of an increased insight into the structural fire behaviour of timber structures, to contribute in demonstrating compliance with the Dutch building code. If self-extinguishment occurs in a compartment burnout, the probability of structural failure is reduced. Despite the high consequences of collapse for a tall building, the lower probability might result in a level of risk and safety as intended by the Dutch building code.

9.4 Fire-safe structure according to Eurocode consequence class 3

The Eurocode recognises the risk associated with failure of the high-rise structure and suggests it to be designed according to a consequences class 3. Failure of the structure due to fire is highly undesirable. This requires the structure to be reliably safe and robust.

The design of tall buildings in consequence class 3 requires a high degree of insight into the structural fire behaviour and potentially additional measures. An in-depth investigation of the risks associated with the fire and the structural response is needed. The Eurocode and NTA provide two options for additional measures for CC 3 buildings to ensure the structure is reliably safe and robust.

1. Structural fire calculations are based on tables and simple methods for CC 1 and 2 buildings. However, designers are to perform a risk analysis of foreseen and unforeseen accidents (including fire) according to Eurocode 1991-1-7 appendix B. If necessary, additional measures are to be taken to ensure sufficient robustness, as set out in chapter 6 of the NTA and Eurocode 1991-1-7, such as second load paths, and key elements, as well as non-structural measures. Additional supervision and control should be implemented during design and execution according to the Eurocode 1990 appendix B.
2. Structural fire calculations are based on advanced “performance-based” methods. The real behaviour of the structure is determined based on realistic natural fire scenarios and an analysis of the thermal and mechanical response. This includes the effects of thermal expansion, material properties at elevated temperatures, the redistribution of forces, and the cooling phase. Both the NTA and the Eurocode offer guidance for advanced calculations.

An assessment of the potential self-extinguishment provides increased insight required for a CC 3 building. Should the timber structure continue burning and eventually collapse, it might not be reliably safe. Furthermore it could result in damage disproportionate to the original cause, i.e. a local fire results in global collapse, rendering the timber structure insufficiently robust as well.

Alternatively, while this would require more research and validation, self-extinguishment could be taken into account as part of an overall fire safety concept for tall timber buildings. The assessment of potential self-extinguishment might be adopted in both options of additional measures.

If simple methods are used, the risk analysis should incorporate the danger of collapse due to the sustained burning of the CLT and assess the potential self-extinguishment. If advanced calculations are used, self-extinguishment could be part of the analysis with regards to its influence on the fire scenario, the thermal and mechanical response, and the effect of active measures and fire-brigade intervention.

This might contribute in demonstrating the structure is reliably safe, because it can maintain its function even in a compartment burnout. Survival of the structure could also ensure additional robustness, because it allows the structure to withstand the fire without being damaged to an extent disproportionate to the original cause.

9.5 Perception and approval

In chapter 2, it was discussed that as an innovative concept with few precedents and limited experience of designers and regulators, tall timber buildings face challenges in approval. Proposals encounter stringent levels of review, and the designer must explicitly demonstrate compliance with the functional statements and objectives in the code. These approval processes can be slow and costly.

Furthermore, some building codes cap the height of structures made from combustible materials or provide more onerous fire resistance requirements. It is reasonable to assume these restrictions are leftover from the transition from a prescriptive- to a performance-based code. The prescriptive rules might anticipate light-frame construction with a low level of inherent fire performance, and the potential superior performance of mass timber might not be taken into account.

As a result, there seems to be reluctance of designers and regulators to say these timber buildings are sufficiently safe. Timber is perceived as a material less suitable for high-rise buildings.

This caution and these restrictions in codes seem reasonable, considering the limited experience with tall timber buildings and some of the uncertainties regarding its performance in fire. However, more insight into self-extinguishment, and its role in the overall fire safety concept and the structural design, could affect the perception of the material and the way it is treated in building regulations and approval.

However, considering the implications that were addressed in the previous two paragraphs, the increased insight into self-extinguishment, its role in a total fire safety concept for tall timber buildings, and its influence on the structural design, could affect this.

With regards to the restrictions in building codes, it is the author's opinion that performance-based codes should focus on functional requirements, instead of specifying which materials can be used. A pragmatic approach might be adopted, in which any material - be it steel, concrete, or timber - poses unique design

challenges, but can be applied as long as it contributes to a safe building. While the combustibility of the timber structure will remain a point of attention, its risk should be managed properly, instead of used to discard the material for high-rise buildings.

While it would require more research and experience, more insight into the structural fire behaviour of timber, including potential self-extinguishment, might contribute to making timber available as a material for high-rise structures. Furthermore, implications of self-extinguishment would not be limited to CLT structures and high-rise buildings only, but might be applied to timber structures in general.

9.6 Conclusions

In chapter 2, regulatory issues were identified for tall timber buildings. It was concluded that more insight into the fire behaviour of the exposed timber structure is required. Self-extinguishment, as part of a complete concept of fire safety for tall timber buildings, might contribute to this.

Currently, self-extinguishment is not part of the fire safety considerations for the structural design of tall timber buildings. Chapter 8 presented a potential assessment method that incorporates self-extinguishment. This chapter explored the implications on the regulatory issues when self-extinguishment would be taken into account. Considering the limitations of this work, more research and validation would be required before self-extinguishment could actually influence these regulatory issues.

With regards to building regulations and approval, self-extinguishment might contribute in demonstrating compliance of a timber structure with the Dutch building code. Self-extinguishment, as part of an increased insight into the structural fire behaviour, reduces the probability of collapse as a result of the fire. Despite the severity consequences of collapse in a high-rise building, this reduction in probability might contribute in achieving a level of risk and safety as intended by the Dutch building code.

Furthermore, an assessment of potential self-extinguishment might be considered in the design of timber buildings according to the Eurocode consequence class 3, which requires a high degree of insight into the structural fire behaviour. Self-extinguishment, as part of an overall fire safety concept, might become part of the risk analysis and the advanced calculations in order to demonstrate the tall timber structure is reliably safe and robust.

Finally, new insight can affect the perception of the material and the way it is treated in building regulations and approval. Due to lack of precedents, limited experience, code limitations, and uncertainties regards the performance in fire, there seems to be reluctance to say tall timber buildings are sufficiently safe. Timber is perceived as a material less suitable for high-rise buildings. More insight into self-extinguishment, and its role in a total fire safety concept and in the structural design for tall timber buildings, could affect this. A more pragmatic approach might be adopted in which any material poses unique design challenges, but can be applied as long as it contributes to safe buildings. While the combustibility of the timber structure will remain a point of attention, its risk should be managed properly, instead of used to discard the material for high-rise buildings.

Eventually, insight into the structural fire behaviour of timber structures, including potential self-extinguishment, could contribute to making timber available as a material for high-rise buildings.

Conclusions and recommendations

10.1 Introduction

Based on the results of this work, this chapter presents conclusions, recommendations, and topics for further research. The main research question can now be answered.

Under what conditions is there a potential for self-extinguishment of unprotected cross-laminated timber in building fires?

Based on this research, it seems there is a potential for cross-laminated timber to self-extinguish if:

- Delamination and fall-off are prevented by applying a sufficiently thick top lamella.
 - The heat flux on the CLT during smouldering is below 5 to 6 kW/m².
 - The airflow over the CLT surface during smouldering should be limited to a speed of 0,5 m/s at heat flux exposures below 6 kW/m².
-

Furthermore, in the introductory chapter a meta-goal was formulated to incorporate the general wish to contribute to the understanding of the performance of timber in fire and translate this to design and regulations:

To increase the understanding of the performance of tall timber structures in fire and to translate new insights to design guidance and regulations.

This chapter will also provide recommendations that contribute to this meta-goal.

10.2 Conclusions

1. Self-extinguishment of CLT follows a number of phases. Under the influence of an initial fire due to burning of room contents, the exposed CLT becomes involved in flaming combustion. Once the room contents have been largely consumed and the initial fire decays, the CLT contribution is expected to decrease as well, transforming from flaming to smouldering combustion. Finally, there will be a transition from smouldering to self-extinguishment.
2. Smouldering CLT self-extinguishes when the externally applied flux is below 5 to 6 kW/m².
3. Additional airflow over a CLT surface influences the transformation from smouldering to self-extinguishment. At a heat flux of 6 kW/m², an airflow with a speed of 0,5 m/s resulted in self-extinguishment, while an airflow with a speed of 1,0 m/s resulted in sustained smouldering.
4. Delamination and fall-off of CLT can sustain flaming combustion or transform smouldering back to flaming combustion. This prevents the CLT from self-extinguishing.
5. Delamination can be prevented by an increased thickness of the top lamella; the charring front does not reach the polyurethane adhesive, which would result in loss of bonding.
6. Exposed CLT increases the heat release rate and total energy released, and extends the duration of a fire. These are further increased when delamination and fall-off result in prolonged flaming.

10.3 Recommendations

1. Self-extinguishment is currently not part of fire safety considerations for timber high-rise buildings. Pending further research, it might become recommendable to consider self-extinguishment as part of a total fire safety concept for tall timber buildings, including the effects of active measures such as sprinkler activation and fire-brigade intervention.
2. It would be recommended to consider an assessment method for potential self-extinguishment of CLT. This work suggests a method based on the calculation of a lamella thickness, to be applied to the outer layer of CLT to prevent delamination, and on limiting the heat flux on the smouldering CLT to 5 kW/m²
3. It would be recommended to consider potential self-extinguishment in demonstrating compliance of a tall timber structure with the Dutch building code. Self-extinguishment might contribute to achieving the level of safety intended by the code by reducing the probability of severe consequences due to structural collapse as a result of the fire.

4. It would be recommended to consider potential self-extinguishment in the design of a timber high-rise building according to the Eurocode consequence class 3. Self-extinguishment, as part of an overall fire safety concept, might become part of the risk analysis and the advanced calculations in order to demonstrate the tall timber structure is reliably safe and robust.
5. Insight into self-extinguishment, and its role in a total fire safety concept and in the structural design for tall timber buildings, could affect the perception of timber and the way it is treated in building regulations and approval. It would be recommended to consider a pragmatic approach in which any material poses unique design challenges, but can be applied as long as it contributes to safe buildings. While the combustibility of the timber structure will remain a point of attention, its risk should be managed properly, instead of used to discard the material for high-rise buildings.
6. It would be recommended to consider the implications of potential self-extinguishment for other, non-CLT timber structures, as well as types of buildings other than high-rise buildings.

10.4 Further research

1. This work featured a limited amount of experiments which were conducted under specific conditions; e.g. with regards to the design fire, fire load, ventilation conditions, CLT build-up, type of adhesive, wood species, and compartment configuration and scale. These conditions can influence the fire and the structural response. Furthermore, even equal conditions can lead to different results. To verify the conclusions and assess the applicability for real CLT structures, further research would be recommended on a larger scale and varying in the conditions above.
2. Self-extinguishment was investigated as passive protection for an exposed CLT structure in a compartment burnout, conservatively assuming no active measures. In a real high-rise building, active measures, such as sprinkler activation and fire brigade intervention, can be expected. It would be recommended to investigate self-extinguishment as part of a total fire safety strategy.
3. The influence of the airflow on the transition from smouldering to self-extinguishment was investigated to a limited degree. It would be recommended to further research a range of airspeeds in combination with a range of heat fluxes. Results should be compared with actual values that can be expected in high-rise compartments, with and without openings in the façade.
4. The transformation from smouldering to self-extinguishment depends partly on the heat flux received by the CLT. In a real fire, this heat flux can be cross-radiation between smouldering CLT surfaces. This cross-radiation is interactive by nature and should be further investigated.
5. A sufficiently thick top lamella, which results in the charring front not reaching the polyurethane adhesive, was applied in one experiment to prevent delamination and fall-off. It would be recommended to conduct more experiments to increase confidence in this approach.

6. Delamination and fall-off due to loss of bonding of the polyurethane adhesive at elevated temperatures might be prevented by development of a new type of glue. As a result, the CLT might perform as a solid slab of wood and the application of a certain lamella thickness to prevent delamination would no longer be required.
7. The assessment method proposed in this work would require further research and validation before it could be generally applied in practice. Furthermore, it could be expanded by incorporating the airflow condition, by taking account the interactions between smouldering surfaces, and by taking into account other objects and surfaces.
8. A parametric charring rate was used in the assessment method. However, parametric fires are restricted by the Eurocode to relative small compartments up to 500 m² and maximum 4 m in height. It would be recommended to expand the parametric charring approach for larger compartments or develop an alternative method based on another design fire.
9. Differences were found between the parametric charring method of the Eurocode, and the formulas from research on which this method is based. The original work corresponds well with experiment data and can lead to reasonable layer thicknesses. It would be recommended to investigate the differences and bring the Eurocode approach in line with experimental results.
10. Predictions of temperatures in the CLT using the Eurocode wood properties at elevated temperatures did not correspond well with the experiments. Furthermore, the predictions did not incorporate the smoulder process propagating through the material. It would be recommended to investigate how this could be incorporated in the Eurocode approach for advanced calculations.
11. Exposed CLT can significantly contribute to the heat release rate and the total energy released, and extent the duration of a fire. It would be recommended to investigate the influence of CLT on the severity and development of the fire. Results could be compared to the standard fire and implications with regards to the fire resistance of members could be discussed.
12. Charring rates in experiments where CLT contributed to the fire were typically higher than suggested by Eurocode 5. It would be recommended to further investigate the influence of the CLT contribution to the fire and of delamination and fall-off on the charring rate. Results could be compared with values in design guidance.
13. This work partially relates to previous research in which the CLT fire behaviour was investigated with fire modelling software. Based on that research, it would be recommended to further investigate the influence of the fuel load on self-extinguishment. Furthermore, differences and similarities could be explored and the results could be tied in with this work.

References

- Babrauskas, V., Peacock, R.D. (1992) Heat release rate: the single most important variable in fire hazard. *Fire Safety Journal*, 18, 255–272.
- Babrauskas, V. (2002) *The cone calorimeter. SFPE Handbook of Fire Protection Engineering*. Quincy: Society of Fire Protection Engineers.
- Baker, R.R. (1977). Combustion and thermal decomposition regions inside a burning cigarette. *Combustion and Flame*, 30, 21-32.
- Bergeron, D. (2003). Role of acceptable solutions in evaluation innovative designs. *Proceedings of the CIB-CTBUH International Conference on Tall Buildings*, 8-10 May 2003, Malaysia
- Bergman, T.L., Lavine, A.S., Incropera, F.P., DeWitt, D.P. (2011) *Fundamentals of heat and mass transfer*. Chichester: John Wiley & Sons.
- Beyler, C.L., Hirschler, M.M. (2002). *Thermal Decomposition of Polymers. SFPE Handbook of Fire Protection Engineering. Quincy: Society of Fire Protection Engineers.*
- Beyler, C.L., Gratkowski, M.T., Sikorski, J. (2006). Radiant smouldering ignition of virgin plywood and plywood subjected to prolonged smouldering. *International Symposium on Fire Investigation and Technology*.
- Bilbao, R., Mastral, J.F., Aldea, M.E., Ceamanos, J., Betran, M., and Lana, J.A. (2001). Experimental And Theoretical Study Of The Ignition And Smoldering Of Wood Including Convective Effects. *Combustion and Flame*, 126, 1363–1372.
- Bolonius Olesen, F., Hansen, T. (1992). *Full-scale tests on loaded glulam beams exposed to natural fires*. Aalborg: Aalborg University.
- Boonmee N, Quintiere J.G. (2002). Glowing and Flaming Autoignition of Wood. *Twenty-ninth International Symposium on Combustion*. The Combustion Institute, 289–296.
- Boonmee N, Quintiere J.G. (2005). Glowing Ignition of Wood: The Onset of Surface Combustion, *Thirtieth Symposium (International) on Combustion*. The Combustion Institute, 2303–2310.
- Browne, F. L., Brenden, J.J. (1964). Heats of combustion of the volatile pyrolysis products of Ponderosa pine. *US Forest Research Paper FPL 19*. United States Department of Agriculture
- Buchanan, A.H. (2009). *Structural Design for Fire Safety*. Chichester: John Wiley & Sons.
- Butler, C.P. (1971). *Notes on charring rats in wood*. Fire research note No, 896.
- CIBSE. (2010). *Fire safety engineering, CISBE guide E*. London: The Chartered Institution of Building Services Engineers
- CUR. (1997). *Probabilites in civil engineering, part 1: Probabilisty design in theory*. Gouda: Stichting CUR.

- Di Blasi, C. (2009). Combustion and gasification rates of lignocellulosic fuels. *Progress in Energy and Combustion Science*, 35, 121-140.
- Dosanjh, S.S., Pagni, P.J., Fernandez-Pello, A.C. (1987). Forced co-current smouldering combustion. *Combustion and Flame*, 68, 131-142.
- Dosanjh, S.S., Pagni, P.J. (1987). Countercurrent Smouldering Combustion. *Proceedings of the 1987 ASME/JSM E Thermal Engineering Joint Conference - Volume 1*. New York: American Society of Mechanical Engineers.
- Drysdale, D. (2011). *An Introduction to Fire Dynamics*. 3rd edition. Chichester: John Wiley & Sons.
- Drysdale, D. (2002). *Thermochemistry. SFPE Handbook of Fire Protection Engineering*. Quincy: Society of Fire Protection Engineers.
- Egerton, A.C., Guban, K., Weinberg, F.J. (1963). The mechanism of smouldering in cigarettes. *Combustion and flame*, 7, 63-79.
- European Committee for Standardization. (2004). *Eurocode 5. Design of timber structures. Part 1-2: General - Structural fire design. EN 1995-1-2*. Brussels:
- FPInnovations. (2013). *Technical Guide for the Design and Construction of Tall Wood Buildings in Canada. 90 % draft*. Pointe-Clair: FPInnovations.
- Frangi, A., Fontana, M., Hugi, E., Jöbstl, R. (2009). Experimental analysis of cross-laminated timber panels in fire. *Fire safety journal*, 44, 1078-1087.
- Gerard, R., Barber, D., Wolski, A. (2013). *Fire Safety Challenges of Tall Wood Buildings: Final Report*. Massachusetts: The fire protection research foundation.
- Gratkowski, M., Dembsey, N., Beyler, C. (2006). Radiant Smoldering Ignition of Plywood. *Fire Safety Journal*, 41, 427–443.
- Green, M.C. (2012). *The Case For Tall Wood Buildings*. Vancouver: mgb Architecture and Design.
- Hadjisophocleous, G.V., Bénichou, N. (2000). Development of performance-based codes, performance criteria and fire safety engineering methods. *International journal on engineering performance-based fire codes*, volume 2, number 4, p. 127-142.
- Hadvig, S., Paulsen, O.R. (1976). One dimensional charring rates in wood. *Journal of Fire and Flammability*, 7, 433-449.
- Hadvig, S. (1981). *Charring of wood in building fires, Report*. Lyngby: Laboratory of heating and air conditioning, Technical University of Denmark.
- Hakkarainen, T. (2002). Post Flashover Fires in Light and Heavy Timber Construction Compartments. *Fire Sciences*, 20.
- Huggett, C. (1980) Estimation of the rate of heat release by means of oxygen consumption. *Journal of fire and materials*, 12, 61–65.
- Janssens, M.L. (1991). Measuring rate of heat release by oxygen consumption. *Fire technology*, 27, 234–249.
- Janssen, M.L. (1993). Cone calorimeter measurements of the heat of gasification of wood. *Interflam '93: Proceedings of the Sixth International Fire Conference*, 549-559. London: Interscience Communications.
- Karlsson, B., Quintiere, J.G. (2000). *Enclosure Fire Dynamics*. Boca Raton: CRC Press
- Kashiwagi, T., Ohlemiller, T.J., Werner, K. (1987). Effects of external radiant heat flux and ambient oxygen concentration on non-flaming gasification rates and evolved products of white pine. *Combustion and Flame*, 69, 331-345.
- Kashiwagi, T., Ohlemiller, T.J. (1982). A study of oxygen effects on non-flaming gasification of PMMA and PE during thermal irradiation. *Proceedings of the Combustion Institute*, 19, 815-823.

- Köning, J., Walleij, L. (1999). *One-dimensional charring of timber exposed to standard and parametric fires in initially unprotected and postprotected situations. Report no. 1*. Stockholm: Träteknik, Swedish institute for wood technology research.
- Law, A., Bartlett, A., Hadden, R., Butterworth, N. (2014). The challenges and opportunities for fire safety in tall timber construction. *2nd International Tall Building Fire Safety Conference*.
- Lilley, D.G. (2012). *Applied Science and Engineering: Fire Dynamics. The Safety Professionals Handbook*. The American Society of Safety Engineers.
- Lim, S., Chew, M. (2007). The Ignition of Green and Preburn Wood by Radiation. *Fire and Materials Conference 2007*. Interscience Communications.
- Madorsky, S.L. (1964). *Thermal Degradation of Organic Polymers*. John Wiley & Sons, Inc., New York.
- McGregor, C., Hadjisophocleous, G., Craft, S. (2012). *Contribution of Cross Laminated Timber Panels to Room Fires*. Ottawa: Carleton University.
- Mikola, E. (1990). Charring of wood. *VTT research report 689*. Technical research centre of Finland.
- Miller, R.B. (1999). *Structure of wood, in Wood Handbook – Wood as an Engineering Material*. Forrester products laboratory general Technical report FPL-GTR-113. Madison: US Department of Agricultural Forest Service.
- Moussa, N.A., Toong, T.Y., Garris, C.A. (1977). Mechanisms of smouldering of cellulosic materials. *Proceeding of the Combustion Institute*, 16, 1447-1457.
- NEN. (2012). *Nederlandse technische afspraak 4614; Covenant high-rise buildings*. (2012). Delft: Nederlands Normalisatie Instituut.
- Ohlemiller, T.J. (2002). *Smouldering Combustion. SFPE Handbook of Fire Protection Engineering*. Quincy: Society of Fire Protection Engineers.
- Ohlemiller, T.J. (1991) Smouldering combustion propagation on solid wood. *Fire Safety Science*, 3, 565-574.
- Ohlemiller, T.J. (1990a). Smouldering combustion propagation through a permeable horizontal fuel layer. *Combustion and Flame*, 81, 341-353.
- Ohlemiller, T.J. (1990b) Forced smouldering propagation and the transition to flaming in cellulosic insulation. *Combustion and Flame*, 81, 354-365.
- Ohlemiller, T.J., Shaub, W. (1988). *Products of Wood Smolder and Their Relation to Wood-Burning Stoves*. Washington DC: National Bureau of Standards.
- Ohlemiller, T.J. (1985). Modelling of smouldering combustion. *Progress in Energy and Combustion Science*, 11, 277-310.
- Ohlemiller, T.J., Lucca, D. (1983). An Experimental Comparison of Forward and Reverse Smolder Propagation in Permeable Fuel Beds. *Combustion and flame*. 54. 131.
- Ohlemiller, T.J., Rogers, F.E. (1978). A survey of several factors influencing smouldering combustion in flexible and rigid polymer foams. *Journal of Fire and Flammability*, 9, 489-509.
- Olesen, F.B., Hansen, T. (1992). *Full-scale tests on loaded glulam beams exposed to natural fires*. Aalborg: Department of Building Technology and Structural Engineering, Aalborg University.
- Olesen, F. B., Köning, J. (1992). *Tests on Glued Laminated Beams in Bending Exposed to Natural Fires*. Aalborg: Department of Building Technology and Structural Engineering, Aalborg University.
- Palmer, K.N. (1957). Smouldering combustion of dust and fibrous materials. *Combustion and Flame*, 1, 129-154.
- Petrella, R.V. (1980). The mass burning rate of polymers, wood and organic liquids. *Journal of Fire and Flammability*, 11.

- Petrella, R.V. (1979). The mass burning rate and mass transfer number of selected polymers, wood and organic liquids. *Polymer and Plastics Technology Engineering*, 13, 83-103.
- Rath, J., Wolfinger, M.G., Steiner, G., Krammer, G., Barontini, F., Cozzani, V. (2003). Heat of wood pyrolysis. *Fuel*, 82, 81-91.
- Rein, G. (2009). Smouldering combustion phenomena in science and technology. *International Review of Chemical Engineering*, 1, 3-18.
- Roberts, A.F. (1971). Problems associated with the theoretical analysis of the burning of wood. *Proceedings of the Combustion Institute*, 13, 893-903.
- Roberts, A.F. (1970). A review of kinetic data for the pyrolysis of wood and related substances. *Combustion and Flame*, 14, 261-272.
- Schaffer, E.L. (1967). Charring rate of selected woods – transverse to grain. *US forest service research paper FPL69*. Madison: Forest products laboratory
- SOM. (2013). *Timber Tower Research Project: Final Report*. Chicago: Skidmore, Owings & Merrill, LLP.
- Spearpoint, M.J., and Quintiere, J.G. (2001). Predicting the Piloted Ignition of Wood in the Cone Calorimeter using an Integral Model. *Fire Safety Journal*, 36, 391–415.
- Spearpoint, M.J. (1999). *Predicting the Ignition and Burning Rate of Wood in the Cone Calorimeter using an Integral Model*. University of Maryland.
- Stevens, M.P. (1999). *Polymer Chemistry: an introduction*. Oxford University press, New York.
- Swann, J.H., Hartman, J.R., Beyler, C.L. (2008). Study of Radiant Smoldering Ignition of Plywood Subjected to Prolonged Heating Using the Cone Calorimeter, TGA, and DSC. *Proceedings of the 9th IAFSS Symposium*, 9, 155-166.
- SP Technical Research Institute of Sweden. (2010). *Fire safety in timber buildings. Technical guideline for Europe*. Stockholm.
- Terwel, K.C., (2014). *Structural safety: Study into critical factors in the design and construction process*. Faculty of civil engineering and Geosciences. Delft: Delft university of Technology.
- Tewarson, A., Pion, R.F. (1976). Flammability of plastics. I. Burning intensity. *Combustion and Flame*, 26, 85-103.
- Thornton, W. (1917). The relation of oxygen to the heat of combustion of organic compounds. *Philosophical magazine and journal of science*, 33.
- Van de Kuilen, J.W.G., Ceccotti, A., Zhouyan Xia, Minjuan He, Shuo Li. (2011) Wood-concrete skyscrapers. *World Conference on Timber Engineering*. Riva del Garda, Italy.
- Van de Kuilen, J.W.G., Ceccotti, A., Zhouyan Xia, Minjuan He. (2011) Very tall wooden building with cross laminated timber. *The twelfth east Asia-pacific conference on structural engineering and construction*.
- White, R.H. (1988). *Charring rates of different wood species*. PhD thesis. Madison: University of Wisconsin.
- Wiedenhoef, A. (2010) *Structure and Function of Wood. Wood Handbook, Wood as an Engineering Material* Madison: United States Department of Agriculture Forest Service.

Appendices

Cross-laminated timber

A.1 Introduction

This appendix provides a brief history of cross-laminated timber and its manufacturing process and is based on the work of Brandner (2013) and the CLT handbook (FPInnovations, 2013).

A.2 Brief history

Cross-laminated timber has its origins in Europe, where it was initially developed in the early 1990s in Switzerland and further developed in Austria and Germany. After a slow start, construction with CLT increased rapidly in the early 2000s in Europe due to a move to sustainable architecture, increased production efficiency, product approvals, code changes, and improved marketing and distribution. These developments took place mainly in Austria and Germany and these countries are currently leading in the use and production of CLT with a current combined production volume of approximately 0,5 m³. On a global scale, Europe is leading in the use of CLT.

Compared to Europe, CLT is still a novel building system in other markets, such as North America. However CLT is receiving more interest, due to potential economic benefits and the desire for a sustainable alternative to steel, concrete, and masonry construction. A number of plants have started producing CLT and several projects are proposed or have been built recently outside of Europe.

A.3 Manufacturing

The manufacturing of Cross-laminated timber consists of several steps, as depicted in figure A.1 and A.2.

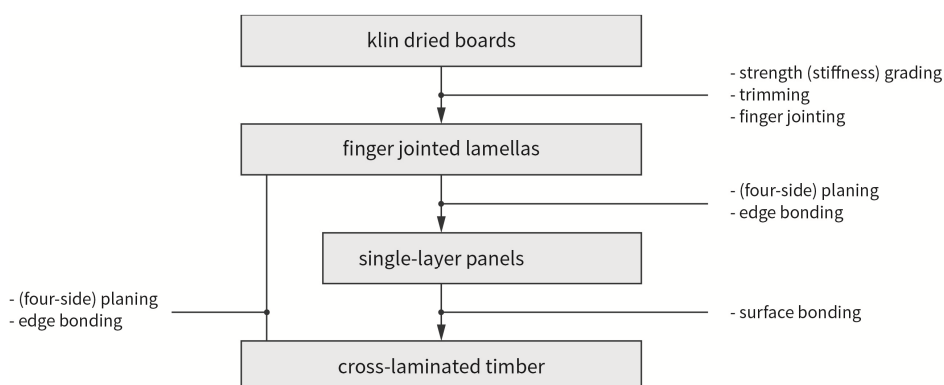


Figure A.1 Overview of the CLT production process. From Brandner (2013).

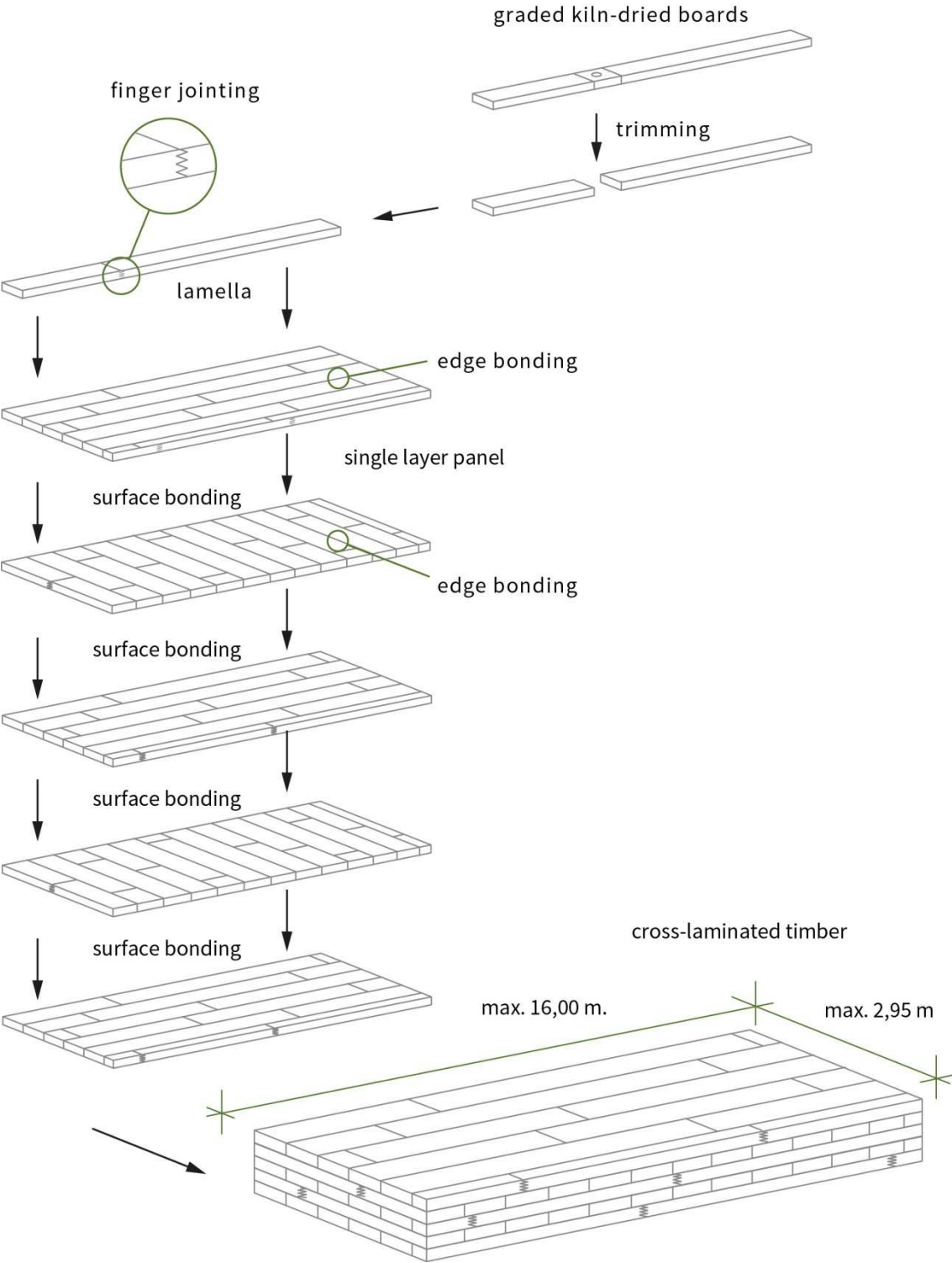


Figure A.2 Overview of the CLT production process. Adapted from Stora Enso.

A.3.1 Base material

The base material of the CLT is sawn timber. The use of softwood is dominant and the main softwood species that is used is Norway spruce (*Picea abies*). Furthermore, species like White fir (*Abies alba*), Scots pine (*Pinus sylvestris*), European larch (*Larix decidua*), Douglas fir (*Pseudotsuga menziesii*) and Swiss stone pine (*Pinus cembra*) are used. The latter species are primary used for CLT of high appearance quality and thus for top layers.

CLT manufactured from hardwoods is also feasible. It is especially the application of hardwood in particular layers within a CLT panel that is of interest, because this allows for optimisation of the mechanical properties of the panel without increasing thickness

Individual boards of the base material are kiln-dried to a moisture content of about 12 %, depending on the end use, to prevent dimensional variations and surface cracking.

The material is visually or mechanically graded to strength or stiffness classes. If required, local growth characteristics with a possible negative impact on the desired strength can be cut out of those boards which do not meet the requirements of the strength class. This is referred to as trimming.

Common strength classes are C24, but it is possible to use a lower grade timber for interior layers. In those cases C24 is often combined with C16 / C18 for the transverse layers, because the bearing capacity of CLT stressed out of plane in bending is primary governed by the resistance of the top layers stressed parallel to grain.

A.3.2 Lamellas

The trimmed board segments are re-joined by means of glued finger joints. This process creates a continuous lamella, without local growth characteristics. The continuous lamella then is cut into boards for use in the layers of CLT. These boards are planed on 4 sides for improved gluing effectiveness and to achieve the required tolerance in thickness. The boards are placed side by side to form one layer of the CLT. This single layer typically ranges in thickness from 20 to 80 mm.

A.3.3 Single layer panels (intermediate step)

As an intermediate step the boards can be bonded to each other to form a single-layer panel by means of edge gluing. As a result, gaps between boards are eliminated or reduced. Most producers of CLT aim to reduce these gaps between the boards, with respected to building physic, e.g. improved fire performance, acoustics, and airtightness. Other reasons are found in improved joining techniques, in particular considering pin-shaped fasteners like nails, screws or dowels, as well as with regards to aesthetics if the outside surface of CLT is left visible in its final use.

A.3.4 Cross laminated timber

The final CLT panel is created by means of surface gluing multiple single layer panels. The adhesive is applied to the faces of the single layer panels and the layers are surface bonded by pressing. The most common method is by means of hydraulic press, but both vacuum pressing or utilising the pressure of screws, brackets, or nails, are used as well. The assembled panels are planed or sanded for a smooth surface.

The process of face gluing, but also of edge gluing and finger jointing, is quite complex. To ensure an optimum performance of the jointing - i.e. sufficiently strong, stiff, and durable - various factors need to be taken into account, including joint geometry, timber species, thickness of layers, type of adhesive and applied quantity, roughness and flatness of the surfaces, bonding pressure, hold time, temperature, and moisture content.

A.3.5 Post-processing

The CLT panels are often post-processed. Panels can be joined by large finger joints between the panels. Furthermore, with the use of computer numerical control (CNC) routers openings for windows, doors, building services and ducts are cut out with high precision.

Depending on end use, the application of additional non load-bearing layers like oriented-strand boards, acoustic panels, and gypsum plaster boards is possible. Cladding can also be installed prior to delivery.

Typical panel widths are up to 2,95 m while lengths can be up to 24 m when finger joints are applied. However, production or transportation capability may impose size limitations. Panel thickness is typically up to 0,3 m, with individual lamella thickness of typically 20 to 80 mm.

A.4 CLT used for the experiments

Stora Enso provided the CLT for the experiments. Stora Enso is of origin a Finnish pulp and paper manufacturer, and now one of the global players in the paper, biomaterials, wood products, and packaging industry.

Table A.1 provides specifications of the CLT used for the experiments. The same CLT was used for both series of experiments. The next two pages contain the product information sheets as specified by Stora Enso.

Table A.1 Specifications of the CLT used in the experiments

Property	Specification
Wood species	Spruce
Grade of lamellas	C24
Face gluing adhesive	Polyurethane
Finger-jointing adhesive	Polyurethane
Edge gluing adhesive	Emulsion polymer isocyanate
Fire rating	Euroclass D-s2, d0
Layer build-up*	20/20/20/20/20 mm crosswise stacked 40/20/20/20/40 mm crosswise stacked

*two types of layer build-up were used in the experiments

Product information

CLT CHARACTERISTICS

04/2012

Use	Primarily as a wall, ceiling and roof panel in homes and other buildings
Maximum width	2.95 m
Maximum length	16.00 m
Maximum thickness	40 cm
Layer structure	Bonded, cross-laminated single-layer panels
Wood species	Spruce (middle layers can contain pine; larch and pine as cover layer on request)
Grade of lamellas	C24 (in accordance with the technical approval 10 % to strength class C16 allowed; other grades on request)
Moisture content	12% ± 2%
Bonding adhesive	Formaldehyde-free adhesives for edge bonding, finger jointing and surface bonding
Surface quality	Non-visible quality, industrial visible quality and visible quality; the surface is always sanded
Weight	5.0 kN/m ³ in accordance with DIN 1055-1:2002, for structural analyses; for ascertaining transport weight: approx. 470 kg/m ³
Change in shape with change in moisture content	Swelling and shrinkage in accordance with DIN 1052:2008 below the fibre saturation level: <ul style="list-style-type: none"> ▪ In the panel layer: 0.02% change in length for each 1% change in timber moisture content ▪ Perpendicular to the panel layer: 0.24% change in length for each 1% change in timber moisture content
Fire rating	In accordance with Commission Decision 2003/43/EC: <ul style="list-style-type: none"> ▪ Timber components apart from floors → Euroclass D-s2, d0 ▪ Floors → Euroclass Dfl-s1
Water vapour diffusion resistance <i>m</i>	According to EN 12524 → 20 to 50
Thermal conductivity <i>l</i>	According to the SP Technical Research Institute of Sweden's expert opinion of 10.07.2009 → 0.11 W/(mK)
Specific heat capacity <i>c_p</i>	According to EN 12524 → 1600 J/(kgK)
Airtightness	CLT panels are made of single-layer panels and are therefore extremely airtight. The airtightness of a 3-layer CLT panel and of panel joints has been tested to EN 12 114 where it was found that that the volumetric rates of flow were outside the measurable range.
Service class/usability	According to EN 1995-1-1, can be used in service classes 1 and 2

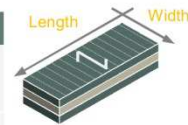


Product information

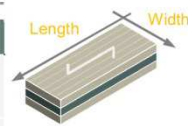
CLT STANDARD DESIGNS

04/2012

C panels									
Nominal thickness [mm]	Designation	Layers	Lamella structure [mm]						
			C	L	C	L	C	L	C
60	C3s	3	20	20	20				
80	C3s	3	30	20	30				
90	C3s	3	30	30	30				
100	C3s	3	30	40	30				
120	C3s	3	40	40	40				
100	C5s	5	20	20	20	20	20		
120	C5s	5	30	20	20	20	30		
140	C5s	5	40	20	20	20	40		
160	C5s	5	40	20	40	20	40		



L panels									
Nominal thickness [mm]	Designation	Layers	Lamella structure [mm]						
			L	C	L	C	L	C	L
60	L3s	3	20	20	20				
80	L3s	3	30	20	30				
90	L3s	3	30	30	30				
100	L3s	3	30	40	30				
120	L3s	3	40	40	40				
100	L5s	5	20	20	20	20	20		
120	L5s	5	30	20	20	20	30		
140	L5s	5	40	20	20	20	40		
160	L5s	5	40	20	40	20	40		
180	L5s	5	40	30	40	30	40		
200	L5s	5	40	40	40	40	40		
160	L5s-2*	5	60	40	60				
180	L7s	7	30	20	30	20	30	20	30
200	L7s	7	20	40	20	40	20	40	20
240	L7s	7	30	40	30	40	30	40	30
220	L7s-2*	7	60	30	40	30	60		
240	L7s-2*	7	80	20	40	20	80		
260	L7s-2*	7	80	30	40	30	80		
280	L7s-2*	7	80	40	40	40	80		
300	L8s-2**	8	80	30	80	30	80		
320	L8s-2**	8	80	40	80	40	80		



* Cover layers consisting of 2 lengthwise layers
 ** Cover layers and inner layer consisting of 2 lengthwise layers

Status: 04/2012

Width (Charged widths): 245 cm, 275 cm, 295 cm
 Length (Production lengths): From minimum production length of 8.00 m per charged width up to max. 16.00 m (in 10 cm increments).



B

Existing data

B.1 Introduction

Various pieces of existing research were investigated in more detail as part of this work on self-extinguishment of CLT. This appendix provides an overview of some of the reviewed existing works. For each reviewed work a short introduction is given first. The test setup and the results are discussed, followed by the conclusions and their relevance to the research on self-extinguishment.

B.2 Tewarson and Pion, and Petrella

Tewarson and Pion (1976) and Petrella (1979) conducted research on the “flammability” of a large range of polymers, including plastic, but also wood and organic liquids by looking at the mass burning rate for steady-state flaming combustion.

Their main goal was to develop a laboratory-scale test that correlates an “ideal” burning rate to small-scale flammability test results, full-scale fires, and other flammability parameters. Furthermore, various properties of the materials were investigated, including the heat of gasification, the heat flux transferred from the flame to the surface, the heat flux lost by the surface, and minimum mole fraction of oxygen required for flame extinction.

B.2.1 Test model

The researchers investigated various samples using a theoretical model for steady state burning in flaming combustion. During steady state combustion, a heat balance can be assumed to operate at the surface of the polymer. This heat balance is given in equation B.1

$$\dot{Q}_F'' + \dot{Q}_E'' = \dot{Q}_G'' + \dot{Q}_L'' \quad (\text{Eq. B.1})$$

Where

\dot{Q}_F''	= total heat flux from the flame to the surface (kW/m ²)
\dot{Q}_E''	= externally applied heat flux to the surface (kW/m ²)
\dot{Q}_G''	= heat flux required to gasify/pyrolyze the polymer (kW/m ²)
\dot{Q}_L''	= total heat flux lost by the polymer (kW/m ²)

The total heat flux incident upon the polymer surface is made up of two components: one is the heat flux transferred from the flame to the surface under experimental conditions, the second is any additional heat

flux received by the surface from external heat sources, for example if flames are much larger than the experimental flame, or from other hot or burning surfaces in a compartment. The incident flux is balanced by two other components: one is the heat losses through the surface under experimental conditions, the second is the flux required to gasify or pyrolyze the polymer and feed the flame and can be expressed in terms of the mass burning rate per unit area times the heat of gasification, as given in equation B.2.

$$\dot{Q}_G'' = \dot{m}'' \cdot L_V \quad (\text{Eq. B.2})$$

Where \dot{m}'' = mass burning rate per unit area (kg/m²s)
 L_V = heat of gasification/pyrolysis/depolymerisation of the polymer initially at ambient temperature

When equation B.2 is substituted in equation B.1, the mass burning rate can be expressed in terms of the other heat fluxes, as given in equation B.3.

$$\dot{m}'' = \frac{\dot{Q}_F'' + \dot{Q}_E'' - \dot{Q}_L''}{L_V} \quad (\text{Eq. B.3})$$

However, this relation is of little use, as the heat flux from the flame to the surface \dot{Q}_F'' is difficult to measure directly. Alternatively, an indirect method can be used.

In equation B.3, $\dot{m}'' \cdot L_V$ can be plotted against the heat flux from the flame to the surface \dot{Q}_F'' . If the losses \dot{Q}_L'' are assumed constant in the experimental setup, a straight line is obtained with $\dot{Q}_E'' - \dot{Q}_L''$ as the y-intercept, as depicted in figure B.1.

Furthermore, it has been found previous studies that $\dot{m}'' \cdot L_G$ is a function of the mole fraction of oxygen N_{O_2} to the power α under a certain externally applied flux \dot{Q}_E'' . This relation was valid over a range of oxygen concentrations for the materials studied. Over a wide range of mole fraction of oxygen N_{O_2} , the mass burning rate \dot{m}'' , increased linearly as the N_{O_2} is increased, thereby showing that $\alpha = 1$.

This linear relation can be combined with the observation that $\dot{Q}_E'' - \dot{Q}_L''$ is the y-intercept of the straight line that describes $\dot{m}'' \cdot L_G$ for different values of \dot{Q}_F'' . As a result the slope of that line can be defined as a constant ξ and the heat flux from the flame to the polymer surface \dot{Q}_F'' can be expressed as equation B.4.

$$\dot{Q}_F'' = \xi \cdot N_{O_2}^\alpha \quad (\text{Eq. B.4})$$

Where ξ = characteristic combustion constant for the polymer (kW/m²)
 $N_{O_2}^\alpha$ = mole fraction of oxygen
 α = constant (=1 for a linear relation)

In this equation, ξ and α indicate the relationship between $\dot{m}'' \cdot L_V$ and the mole fraction of oxygen N_{O_2} at a constant $\dot{Q}_E'' - \dot{Q}_L''$. When equation B.4 is substituted into equation B.3 the result is equation B.5.

$$\dot{m}'' = \frac{\xi \cdot N_{O_2}^\alpha}{L_V} + \frac{\dot{Q}_E'' - \dot{Q}_L''}{L_V} \quad (\text{Eq. B.5})$$

From the equation B.5, values for ξ , L_G , and \dot{Q}_L'' can be obtained if the mass burning rate \dot{m}'' is measured at different values for the mole fraction of oxygen N_{O_2} and externally applied flux \dot{Q}_E'' . The relations become clearer if it is thought of as a straight line, as presented in equation B.6 and figure B.1.

$$y = a \cdot x + b \quad (\text{Eq. B.6})$$

Where	a	= (ξ / L_G)
	b	= $(\dot{Q}_E'' - \dot{Q}_L'') / L_V$
	x	= N_{O_2}
	y	= \dot{m}''

With $\alpha = 1$, a plot of \dot{m}'' versus the mole fraction of oxygen N_{O_2} at a certain external heat flux \dot{Q}_E'' yields a straight line with slope (ξ / L_V) and the intercept $(\dot{Q}_E'' - \dot{Q}_L'') / L_V$ at $N_{O_2} = 0$.

The value for the heat of gasification L_V is well-known for many materials and can independently be determined with a calorimeter. Alternatively, using the equations presented above, a plot of \dot{m}'' versus the external heat flux \dot{Q}_E'' at a constant mole fraction of oxygen N_{O_2} yields a straight line with the slope $1/L_V$. With L_V determined, the value for ξ and \dot{Q}_L'' are calculable. As a result the heat flux from the flame to the surface Q_F'' can be determined from equation B.4.

With these parameters the mass burning rate of the polymer can be calculated over a wide range of fuel and air mixes and over externally applied heat fluxes, ranging from small-scale tests with $\dot{Q}_E'' = 0$ to full scale tests with $\dot{Q}_E'' \gg 0$.

Furthermore, the “ideal” burning rate can be defined, where the externally applied flux completely compensates the losses, i.e. $\dot{Q}_E'' = \dot{Q}_L''$, then equation B.5 reduces to equation B.7, in which $N_{O_2} = 0,21$ for ambient air.

$$\dot{m}''_{ideal} = \frac{\xi \cdot N_{O_2}}{L_V} \quad (\text{Eq. B.7})$$

Where \dot{m}''_{ideal} = ideal mass burning rate per unit area (kg/m²s)

Substitution equation B.7 into equation B.5 yields equation B.8.

$$\dot{m}'' = \dot{m}''_{ideal} + \frac{\dot{Q}_E'' - \dot{Q}_L''}{L_V} \quad (\text{Eq. B.8})$$

Equation B.8 relates the mass burning rate at ideal conditions in ambient air to those of lab-scale tests and end-use conditions. In other words, with this equation it is possible to calculate the mass burning rate in various scenarios, based on the ideal rate and a modification for externally applied flux and losses.

Furthermore, with equation B.5 it is possible to investigate and plot the relation between the various parameters. These include the influence of the mole fraction of oxygen N_{O_2} on the mass burning rate \dot{m}'' , as in equation B.6, but also the influence of externally applied flux \dot{Q}_E'' (or $\dot{Q}_E'' - \dot{Q}_L''$) on the burning rate \dot{m}'' , and the influence of variation of the externally applied heat flux and mole fraction of oxygen on extinction of the flame.

B.2.2 Test Setup

With this theoretical model and a test apparatus that can impose an externally applied flux and regulate the available oxygen, the samples were studied in flaming combustion. The experiments were conducted with a “mass burning apparatus”, as depicted in the figure B.2.

Samples of 60 to 100 cm² and 30 to 50 mm thick were placed in horizontal configurations within a quartz tube. The total flow rate of air or air mixtures with N₂ or O₂ was measured. An external heat flux was applied to the samples with two radiant heaters. The mass burning rate was measured with a load cell assembly capable of detecting losses of 0,1 g/s.

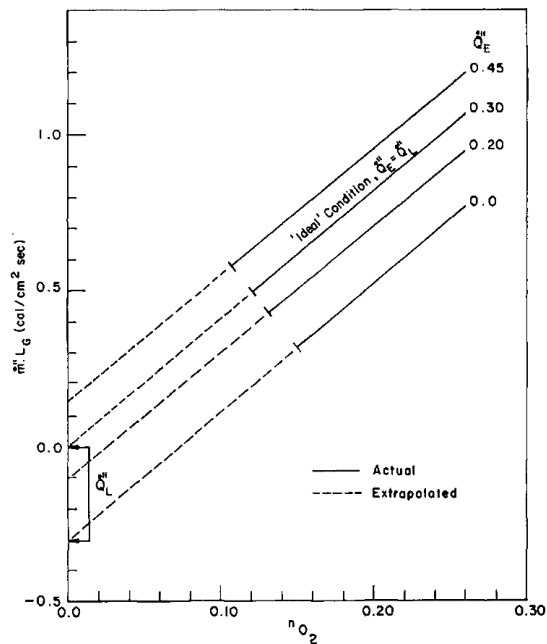


Figure B.1 $\dot{m}'' \cdot L_G$ as a function of the mole fraction of oxygen N_{O_2} . From Tewarson and Pion (1976).

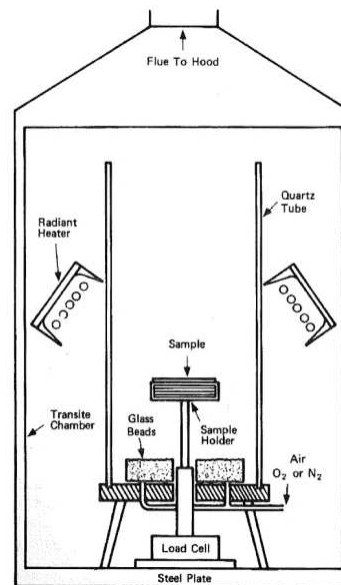


Figure B.2 Schematic representation of the mass burning apparatus. From Petrella (1979).

B.2.3 Test results

The effects of varying heat flux conditions on the mass burning rate were investigated for a large range of polymers. This allowed for the correlation of the ideal burning rate to small-scale flammability test results and full-scale fires.

In small-scale experiments where the only source of heat flux to the surface is the flame from the material itself, it can be expected however that $\dot{Q}_E'' < \dot{Q}_L''$, resulting in $\dot{m}'' < \dot{m}''_{ideal}$. In full-scale fires where the surface receives additional heat flux, it can be expected that the externally applied flux will overcompensate the losses, i.e. $\dot{Q}_E'' > \dot{Q}_L''$. The mass burning rate will be higher than the ideal rate, i.e. $\dot{m}'' > \dot{m}''_{ideal}$.

Furthermore, various flammability parameters of the samples were investigated. Only the results for wood are presented below. Tewarson and Pion investigated a sample of Douglas fir, while Petrella investigated ten different species of wood. The results of Petrella are summarized in table B.1. It should be noted that the values reported here apply to the size and geometry used in these specific experiments.

Table B.1 Mass burning rate data for materials burning in air. From Petrella (1979).

Sample	ξ cal/cm ² sec	\dot{Q}_T'' cal/cm ² sec	\dot{Q}_L'' cal/cm ² sec	L_G cal/gm	$\dot{m}''_{ideal} \times 10^4$ gm/cm ² sec	$\dot{m}'' \times 10^4$ gm/cm ² sec	$\frac{\dot{Q}_T''}{\dot{Q}_L''}$
Ponderosa Pine	3.76	0.79	0.77	667	11.8	0.3	1.03
Douglas Fir	1.81	0.38	0.25	791	4.8	1.8	1.52
Red Oak	3.89	0.82	0.94	417	19.6	- 3.0	0.87
Chipboard	3.09	0.65	0.64	568	11.4	0.1	1.02
Black Cherry	5.04	1.06	1.09	719	14.7	- 0.4	0.97
White Oak	4.06	0.85	1.07	338	25.7	- 6.4	0.79
Hard Maple	4.08	0.86	1.04	483	17.7	- 3.8	0.83
Cedar	4.39	0.92	1.10	539	17.1	- 3.4	0.84
Walnut	3.25	0.68	0.59	772	8.8	1.2	1.15
African Mahogany	5.42	1.14	1.24	667	17.1	- 1.5	0.92

The values for the heat of gasification showed good agreement with values found in literature or measured with different techniques, such as a calorimeter. Tewarson and Pion found for the Douglas fir sample a value of 435 cal/g or 1,82 kJ/g. Petrella found results in the range of 338 to 791 cal/gm or 1,41 to 3,31 kJ/g, depending on the species of wood.

Tewarson and Pion found for the Douglas fir sample that the heat flux transferred from the flame to the surface \dot{Q}_F'' is just able to compensate the heat flux lost by the surface \dot{Q}_L'' , i.e. $\dot{Q}_F'' \approx \dot{Q}_L''$. Values for both fluxes of 0,57 cal/cm² or 24 kW/m² were reported in normal ambient air. Petrella's data even shows that wood tends to dissipate heat at a rate slightly faster than is supplied by the flame, i.e. $\dot{Q}_T'' < \dot{Q}_L''$.

Furthermore, the "ideal" mass burning rate was determined for the materials. The results correlated well with full-scale fire test classifications. For the Douglas fir sample in the experiment by Tewarson and Pion an ideal burning rate was found of 13 g/cm² s. This value was a peak burning rate, as the burning rate of the wood samples was not constant due to the charring behaviour. Petrella found values in the range of 4,8 to 25,7 g/cm² s, linear dependent on the heat of gasification of the various species of wood.

Tewarson and Pion found a mole fraction of oxygen required for flame extinction of 0,289 for Douglas fir.

B.2.4 Conclusions and relevance

Using the theoretical model of steady state burning, Tewarson and Pion developed a laboratory-scale technique which provides mass burning rate data that correlates small-scale testing with the full-scale test data. They also formulated the effects of varying heat flux conditions in full-scale fires on this burning rate. Furthermore, various properties of samples of combustibles have been derived, including the “ideal” burning rate, heat of gasification, heat flux transferred from the flame to the surface, heat flux lost, and mole fraction of oxygen at flame extinction.

The work of Tewarson and Pion, and Petrella, is relevant for this research in the values of the heat fluxes that drive the burning process.

For self-sustained combustion in normal air, the heat flux transferred from the flame to the surface \dot{Q}_F'' should be larger than the heat flux lost by the surface \dot{Q}_L'' . Tewarson and Pion found under experimental conditions the heat transfer from the flame to the wood is just sufficient to match the heat losses, i.e. $\dot{Q}_F'' \approx \dot{Q}_L''$.

Petrella indicates that generally losses even are generally slightly higher, i.e. $\dot{Q}_F'' < \dot{Q}_L''$. This indicates that combustion would not be sustained without any externally applied flux \dot{Q}_E'' in normal air.

It is interesting to note that, based on the model, if in a compartment the mole fraction of oxygen in the air drops, so would the heat flux transferred from the flame to the surface \dot{Q}_F'' . As a result a higher external flux would be required for sustained burning.

The idea that wood burns poorly without an additional heat is supported by the result with regards to the mole fraction of oxygen required for flame extinction. For wood a value of 0,289 was found, which is higher than 0,21 for ambient air. In other words, oxygen needs to be additionally provided to prevent extinguishment if an externally applied heat flux is absent. The supply of oxygen increases the combustion and as a result the heat flux transferred from the flame to the surface.

B.3 Ohlemiller

Ohlemiller (1991) has conducted research on the smoulder propagation on solid wood in a configuration designed to enable self-sustained smouldering. The research was conducted with a focus on how smouldering relates to wood-burning stoves and the findings most pertinent to this application were presented in separate reports by Ohlemiller (1985, 1988). The work discussed here however is more focused on the factors controlling the smoulder process and on the spread of smouldering combustion.

B.3.1 Test setup

The test samples were designed as a U-shaped channels of 74 cm long with 6,4 cm thick walls. These samples were designed so that radiative interactions among the concave interior surface allowed the possibility of sustained smouldering without an additional applied flux.

Samples were placed in an enclosed steel chamber for control of air flow and for analysis of combustion products. A controlled laminar air flow at ambient temperature was led over the surface. For various flow speeds, smoulder propagation was investigated.

Mostly white pine, but also samples of red oak were used to investigate the influence of varying material properties. Smouldering was initiated at either end of the channel or at mid-length, yielding, forward or reverse smouldering, or a combination of both smoulder modes.

The smouldering process and rate of spread were observed visually. Exhaust gasses were gathered and analysed. Furthermore, information was obtained on the internal temperature profiles in the wood. Thermocouples were embedded in the bottom of the wooden channel. For a small number of tests gas temperatures in the channel were measured with thermocouples.

B.3.2 Test results

The spread of smouldering on the wood was observed visually for up to seven hours as an orange glow in the oxidation zone. Smouldering occurred on all three surfaces of the trench.

The smoulder process occurred both inward into the walls of channel and along the length of the channel. The inward burning terminated when the thinnest regions of the wall were about 0,5 cm thick. Because the spread of smouldering along the surface depends on the ability to transfer heat from the hot region to the unburned wood, termination of the inward spread could also terminated the spread along the wood.

For forward smouldering, the spread rate along the wood surface and the surface temperature increased with flow of air. The increased flow of air accelerates the rate of transfer of oxygen to the wood char surface. This increased the oxydation rate and thus the locate heat release, temperature, and rate of heat transfer to the unburned wood downstream. This causes the smoulder front to propagate faster.

For reverse smouldering and combinations of the forward and reserve smouldering results of the spread rate and temperature were more complex. While it is beyond the scope of this review to go in depth, it should be noted that in reverse smouldering, high air flows might partially cool and shorten the pre-heated wood regions. This counteracts the increased char oxidating, resulting in lower spread rates.

For both forward and reverse smouldering the process was prone to extinction at low air speeds and likely to transsition into flaming combustion at high air speeds. For both types of propagation this range was

about the same and rather narrow: from 0,05 m/s to 0,2 m/s. At the limits of this range smouldering could be sustained for hours, but would eventually extinguish or transform into flaming combustion. The transition process to flaming in the gas phase was associated with localized regions of higher char surface temperature.

To gain further understanding of the charring behaviour an energy balance model was made for the steady-state smouldering process. This model does not describe the propagation, but indicates the driving forces of the process. A portion of oxidizing char was modelled that exchanges radiation with other regions of hot char and with the cooler wood beyond the smoulder front. Furthermore, it is also subject to conductive and convective heat losses.

The model indicated a central role for radiative transfer in sustaining the smoulder process. The observation that the heat transfer rate, rather than oxygen consumption limitation, played a central role in the smoulder propagation over the channel surface was reinforced by analysis of the gasses. This analysis showed there was always plenty of oxygen available in the air flow ranging from 12 % to 15 %. However, this does not exclude a key role of oxygen supply rate in the smoulder propagation process as it influences the temperature of the radiating surfaces. The model also corresponded well with regards to the extinction limits found in the tests.

The rate of heat release during smouldering was estimated from the oxygen consumption rate, as described in a separate report by Ohlemiller *et al.* (1988). The rate ranged from about 0.5 to 2 kW. Based on the area visibly glowing, this yields roughly 10 to 30 kW/m².

Smoulder spread rates for white pine and red oak were essentially equal for a give air flow rate. An analysis based on thermocouple data suggests heat conduction through the wood was the least significant heat transfer mode. The higher conductivity of oak did not yield in a more rapid spread.

B.3.3 Conclusions and relevance

The research by Ohlemiller is of interest to this research as it is one of the studies in which the solid wood itself is studied. In other research (wood-based) products with a greater permeability with regards to oxygen are investigated.

However, the experiments by Ohlemiller focussed on smouldering on the surface of the wood, not inward into the material. In a post-flashover fire in a CLT compartment it is reasonable to assume all timber surfaces to be involved with the fire. Subsequently, it is the propagation of smouldering inward into the material that is important to investigate for the potential of self-extinguishment. Nevertheless, the results of these experiments can have qualitative value.

The test results implied a central role for radiative heat transfer between the smouldering surfaces in sustaining a smoulder processes. Furthermore, it was observed that an externally applied flux is required in order to keep the smouldering process going. Values for this flux are not reported, although mention is made of 10 kW/m² as an unpublished value found by preliminary research by Ohlemiller (2002). As a

result a single flat and thermally thick slab of wood will not smoulder unless the smoulder-derived heat is supplemented by an external radiant flux.

Ohlemiller also indicated that the airflow over the surface is important in controlling the smoulder process, as it determines the oxidation rate. Furthermore, because oxygen was always present in excess in the channel, the oxygen supply rate to the reaction zone, not the total oxygen available, appear to limit the rate of propagation.

It was also found that a minimum air flow rate of 0,05 m/s was required to prevent extinction of forward or reverse smouldering over the surface, while an air flow of 0,2 m/s transformed the fire to flaming. The influence of air velocity on inward smouldering is not reported.

While the work of Ohlemiller was focussed on smouldering on the surface of the material, it can be expected that an externally applied flux is required for smouldering inward into the materials as well. Furthermore, airflow over the material surface will heavily influence the process. This would then be relevant for the self-extinguishment of CLT compartment fires.

Conduction had a minor role in the heat transfer between the zones. This indicates the smoulder process is independent of the wood properties, such as density. However, in the case of smouldering inward into the material, conduction might be of more importance, as described by the model of Moussa *et al.* (1977).

B.4 Swann *et al.*

Swann *et al.* (2008) performed research on the radiant smoulder ignition of maple plywood subjected to prolonged pre-heating. The research was conducted to investigate a long standing hypothesis that wood subjected to prolonged preheating will form a reactive char that enhances the ignitability of wood, often referred to as “pyrophoric carbon”.

While the research is aimed towards the influence of pre-heating on the ignitability of wood, it is accompanied by a literature review regarding the radiative ignition of wood at low fluxes. This review and the results regarding the radiative ignition of wood at low heat fluxes is of interest to this research, as it might indicate if self-extinguishment can occur.

B.4.1 Literature review

Bilbao *et al.* (2001) investigated pine wood in a range of heat fluxes and air flow velocities. Smouldering ignition was observed only at fluxes higher than 20 kW/m².

Spearpoint and Quintiere (1999, 2001) studied the minimum heat flux for piloted ignition of several wood species along the grain and perpendicular to the grain. Along the grain exposure required a heat flux of 12 kW/m² for piloted ignition, while end grain exposure resulted in piloted ignition at heat fluxes of 8 kW/m². Only limited data was reported for smouldering ignition at low heat fluxes. For maple exposed to 12 kW/m² the time to glowing ignition was about an hour and piloted flaming ignition occurred 10 minutes later. Glowing ignition prior to flaming ignition for specimen subjected along the grain to heat fluxes less than 10 kW/m² was also observed, but no specific data was provided.

Boonmee and Quintiere (2002, 2005) investigated the glowing and flaming ignition of wood in a vertical orientation along the grain and perpendicular to the grain. Above 40 kW/m² flaming ignition was observed, while below 40 kW/m² glowing was observed first. Furthermore, they reported glowing ignition within 2 hours with a 10 kW/m² exposure and considered that value to be the critical heat flux for glowing ignition.

Lim and Chew (2007) studied piloted flaming ignition of Nyatoh hardwood. The critical flux for ignition was 10 kW/m².

Gratkowski *et al.* (2006) investigated the smouldering ignition of maple plywood. The critical radiant flux was 7,5 kW/m².

B.4.2 Test setup

Swann *et al.* investigated the critical heat flux for radiative smouldering ignition, the ignition temperature and the kinetic parameters of both virgin and pre-treated wood in order to determine if there is any evidence for a change in ignitability. Maple plywood samples of 18 mm thick were heated at 180 °C for up to a month to achieve varying degrees of thermal decomposition and charring, resulting in residual weights of 30, 50 and 70 % of the original weight.

Ignitability of the samples was examined in the cone calorimeter without pilot to a heat flux between 6 and 15 kW/m². These tests were conducted until smouldering/glowing combustion was observed or if after eight hours no ignition was observed. Furthermore, the chemical kinetics of the samples (i.e. the

reaction rates and mechanisms) were investigated by thermogravimetric analysis (TGA) and differential scanning calorimetry (DSC).

B.4.3 Test Results

No measurable differences were found between the various pre-treated samples and the virgin material with regards to the minimum heat flux for ignition.

The minimum heat flux for smouldering ignition was in the range of 7 to 8 kW/m². However, the time to ignition was reduced from nearly 4 hours for the virgin material to less than one hour for the treated samples. Discussion about the TGA and DSC results is beyond the scope of this review.

B.4.4 Conclusions and relevance

The data from the cone calorimeter, TGA, and DSC do not suggest the presence of pyrophoric carbon in the pre-heated wood samples. The pre-heated wood samples follow the same combustion mechanism as the virgin wood, but start further along “the pathway”. As a result, the cone calorimeter shows the minimum flux required for ignition of 7-8 kW/m² is not affected by pre-heating. However, the time to ignition is shortened for the thermally treated samples.

The reduction in heating time is expected since a smouldering ignition mechanism requires charring as the first step. Since this step has already been accomplished in whole or in part in the thermally pre-heated materials, the ignition can occur more quickly. In addition the thermal inertia of the thermally pre-heated wood is lowered.

A flux minimum heat flux of 7-8 kW/m² without pilot was found to be required for the onset of smouldering combustion in virgin wood after 4 hours of exposure. While this result regards the initiation of smouldering and not sustaining the smouldering, it can be expected that it indicates that smouldering might not occur below this flux. As a result, it suggests a potential of self-extinguishment. Furthermore, the literature review also suggests a potential for self-extinguishment at heat fluxes below approximately 10 kW/m².

B.5 McGregor - CLT Room Fires

McGregor *et al.* (2013) carried out a series of 5 fire tests on CLT rooms. Setups with different fuels (propane and bedroom furniture) and different room lining configurations (fully passive protected and unprotected) were investigated. The goal of the research was to assess the contribution of CLT panels to the development, duration, and intensity of room fires.

B.5.1 Test setup

The tests were conducted in rooms 3,5 m wide, 4,5 long, and 2,5 m high. The walls and ceiling were constructed from 105 mm thick 3-ply CLT panels. A single door opening in the front wall 1.07 x 2 m was included in all tests.

In the protected configurations two layers of gypsum board were installed directly over the CLT panels on the walls and ceiling. The floors were protected with a gypsum layer with cement board on top. For the furniture tests hardwood flooring was installed.

A propane design fire was used that represented an extreme case for a primary bedroom in a multi-family dwelling, based on a fire load density of 753 MJ/m². The fire was modelled as a fast growing fire. The ventilation limited peak HHR was calculated to be 4.54 MW. This peak was sustained until 60 % of the fuel load had been consumed. Subsequently, a t-squared decay phase was used, resulting in a test duration of approximately 60 minutes, as depicted in figure B.3. However, a revised peak HHR of 3 MW was used in the actual testing, because extensive flaming was observed outside the compartment during the first test, indicating a large amount of volatiles being combusted outside the compartment.

The furniture fires tests were performed with real room contents. The total fuel load was estimated to be around 533 MJ/m².

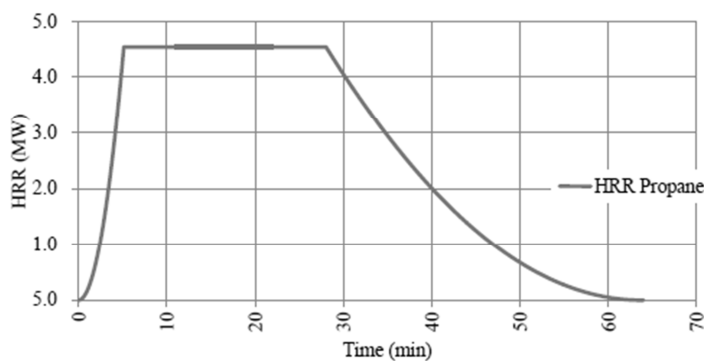


Figure B.3 Design fire profile with unrevised peak value. From McGregor *et al.* (2013).

Visual observations, such as fire stages, were recorded during the tests. Data was collected on the heat release rate using a full-scale tunnel test facility that features a system for measuring HRR using oxygen consumption. A flow meter was used to measure the propane flow, from which the propane HRR was calculated.

Room temperatures were measured with a plate thermometer and with thermocouples at different heights and location. Temperatures of CLT were measured with thermocouples embedded in the structure at different depths.

Charring rates were calculated by using these thermocouples to track the progress of the char front. Final char depths were measured by removal of the char layer after testing.

B.5.2 Test Results

The test results presented by McGregor are numerous. The review here is limited to the most important observations with regards to contribution of the CLT to the fire and possible self-extinguishment. The results are discussed per configuration.

Protected CLT with propane design fire

The aim of test 1 was to establish a reference fire and to observe the performance of protected CLT panels in the controlled propane design fire. The HRR development of the test is depicted in figure B.4.

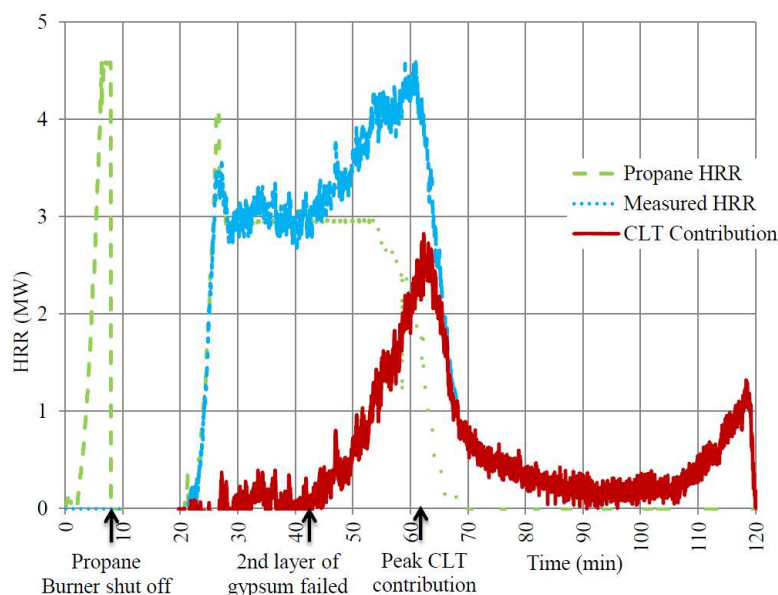


Figure B.4 Protected CLT with propane design fire heat release rate. From McGregor et al. (2013).

The fire was initiated and room temperatures quickly exceeding 1000 °C, before entering a slower growth phase. The room temperature stabilised near 1130 °C, or 1200 °C for the plate thermometer.

Localized failure of the gypsum occurred near the burner at 48 minutes, possible due to the concentrated fire load. The CLT became involved in the fire and the total heat release peaked at 4,6 MW at 60 minutes. At that time, the heat release from the propane burning was decreased, indicating decay of the design fire load. The contribution of the CLT increased to 2,8 MW, but then decayed as well, followed by a sharp drop in temperature.

Flaming combustion transformed to smouldering combustion which continued at room temperatures of 480 °C, or 400 °C for the plate. The first layer of the exposed CLT delaminated, exposing a second layer

which burned in flaming combustion. This caused a second growth phase, approximately at 115 minutes. The fire was extinguished after the flames started to exit the room.

The total energy released by the propane was calculated to be 486 MJ/m². The CLT contribution to the fire was calculated to be 200 MJ/m².

Protected CLT with furniture fire

The aim of test 2 and test 4 was to observe the performance of protected CLT panels in a furniture room fire. Data of test 2 was lost, so test 4 is review here. The HRR development of the test is depicted in figure B.5.

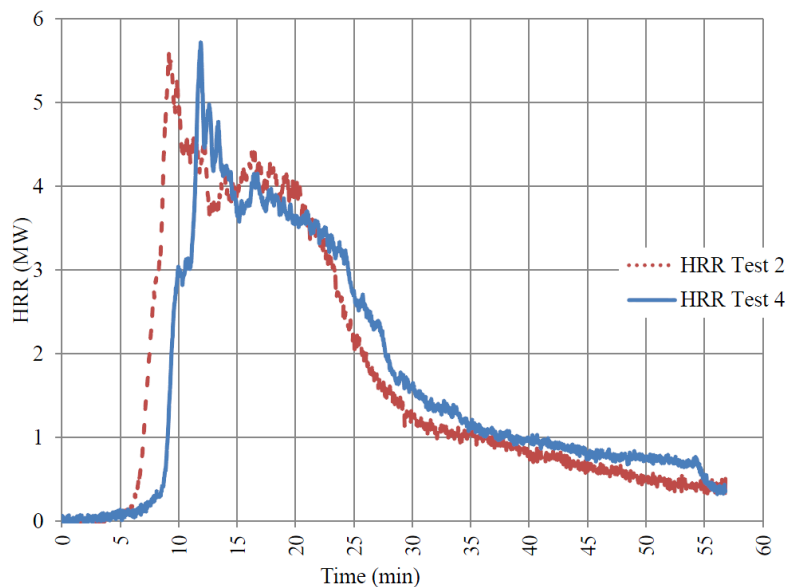


Figure B.5 Protected CLT with furniture fire heat release rate. From McGregor et al. (2013).

At the start of the test the bedding was ignited. Temperatures increased quickly and at 9,5 minutes all items in the room appeared to be involved in the fire, indicating flashover. The HRR peaked at approximately 5,7 MW at 12 minutes and stabilized at 4 MW. Temperature peaked at approximately 1000 °C at 16 – 20 minutes, or approximately 1100 for the plate thermometer.

Both HHR and temperatures entered a sharp decay phase at approximately 24 minutes. Most flaming was contained within the room by 25 minutes and most flaming extinguishing after 30 minutes. The fire was extinguished at 53,5 minutes.

The majority of the gypsum remained in place, with the exception of the first layer at some locations. No contribution of the CLT was observed. The total energy released during these fires was 379 MJ/m² and 364 MJ/m², equivalent to 69% and 64% of the estimated fuel load of the room.

Unprotected CLT with propane design fire

The aim of test 3 was to observe the involvement of unprotected CLT panels in the controlled propane design fire. The HRR development of the test is depicted in figure B.6.

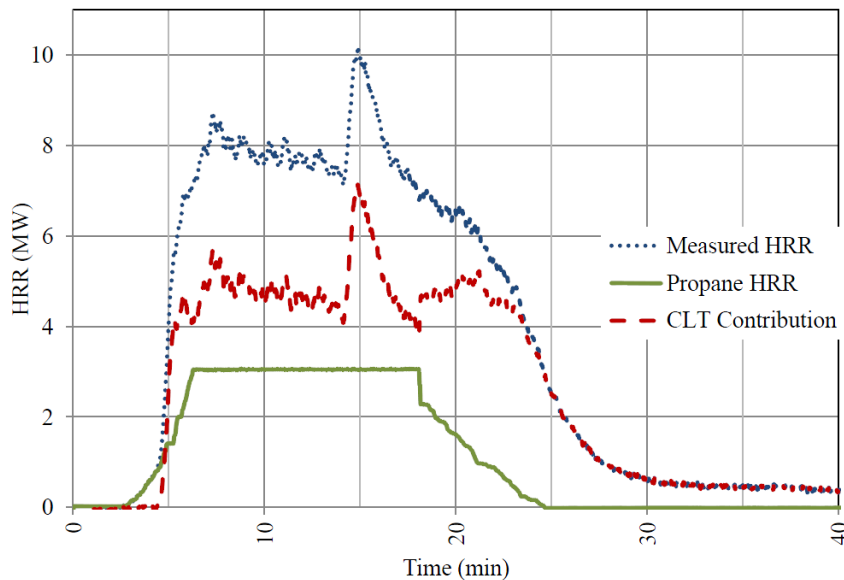


Figure B.6 Unprotected CLT with propane fire heat release rate. From McGregor et al. (2013).

The CLT became involved in the fire at 4,5 minutes, indicated by the HHR increasing above that of solely the propane fire. Temperatures rose fast at 5 minute, indicating flashover. The total HHR then reached a peak of 8,75 MW at 7,5 minutes. At that moment the CLT contribution reached a peak of 5,7 MW. Both the total HHR and the CLT contribution stabilized. The CLT contribution remained constant at 4,5 MW, indicating uniform charring and pyrolysis of all the surfaces. Maximum temperatures were achieved of approximately 980 °C, or 1140 for the plate, at 10 – 24 minutes.

The propane flow was reduced at 17 minutes, initiating the decay of the design fire. Temperature dropped along with the heat release rate. No significant change was noticed in the CLT contribution to the HHR until 21 minutes when it also entered a period of decay. Only smouldering combustion was observed in the room at 29 minutes and the HHR stabilized at 0,45 MW at 35 minutes. The glowing combusting was mostly observed near the floor and in the corners of the room. Some unsustainable localised flaming was observed at 58 minutes at locations where minor delamination was observed. The room was cooled with water at 60 minutes.

The total energy released by the propane was calculated to be 182 MJ/m². The CLT contribution to the fire was calculated to be 408 MJ/m².

Unprotected CLT with furniture fire

The aim of test 5 was to observe the performance of unprotected CLT panels in a furniture room fire. Figure B.7 depicts the development of the HRR and compares it with the tests with protected CLT and furniture fire, to estimate the contribution of the CLT.

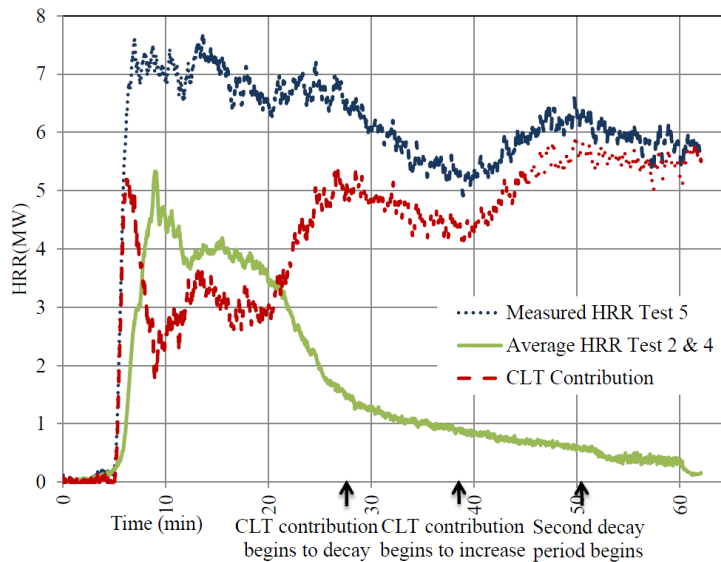


Figure B.7 Unprotected CLT with furniture fire heat release rate. From McGregor et al. (2013).

The test started and the bedding was ignited. The CLT became involved in the fire and the estimated contribution of the CLT increased rapidly to 5 MW. Temperatures quickly rose at flashover, slowing at 825 °C, but increased again to 980 °C and stabilized. After a small drop, temperatures reached 1000 °C, or 1170 °C for the plate, and stabilized. The total HRR reached a peak of 7,64 MW at 7 minutes, after which the fire burned steady at 7 MW. At 27 minutes a decay was initiated at the moment the estimated contribution from the furniture and hardwood floor dropped below approximately 1,5 MW.

At 39 minutes pieces of the first layer of the CLT delaminated and fell off, exposing a second layer of CLT. The delamination contributed to the fire load in the room and exposed unburned wood that caused the HRR to rise again. The contribution of the CLT increased to 6 MW. A second peak of 6.6 MW was reached at 50 minutes, after which the HRR stabilized at 5.7 MW at 57 minutes. The test was stopped at 63 minutes to protect the test facility from being damaged.

The total energy released by the furniture was estimated to be 336 MJ/m². The CLT contribution to the fire was estimated to be 612 MJ/m².

Other results

Overall charring rates were found to be consistent with those presented in the Eurocode for solid timber, as well as for initially protected timber members after the fire protection has fallen off. In some tests charring continued hours after the fire was extinguished at the gypsum-CLT interface where gypsum remained in place. In all tests the exterior faces of the walls did not experience any significant increase in temperature and remained safe to touch due to the low conductivity of the wood.

B.5.3 Conclusions and relevance

The work by McGregor is of interest to this research because it investigates CLT room fires. The research illustrates the various phases of a CLT room fire in terms of HHR and temperature and the transitions between flaming and smouldering combustion. The research also describes the particular behaviour of CLT in a fire, including phenomena such as delamination. Furthermore, the contribution of the CLT to the fire was determined.

Figure B.8 provides a comparison of the total energy released for all tests.

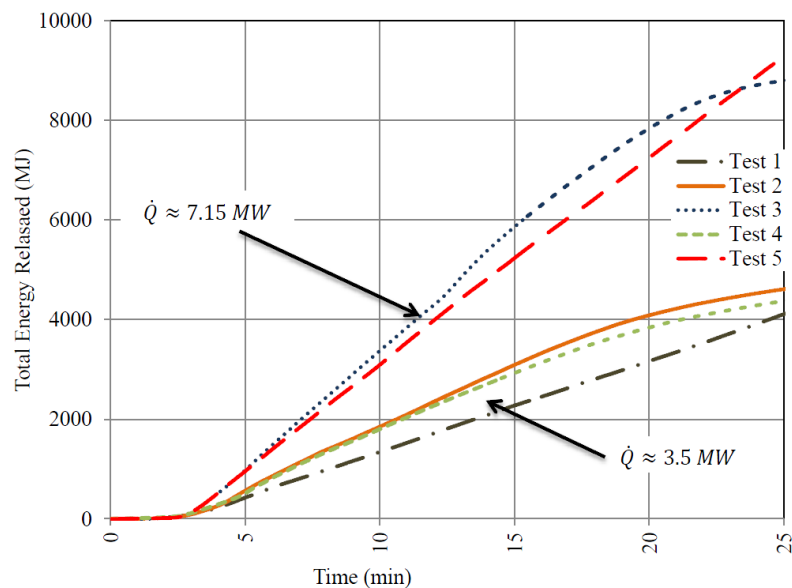


Figure B.8 Comparison of total energy released for all tests. From McGregor et al. (2013).

McGregor concluded that in protected room tests with furniture as fuel (tests 2 and 4), the fires self-extinguished when all combustibles were consumed. The CLT panels did not contribute to the growth, duration, or intensity of the fire.

In the tests with unprotected CLT (tests 3 and 5), the CLT quickly became involved in flaming combusting and increased fire growth rates were observed, which reduced time to flashover. Furthermore, increased rates of energy release were observed; approximately twofold in these test, as well as the total energy released.

In the test 3 with unprotected CLT the propane design fire entered a phase of decay. The CLT contribution was observed to decay as well. The material changed from flaming to smouldering combustion and the heat release dropped. The CLT did not delaminate and smouldering occurred until the test was extinguished with water. These observations suggest that the contribution of exposed CLT to the fire is most significant in the flaming combustion phase when heat release is high. Furthermore, they suggest a smouldering phase can be expected after cessation of the flames if the CLT does not delaminate.

Glowing / smouldering combusting in test 3 was observed until the end of the test, but gradually faded, indicating possible self-extinguishment. This smouldering occurred predominantly at the corners and at the floor-wall joint. This can be explained due to the higher radiative configuration factors at these locations.

In those tests where charring caused delamination of the CLT panels (test 1 where the gypsum failed in a propane fire; and tests 5 with unprotected CLT and a furniture fire), the energy release rates increased, extending the duration of the fire. The CLT panels provide fuel to the fire as it uncovered unburned wood. This indicated that the CLT panels can contribute significantly to the fire load in a room.

In the test 5 with unprotected CLT and furniture fire the CLT delaminated and exposed new layers of wood. As a result the fire did not transform into smouldering combusting, but flaming was sustained. A similar event occurred in the test 1 with protected CLT in a propane fire. The gypsum board protection failed and the CLT panels contributed to the fire, increasing the energy release. Due to delamination the fire transformed from smouldering back into flaming combustion and heat release increased again.

These observations suggest that delamination of the CLT can sustain flaming or transforms the fire back to flaming. If a potential for self-extinguishment exist, it will be when the CLT does not delaminate and the fire can enter a smouldering phase. Subsequently this smouldering might self-extinguish. However, these tests were terminated and cooled with water before complete burnout occurred and potential self-extinguishment was not investigated.

Furthermore, McGregor also observed that temperatures of the thermocouples converged. This indicates that the dominating mode of heat transfer was transitioning from convective to radiative.

B.6 Frangi *et al.* - CLT Charring

Frangi *et al.* (2009) investigated CLT panels in fire, with an emphasis on the charring behaviour. Design models of timber structures in fire usually take into account the loss in cross-section due to charring of wood. The cross-section in a fire is determined by reducing the unaffected cross-section with a charred layer. The depth of this charred layer is calculated as the charring rate times the duration of exposure.

Charring rates are available in design guidance for various timber products, including solid timber and wood panelling. However, little information is available about the charring behaviour of CLT. The study of Frangi *et al.* is focussed on CLT charring behaviour under ISO-fire exposure and compares it to other timber products. Particular attention was given to the influence of the adhesive with regards to delamination of the panels.

B.6.1 Test setup

CLT tests specimen were made of 1,15 x 0,95 m. spruce boards. Layers of 10, 20 and 30 mm were used; but the total thickness of the CLT panels was 60 mm in each test. Thermocouples were placed between the layers and an additional timber layer of 30 mm was glued on the fire unexposed side to allow for complete charring of the samples.

Five different polyurethane (PU) adhesives and one melamine urea formaldehyde (MUF) adhesive were tested. These adhesives are commonly used in Europe for the production of CLT panels. To study the influence of the orientation of the layers, one specimen was manufactured with all layers orientated in the same direction.

In total, eleven samples were subjected to ISO 834 fire exposure in an unfavourable orientation with regards to charring; exposure from below in a horizontal configuration. Tests were stopped when the 300 °C isotherm reached the interface between CLT and the additional timber layer; indicating complete charring. At the end of the tests, the specimens were cooled with water.

B.6.2 Test results

Falling off of the charred layers was observed for all specimens with the PU adhesives. However, the tests with MUF adhesive showed not char fall-off.

Thermocouple-data reinforced this. For the PU specimen the temperatures between the layers rose rapidly from 300 °C to furnace temperature; indicating delamination the moment the complete layer was charred. Note that the 300 °C isotherm is used as indication of the location of the char front. Delamination could be visually observed, as depicted in figure B.9.

For the MUF specimen these temperatures did not increase so rapidly and were always lower than the furnace temperature.

The charring depth vs. time and the charring rate were determined for all specimens with the 300 °C isotherm. Results were compared with charring rates in the Eurocode for of solid timber and timber panelling.

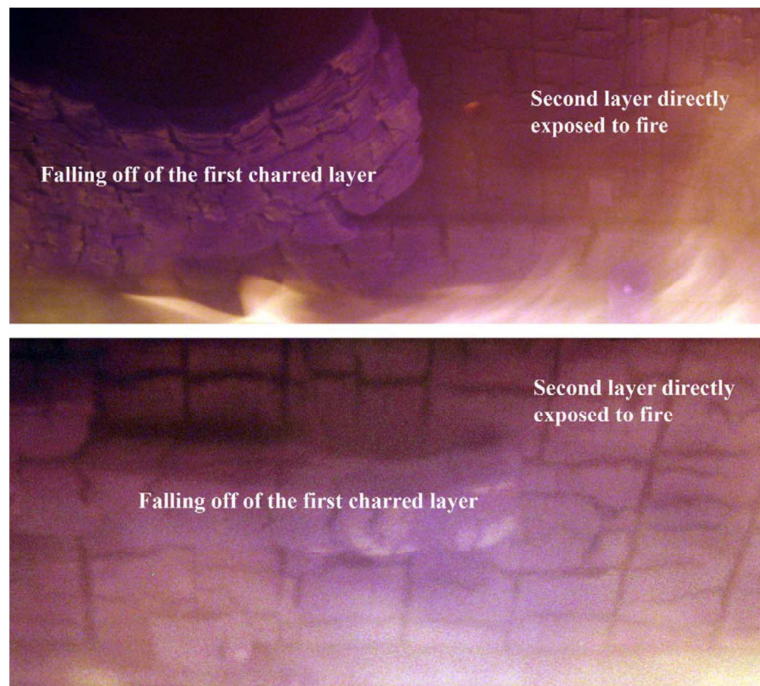


Figure B.9 Falling off of the first charred layer, exposing a second. From Frangi et al. (2009).

It was observed for the MUF glued specimens that the charring rate of all individual layers was constant by approximation. As the charred layers remained in place, the uncharred material was protected against the increasing high temperatures of the ISO exposure. As a result, the CLT behaved similar to solid timber panels. The measured charring rate of about 0,60mm/min was even slightly lower than the one-dimensional charring rate of 0,65mm/min assumed for solid timber in EN 1995-1-2.

For the PU glued specimens it was observed that the charring rate of the individual layers was not constant. The charring rate increased after the first layer was completely charred and fell off. Furthermore, the later the layer became exposed, the more the charring rate increased. This was assumed due to increasing fire temperature of the ISO exposure, while no protective char could reduce its effect on the next layer. This effect amplified with increasing number of layers and decreasing individual layer thickness. As a result, the total charring rate of these PU glued CLT panels was also higher compared to solid timber, in the range of 0,85 to 1,10 mm/min. No significant differences were observed between the various PU adhesives and for the specimen with alternative layer orientation.

The effect of an increased charring rate observed in the PU glued specimens is also known for initially protected timber members after the fire protection has fallen off. The simplified bilinear model in EN 1995-1-2 for initially protected surfaces was adopted for the CLT test results. This new CLT model uses the 0,65 mm/min of one-dimensional charring of solid timber for the first layer. After fall-off of this layer, the model adopts the EN 1995-1-2 approach of a double rate of charring of 1,3 mm/min. For layers with a thickness of more than 25 mm, the rate is reduced to 0,65 mm/min after charring 25 mm into that layer. This model lead to safe estimations of the charring depth of the PU glued specimens; as shown in Figure B.10.

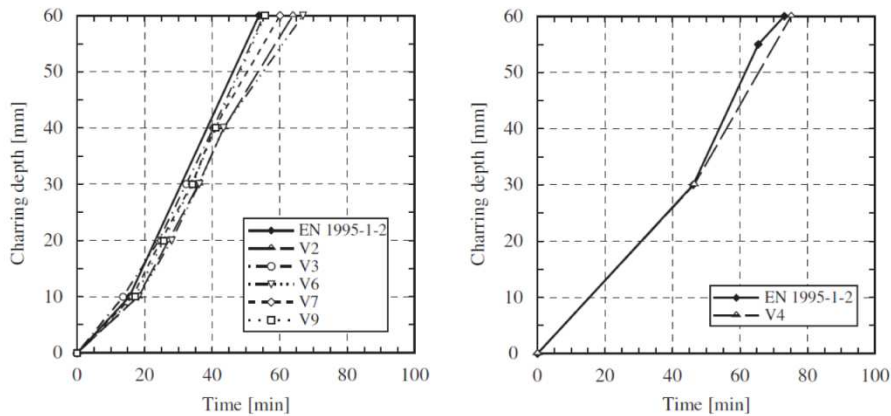


Figure B.10 Comparison of the measured charring depth with the charring depth calculated using the bilinear model adopted from EN 1995-1-2: CLT panels of 4 x 10mm + 20 mm and various PU glues and orientations (left) and 2 x 30 mm (right). From Frangi et al. (2009).

B.6.3 Conclusions and relevance

The research was aimed towards enlarging the experimental background on the charring behaviour of CLT panels and the development of a charring model. While this is important in the design of CLT structures in fire, it is the influence of the adhesive and possible delamination of the panels that is of particular interest to this research. It was observed in the tests performed by McGregor (2013) that delamination of the CLT panels transformed the smouldering fire back to a flaming fire. As a result, delaminating of the CLT can sustain flaming combustion and prevent any potential of self-extinguishment.

Frangi *et al.* concluded that the fire behaviour of CLT panels is strongly dependent on the adhesive used. PU glued specimens were found to delaminate in the unfavourable horizontal configuration when the layer was completely charred. After fall-off of a charred layer, an increased charring rate was observed due to the newly exposed layer being subjected to high temperatures without protecting char. As the ISO-exposure increases in temperature, the later the char falls off, the more the charring rate increased. Furthermore, thick lamellas perform better than thin ones, as falling off occurs less frequently. This might be relevant in achieving self-extinguishment of PU-based CLT, when it can occur within the thickness of a single lamella, before the layer delaminates.

A bi-linear model adopted from EN 1995-1-2 for initially protected surfaces can be used for the calculation of charring of CLT panels that delaminate in a fire.

MUF glued specimens did not show such behaviour and the char protection stayed in place. The charring rate for these specimens was slightly lower than the one-dimensional charring rate of 0.65mm/min for solid timber and much lower than the charring rate of 0,9 mm/min for wood panelling in EN 1995-1-2.

The samples were tested in an unfavourable orientation with regards to charring; from below in a horizontal configuration. It was noted that a vertical orientation or a horizontal orientation but heated from above, might be less unfavourable and will prevent, or show less, delamination and fall-off.

Post-processing of data in experiment series 1

Once an experiment was performed, data from the various devices was post-processed in order to make it presentable and suitable for discussion.

During each experiment, up to three devices gathered measurements and provided output data.

- The cone calorimeter measured the sample mass and analysed the exhaust gases during the exposure of 75 kW/m^2 . Output was provided on the sample weight, mass loss rate, heat release rate, and effective heat of combustion.
- The thermocouples provided output on the temperature at various locations in the sample for the total test duration.
- The scale provided output on the sample weight during the second exposure.

These 3 data sets needed to be combined to allow for discussion of the results as a post-processing step. Combining of the sets was achieved by making use of three “events” that occurred during the experiments and that were reflected in these data sets.

A first event occurred at the start of an experiment and was marked by the opening of the shutters in the calorimeter, exposing the sample to a 75 W/m^2 heat flux. The cone calorimeter presents this event at $t=0$ in its output. This event is also marked in the thermocouple data by an immediate rise in temperature of the surface thermocouples. This was used to combine the cone data with the thermocouple data.

A second event occurred when the sample is removed from the cone calorimeter. The weight measurement of the load cell drops, as does the temperature of the surface thermocouples. If both data sets were successfully combined at the start of the test, they arrived at this moment simultaneously.

A third event occurred when the sample was placed on the scale of the second setup. It was established during testing that it takes approximately 20 seconds to switch the sample to the second setup. Therefore, the scale data set was combined with the other two data sets 20 seconds after removing the sample from the cone calorimeter.

D

Temperature profile prediction experiment series 1

This appendix presents a prediction of the temperatures in the CLT of the first series of experiments. This prediction is based on a finite difference method, a numerical method for approximating the solutions of differential equations using finite difference equations to approximate derivatives. The method used is presented in “Fundamentals of Heat and Mass Transfer” (Bergman *et al.* 2011).

The thermal properties of the wood and the charcoal (the thermal conductivity, specific heat capacity, and density ratio); are obtained from Eurocode 1995-1-2 for advanced calculations. Tables D.1 to D.3 depict these properties. A density of 450 kg and an initial moisture content of 12 % at 25 °C are assumed.

Table D.2 temperature – specific heat relationship for wood and the char layer. From Eurocode 1995-1-2.

Temperature [°C]	Specific heat capacity	
	[Wm ⁻¹ K ⁻¹]	[Jkg ⁻¹ K ⁻¹]
20	1,53	1530
99	1,77	1770
99	13,6	13600
120	13,5	13500
120	2,12	2120
200	2,00	2000
250	1,62	1620
300	0,71	710
350	0,85	850
400	1,00	1000
600	1,40	1400
800	1,65	1650
1200	1,65	1650

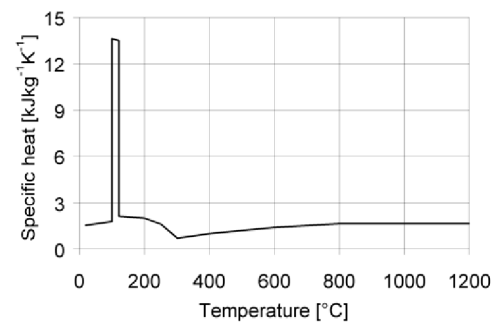


Table D.1 temperature – thermal conductivity relationship for wood and the char layer. From Eurocode 1995-1-2.

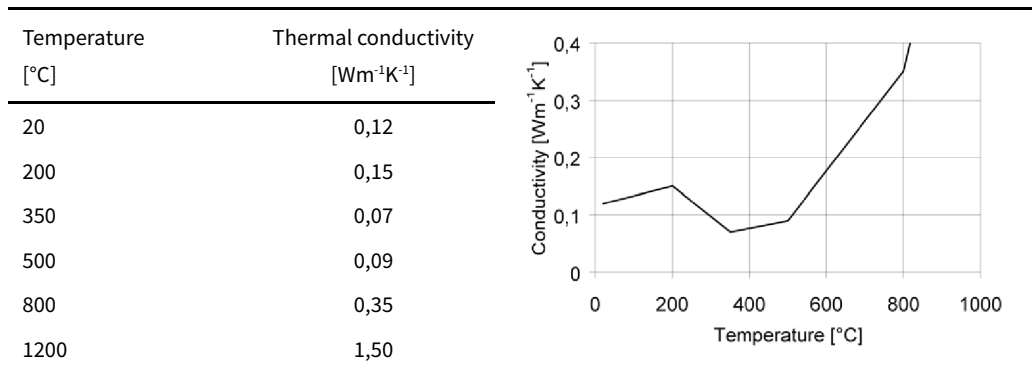
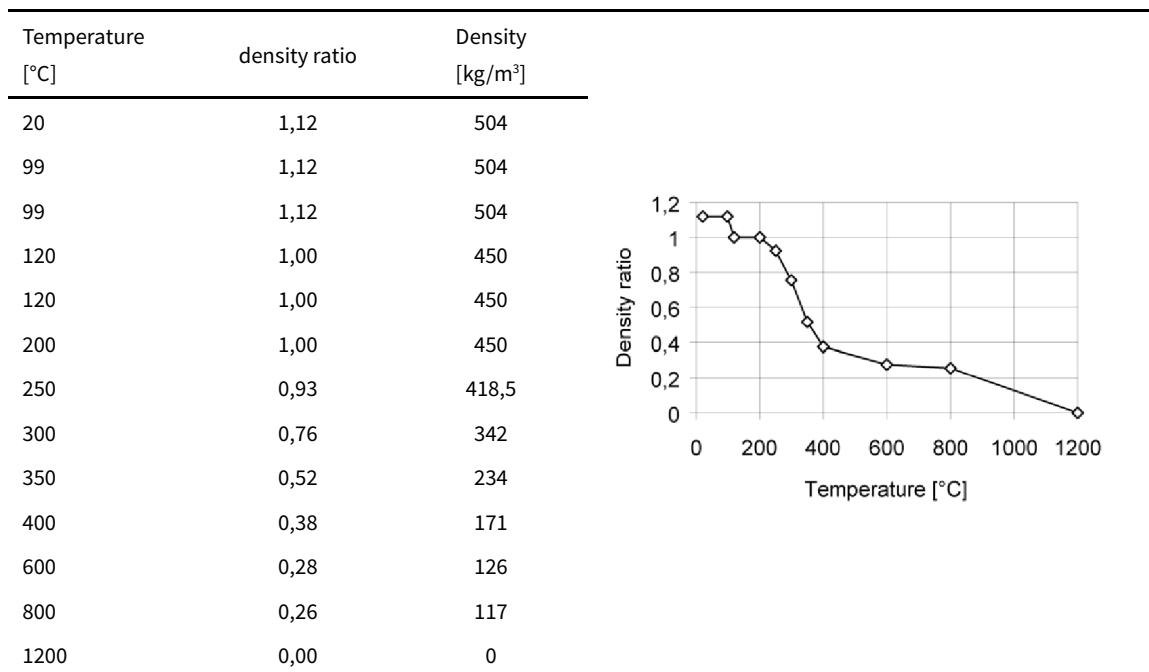


Table D.3 temperature – density ratio relationship for wood and the char layer. From Eurocode 1995-1-2.



Based on these thermal properties, the thermal diffusivity, i.e. the ability of the material to conduct thermal energy relative to its ability to store thermal energy, was determined, as shown in table D.4.

The CLT specimen was divided in elements of thickness 0,005 m. A time step of 1 second was chosen for the numerical process. The Fourier and Biot numbers were determined that characterizes the conduction problem and are used in each step of the numerical calculation.

Based on these numbers, the numerical process was found to be stable at the chosen time step and element size, provided that temperatures did not exceed 1000 °C.

Table D.4 Thermal diffusivity, Fourier and Biot numbers at various important temperatures.

Temp. [°C]	Thermal Conductivity [Wm ⁻¹ K ⁻¹]	Density [kg/m ³]	Specific heat capacity [Wm ⁻¹ K ⁻¹]	thermal diffusivity [m ² /s]	Fourier Number		Biot Number	
20	0,12	504	1530	1,56E-07	0,01	OK	1,46	OK
99	0,13	504	1770	1,49E-07	0,01	OK	1,31	OK
99	0,13	504	13600	1,94E-08	0,00	OK	1,31	OK
120	0,14	450	13500	2,25E-08	0,00	OK	1,28	OK
120	0,14	450	2120	1,43E-07	0,01	OK	1,28	OK
200	0,15	450	2000	1,67E-07	0,01	OK	1,17	OK
250	0,12	419	1620	1,82E-07	0,01	OK	1,42	OK
300	0,10	342	710	3,98E-07	0,02	OK	1,81	OK
350	0,07	234	850	3,52E-07	0,01	OK	2,50	OK
400	0,08	171	1000	4,48E-07	0,02	OK	2,28	OK
600	0,18	126	1400	1,00E-06	0,04	OK	0,99	OK
800	0,35	117	1650	1,81E-06	0,07	OK	0,50	OK
900	0,64	88	1650	4,40E-06	0,18	OK	0,27	OK
1000	0,93	59	1650	9,58E-06	0,38	OK	0,19	OK
1199	1,50	0	1650	3,10E-03	124,08	TOO BIG	0,12	TOO BIG

For the calculation, a convective heat transfer coefficient of 35 W/m²K was assumed on the interface between the gas and the wood, as suggested by Eurocode 1991-1-2 for advanced calculations.

A convective heat transfer coefficient of 4 W/m²K was assumed on the interface between the last element of CLT and the back side, as suggested in Eurocode 1991 for the non-exposed side.

The wood surface emissivity was assumed to be 0,8, as suggested by Eurocode 1995-1-2. The ambient temperature was set as 22 °C.

In the model, heating of the material occurs by means of a gas temperature. However, in the actual experiments the samples were subjected to a radiative heat flux. An equivalent gas temperature was unknown. Therefore, in this calculation, the gas temperature was assumed to be the temperature of the cone heater. This is a simplification, but was found fairly accurate with regards to the surface temperatures that were measured.

With all material properties and transfer characteristics known, the temperature of each element is calculated for the subsequent time steps, based on the mechanism of heat transfer (conduction, convection, and radiation).

The temperature of a certain element is based on its temperature in the previous time step, its thermal diffusivity (including the ability to conduct thermal energy to adjacent elements and the ability to store thermal energy), and (if located at either surface) the convective and radiative interactions with the gas or the ambient air.

Figure D.1 depicts the result of the prediction for a 75 kW/m² heat flux exposure (gas temperature of 913 °C assumed), followed by a 6 kW/m² heat flux exposure (gas temperature of 449 °C assumed). Furthermore, on the next page, the first 30 seconds of the calculation sheet are presented.

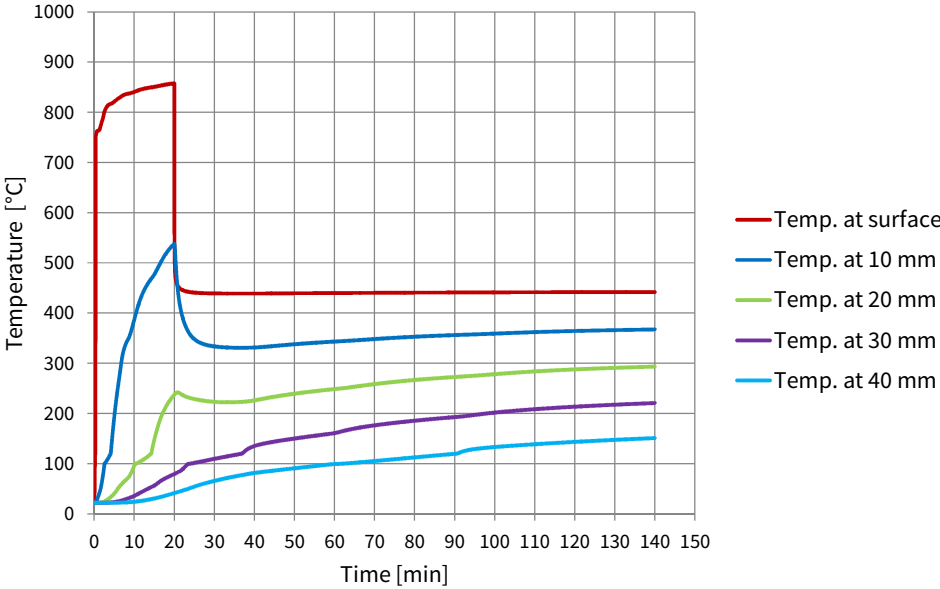


Figure D.1 Prediction of CLT temperatures at a 75 kW/m² and subsequent 10 kW/m² exposure.

t	Tgas	t	x	Temp. at surface	Temp. at 10 mm	Temp. at 20 mm	Temp. at 30 mm	Temp. at 40 mm	LAST NODE			
0.0000	0	20	0	0.005	0.01	0.015	0.02	0.025	0.035	0.04	0.045	0.05
0.0167	22.00	50	1	22.00	21.99	20.02	21.99	22.00	22.00	22.00	22.00	22.00
0.0333	24.25	100	2	22.00	21.98	20.05	21.98	22.00	22.00	22.00	22.00	22.00
0.0500	27.05	150	3	22.02	21.96	20.07	21.96	22.00	22.00	22.00	22.00	22.00
0.0667	31.06	200	4	22.05	21.95	20.10	21.95	22.00	22.00	22.00	22.00	22.00
0.0833	36.37	250	5	22.10	21.94	20.12	21.94	22.00	22.00	22.00	22.00	22.00
0.1000	43.08	300	6	22.19	21.93	20.14	21.93	22.00	22.00	22.00	22.00	22.00
0.1167	51.31	350	7	22.32	21.92	20.16	21.92	22.00	22.00	22.00	22.00	22.00
0.1333	61.22	400	8	22.50	21.91	20.19	21.91	22.00	22.00	22.00	22.00	22.00
0.1500	72.95	450	9	22.73	21.91	20.21	21.90	22.00	22.00	22.00	22.00	22.00
0.1667	86.66	500	10	23.04	21.90	20.23	21.89	22.00	22.00	22.00	22.00	22.00
0.1833	102.52	550	11	23.43	21.90	20.25	21.88	22.00	22.00	22.00	22.00	22.00
0.2000	104.94	600	12	23.91	21.90	20.27	21.87	22.00	22.00	22.00	22.00	22.00
0.2167	107.89	650	13	24.40	21.90	20.29	21.86	22.00	22.00	22.00	22.00	22.00
0.2333	111.46	700	14	24.90	21.90	20.31	21.85	21.99	22.00	22.00	22.00	22.00
0.2500	115.76	750	15	25.42	21.91	20.33	21.84	21.99	22.00	22.00	22.00	22.00
0.2667	120.94	800	16	25.96	21.93	20.35	21.83	21.99	22.00	22.00	22.00	22.00
0.2833	160.38	850	17	26.53	21.94	20.37	21.83	21.99	22.00	22.00	22.00	22.00
0.3000	206.29	900	18	27.33	21.96	20.39	21.82	21.99	22.00	22.00	22.00	22.00
0.3167	254.92	910	19	28.40	21.98	20.41	21.81	21.99	22.00	22.00	22.00	22.00
0.3333	320.31	910	20	29.77	22.01	20.42	21.80	21.99	22.00	22.00	22.00	22.00
0.3500	493.37	910	21	31.52	22.05	20.44	21.80	21.99	22.00	22.00	22.00	22.00
0.3667	665.09	910	22	34.31	22.10	20.46	21.79	21.99	22.00	22.00	22.00	22.00
0.3833	737.28	910	23	38.13	22.17	20.48	21.78	21.98	22.00	22.00	22.00	22.00
0.4000	750.68	910	24	42.34	22.25	20.50	21.77	21.98	22.00	22.00	22.00	22.00
0.4167	752.99	910	25	46.57	22.37	20.52	21.77	21.98	22.00	22.00	22.00	22.00
0.4333	753.83	910	26	50.75	22.51	20.54	21.76	21.98	22.00	22.00	22.00	22.00
0.4500	754.47	910	27	54.88	22.67	20.56	21.75	21.98	22.00	22.00	22.00	22.00
0.4667	755.10	910	28	58.95	22.86	20.58	21.75	21.98	22.00	22.00	22.00	22.00
0.4833	755.71	910	29	62.97	23.07	20.60	21.74	21.98	22.00	22.00	22.00	22.00
0.5000	756.31	910	30	66.94	23.30	20.62	21.74	21.98	22.00	22.00	22.00	22.00

E

Design fire experiment series 2

For the second series of experiments, a design fire was chosen. Eurocode 1991-1-2 appendix E suggest the use of an t^2 growth phase, followed by a steady burning HRR, followed by a linear decay phase once 70 % of the fuel load has been consumed.

However, it was decided to make the growth and the decay phase discrete and jump to the steady state HRR at the start of the experiment, and back to 0 once the CLT was charred 20 mm. This was done to eliminate difficulties in creating the t^2 growth phase and the linear decay phase and because it was expected the exact development of these phases will not influence the outcome of the experiment.

The level of steady state HRR was initially determined using the Eurocode1991-1-2 table E.5. Based on this table, a value of 250 kW/m² was chosen as a representative value for office and residential functions. Considering the size of the compartment, this would result in a HRR of 75 kW.

An estimation of the ventilation controlled heat release rate was performed using both formula E.6 from Eurocode 1991-1-2, as well as a similar formula offered by Drysdale (2012). These calculations can be found in table E.1 and suggested the HRR inside the compartment would be constrained by 89 - 95 kW due to amount of oxygen available.

Table E.1 Ventilation controlled HRR

	EC 1991-1-2 E.6		Drysdale	
opening height	h	0.5 m	h	0.5 m
opening width	w	0.18 m	w	0.18 m
opening area	Av	0.09 m ²	Av	0.09 m ²
mean height	heq	0.5 m	heq	0.5 m
net calorific value of wood	Hu	17.5 MJ/kg		
combustion factor	m	0.8		
ventilation controlled HRR	Qmax	$0,10 \cdot m \cdot Hu \cdot Av \cdot heq^{0.5}$	Qmax	$1.5 \cdot Av \cdot heq^{0.5}$
		89.09545 kW		95.45942 kW
		356.3818 kW/ m ²		381.8377 kW/ m ²

However, the burners use a premixed flame. As a result, the HRR of the burners will not contribute towards the ventilation controlled HRR. The ventilation controlled HRR would only limit the contribution of the CLT, should it exceed approximately 90 kW. This was not expected.

Eventually, it was decided to use a slightly lower HRR of 63 kW, because it was suspected much external flaming would occur at higher values. Indeed, in the first experiment, significant flaming was observed outside the compartment, while only 1 CLT wall was involved additionally in the fire. To protect the experiment setup and to allow for more CLT to become involved in the fire without even more external flaming, the decision was made to reduce the flow rate of propane until most combustion was contained within the room.

The steady state HRR of the propane was lowered to 41 kW and this value was then used in each experiment subsequently.

F

Results experiment series 1

This appendix presents all results from the first series of experiments. An overview is provided in table F.1.

Table F.1 Overview of the first series experiments

Experiment	Initial flux[kW/m ²]	Second flux [kW/m ²]	Remark
1	75	0	-
2	75	0	-
3	75	5	-
4	75	5	-
5	75	10	-
6	75	10	-
7	75	8	-
8	75	8	-
9	75	6	-
10	75	6	-
11	75	6	Additional air flow (0,5 m/s) during second exposure
12	75	6	Additional air flow (1,0 m/s) during second exposure
13	75	75	Samples are not switched
14	75	75	Samples are not switched
15	75	75	Samples are not switched / No thermocouples
16	75	75	Samples are not switched / No thermocouples

F.1 Experiment 1 – 75 kW/m² → 0 kW/m²

F.1.1 Temperatures

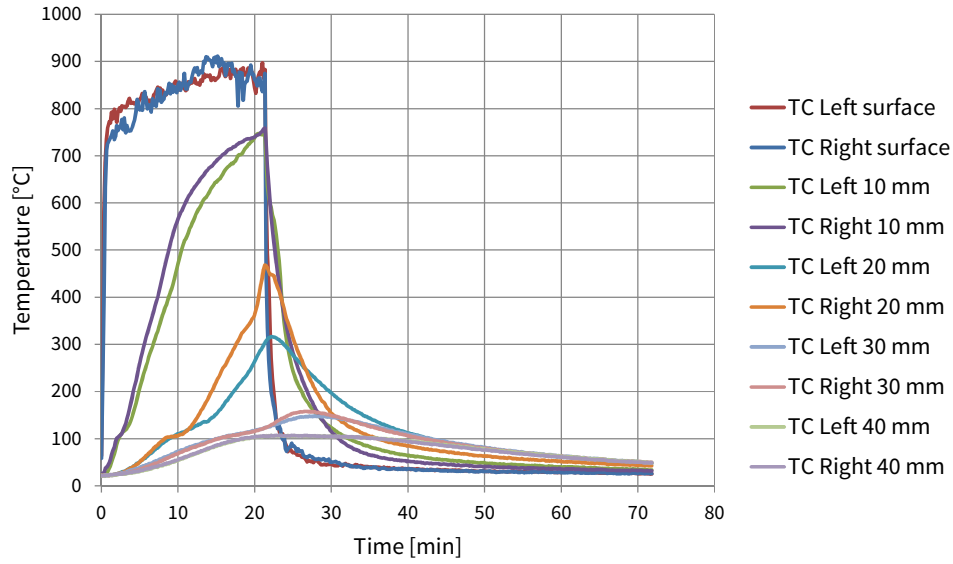


Figure F.1 CLT temperatures in experiment 1.

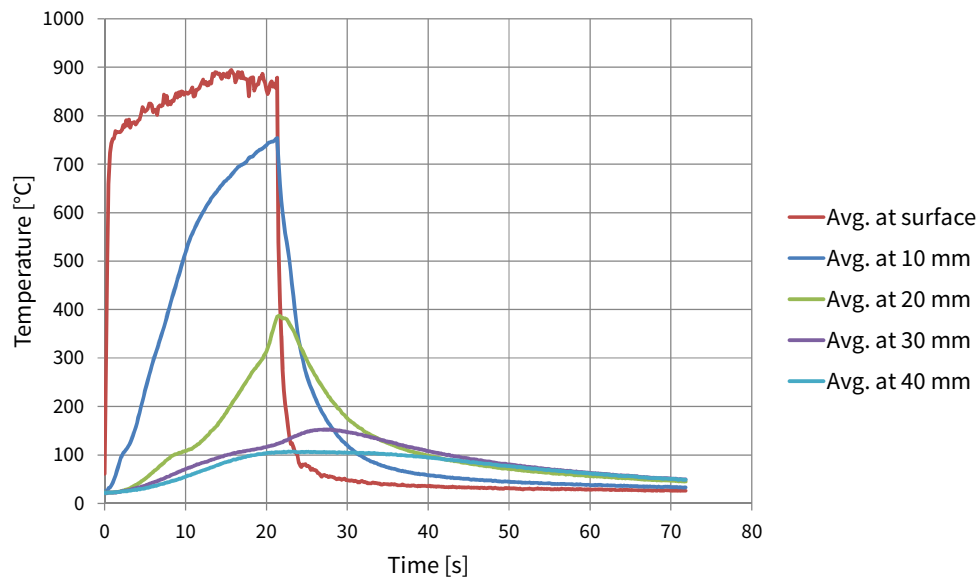


Figure F.2 Average CLT temperatures in experiment 1.

F.1.2 Mass loss

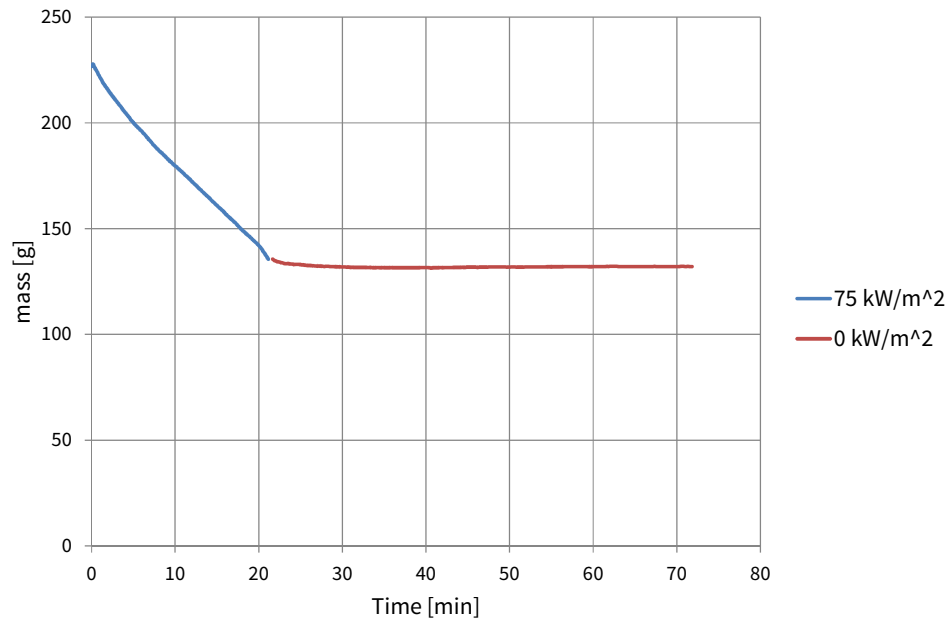


Figure F.3 Sample mass in experiment 1.

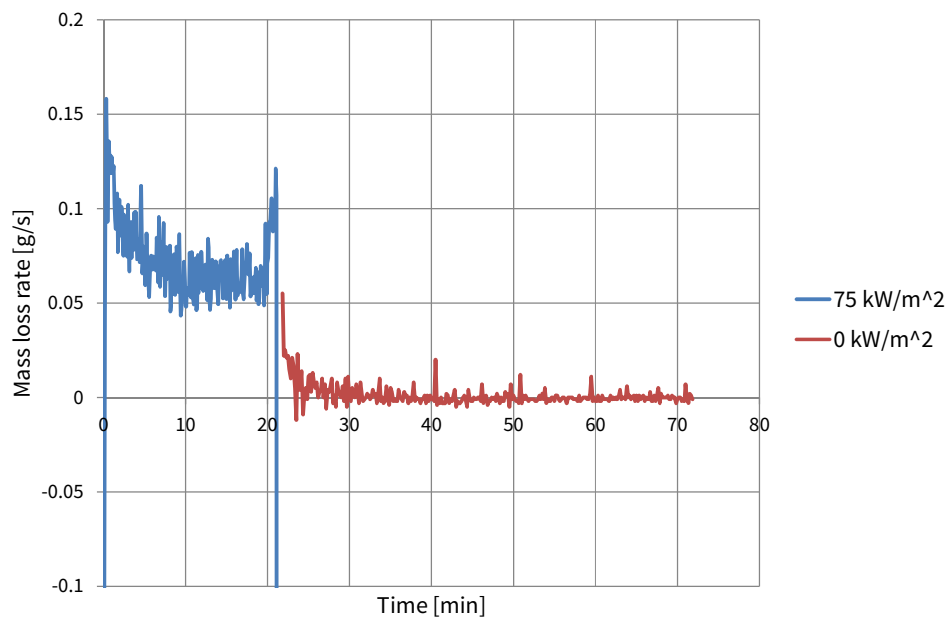


Figure F.4 Mass loss rate in experiment 1.

F.1.3 Heat release rate and heat of combustion

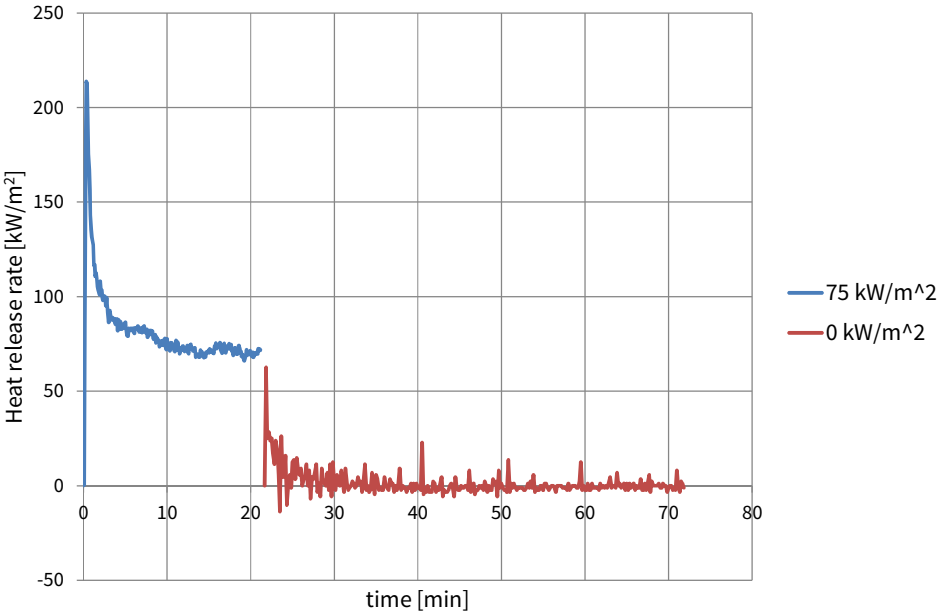


Figure F.5 Heat release rate in experiment 1 (the heat release rate during second exposure is based on the mass loss rate and average effective heat of combustion during the 75 kW/m² exposure).

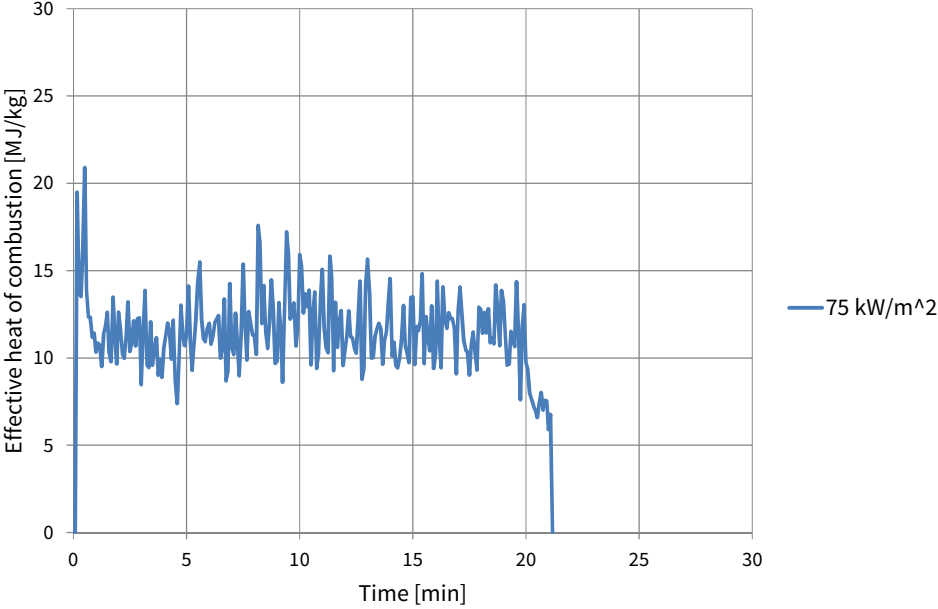


Figure F.6 Effective heat of combustion during the 75 kW/m² exposure in experiment 1.

F.2 Experiment 2 – $75 \text{ kW/m}^2 \rightarrow 0 \text{ kW/m}^2$

F.2.1 Temperatures

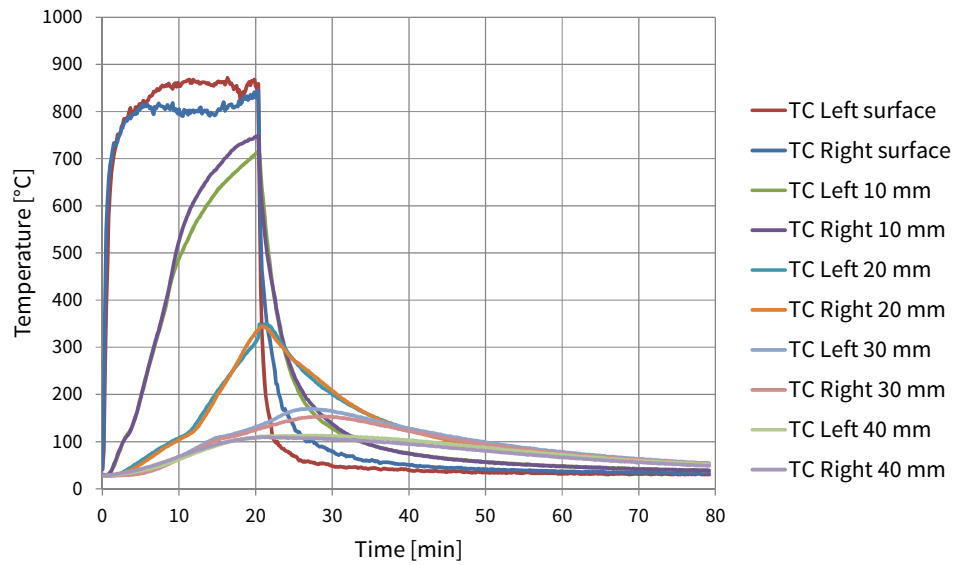


Figure F.7 CLT temperatures in experiment 2.

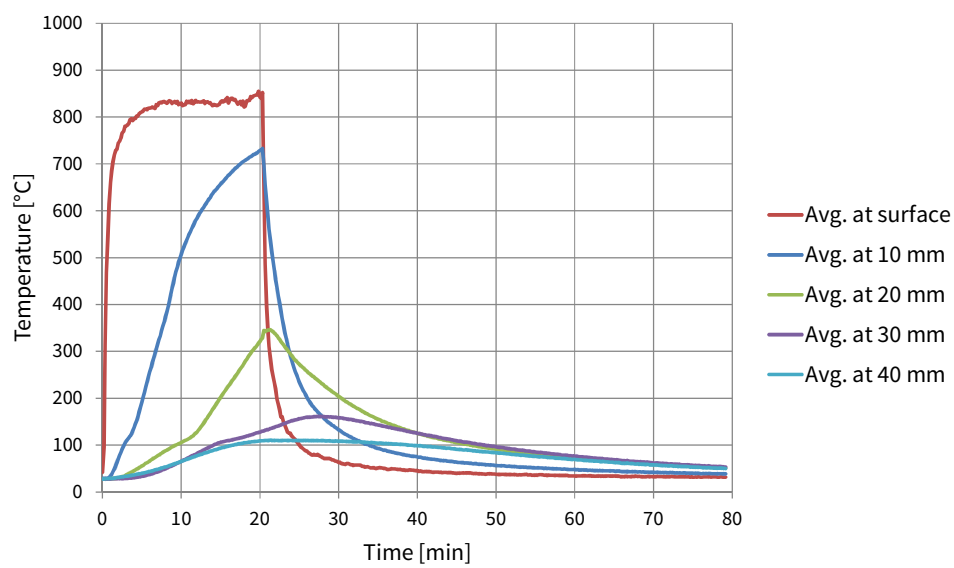


Figure F.8 Average CLT temperatures in experiment 2.

F.2.2 Mass loss

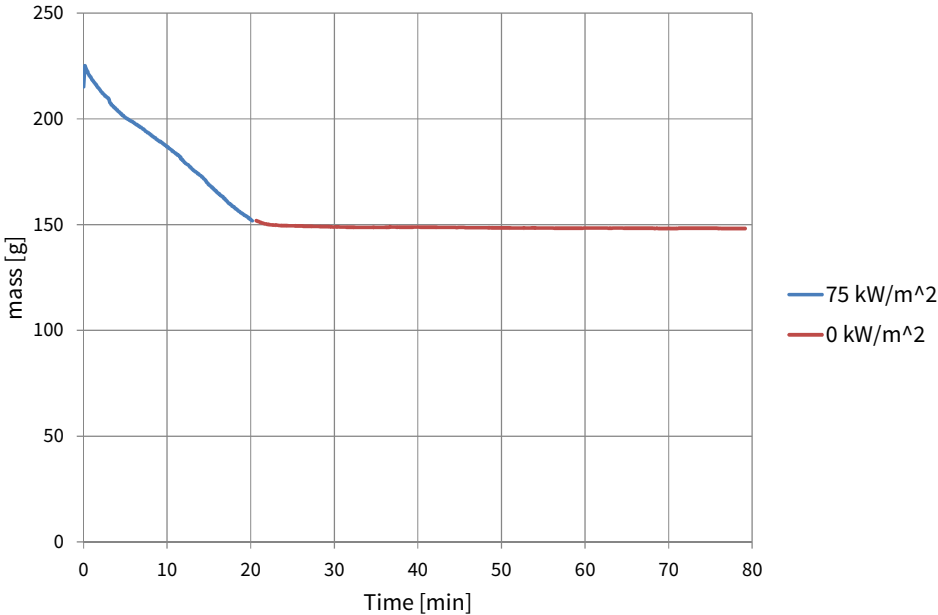


Figure F.9 Sample mass in experiment 2.

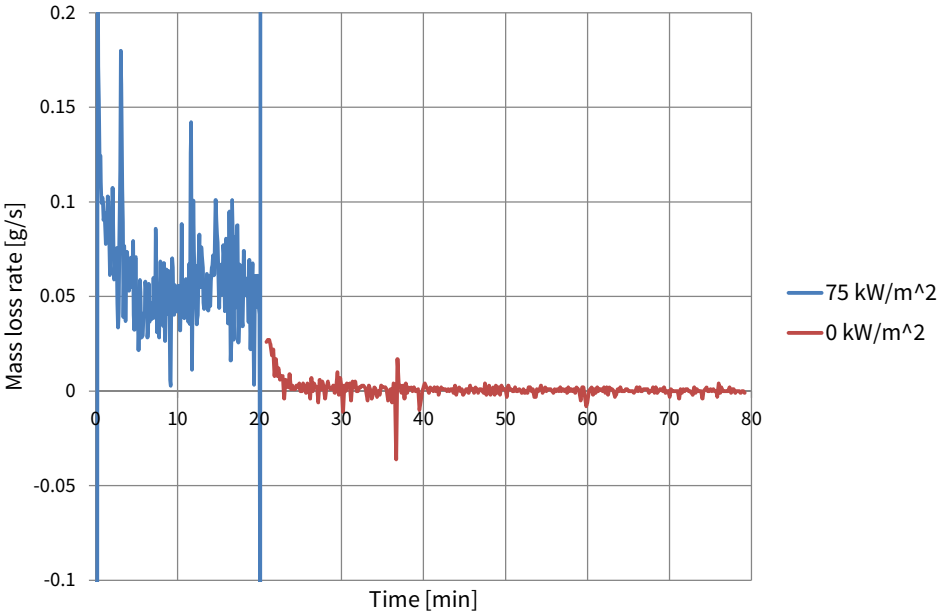


Figure F.10 Mass loss rate in experiment 2.

F.2.3 Heat release rate and heat of combustion

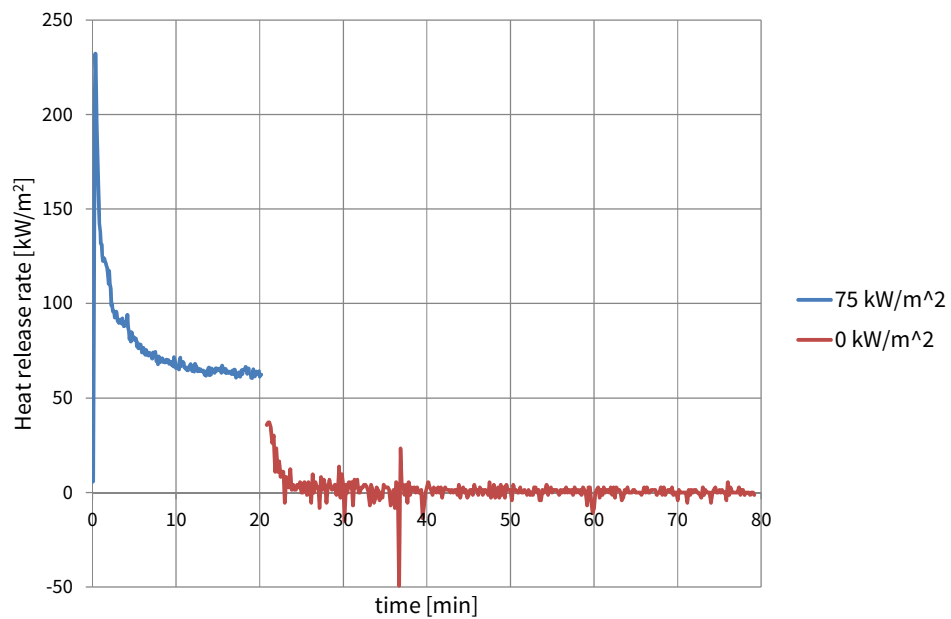


Figure F.11 Heat release rate in experiment 2 (the heat release rate during second exposure is based on the mass loss rate and average effective heat of combustion during the 75 kW/m² exposure)

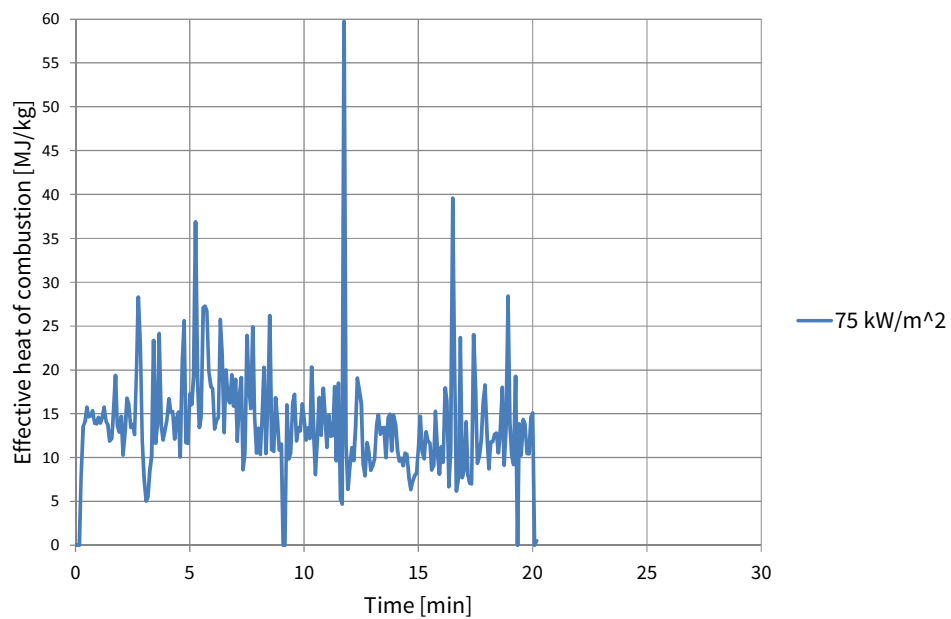


Figure F.12 Effective heat of combustion during the 75 kW/m² exposure in experiment 2.

F.3 Experiment 3 – 75 kW/m² → 5 kW/m²

F.3.1 Temperatures

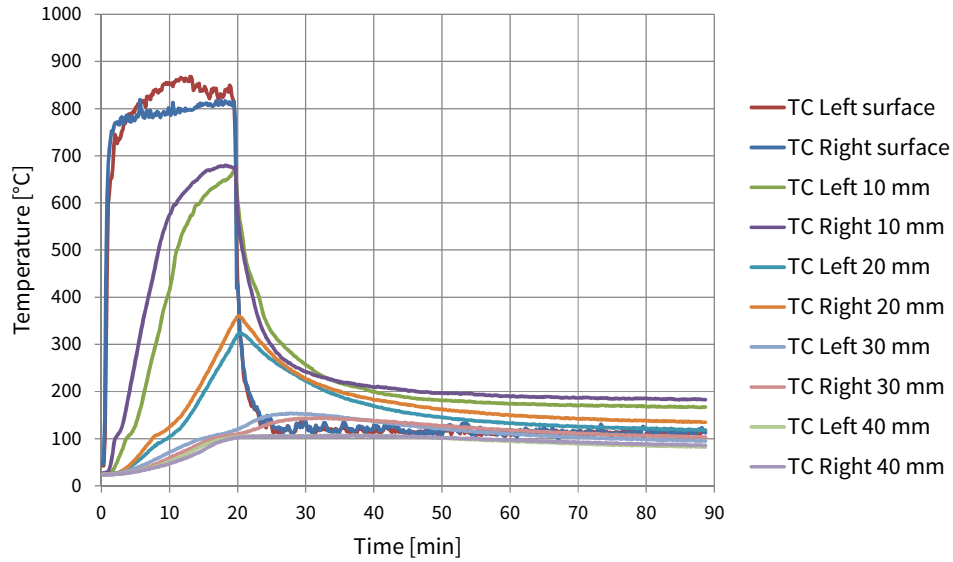


Figure F.13 CLT temperatures in experiment 3.

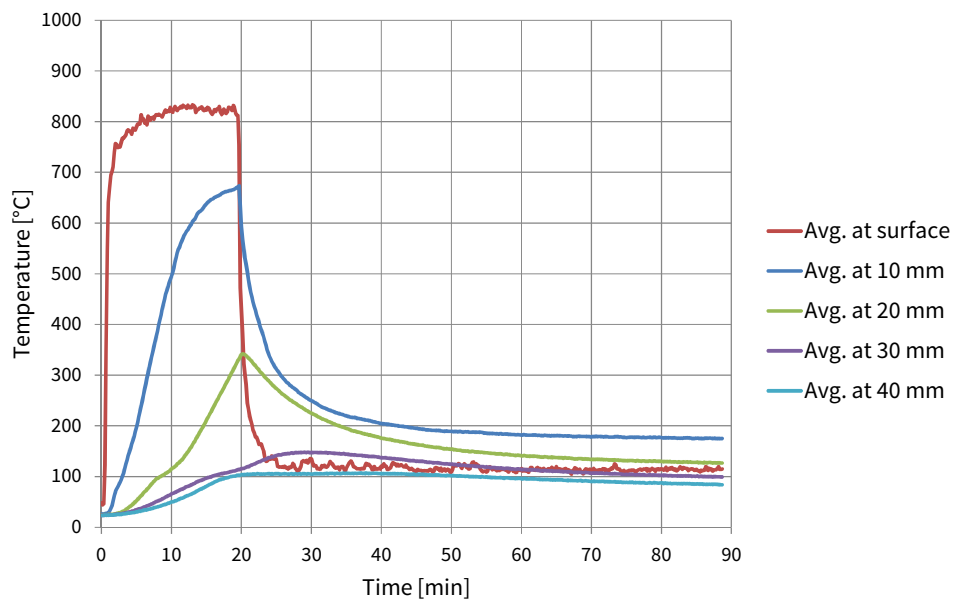


Figure F.14 Average CLT temperatures in experiment 3.

F.3.2 Mass loss

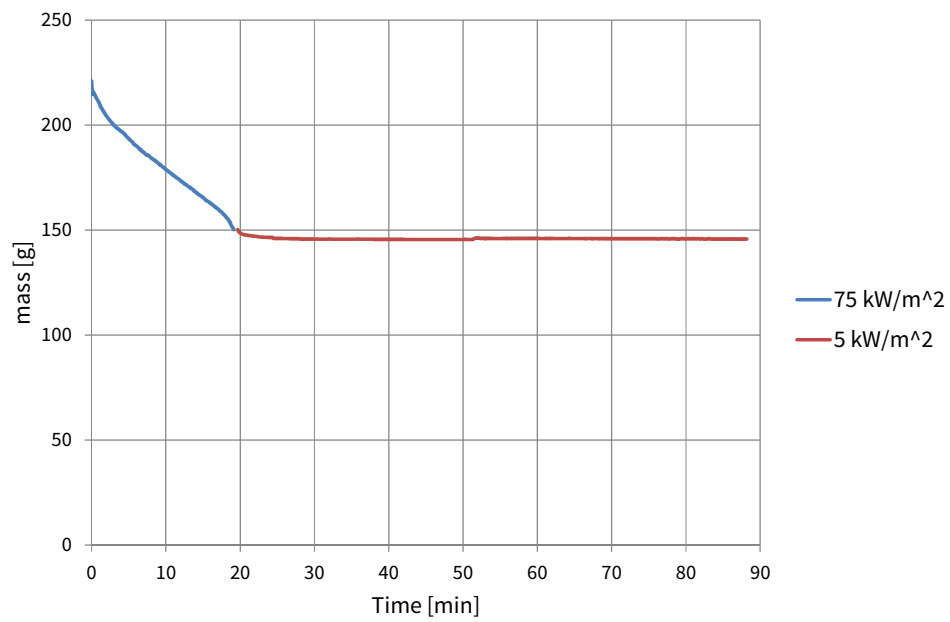


Figure F.15 Sample mass in experiment 3.

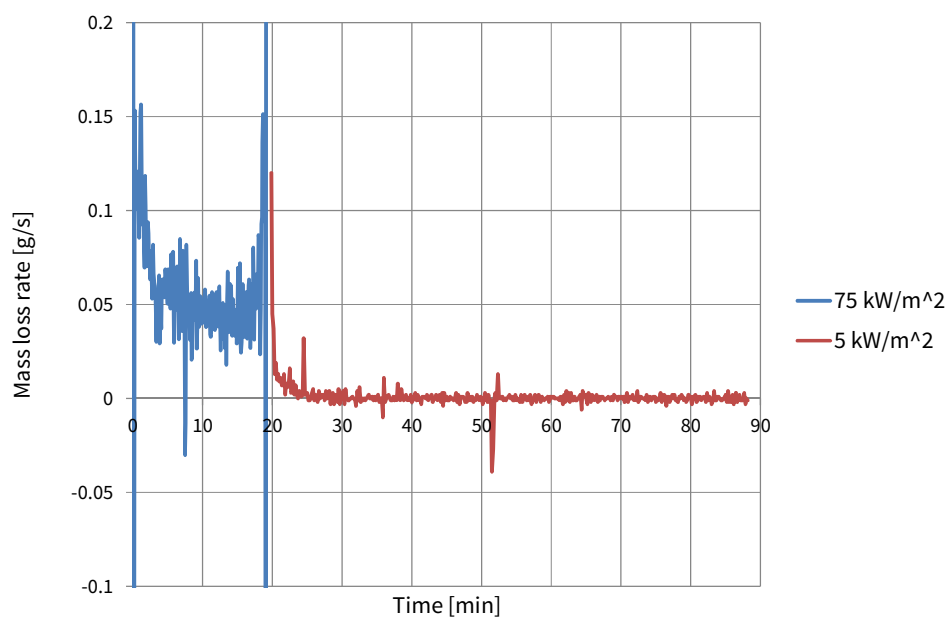


Figure F.16 Mass loss rate in experiment 3.

F.3.3 Heat release rate and heat of combustion

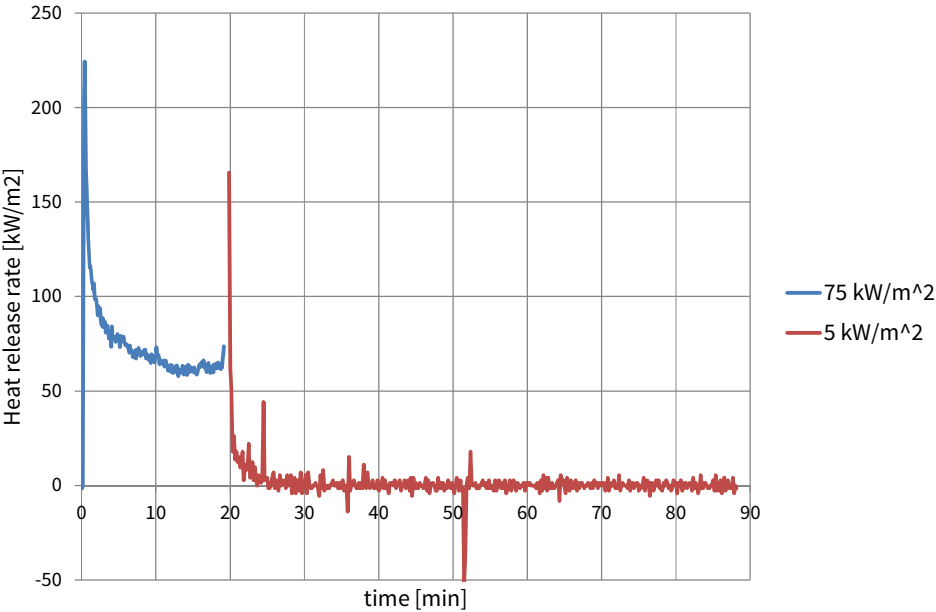


Figure F.17 Heat release rate in experiment 3 (the heat release rate during second exposure is based on the mass loss rate and average effective heat of combustion during the 75 kW/m² exposure)

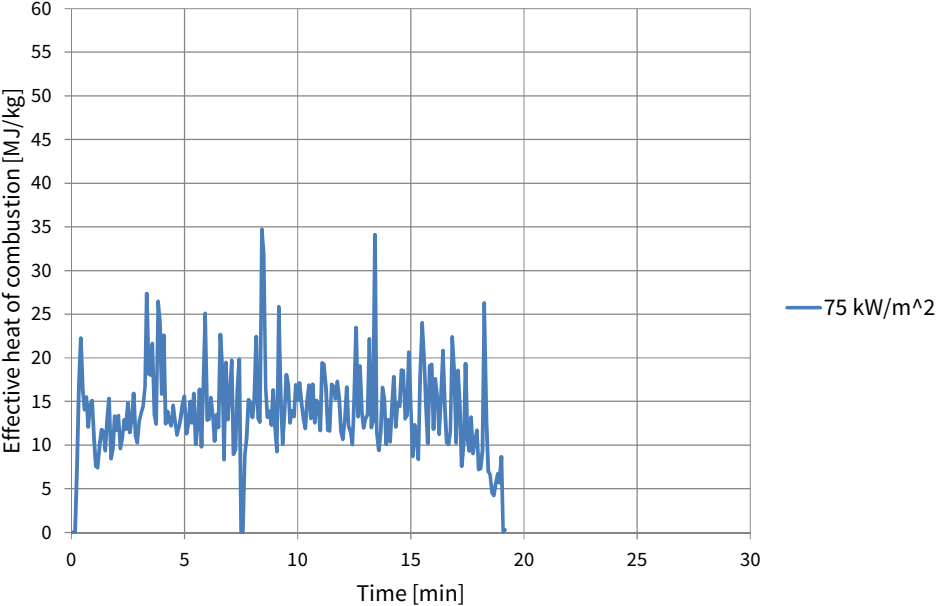


Figure F.18 Effective heat of combustion during the 75 kW/m² exposure in experiment 3.

F.4 Experiment 4 – $75 \text{ kW/m}^2 \rightarrow 5 \text{ kW/m}^2$

F.4.1 Temperatures

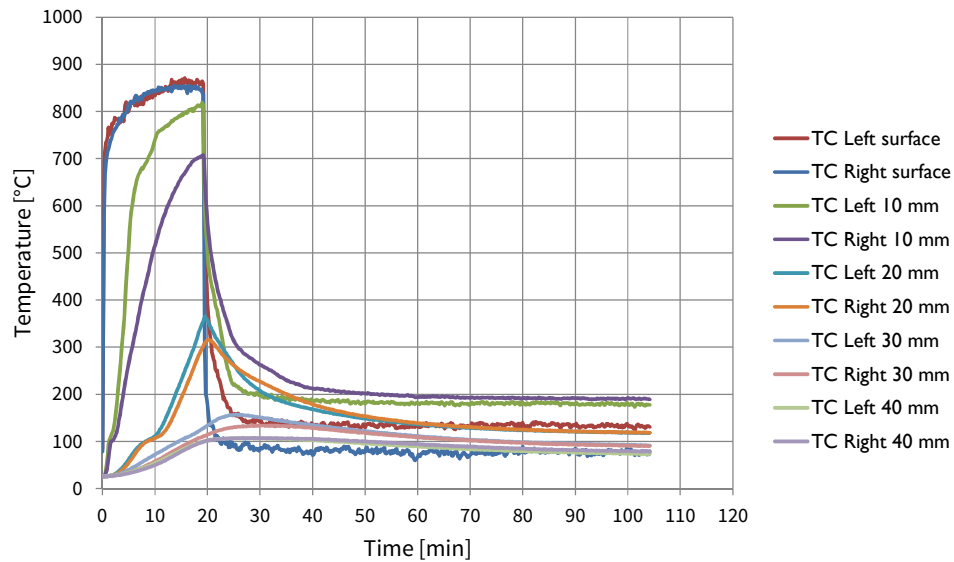


Figure F.19 CLT temperatures in experiment 4.

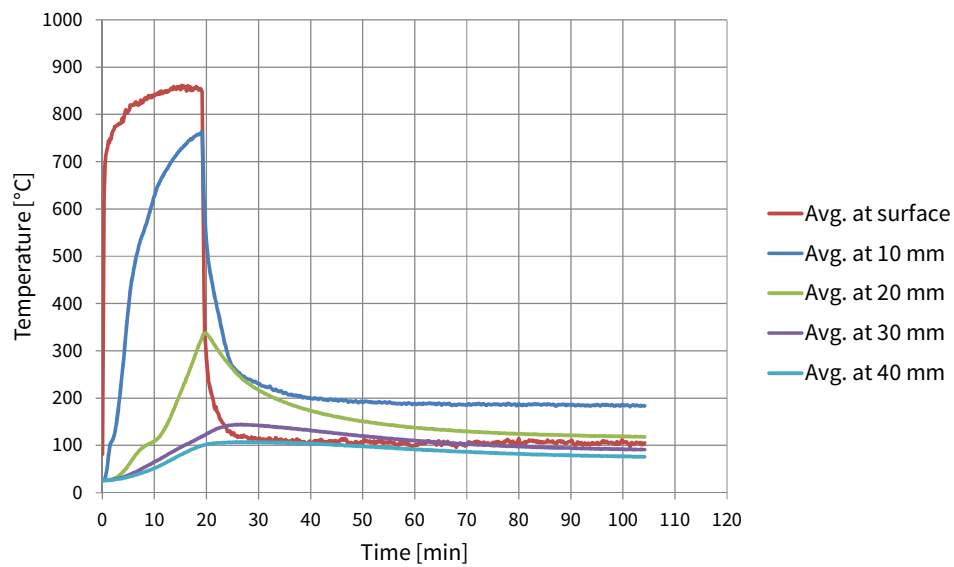


Figure F.20 Average CLT temperatures in experiment 4.

F.4.2 Mass loss

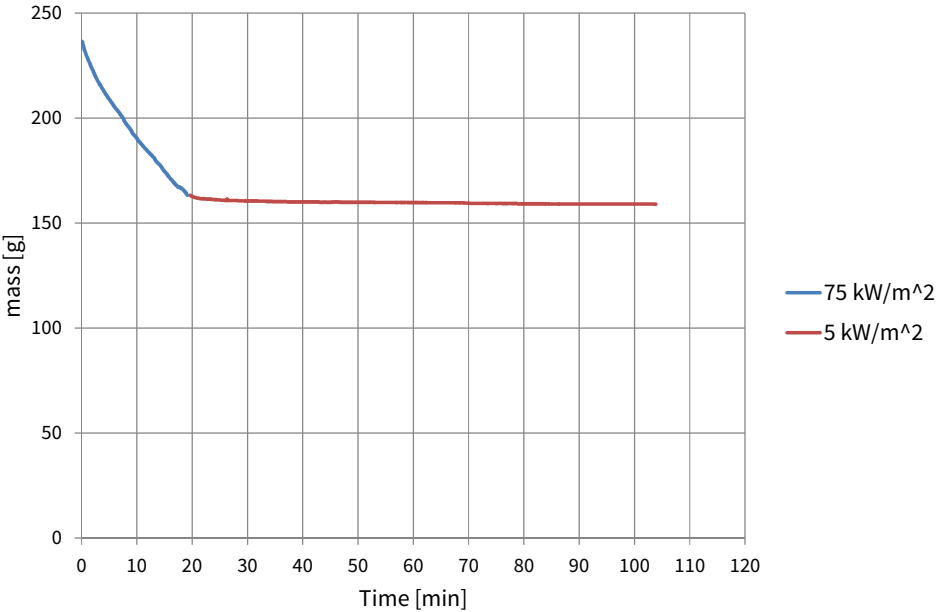


Figure F.21 Sample mass in experiment 4.

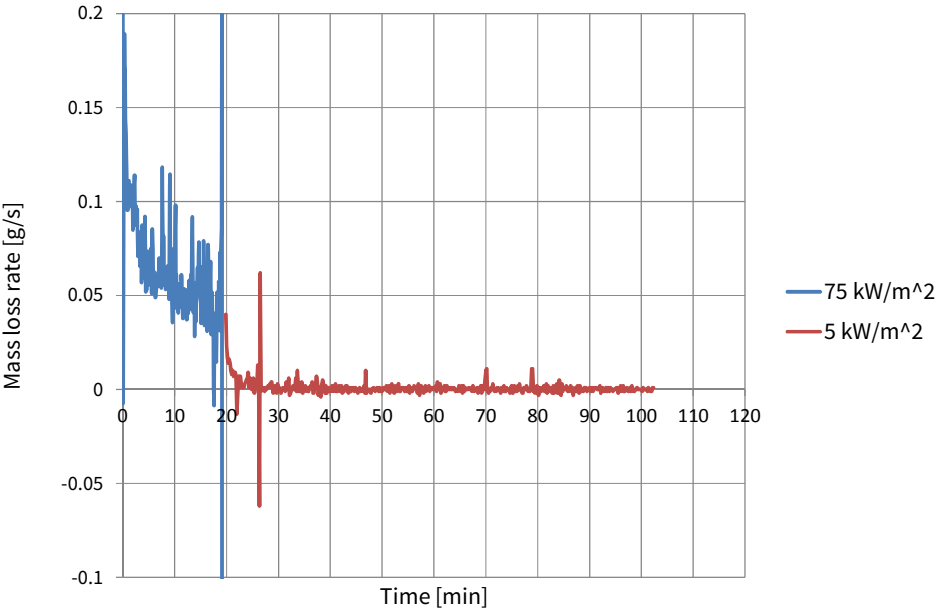


Figure F.22 Mass loss rate in experiment 4.

F.4.3 Heat release rate and heat of combustion

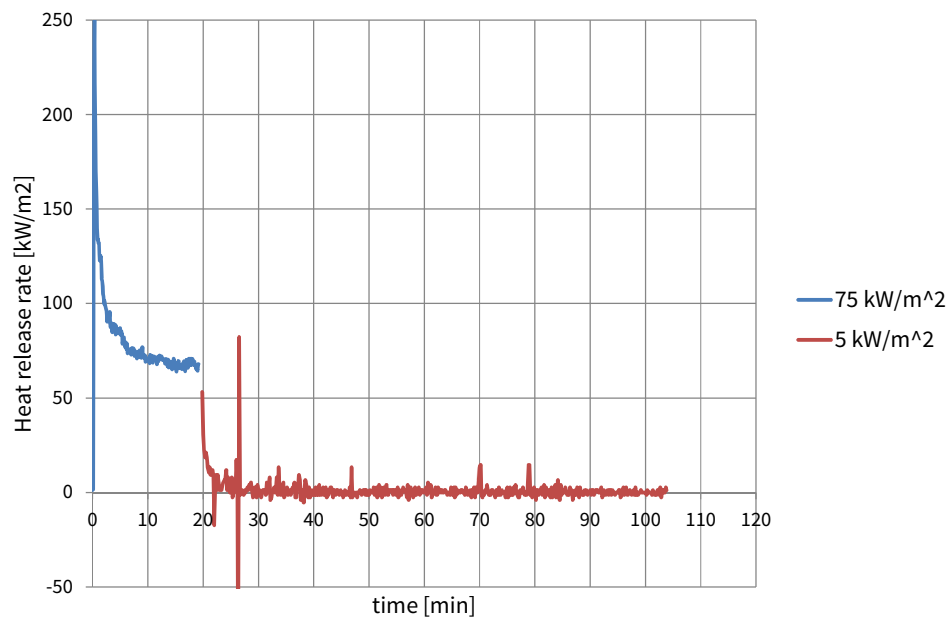


Figure F.23 Heat release rate in experiment 4 (the heat release rate during second exposure is based on the mass loss rate and average effective heat of combustion during the 75 kW/m² exposure)

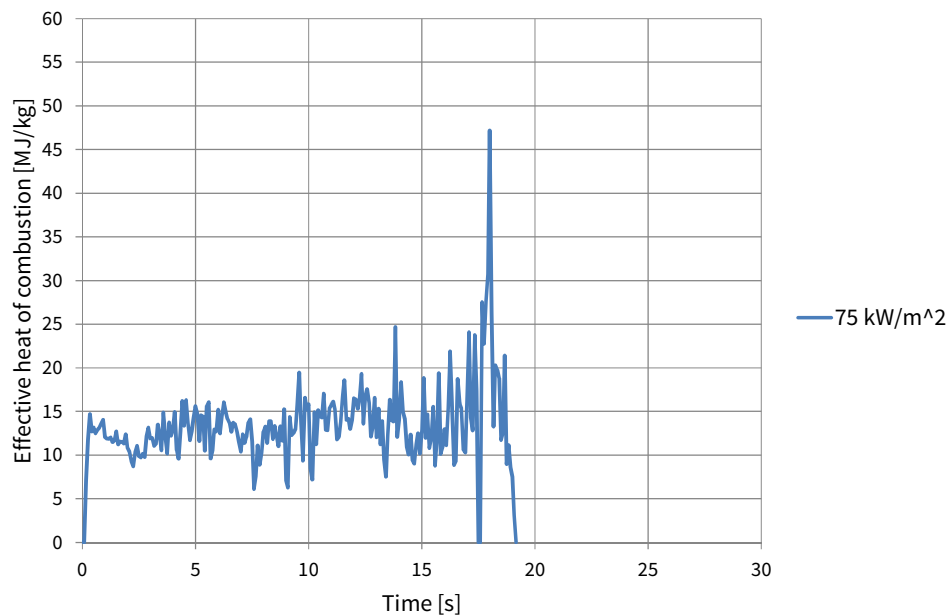


Figure F.24 Effective heat of combustion during the 75 kW/m² exposure in experiment 4.

F.5 Experiment 5 – 75 kW/m² → 10 kW/m²

F.5.1 Temperatures

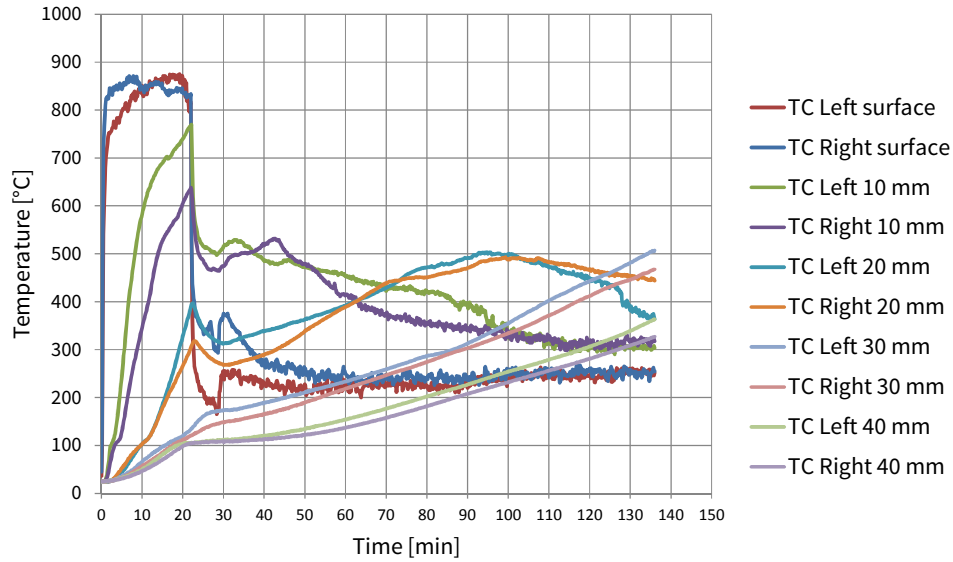


Figure F.25 CLT temperatures in experiment 5.

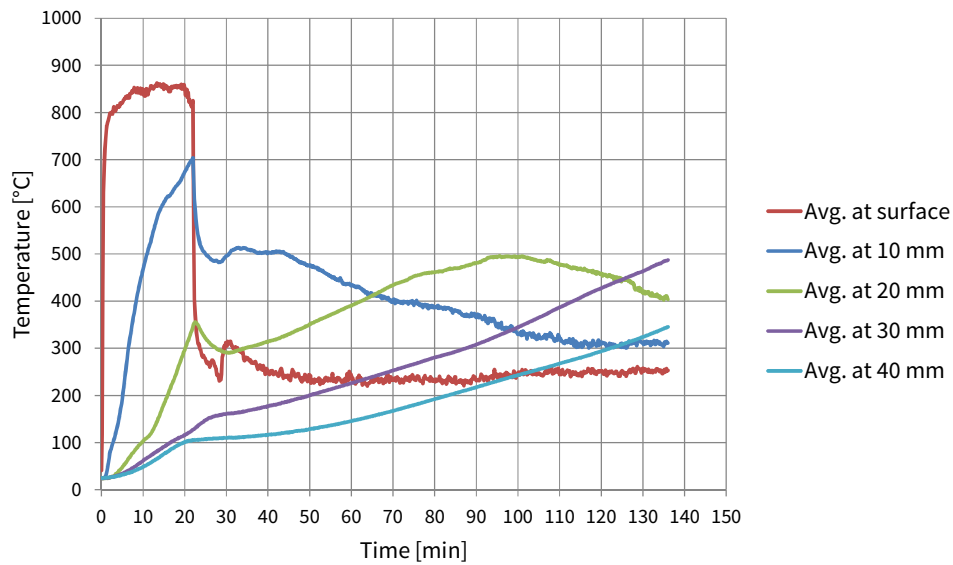


Figure F.26 Average CLT temperatures in experiment 5.

F.5.2 Mass loss

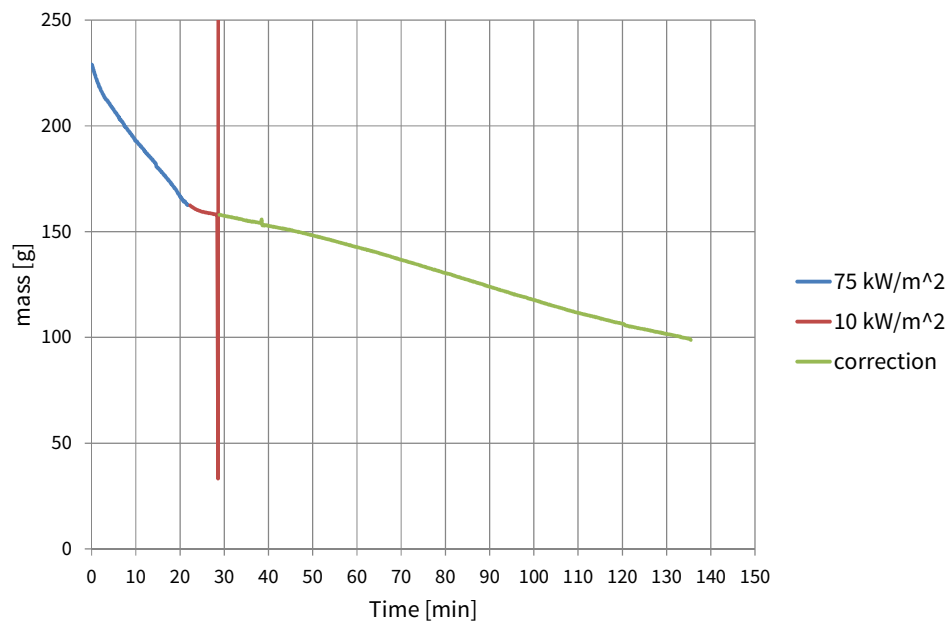


Figure F.27 Sample mass in experiment 5. The sample holder was found missing and was placed at approximately 29 minutes. The mass measurement was corrected for the sample holder weight to show a continuous graph.

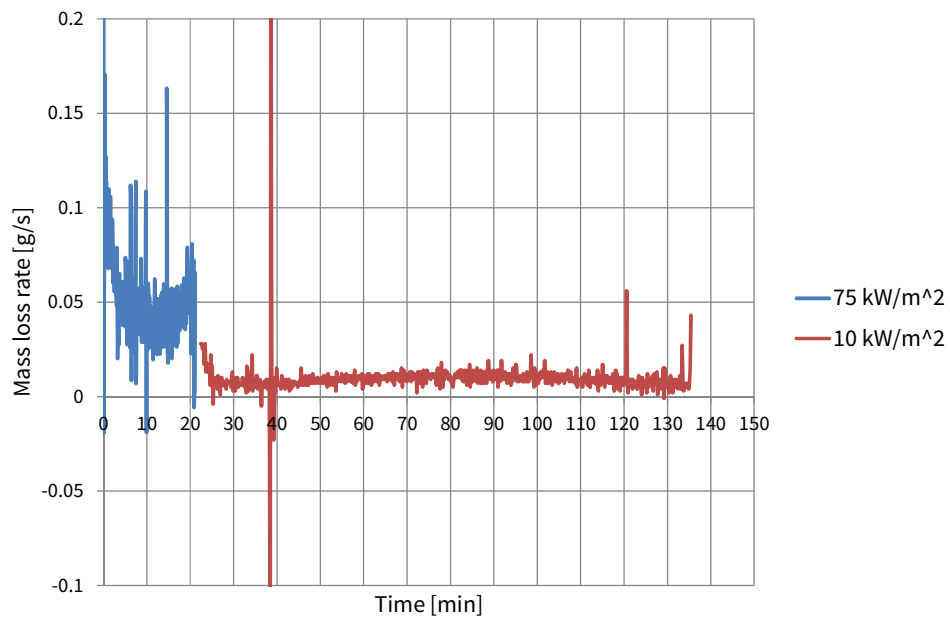


Figure F.28 Mass loss rate in experiment 5.

F.5.3 Heat release rate and heat of combustion

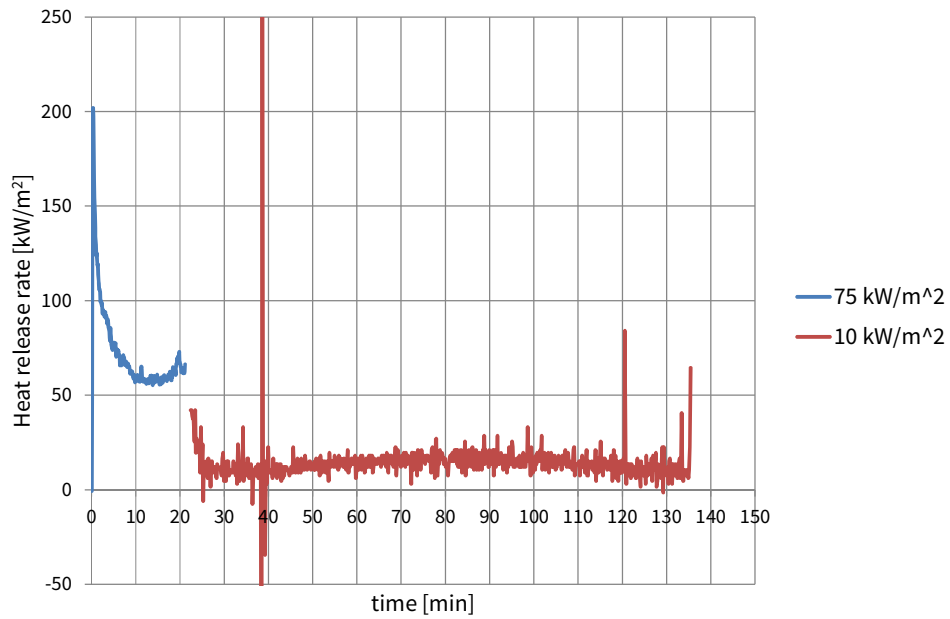


Figure F.29 Heat release rate in experiment 5 (the heat release rate during second exposure is based on the mass loss rate and average effective heat of combustion during the 75 kW/m² exposure)

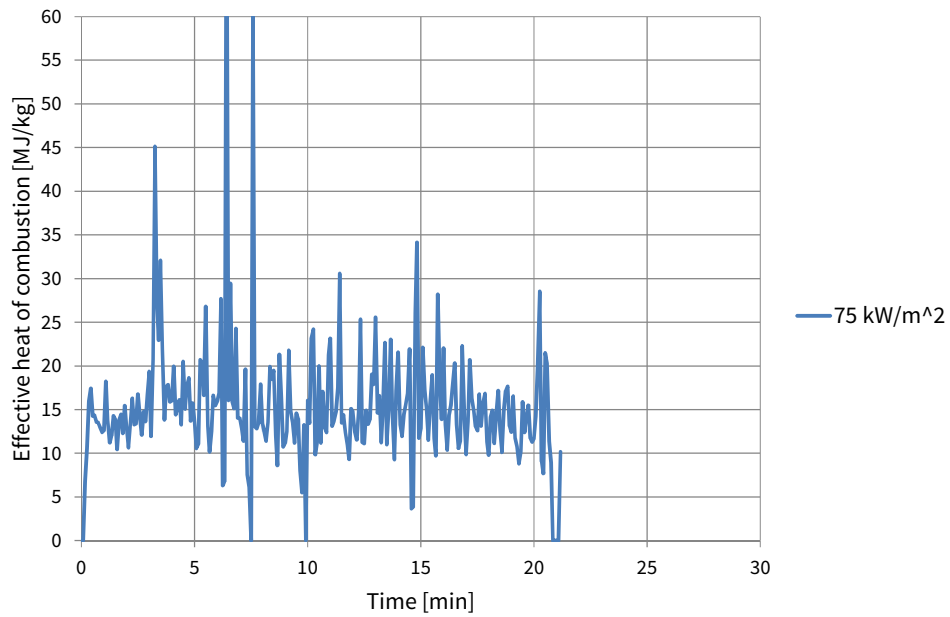


Figure F.30 Effective heat of combustion during the 75 kW/m² exposure in experiment 5.

F.6 Experiment 6 – $75 \text{ kW/m}^2 \rightarrow 10 \text{ kW/m}^2$

F.6.1 Temperatures

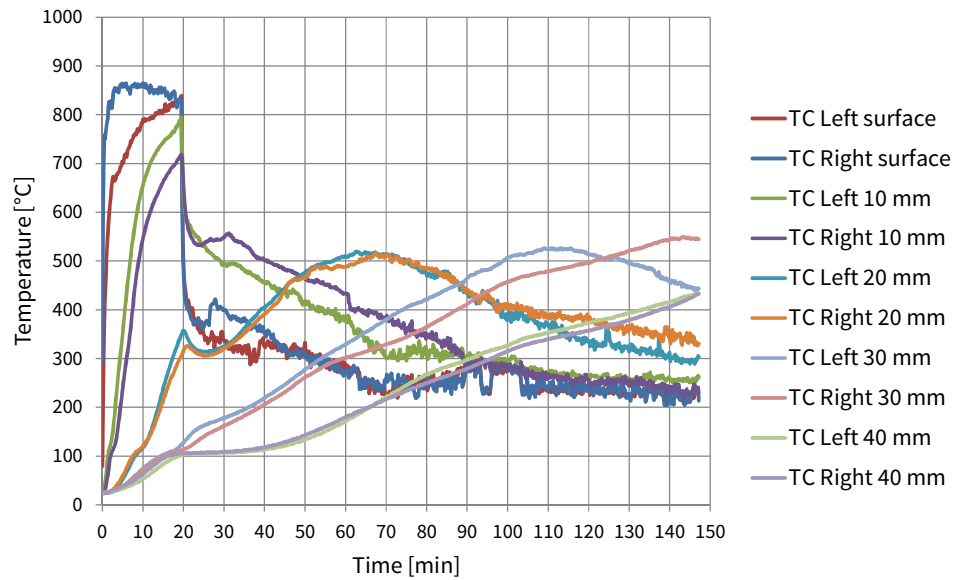


Figure F.31 CLT temperatures in experiment 6.

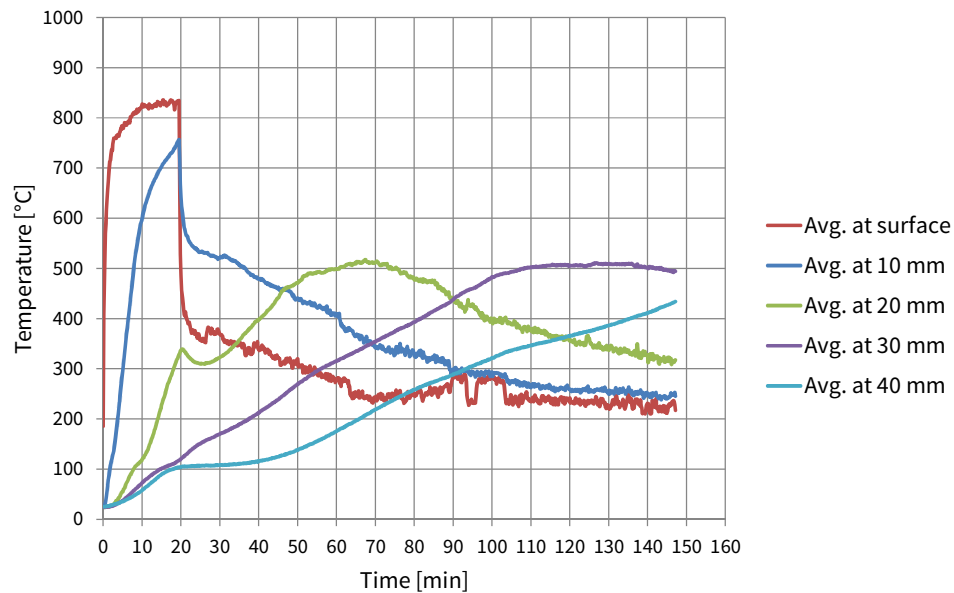


Figure F.32 Average CLT temperatures in experiment 6.

F.6.2 Mass loss

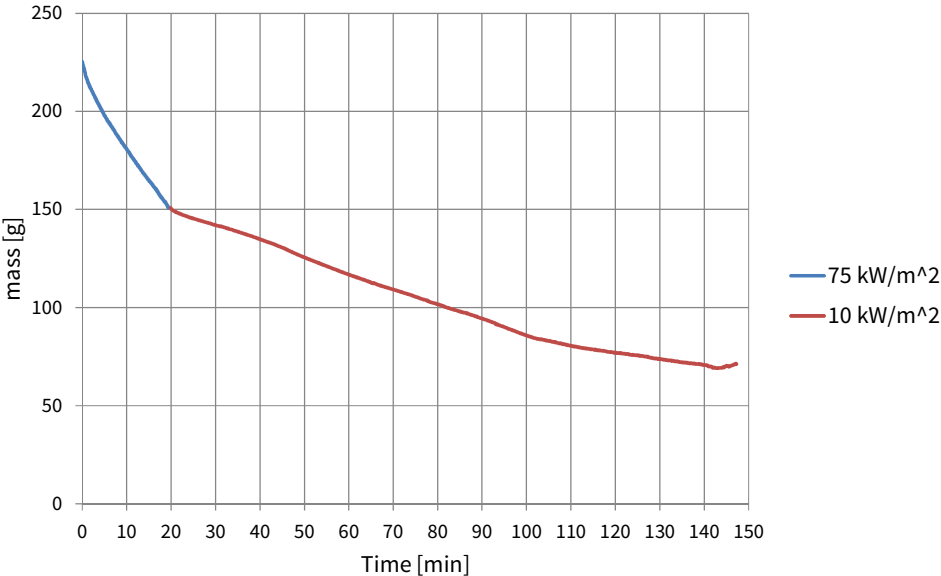


Figure F.33 Sample mass in experiment 6.

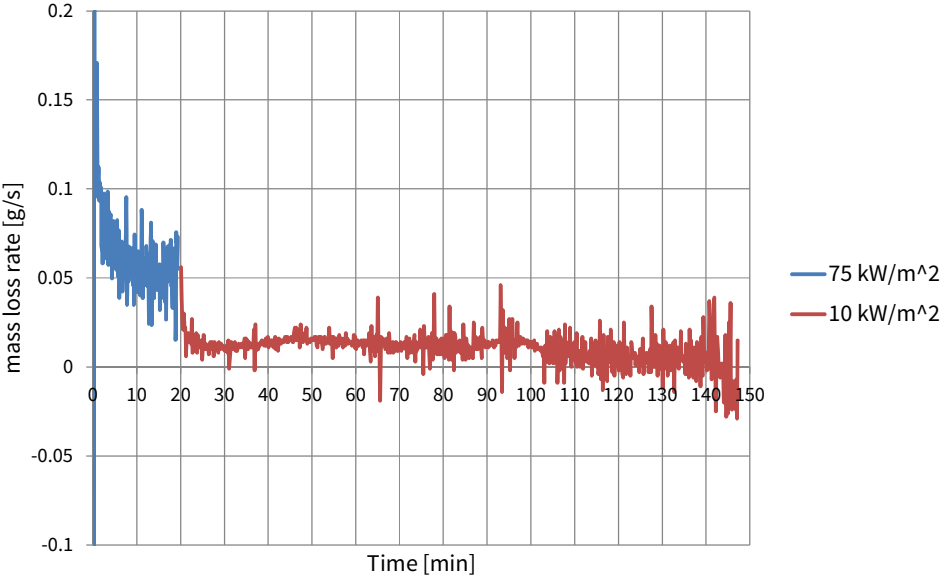


Figure F.34 Mass loss rate in experiment 6.

F.6.3 Heat release rate and heat of combustion

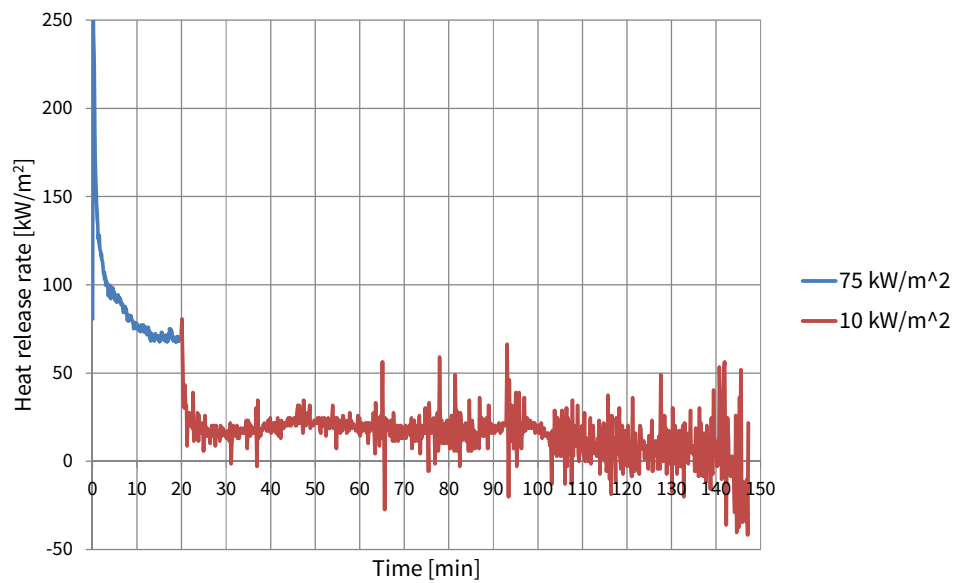


Figure F.35 Heat release rate in experiment 6 (the heat release rate during second exposure is based on the mass loss rate and average effective heat of combustion during the 75 kW/m² exposure)

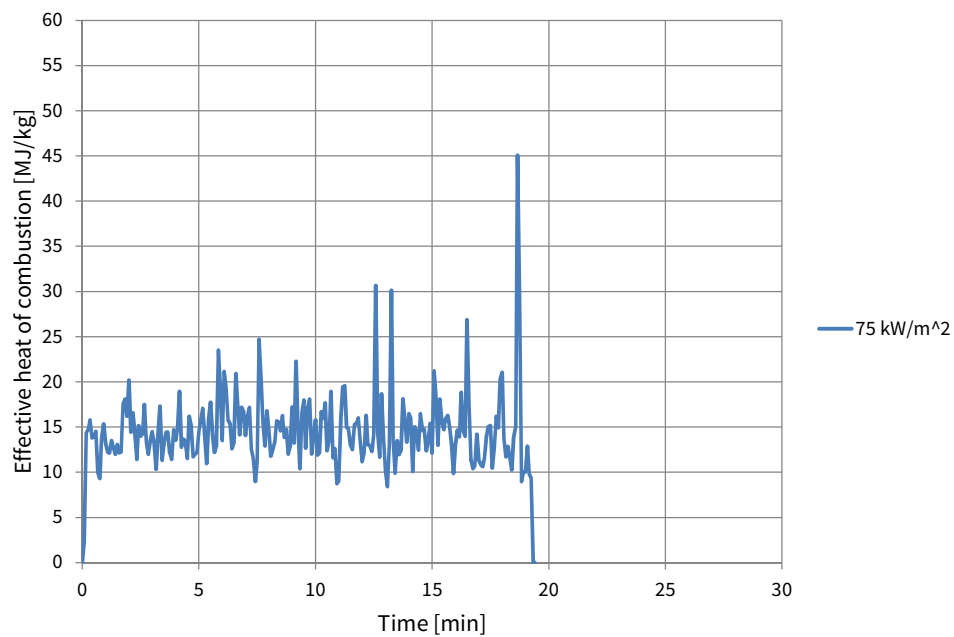


Figure F.36 Effective heat of combustion during the 75 kW/m² exposure in experiment 6.

F.7 Experiment 7 – 75 kW/m² → 8 kW/m²

F.7.1 Temperatures

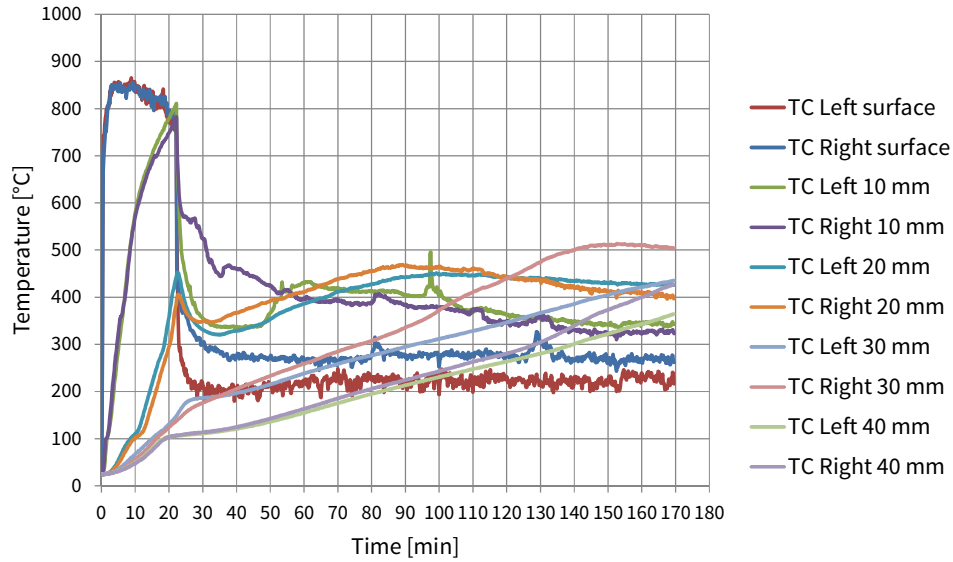


Figure F.37 CLT temperatures in experiment 7.

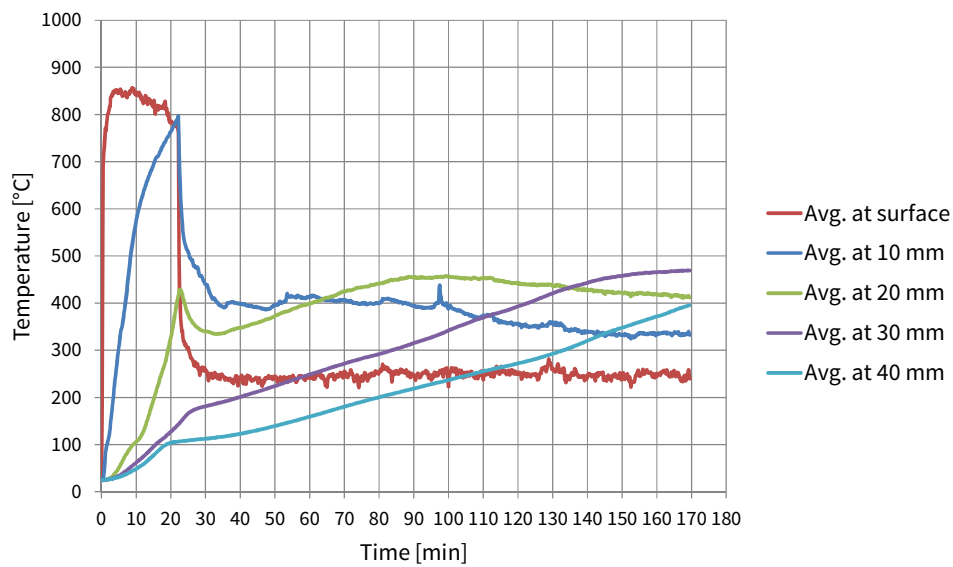


Figure F.38 Average CLT temperatures in experiment 7.

F.7.2 Mass loss

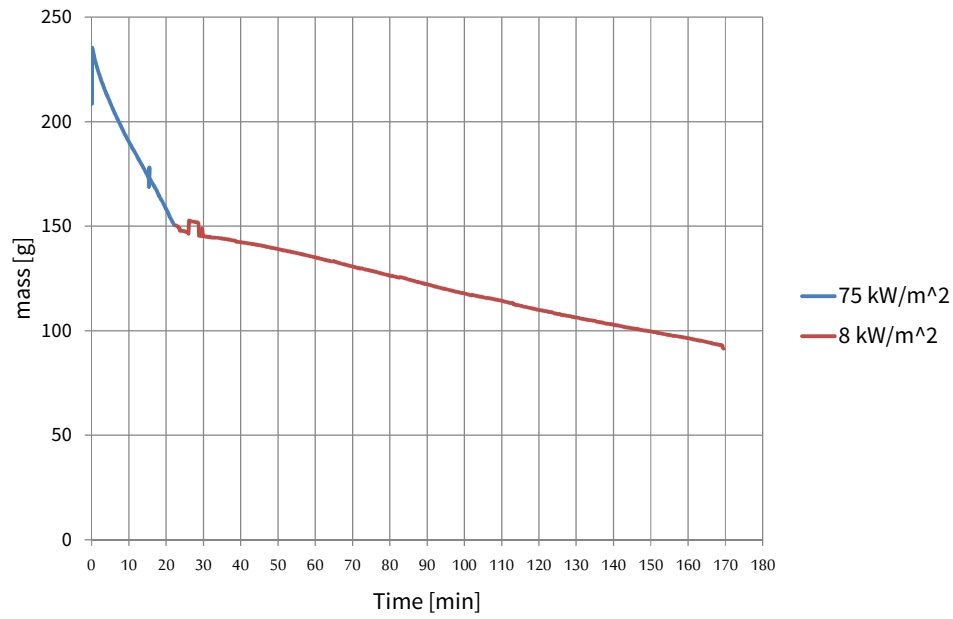


Figure F.39 Sample mass in experiment 7.

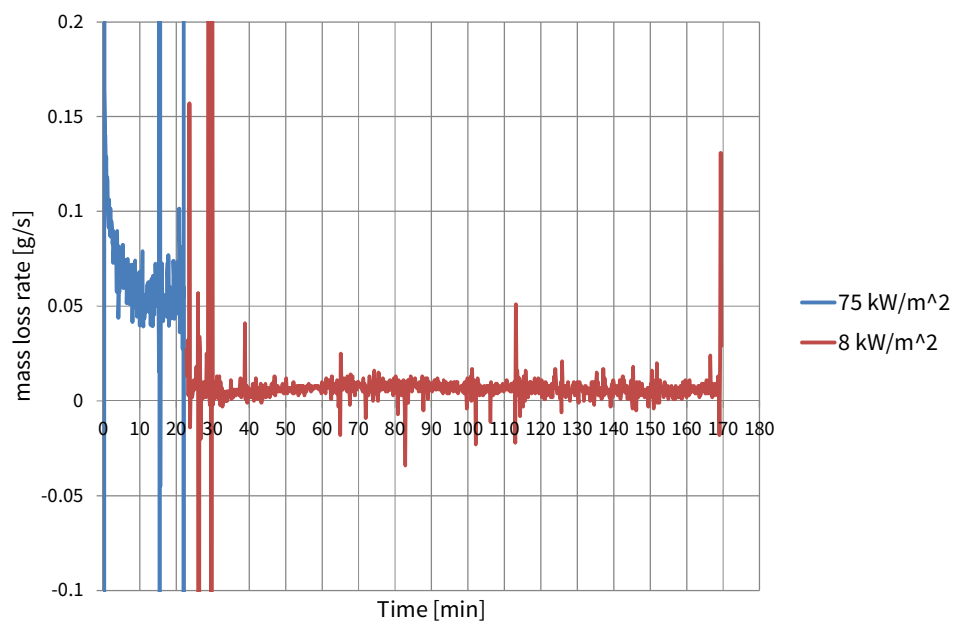


Figure F.40 Mass loss rate in experiment 7.

F.7.3 Heat release rate and heat of combustion

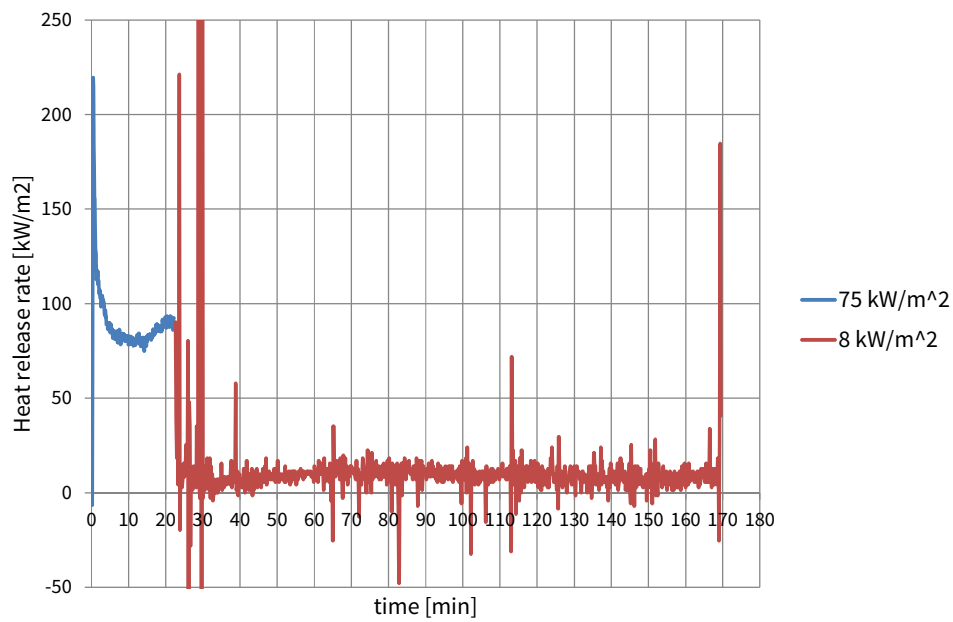


Figure F.41 Heat release rate in experiment 7 (the heat release rate during second exposure is based on the mass loss rate and average effective heat of combustion during the 75 kW/m² exposure)

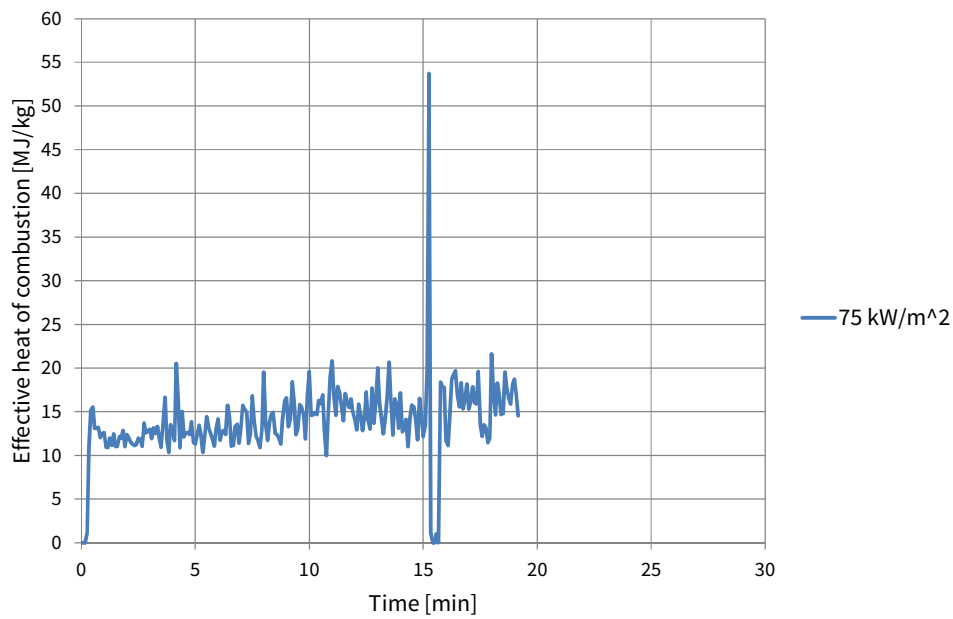


Figure F.42 Effective heat of combustion during the 75 kW/m² exposure in experiment 7.

F.8 Experiment 8 – $75 \text{ kW/m}^2 \rightarrow 8 \text{ kW/m}^2$

F.8.1 Temperatures

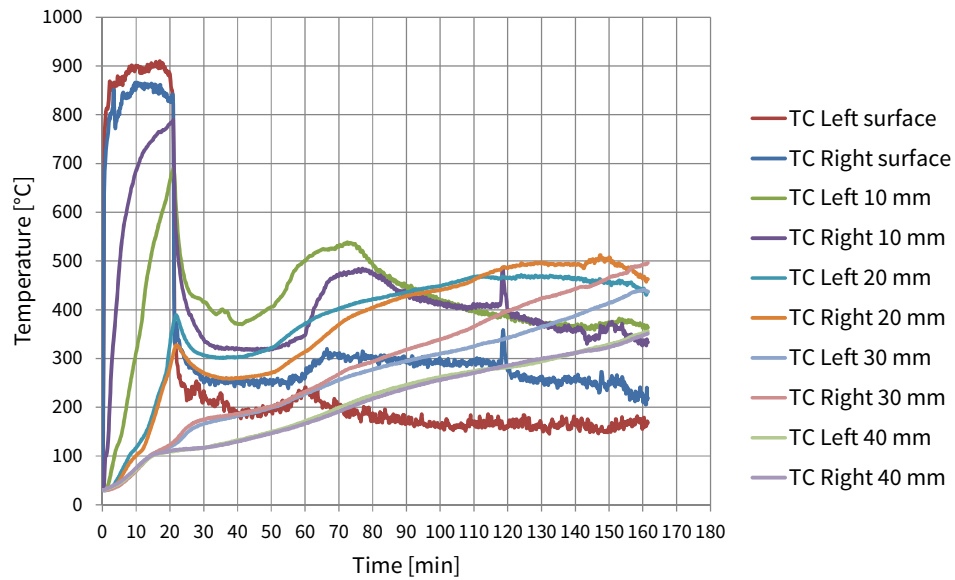


Figure F.43 CLT temperatures in experiment 8.

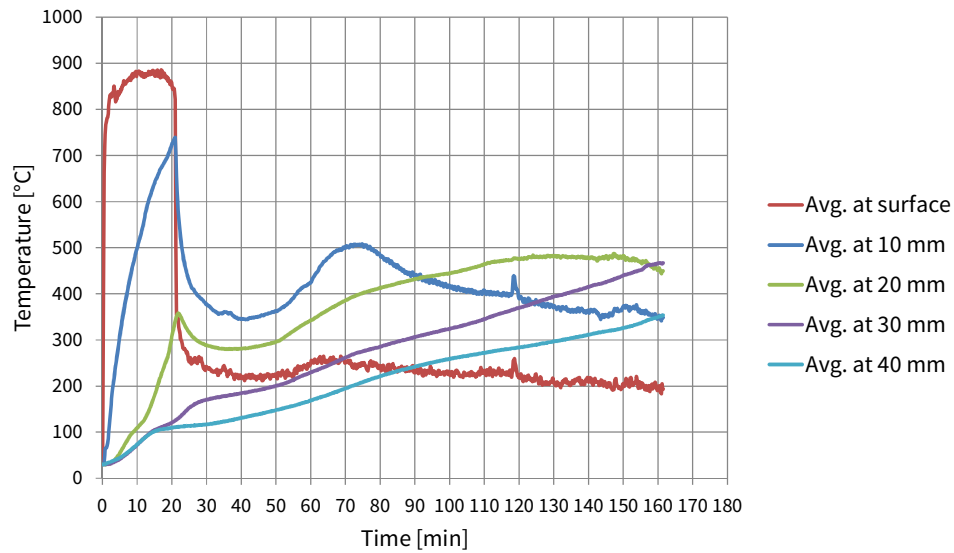


Figure F.44 Average CLT temperatures in experiment 8.

F.8.2 Mass loss

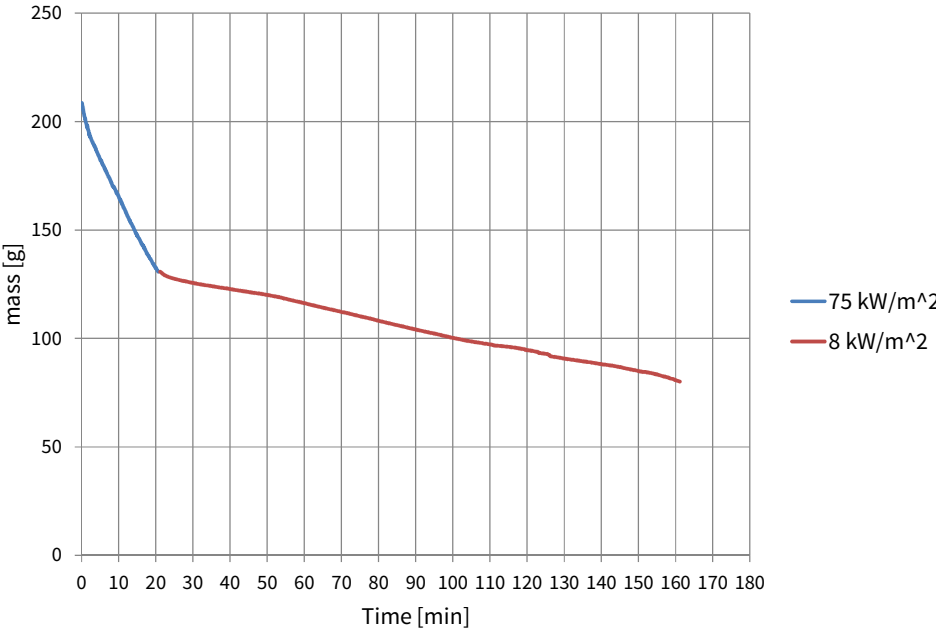


Figure F.45 Sample mass in experiment 8.

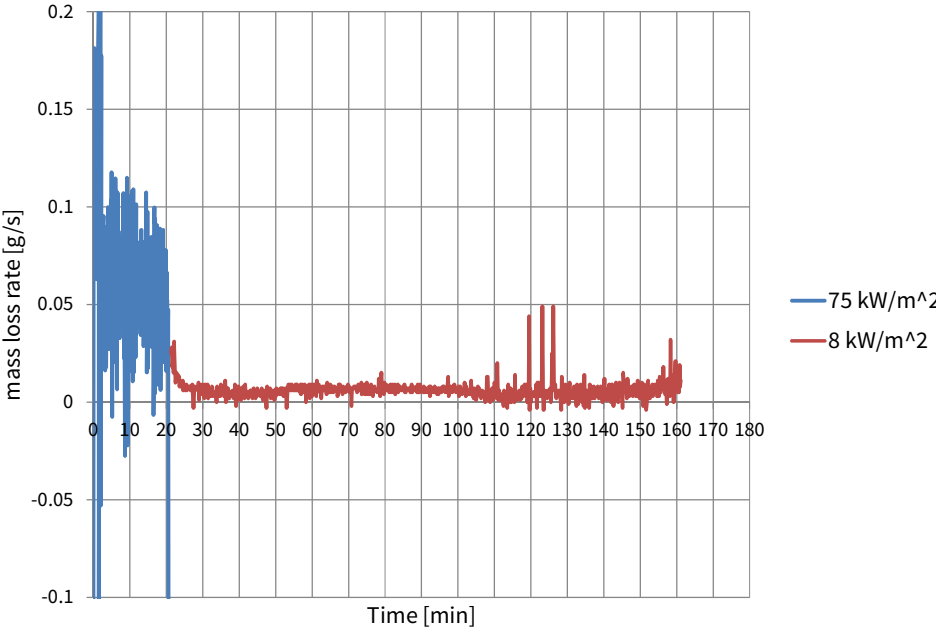


Figure F.46 Mass loss rate in experiment 8.

F.8.3 Heat release rate and heat of combustion

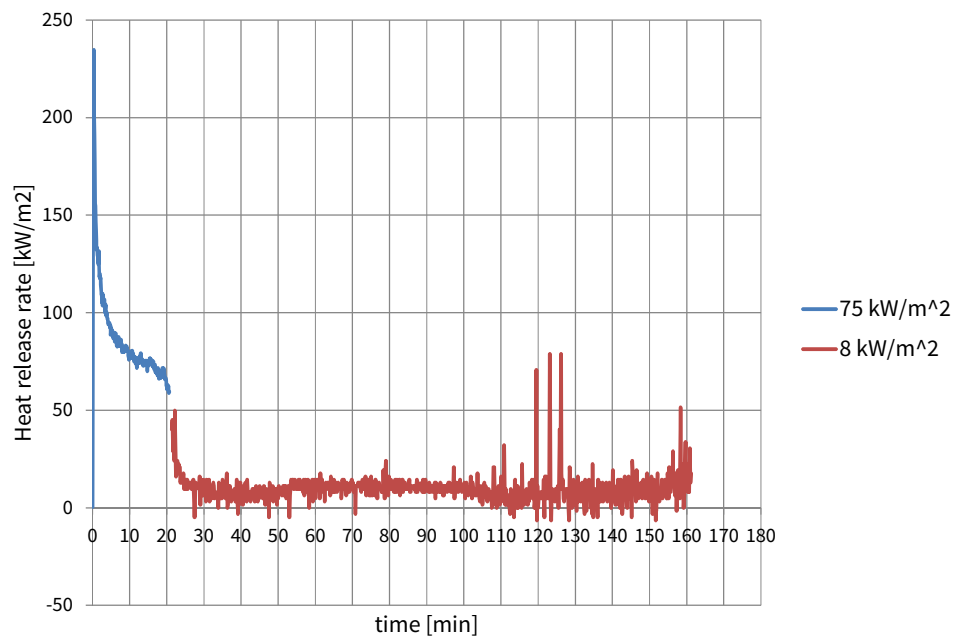


Figure F.47 Heat release rate in experiment 8 (the heat release rate during second exposure is based on the mass loss rate and average effective heat of combustion during the 75 kW/m² exposure)

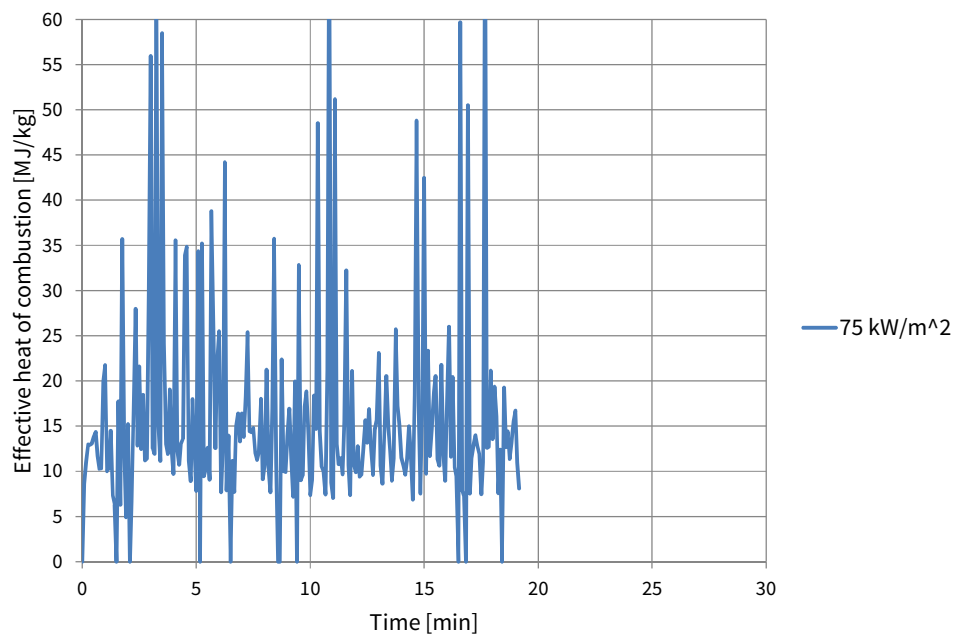


Figure F.48 Effective heat of combustion during the 75 kW/m² exposure in experiment 8.

F.9 Experiment 9 – 75 kW/m² → 6 kW/m²

F.9.1 Temperatures

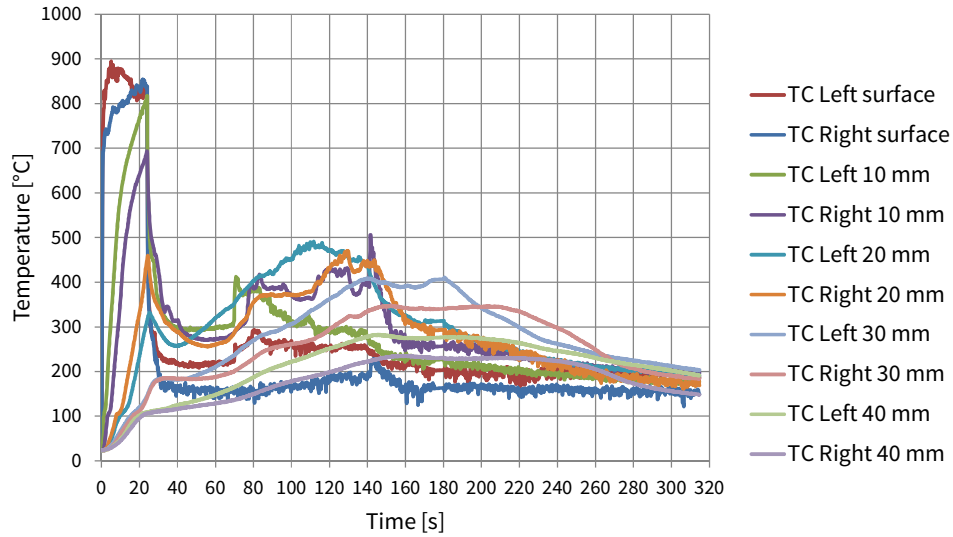


Figure F.49 CLT temperatures in experiment 9.

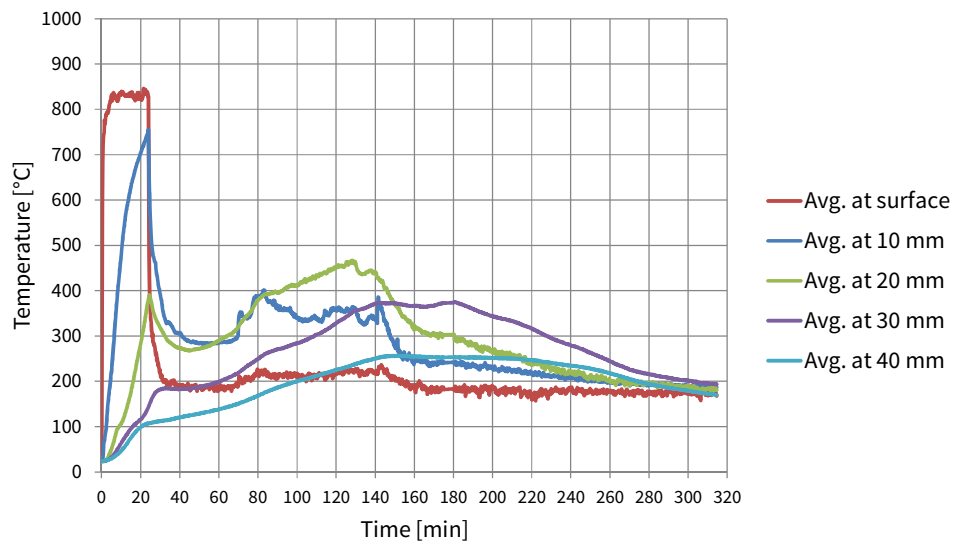


Figure F.50 Average CLT temperatures in experiment 9.

F.9.2 Mass loss

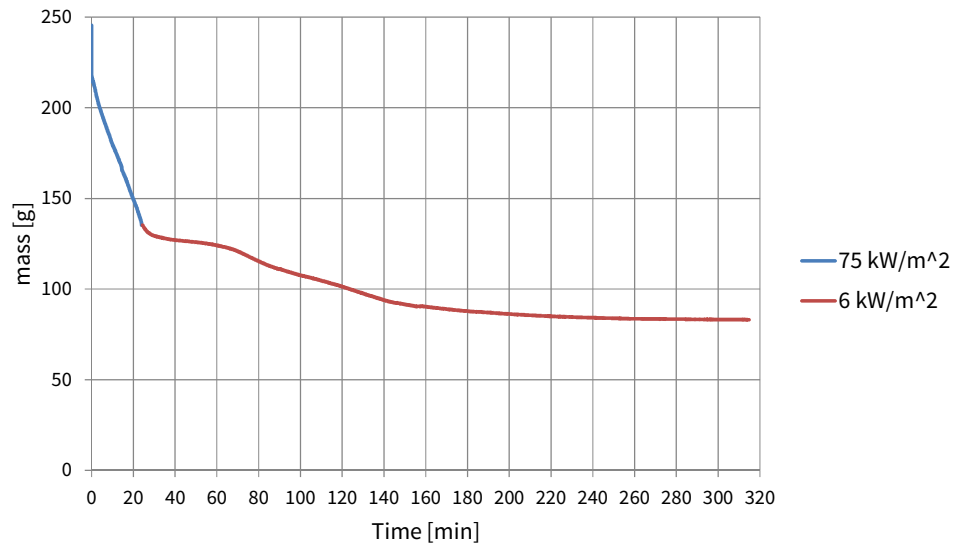


Figure F.51 Sample mass in experiment 9.

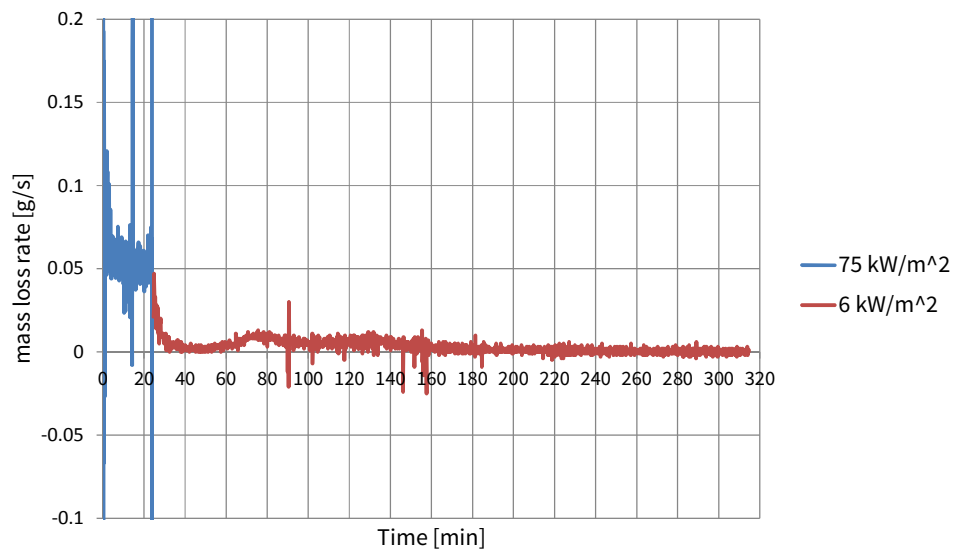


Figure F.52 Mass loss rate in experiment 9.

F.9.3 Heat release rate and heat of combustion

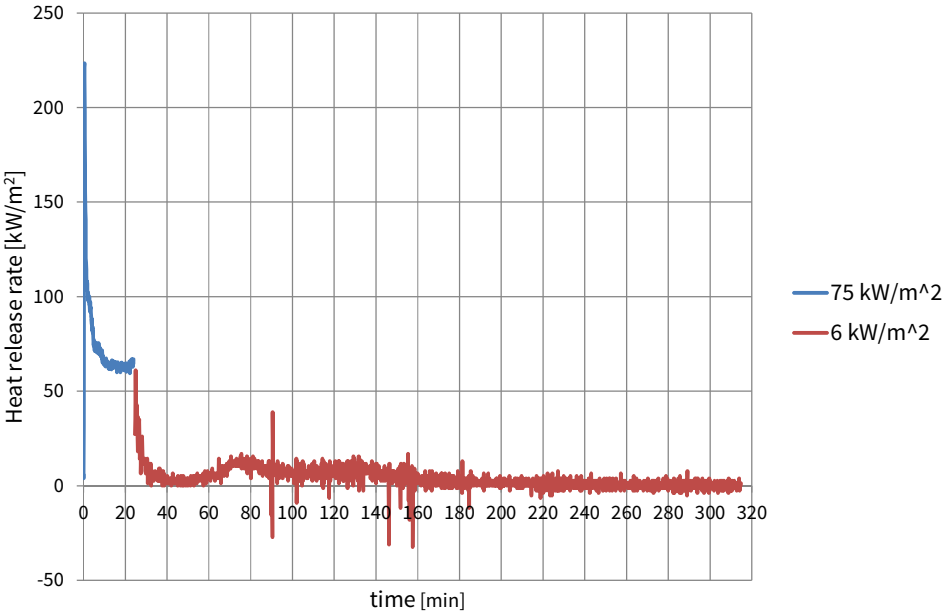


Figure F.53 Heat release rate in experiment 9 (the heat release rate during second exposure is based on the mass loss rate and average effective heat of combustion during the 75 kW/m² exposure)

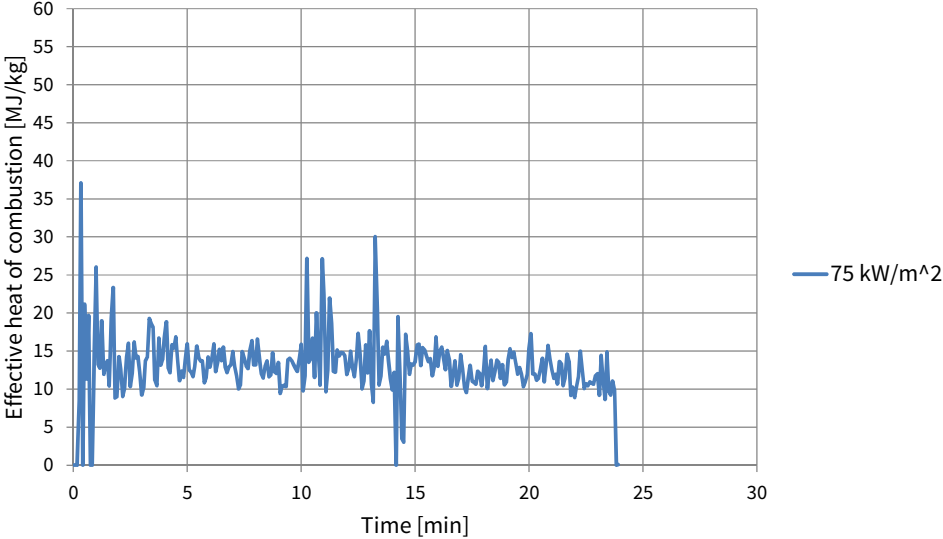


Figure F.54 Effective heat of combustion during the 75 kW/m² exposure in experiment 9.

F.10 Experiment 10 – $75 \text{ kW/m}^2 \rightarrow 6 \text{ kW/m}^2$

F.10.1 Temperatures

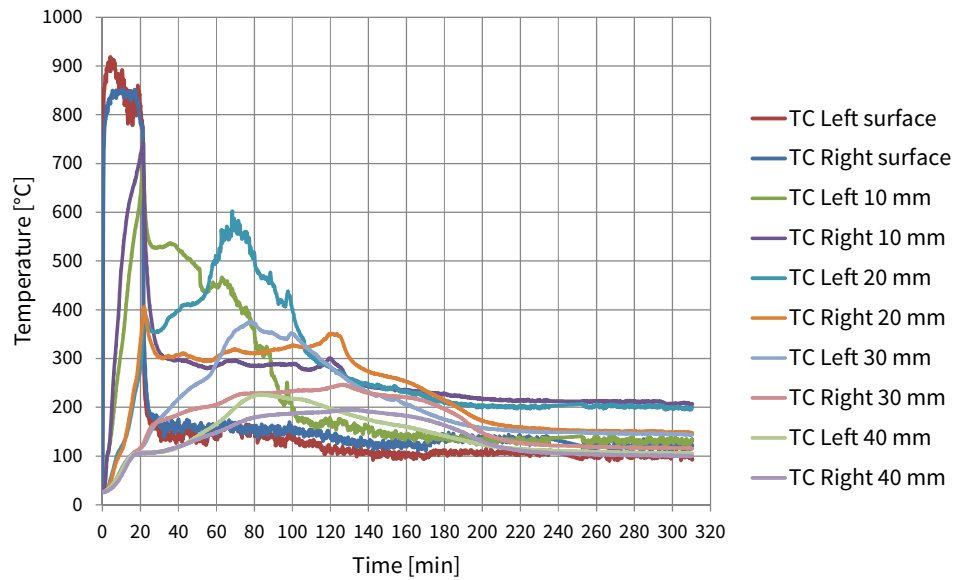


Figure F.55 CLT temperatures in experiment 10.

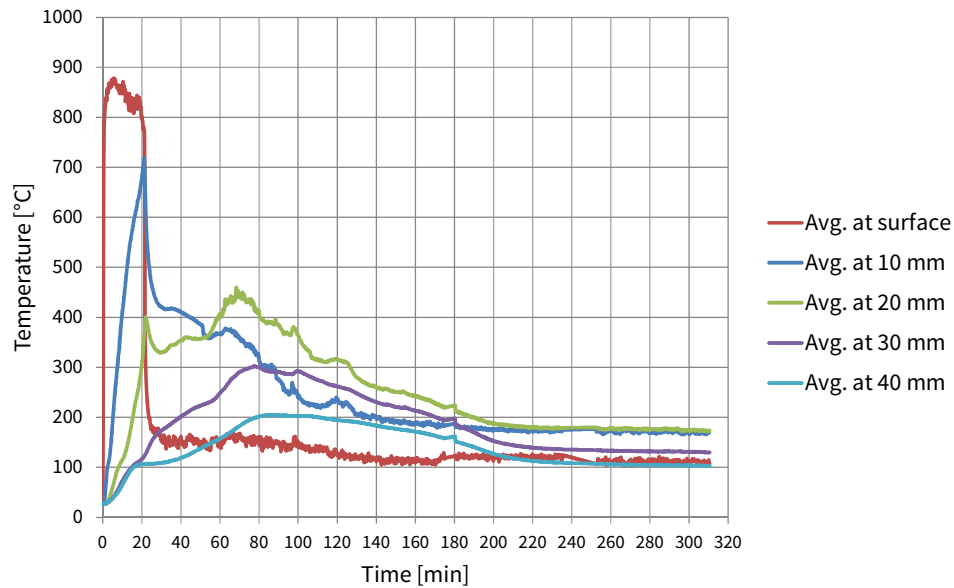


Figure F.56 Average CLT temperatures in experiment 10.

F.10.2 Mass loss

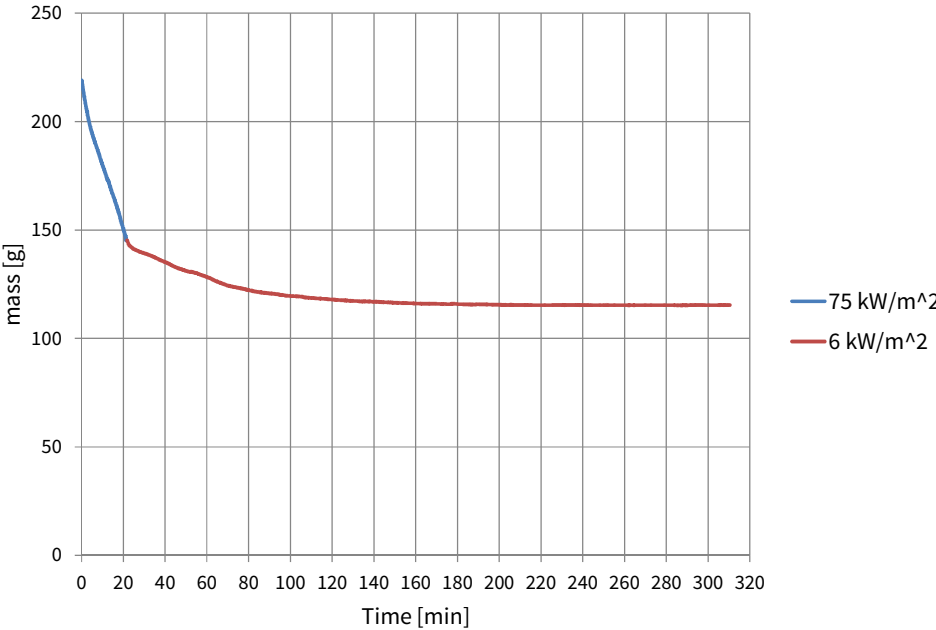


Figure F.57 Sample mass in experiment 10.

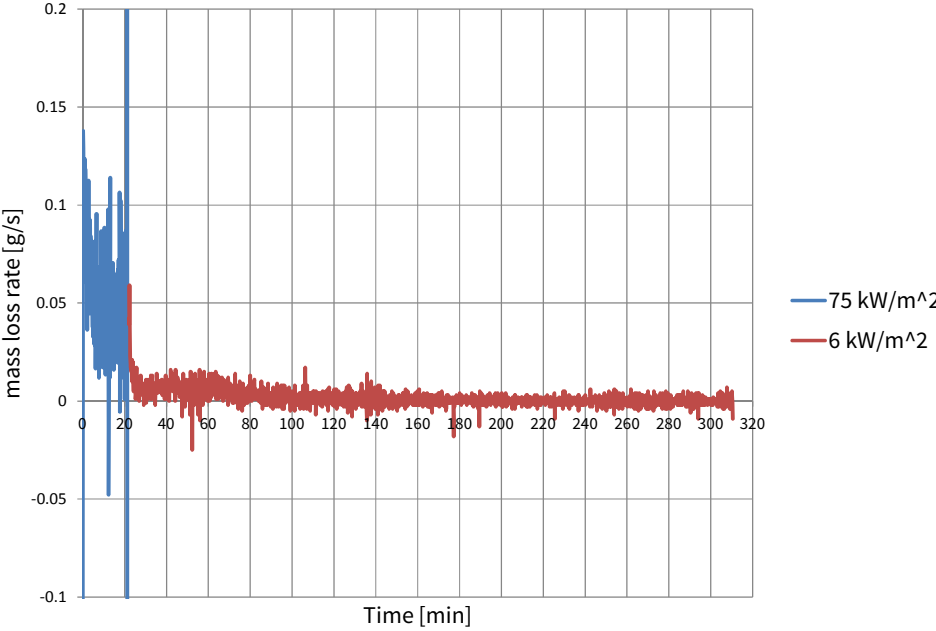


Figure F.58 Mass loss rate in experiment 10.

F.10.3 Heat release rate and heat of combustion

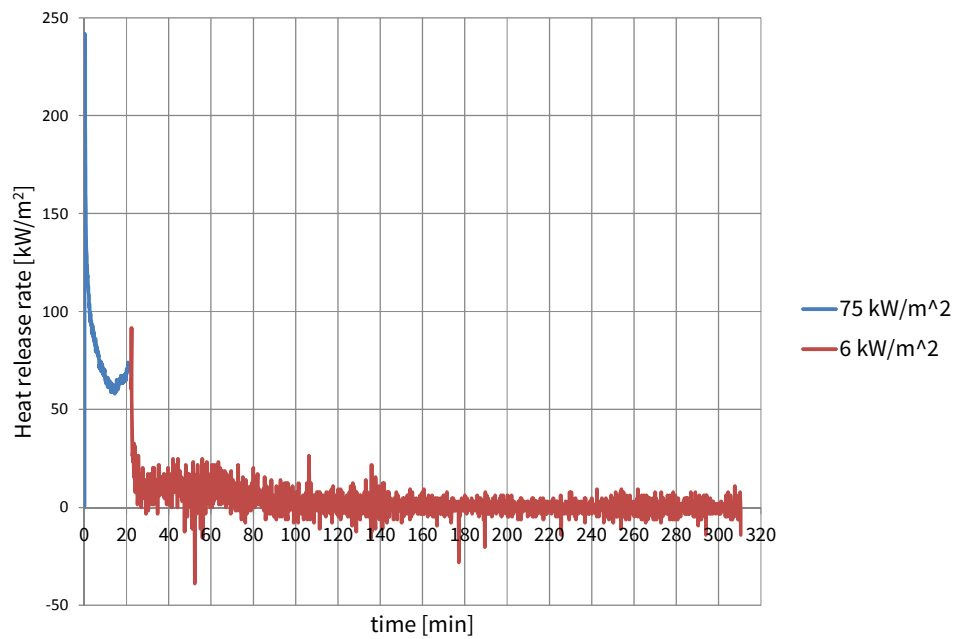


Figure F.59 Heat release rate in experiment 10 (the heat release rate during second exposure is based on the mass loss rate and average effective heat of combustion during the 75 kW/m² exposure)

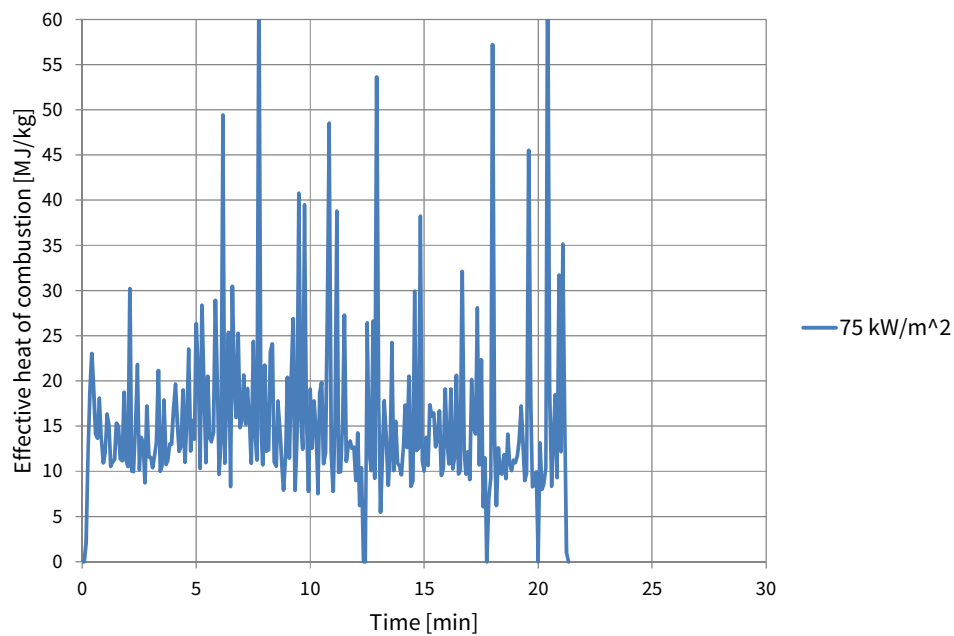


Figure F.60 Effective heat of combustion during the 75 kW/m² exposure in experiment 10.

F.11 Experiment 11 – $75 \text{ kW/m}^2 \rightarrow 6 \text{ kW/m}^2 + 0,5 \text{ m/s}$ additional air flow

F.11.1 Temperatures

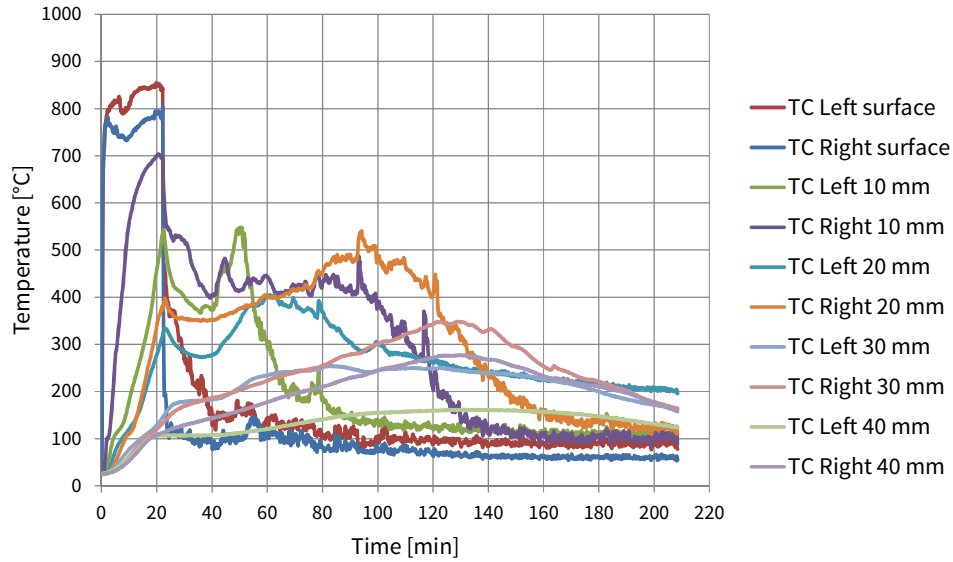


Figure F.61 CLT temperatures in experiment 11.

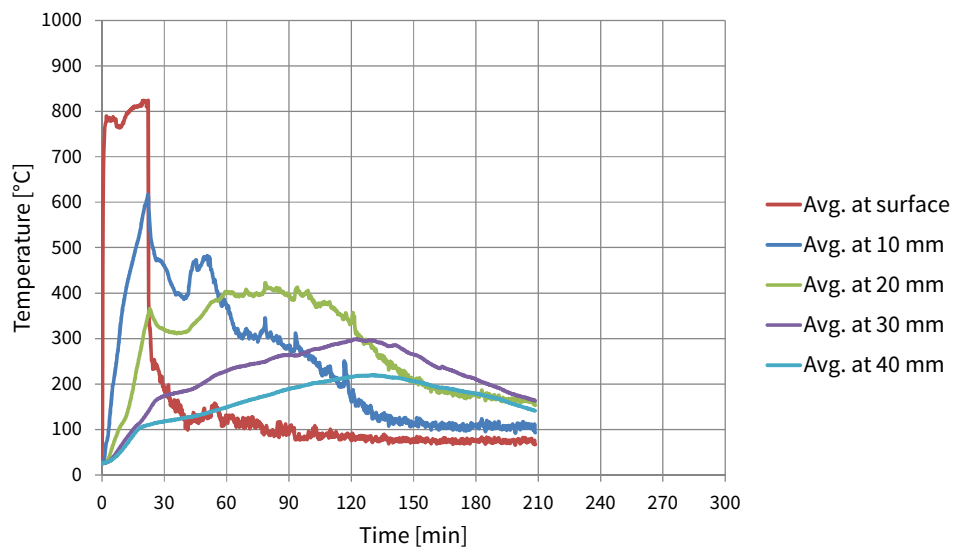


Figure F.62 Average CLT temperatures in experiment 11.

F.11.2 Mass loss

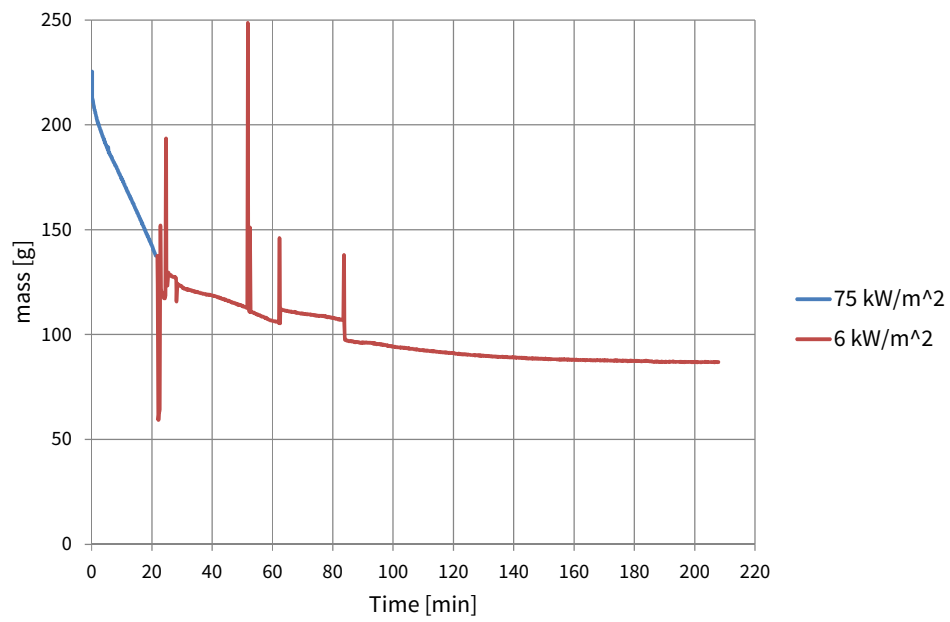


Figure F.63 Sample mass in experiment 11.

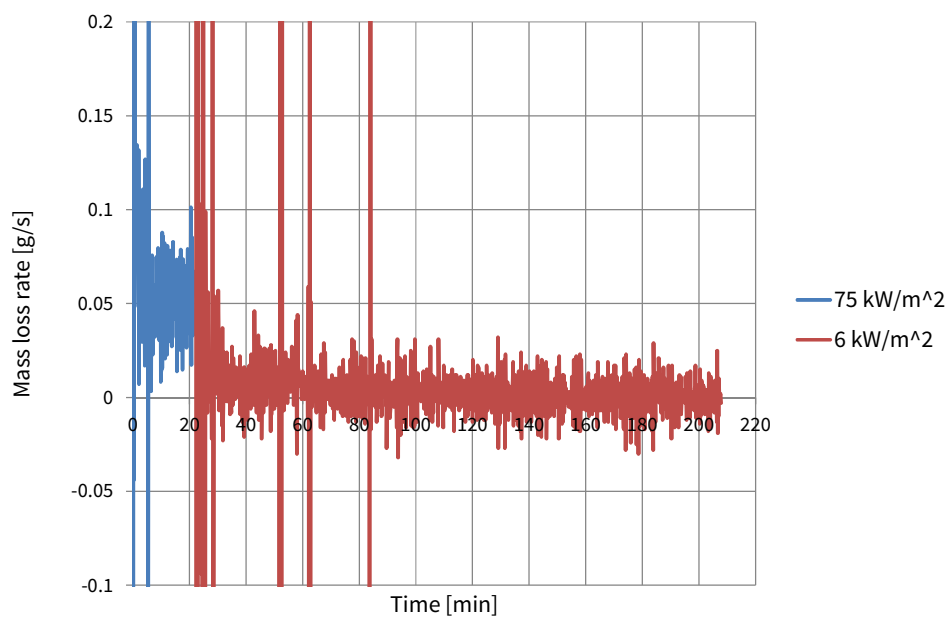


Figure F.64 Mass loss rate in experiment 11.

F.11.3 Heat release rate and heat of combustion

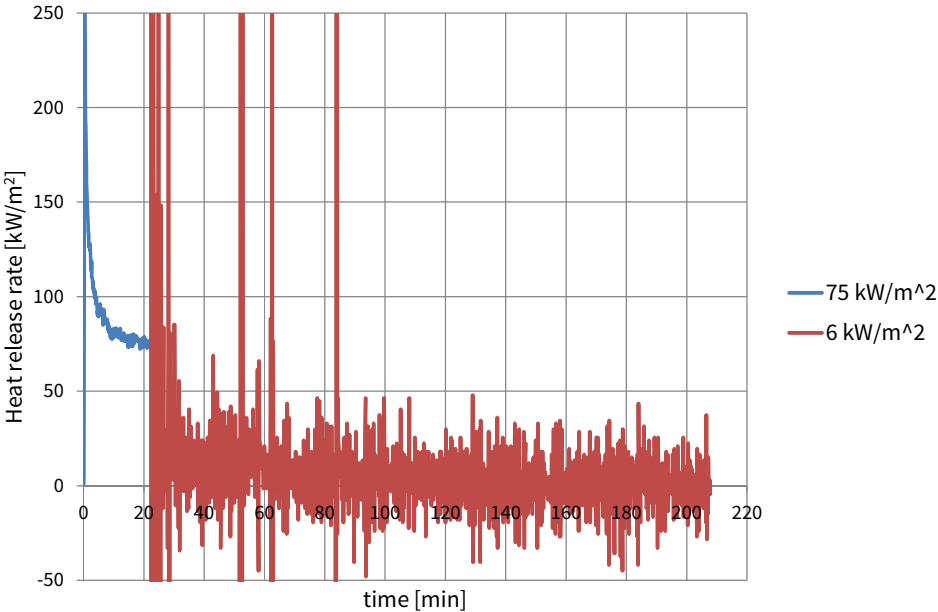


Figure F.65 Heat release rate in experiment 11 (the heat release rate during second exposure is based on the mass loss rate and average effective heat of combustion during the 75 kW/m² exposure)

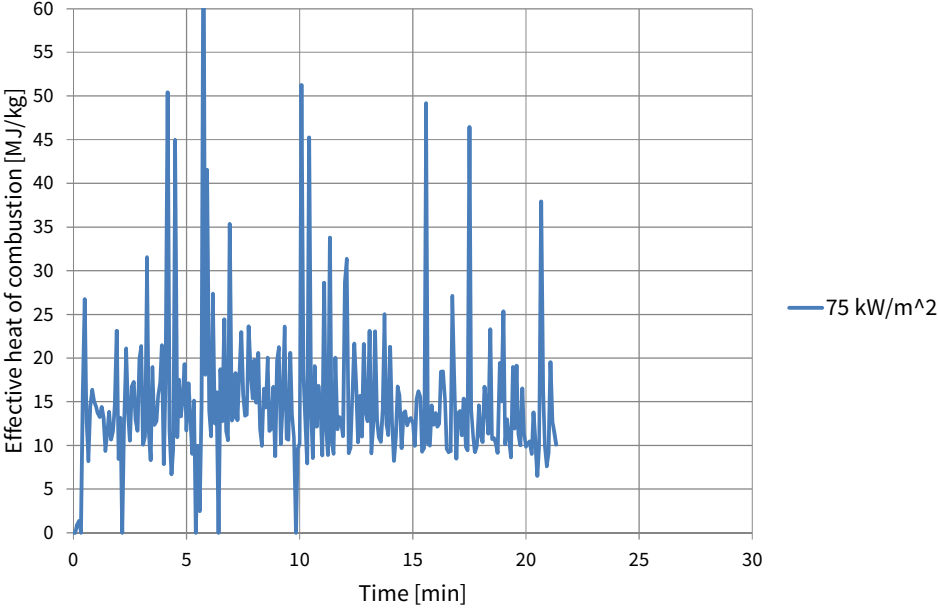


Figure F.66 Effective heat of combustion during the 75 kW/m² exposure in experiment 11.

F.12 Experiment 12 – $75 \text{ kW/m}^2 \rightarrow 6 \text{ kW/m}^2 + 1,0 \text{ m/s}$ additional air flow

F.12.1 Temperatures

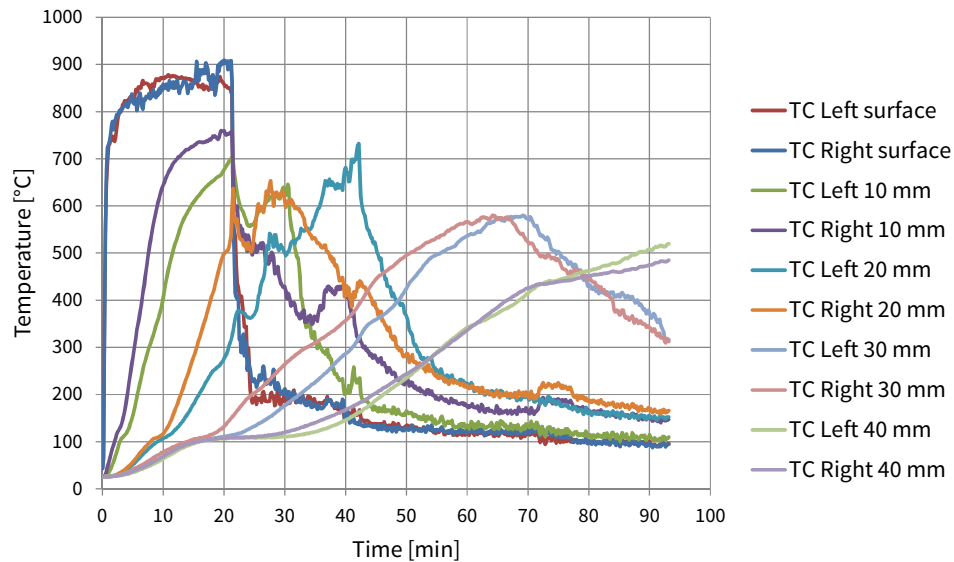


Figure F.67 CLT temperatures in experiment 12.

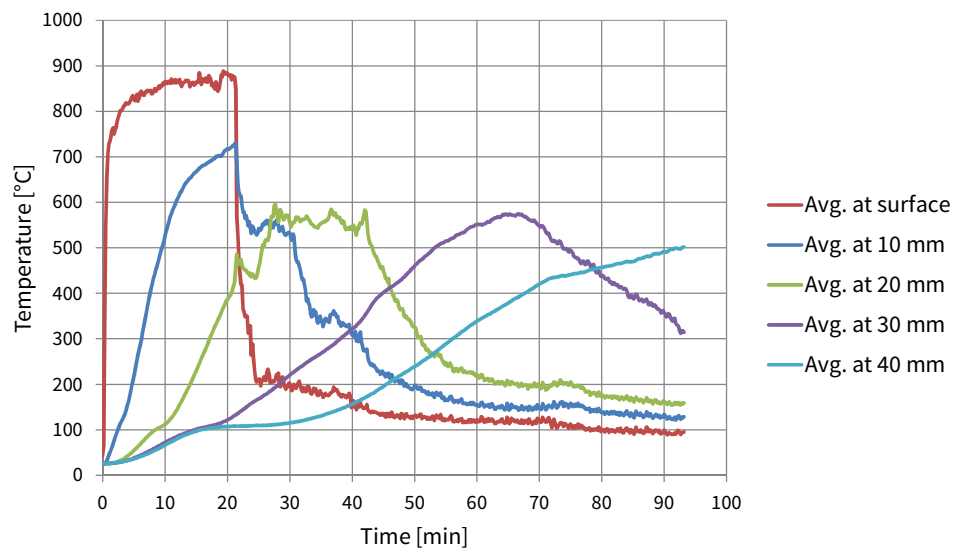


Figure F.68 Average CLT temperatures in experiment 12.

F.12.2 Mass loss

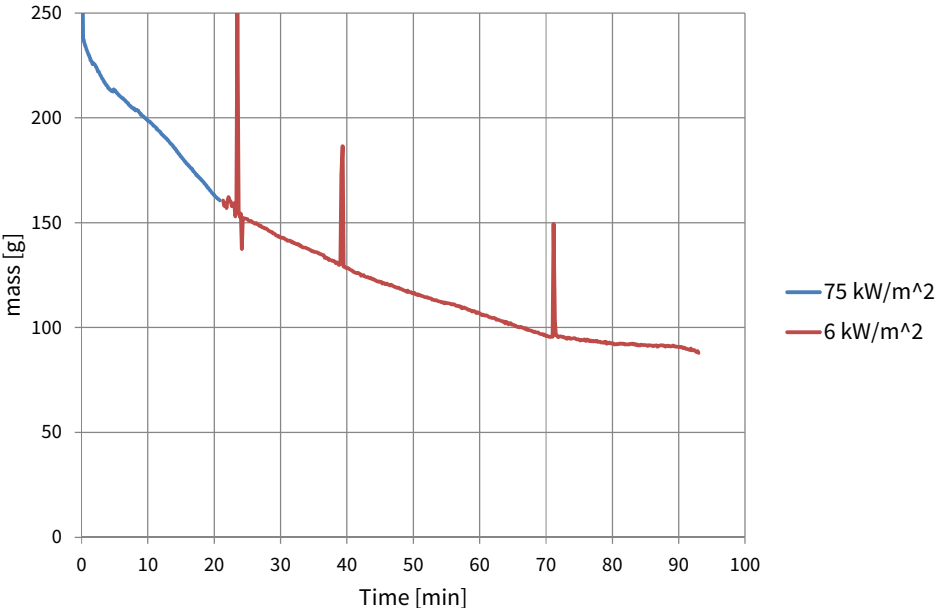


Figure F.69 Sample mass in experiment 12.

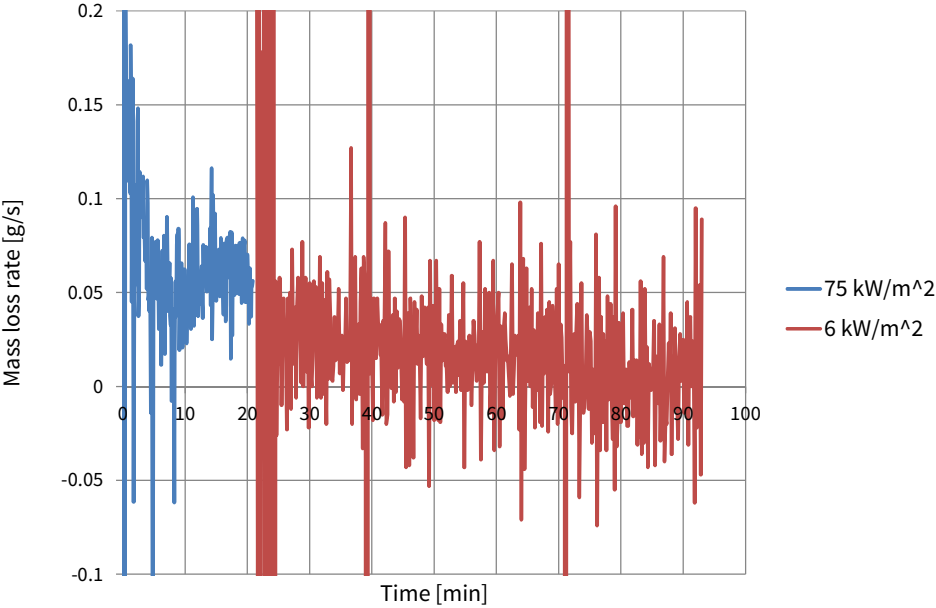


Figure F.70 Mass loss rate in experiment 12.

F.12.3 Heat release rate and heat of combustion

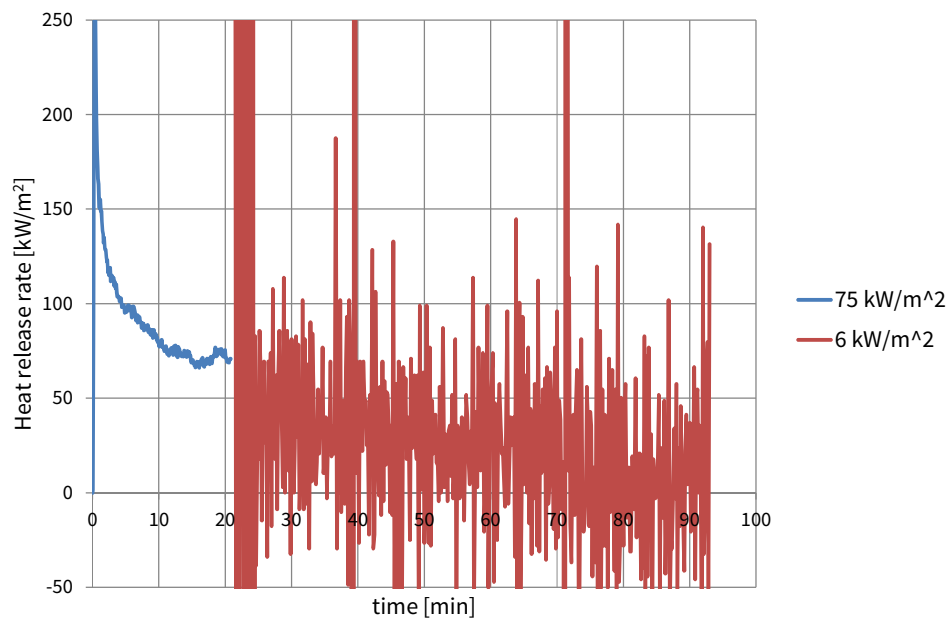


Figure F.71 Heat release rate in experiment 12 (the heat release rate during second exposure is based on the mass loss rate and average effective heat of combustion during the 75 kW/m² exposure)

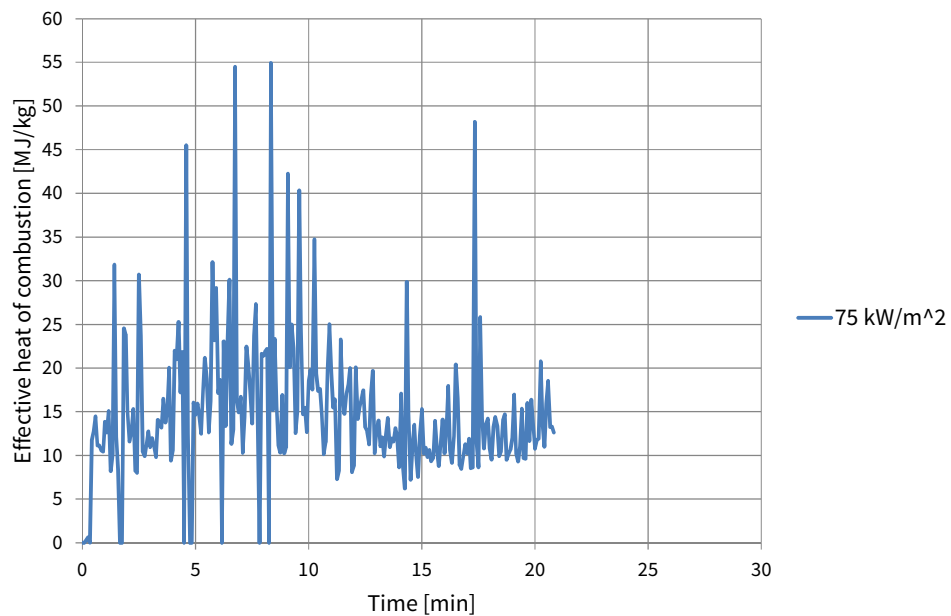


Figure F.72 Effective heat of combustion during the 75 kW/m² exposure in experiment 12.

F.13 Experiment 13 – 75 kW/m² continued

F.13.1 Temperatures

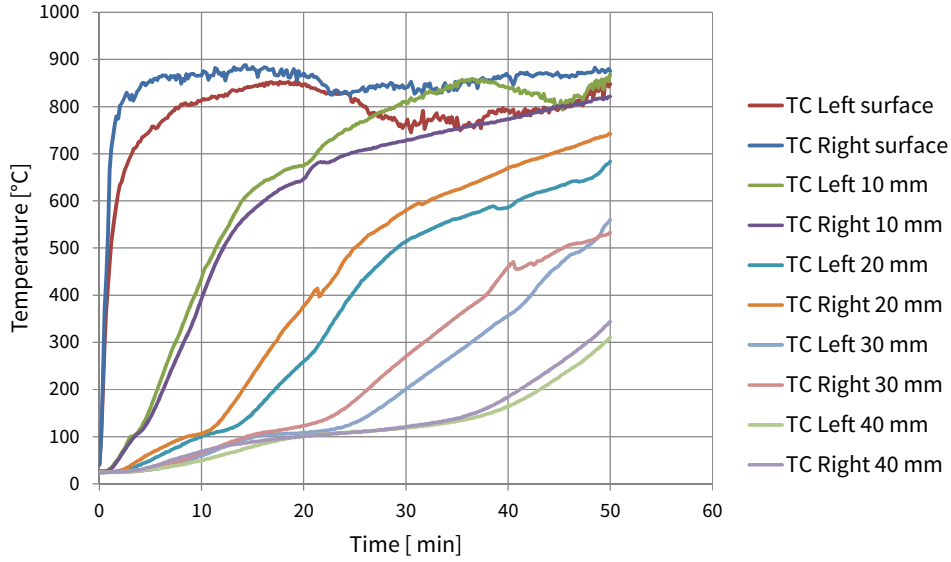


Figure F.73 CLT temperatures in experiment 13.

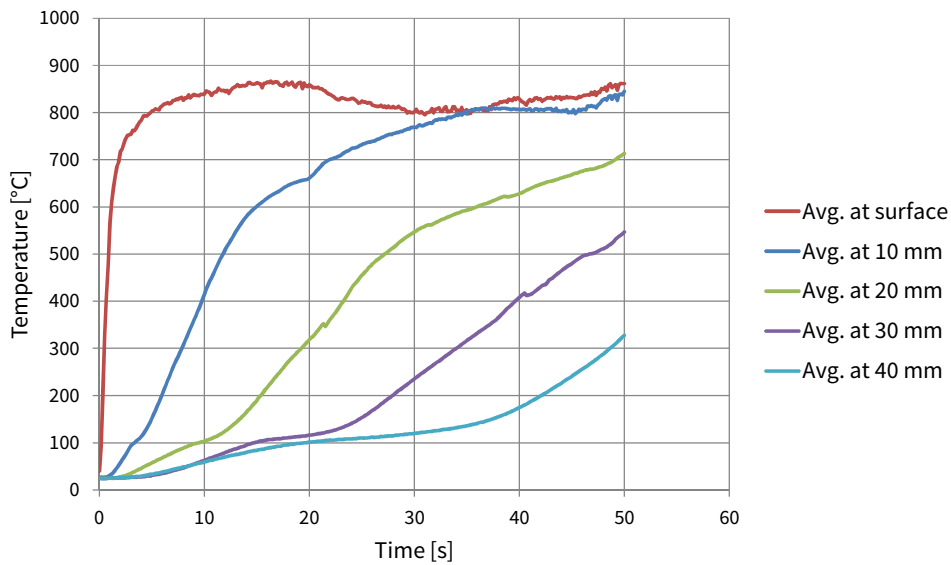


Figure F.74 Average CLT temperatures in experiment 13.

F.13.2 Mass loss

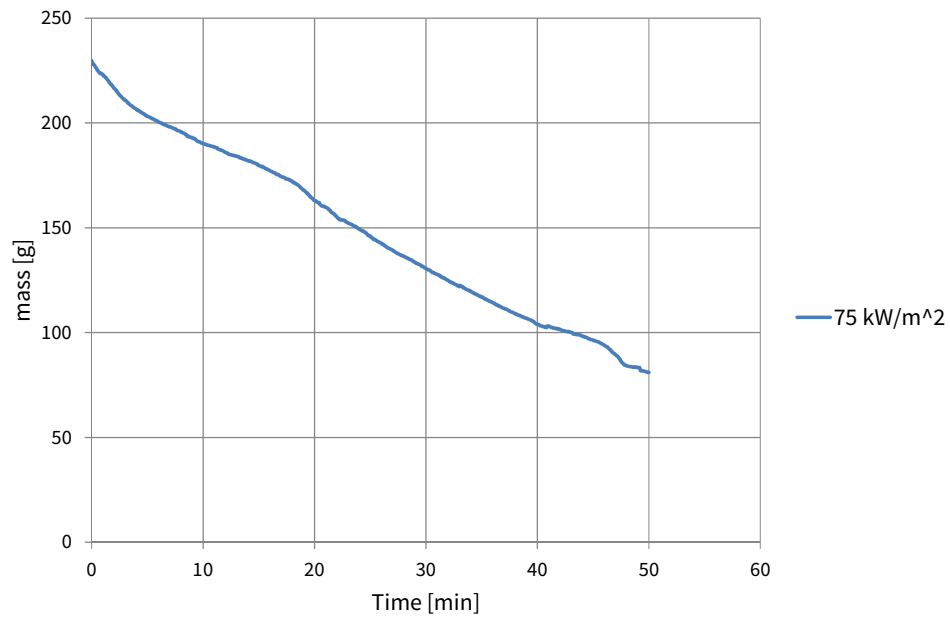


Figure F.75 Sample mass in experiment 13.

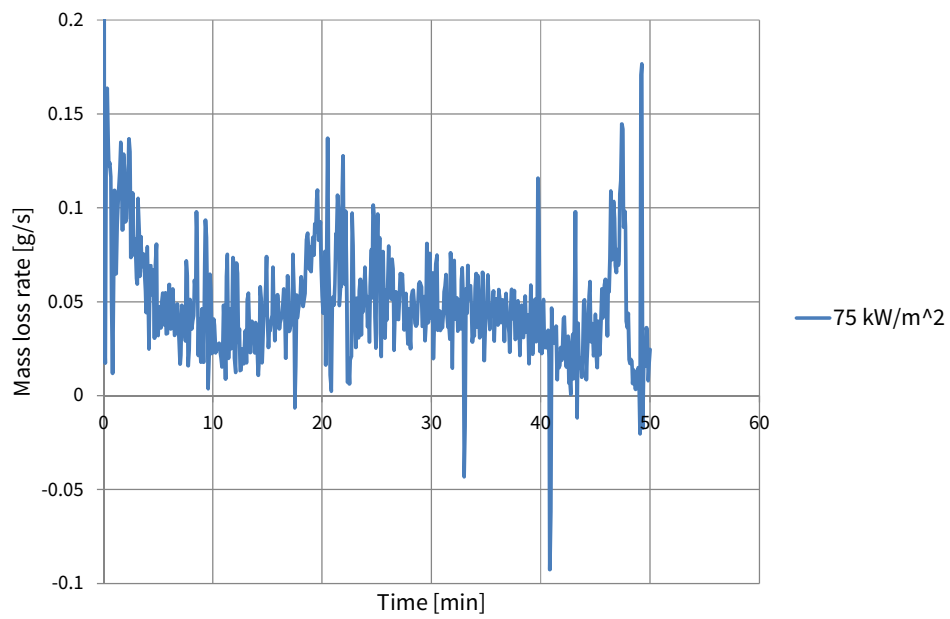


Figure F.76 Mass loss rate in experiment 13.

F.13.3 Heat release rate and heat of combustion

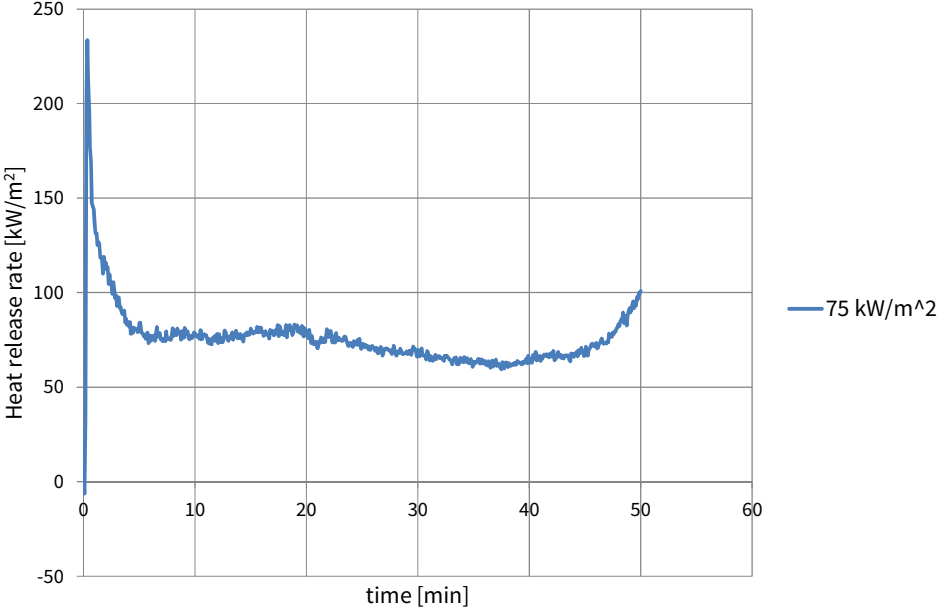


Figure F.77 Heat release rate in experiment 13.

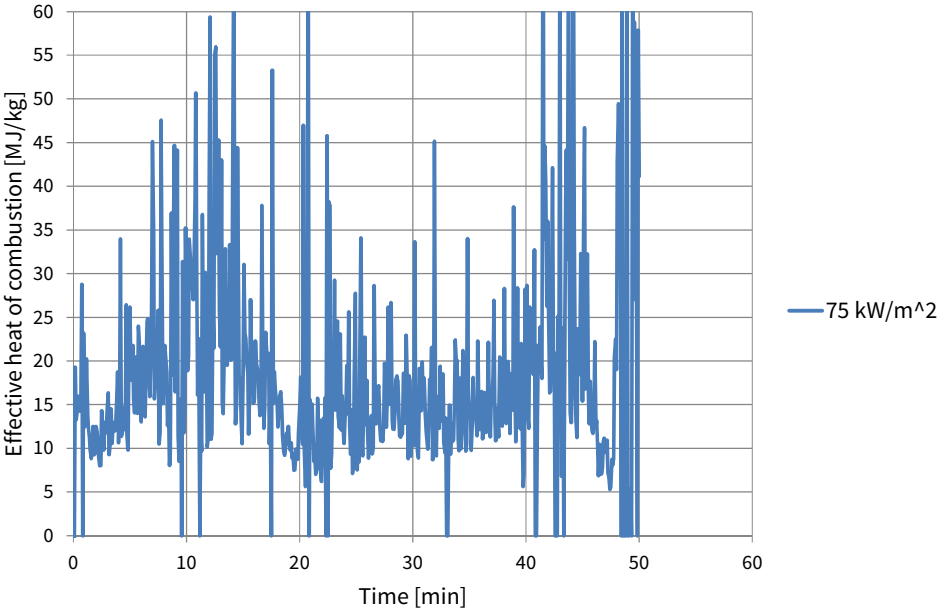


Figure F.78 Effective heat of combustion during the 75 kW/m² exposure in experiment 13.

F.14 Experiment 14 – 75 kW/m² continued

F.14.1 Temperatures

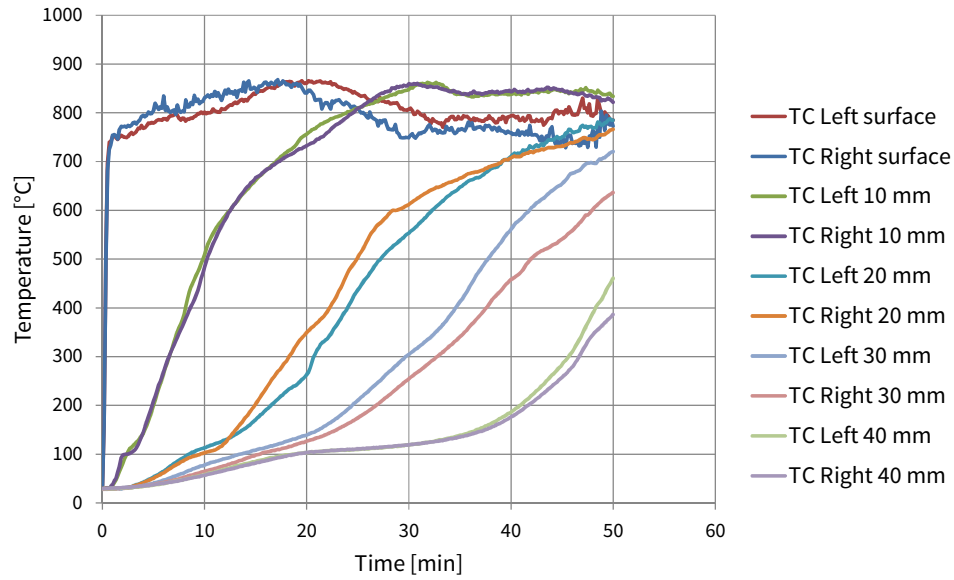


Figure F.79 CLT temperatures in experiment 14.

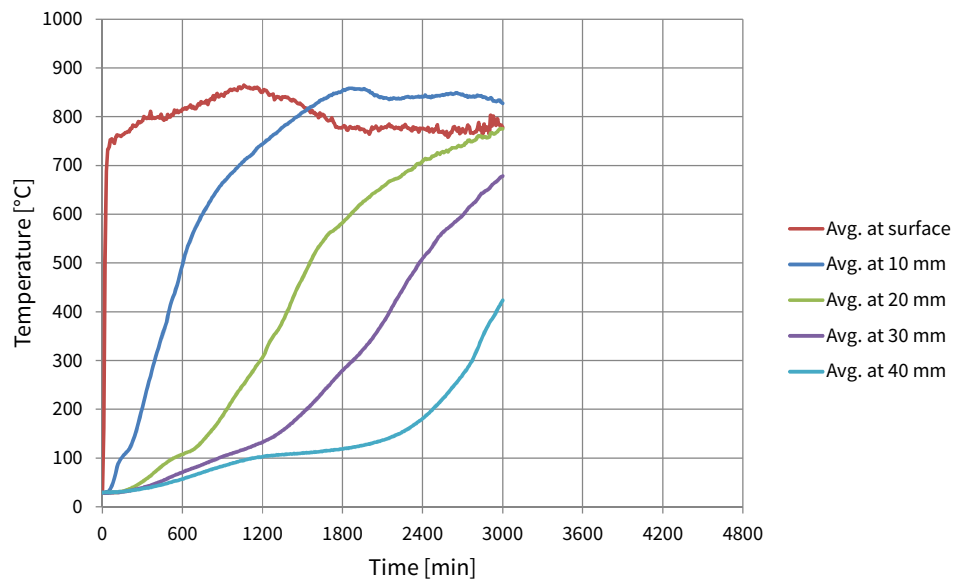


Figure F.80 Average CLT temperatures in experiment 14.

F.14.2 Mass loss

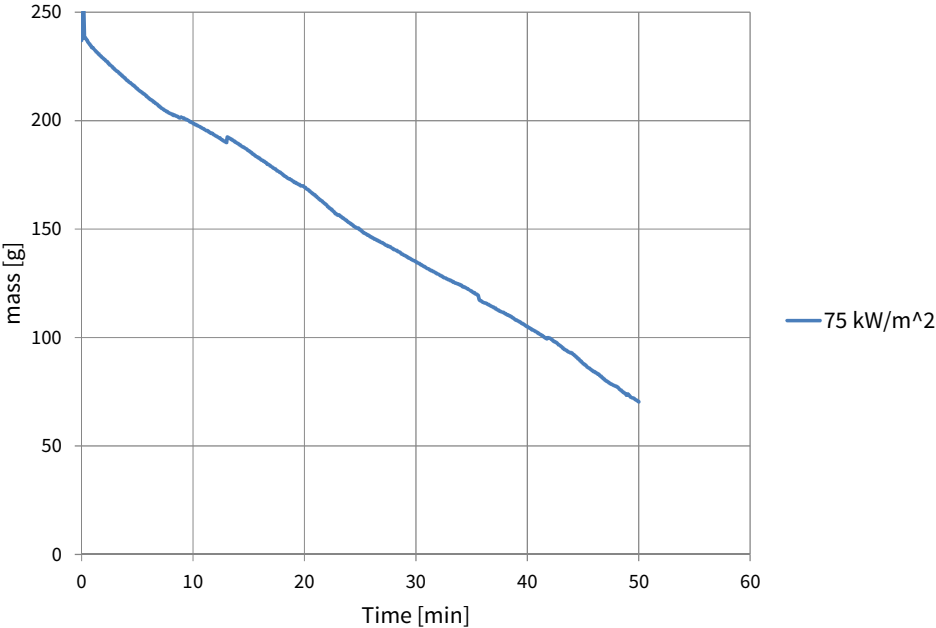


Figure F.81 Sample mass in experiment 14.

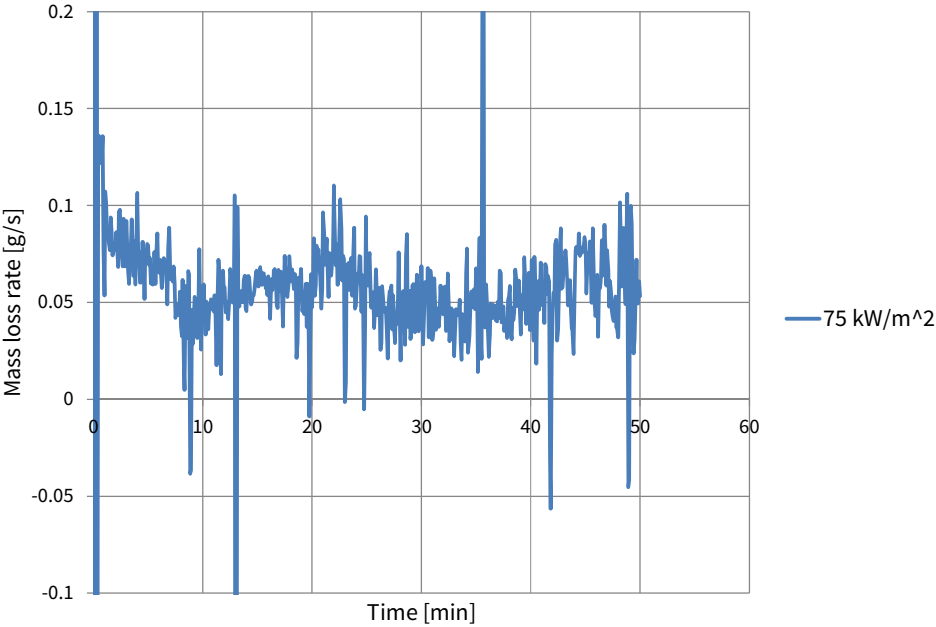


Figure F.82 Mass loss rate in experiment 14.

F.14.3 Heat release rate and heat of combustion

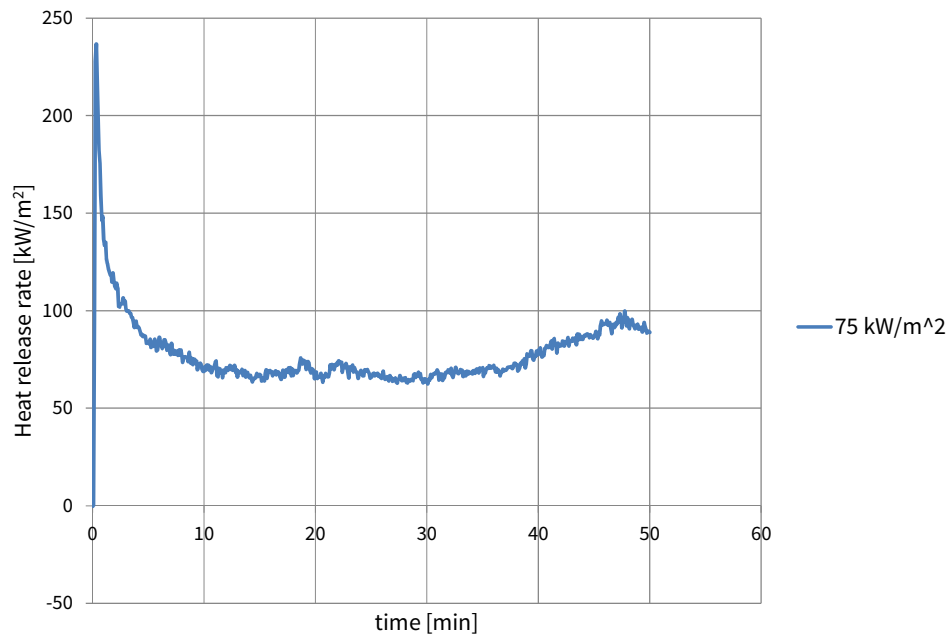


Figure F.83 Heat release rate in experiment 14.

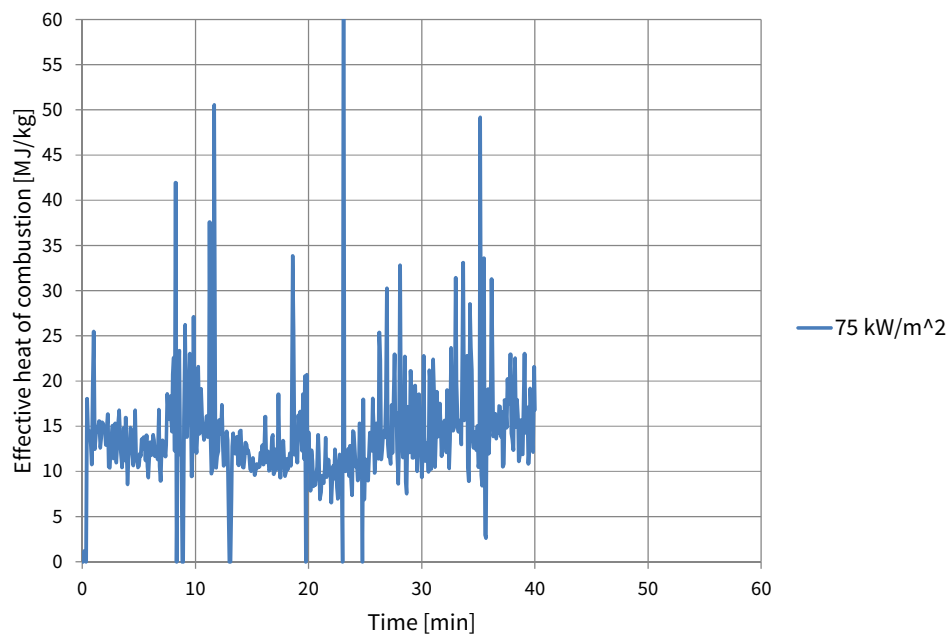


Figure F.84 Effective heat of combustion during the 75 kW/m² exposure in experiment 14.

F.15 Experiment 15 – 75 kW/m² continued, no thermocouples

F.15.1 Mass loss

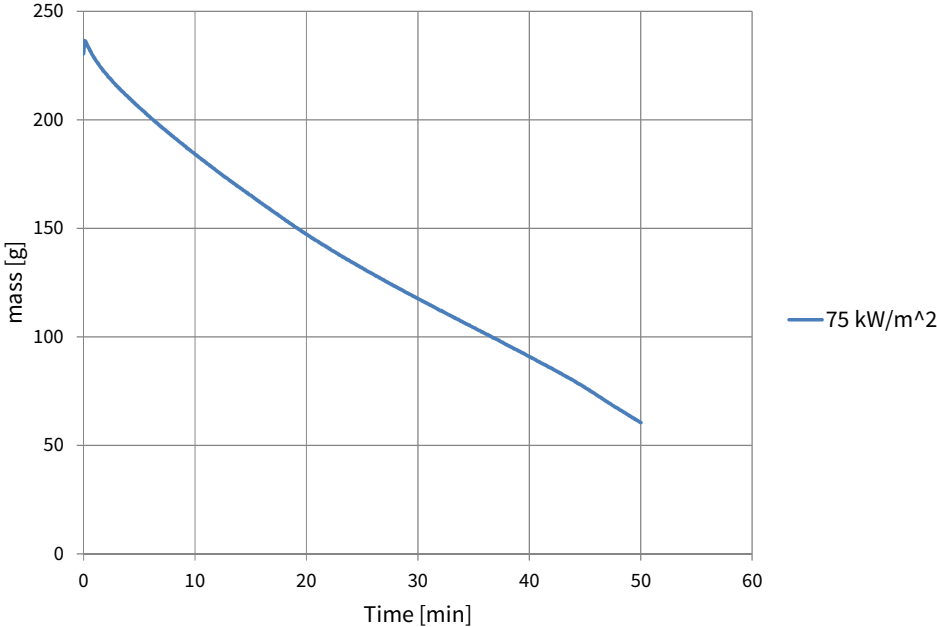


Figure F.85 Sample mass in experiment 15.

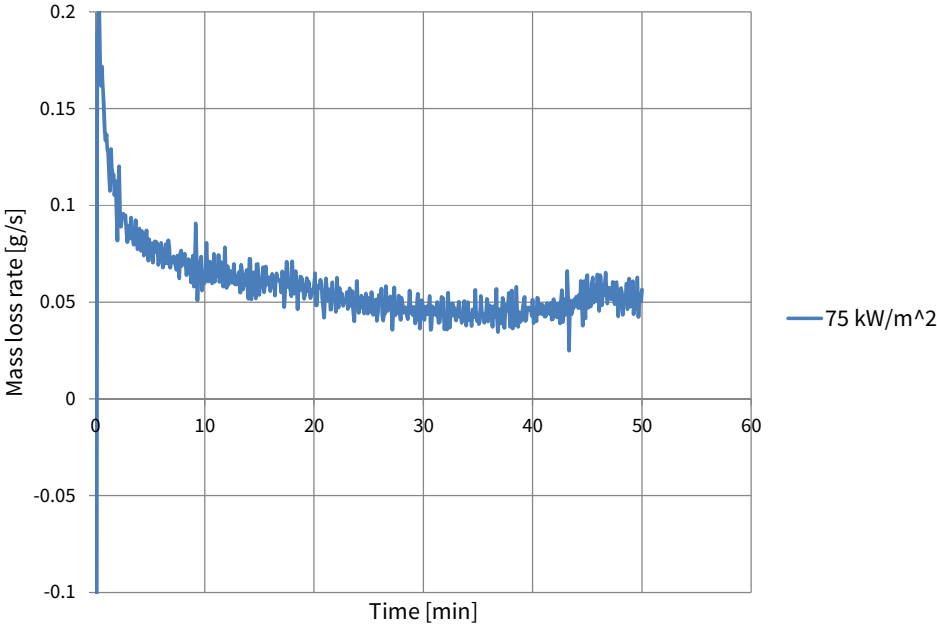


Figure F.86 Mass loss rate in experiment 15.

F.15.2 Heat release rate and heat of combustion

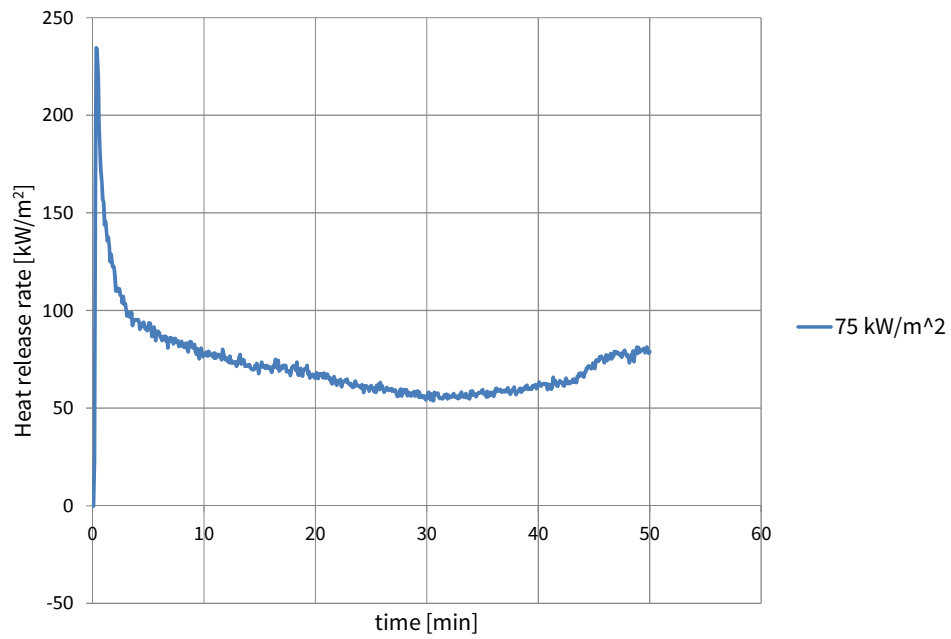


Figure F.87 Heat release rate in experiment 15.

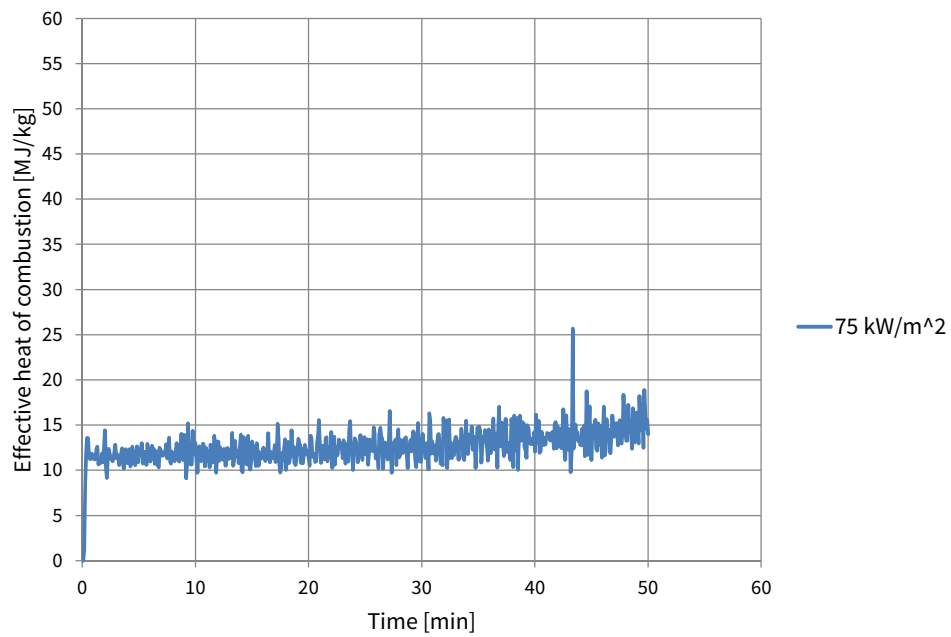


Figure F.88 Effective heat of combustion during the 75 kW/m² exposure in experiment 15.

F.16 Experiment 16 – 75 kW/m² continued, no thermocouples

F.16.1 Mass loss

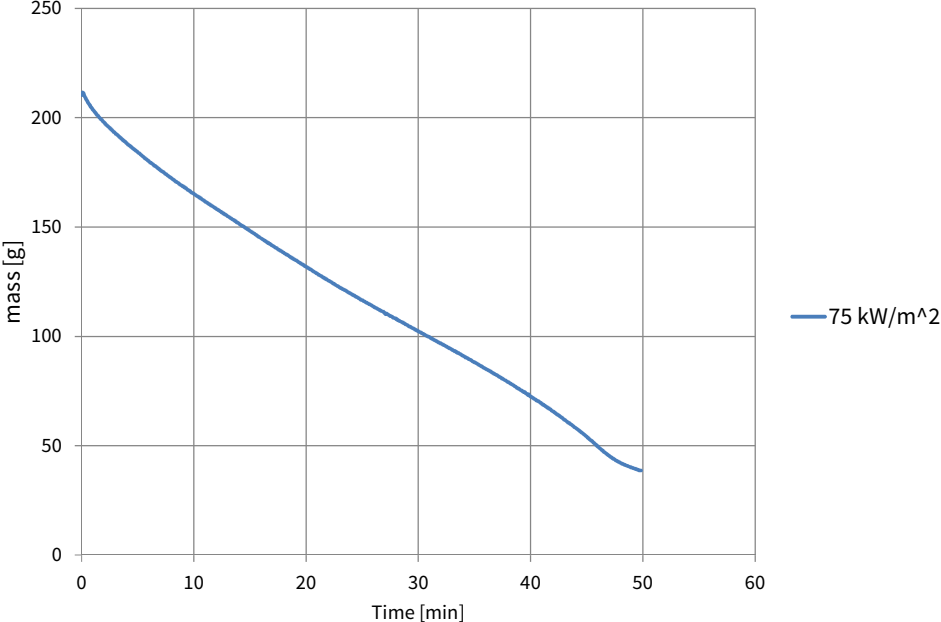


Figure F.89 Sample mass in experiment 16.

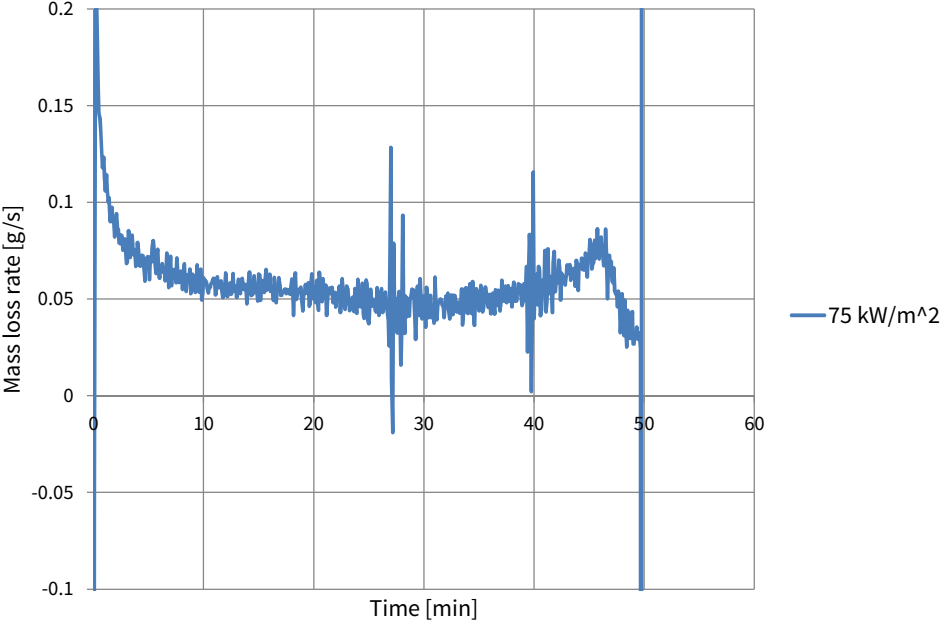


Figure F.90 Mass loss rate in experiment 16.

F.16.2 Heat release rate and heat of combustion

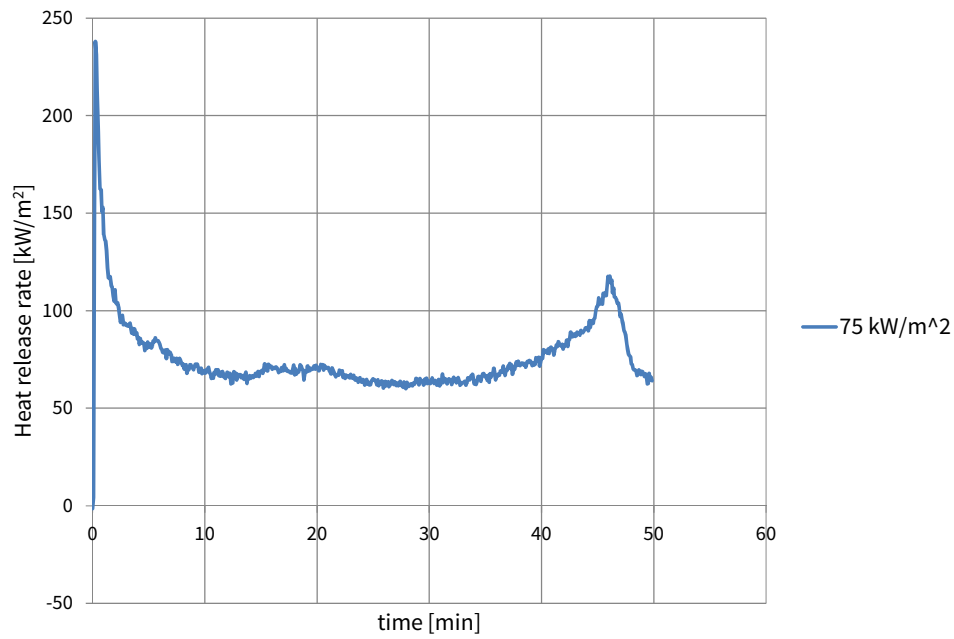
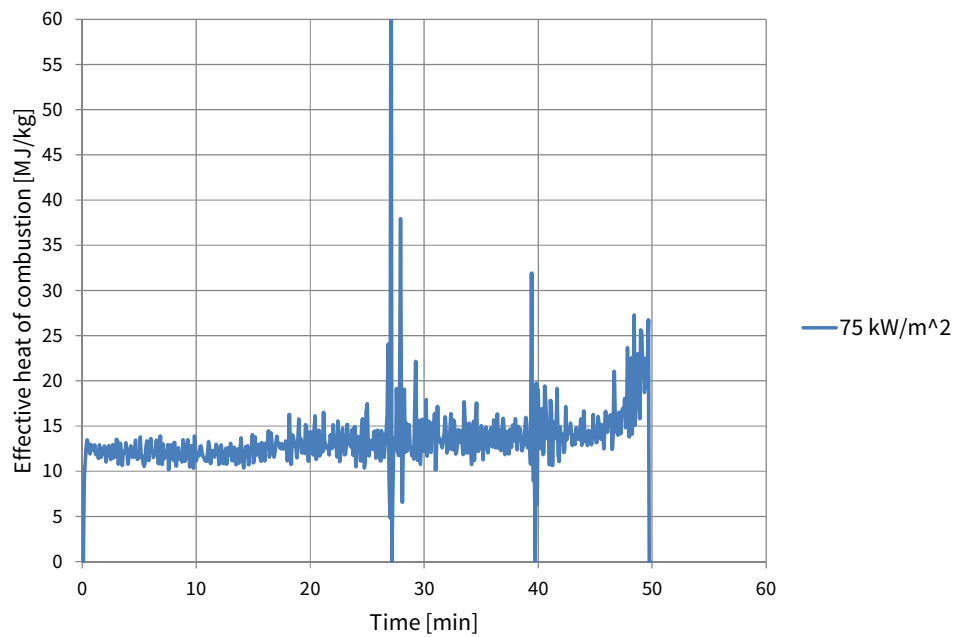


Figure F.91 Heat release rate in experiment 16.

Figure F.92 Effective heat of combustion during the 75 kW/m² exposure in experiment 16.

G

Fluctuations experiment series 1

G.1 Introduction

Various measurements fluctuated during the experiments. This appendix discusses these fluctuations and the influence of the thermocouples on the measurements.

G.2 Fluctuations in experiments 1-12

Experiments 1 – 12 were carried out at a 75 kW/m^2 heat flux and subsequent various lower second exposures. Experiments 11 and 12 were conducted with an additional airflow over the sample surface. In all these experiments thermocouples were embedded in the samples.

G.2.1 Mass loss rate

In most experiments the MLR fluctuated during both the 75 kW/m^2 exposure, (when mass was measured by the cone calorimeter load cell) and during the various second exposures (when mass was measured by a separate scale).

Values of the MLR were obtained of the magnitude $0,050 \text{ g/s}$ during the 75 kW/m^2 exposure, and much lower, i.e. approximately $0,010 \text{ g/s}$, during the second exposures.

The MLR fluctuated with $\pm 0,002 \text{ g/s}$ in most experiments. In some cases, these fluctuations were larger: up to $\pm 0,005 \text{ g/s}$.

It can be expected these fluctuations were due to the sensitive nature of the load cell and the scale. Furthermore, the measurements were conducted at a relative short interval of 5 and 10 seconds respectively. At this short interval, the mass loss is relatively small. Considering the sensitive nature of the equipment, the natural variation the material, and the small mass loss in the short time interval, this resulted in relative large fluctuations.

The experiments with additional air flow fluctuated even more, up to $\pm 0,050 \text{ g/s}$. This can be attributed to the disturbing influence of the wind on the sensitive mass loss measurements. The air flow will likely consist of vortices, which can influence mass measurements.

However, when comparing the results of multiple experiments, it does not seem likely the fluctuations influenced the average MLR over a longer period of time, even though individual measurements were either quite high or quite low.

In addition to these fluctuations, in most experiments, some positive and negative “spikes” were observed in the MLR data. These spikes occurred typically at the start of the experiment and at the moment of switching when the samples were removed from the load cell and placed on the scale. As a result, the load cell and the scale experienced an impulse, which became visible in the measurements.

Furthermore due to the sensitive nature of the load cell and the scale, some other spikes were observed. These could be due to slight bumps to the setup.

G.2.2 Heat release rate

The HRR did not fluctuate much during the 75 kW/m^2 exposures; approximately $\pm 2 \text{ kW/m}^2$ compared to average values of approximately 70 kW/m^2 . This might be due to the fact that oxygen consumption measurement is not very sensitive.

However, the HRR of the various second exposures was not measured directly, but was based on the MLR data. As a result, the fluctuations and spikes that were present in the MLR can also be found in the HRR. The HRR was observed in most experiments to fluctuate with $\pm 3 \text{ kW/m}^2$. In some experiments, fluctuations were larger; up to $\pm 10 \text{ kW/m}^2$. The experiments with additional air flow fluctuated heavily; up to $\pm 100 \text{ kW/m}^2$. Furthermore, due to the fluctuation in the MLR negative values for the HRR were obtained, which are unlikely.

G.2.3 Effective heat of combustion

The EHC was determined during the 75 kW/m^2 exposures, when both a HRR and a MLR measurement were done. The EHC is calculated by dividing the HRR by the MLR.

The degree of fluctuation in the EHC was found to vary significantly between experiments. In some cases, the EHC fluctuated between 8 and 18 MJ/kg . In extreme cases, such as the experiments with an additional air flow, values ranged from 0 to well over 30 MJ/kg . Furthermore, occasionally positive spikes or zeros were present to match high or low values in the MLR data.

Despite the variation in fluctuation, the average EHC ranged from 11,3 to $16,1 \text{ MJ/kg}$; an average of $14,0 \text{ MJ/kg}$. This suggested that even though individual (momentary) measurements of the EHC varied, the average over a longer period was fairly constant.

Considering this average EHC, the fluctuations were large. The reason for this high fluctuation can be found in the fact that the HRR and MLR measurement each fluctuate themselves. Especially the MLR, which is the denominator, is quite small but showed a large fluctuation. This is translated in a large fluctuation of the EHC.

G.3 The effect of thermocouples

Experiments 13 to 16 investigated the samples at a constant 75 kW/m^2 exposure. Experiments 15 and 16 were conducted without thermocouples in the samples.

G.3.1 Mass loss and mass loss rate

Thermocouples were embedded in most samples. This could influence the weight measurements. To decrease any additional weight, the wires were connected to a supporting structure close to the sample. To avoid the wires influence the measurements due to their bending stiffness, the wires were attached as hinges to the supporting structure. To avoid uplift of the sample due to the heavy “back-span”, the back-span was connected to the supporting structure.

Despite these measures, the thermocouples were found to influence the weight in absolute sense. This means that the thermocouples might press the sample on the load cell or scale, or lift it up, resulting in additional or less weight measured. The starting weight of the samples was set to the pre-testing measured value (without thermocouples attached to the samples). As a result, the initial disturbance of the thermocouples was removed from the data.

This was also done when the samples were switch from the cone calorimeter to the scale with the separate cone. The setup was adjusted and the thermocouples again created a difference between the final measurement of the cone and the first measurement of the scale, virtually increasing or decreasing the sample in weight with a discrete step. This step was removed in the data as a post processing step, by setting these two measurements equal to each other.

The relative influence of the thermocouples was investigated during testing. The samples without thermocouples lost more mass than the samples with thermocouples. This difference was established during the first 5 to 15 minutes of testing, as can be seen in figure G.1. It seems the thermocouples resist some of the mass loss, possible due to some stiffness of the thermocouples wires. The setup was made to prevent this effect as much as possible, but a small effect remained present. However, subsequently, the mass graphs are parallel; indicating this influence of the thermocouples on the mass loss remained limited to a certain amount.

Furthermore, if the mass loss is plotted for the other experiments, all conducted with thermocouples in the samples, these are in between the lines of the experiments 13 to 16, as can be seen in figure G.2 This indicates there also might be a natural variation resulting in differences in mass loss; and not necessarily solely an influence of the thermocouples.

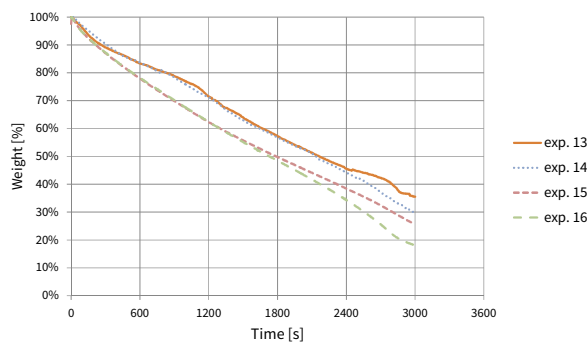


Figure G.1 Sample weight, expressed as a percentage from the starting sample weight.

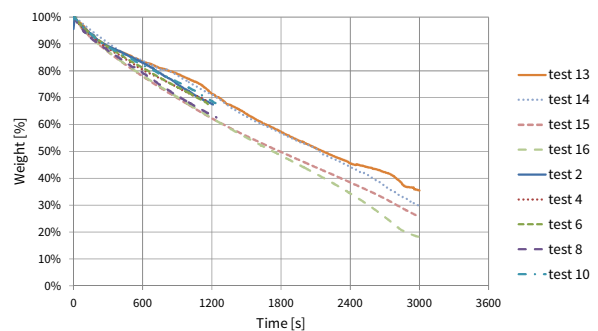


Figure G.2 Sample weight, expressed as a percentage from the starting sample weight.

Figures G.3 and G.4 depict the MLR for an experiment with and without thermocouples. The amount of fluctuation increased when thermocouples were present. This might be in part due to the influence of the stiffness of the thermocouples wire on the sensitive load cell measurements.

However, when the average MLR of experiments with and without thermocouples are compared, the values are within the same range. The average MLR over a longer period of time was not much affected by the thermocouples, even though they influenced individual measurements. This reinforces the idea that the relative influence of the thermocouples was small.

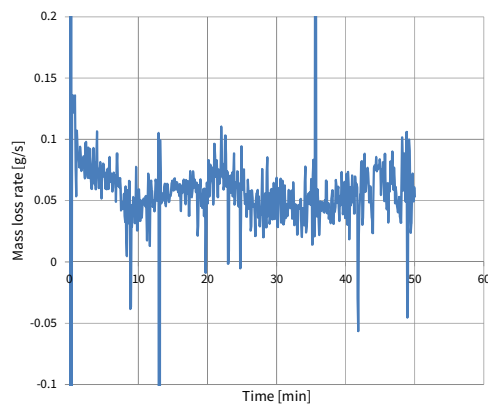


Figure G.3 Mass loss rate during the 75 kW/m² exposure in experiment 14.

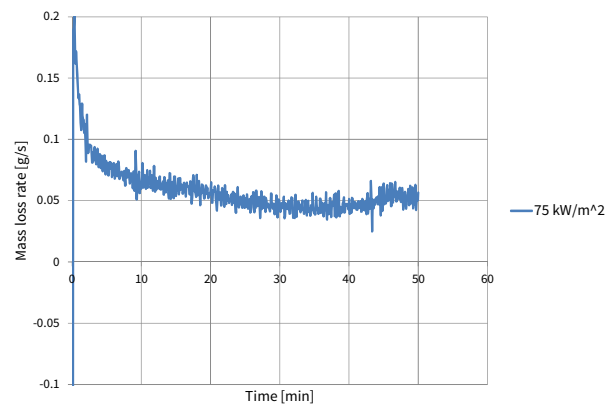


Figure G.4 Mass loss rate during the 75 kW/m² exposure in experiment 15.

G.3.2 Heat release rate

The HRR was not affected by the thermocouples.

G.3.3 Effective heat of combustion

A significant difference was observed in the amount of fluctuation between the tests with and without thermocouples. As explained in the previous paragraph, the fluctuations in the ECH can be attributed in part to the fluctuations in the MLR. Because the thermocouples were found to increase the fluctuations of the MLR, they also increase the fluctuations of the EHC.

However, average values of the experiments without thermocouples were consistent with the values of those with thermocouples. This suggests that even though the couples influenced individual measurements, the average over a longer period was not affected.

H

Charring rates experiment series 1

H.1 Introduction

Charring rates are obtained for both the 75 kW/m² and the various second lower exposures using the location of the 300 ° C isotherm.

The location of the 300 ° C isotherm was determined with the average of the two thermocouple temperatures at a certain depth (0, 10, 20, 30, and 40 mm from the CLT surface).

Charring during the initial exposure of 75 kW/m²

Table H.1 presents the charring rates obtained for the initial 75 kW/m² exposure. The values represent average charring rates for the corresponding 10 mm layer of CLT, because thermocouples were spaced 10 mm over the depth of the material.

Table H.1 Charring rates during the 75 kW/m² exposure.

Charring rate [mm/min]	1	2	3	4	5	6	7	8	9	10	11	12	Average
1st 10 mm	1,62	1,46	1,50	2,31	1,54	1,94	2,00	2,00	1,54	1,30	1,20	1,58	1,67
2nd 10 mm	0,74	0,82	0,85	0,72	0,73	0,77	0,69	0,67	0,70	0,82	0,87	0,92	0,78
total 20 mm	1,02	1,05	1,08	1,10	0,99	1,10	1,03	1,01	0,96	1,01	1,01	1,17	1,04

The charring rate for the first 10 mm of CLT ranged from 1,20 to 2,31 mm/min, and was on average 1,67 mm/min. The charring rate for the second 10 mm of CLT ranged from 0,70 to 0,92 mm/min, and was on average 0,78 mm/min.

Combining these results, the charring rate for the total 20 mm CLT charred during the 75 kW/m² exposure ranged from 0,96 to 1,17 mm/min, and was on average 1,04 mm/min.

Charring when the 75 kW/m² heat flux exposure was continued

Charring rates were also obtained for experiments 13 and 14 in which the 75 kW/m² exposure was continued. Table H.2 presents these charring rates

Table H.2 Charring rates during the (continued) 75 kW/m² exposure.

Charring rate [mm/min]	Average Experiment 1-12	13	14	Average Experiment 1-14
1st 10 mm	1,67	1.25	1.50	1,62
2nd 10 mm	0,78	0.88	0.76	0,78
3rd 10 mm	-	0,68	0,87	0,78
4th 10 mm	-	0,68	0,66	0,67

It is unclear why the charring rate for the 3rd 10 mm of CLT in experiment 14 is higher than the charring rate obtained for the 2nd 10 mm of CLT. It would have expected that the charring rate would drop, due to the protective function of the residual char and ash layer. Perhaps a nearby crack in the char resulted in a faster propagation of the charring front at the location of the thermocouples.

The charring rate of the 4th 10 mm of CLT was on average 0,67 mm/min.

Charring during the various second exposures

Charring rates for the various second lower exposures and were found depended on the level of heat flux and any additional air flow. Table H.3 presents these charring rates.

Table H.3 Charring rates for the various second heat flux exposures.

Charring rate [mm/min]	0 kW/m ²		5 kW/m ²		10 kW/m ²		8 kW/m ²		6 kW/m ²		6 kW/m ²	
	1	2	3	4	5	6	7	8	9	10	0,5 m/s	1,0 m/s
3rd 10 mm	-	-	-	-	0,15*	0,26	0,16	0,15	0,11	0,18	-	0,48
4th 10 mm	-	-	-	-	0,29	0,27	0,20	0,22	-	-	-	0,56
total 20 mm	-	-	-	-	0,20	0,27	0,18	0,18	-	-	-	0,51

*this charring rate was obtained with a slightly larger distance from cone heater to the sample the first minutes after switching and is therefore lower than the value obtained in the experiment 6

Significantly lower charring rates were obtained than for the 75 kW/m² exposure. If the thermocouples temperatures at a certain depth were not observed to exceed 300 °C, the char front did not reach this depth and therefore no charring rate is obtained.

Quite high charring rates were obtained in experiment 12 with 6 kW/m^2 and an additional air flow with speed $1,0 \text{ m/s}$ showed. An average of $0,51 \text{ mm/min}$ was obtained for the total of 20 mm charred CLT.

It is interesting to note an increase in charring rate between the third and the fourth 10 mm of CLT in the experiments where burning-through was observed. This effect could be the result of edge effects. Samples became thin near the end of the experiments. As a result, there is less wood that needs to be heated below the reaction zone. The smoulder speed increases because the losses to the deeper layers of wood decrease. Furthermore, this effect could also be the result of an increase of insulation due the growing residual ash and char layer. The smoulder speed would increase because the losses to the surfaces decrease. These explanations are theory only, however in the experiments there were no measurements that suggest otherwise.

Comparison of charring rates with predictions and Eurocode guidance

The charring rates that were obtained can be compared to the predicted values and those provided by Eurocode 5.

The average charring rate for the first 10 mm of $1,62 \text{ mm/min}$ is consistent with the prediction based on the work of Butler (1971) of $1,65 \text{ mm/min}$. However, as the protective char and ash layer was built up, the charring rates decreased to much lower values.

A charring rate of $0,67 \text{ mm/min}$ for the deepest layers of the wood in experiments 13 and 14 was found consistent with the Eurocode charring rate of $0,65 \text{ mm/min}$. Note however that the latter is based on a standard fire exposure, not on a constant heat flux exposure of 75 kW/m^2 . Nevertheless, these charring rates are almost equal, suggesting the 75 kW/m^2 heat flux was an appropriate post-flashover exposure.

The charring rates of the second lower heat flux exposures cannot be compared to Eurocode guidance. However, these can be compared to predictions based on the work of Butler. The results corresponded well to the predictions; a charring rate of $0,18 \text{ mm/min}$ was obtained as well as predicted for 8 kW/m^2 . A charring rate of $0,24 \text{ mm/min}$ was obtained compared to the $0,22 \text{ mm/min}$ predicted at 10 kW/m^2 . The formula by Butler is not applicable for exposures $< 8 \text{ kW/m}^2$. Indeed, at $0, 5$ and 6 kW/m^2 , the samples extinguished and no charring rates were obtained.

Note that the predictions by Butler seem to correspond well at these low fluxes, despite the fact that a char layer had formed. At the high exposure of 75 kW/m^2 , the prediction corresponded well during the period that the char layer had not formed yet. No explanation has been found for this.

Mechanisms experiment series 1

I.1 Introduction

The distribution of temperatures and their propagation through the CLT samples offer an explanation of the mechanisms during self-extinguishment and burn-through, as well as the effect of additional airflow.

Burn-through

Figure I.1 depicts a linear approximation of the temperature profiles at 30, 60 and 120 minutes in experiment 6 with a 10 kW/m^2 heat flux exposure. From these profiles the various zones of the smouldering mechanism, as discussed in chapter 3, can be observed propagating through the material. These zones are shown on the left side of the graph for the temperature profile at 60 minutes.

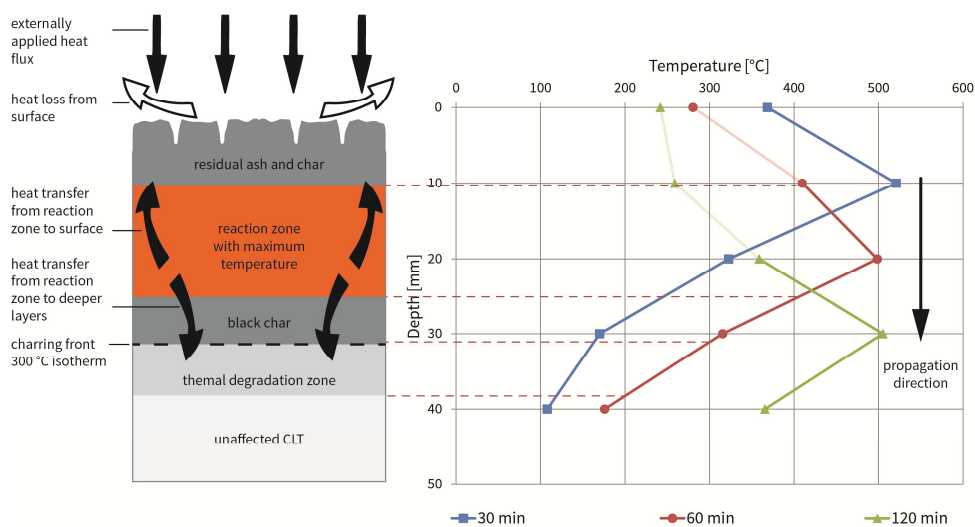


Figure I.1 Smoulder propagation through the sample in experiment 6 during the 10 kW/m^2 exposure. The light lines indicate measurements above the reduced surface, i.e. in the air above the char and ash.

At the surface a residual ash and char layer is present. This layer is the result of the oxidation of the char. The temperature is low ($<300 \text{ °C}$), because the surface is subjected to significant heat losses.

Below this residual layer, the reaction zone is present. Here char is oxidized and heat is being produced that drives the smouldering process. The temperature is high ($>400 \text{ °C}$). Heat is conducted from this zone to the surface and deeper into the sample to the thermal degradation zone. While this zone is well

insulated by the ash and char layer, the losses can become too large. As a result, the process can no longer be self-sustaining and the sample extinguishes. Therefore, losses need to be partially reduced and compensated by an externally applied heat flux. In the experiments where burn-through occurred, the externally applied heat flux was able to do this.

The heat conducted from the reaction zone to the deeper layers of the CLT, elevates the temperature above 200 °C, which will result in thermal degradation. When the temperature is elevated above 300 °C, the material can be considered to be transformed into char. While these zones propagate through the sample, this char will become the reaction zone, and the former reaction zone will become a residual layer.

It was observed that the maximum temperature in the reaction zone is higher than the temperature of the cone heater. In this example, the cone temperature was 449 °C, while the maximum temperature in the sample was > 500 °C. When the configuration factor from the cone to the sample is taken into account, this phenomenon illustrates energy is generated by the smoulder process.

Self-extinguishment

Figure I.2 depicts the temperature profiles at 60, 120, 180 and 240 minutes in an experiment with a 6 kW/m² heat flux exposure (experiment 9). In this experiment, the sample initially smouldered, but then extinguished nevertheless.

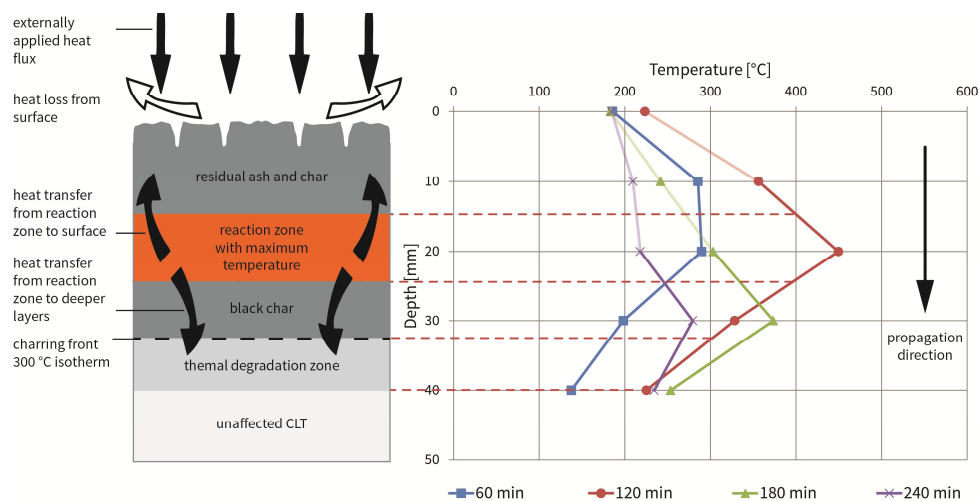


Figure I.2 Smoulder propagation though the sample in experiment 9 during the 6 kW/m² exposure. The light lines indicate measurements above the reduced surface, i.e. in the air above the char and ash.

From these temperature profiles we can observe all temperatures in the CLT were < 300 °C at 60 minutes. However, at 120 minutes, a smouldering reaction was established and generated heat in the char layer at approximately 20 mm depth. The smoulder zones could clearly be observed.

Subsequently, the 300 °C isotherm penetrated further into the material. However, losses overcame the heat generated by the smouldering and supplemented by the 6 kW/m² applied flux. The reaction was not able to sustain itself and temperatures dropped. At 240 minutes, all temperatures had dropped.

Effect of additional air flow

When experiment 11 with additional air flow of speed 0,5 m/s, is compared to experiments 9 and 10 without this additional air flow, it can be observed that temperatures in the CLT were approximately 100 °C lower. Furthermore, peak temperatures were sustained for a shorter period of time. These observations suggest a cooling effect might occur due to additional air flow.

However, despite this cooling effect, similar mass loss rates were obtained and the samples lost approximately the same percentage of mass. This suggests that a forced oxygen supply due to the additional airflow might (partially) counteract this cooling by speeding up the smoulder reaction. Nevertheless, as a net result, the effect of the 0,5 m/s speed air flow promoted self-extinguishment.

When experiment 12 with an additional air flow of 1,0 m/s, is compared to those without, it can be seen that the temperature at the surface was approximately 100 °C lower, while temperatures in deeper layers were actually > 100 °C higher. Furthermore, experiments 9, 10, and 11 extinguished, but experiment 12 burned-through quickly, and a high mass loss rate and charring rate were obtained.

This suggests that forced oxygen supply might overcome the cooling effect at an additional air flow of speed 1,0 m/s. While the surface is cooled, deeper layers reach higher temperatures, because the smouldering reaction speeds up due to forced oxygen supply. This results in more heat being generated, a higher MLR and a faster propagation of the smouldering zones and the charring front. As a net result, the effect of the 1,0 m/s speed air flow promoted burn-through

These two mechanisms; additional surface cooling and additional heat generated due to an increased reaction speed as a result of forced oxygen supply, are depicted in figure I.3.

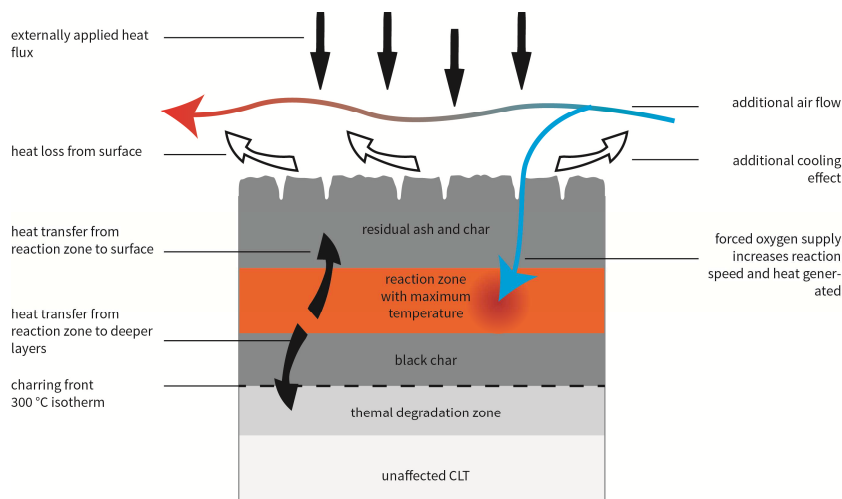


Figure I.3 Smouldering zones, heat transfers, and the effect of additional air flow

These mechanisms might compete in slowing down or speeding up the smoulder reaction. Both effects of the additional air flow were also recognized in the experiments carried out by Ohlemiller (1985, 1988), as discussed in the appendix B.

Their net result might be dependent on the speed of the additional airflow and possible on the level of the externally applied heat flux. More research on this would be recommended.

Shape of burn-through

Burn-through typically occurred in a cone-shaped or circular pattern. This pattern began as large crack in the middle of char. The location of the thermocouples was chosen in such a way that they were located inside this circular area where burn-through occurred.

It can be expected the sample burned-through in this shape because the radiative configuration would be favourable in the large crack, resulting in a high cross-radiation. Furthermore, in the middle area of the sample heat losses are lower, because it is surrounded by hot char along the sides. This allows the smoulder reaction to be sustained there better. Even though the cone heater aims towards providing a uniform exposure over the complete sample surface, the exposure in the middle is always slightly higher.

Charring rates experiment series 2

J.1.1 Introduction

Charring rates are obtained for the second series of experiments using the location of the 300 ° C isotherm. The location of the 300 ° C isotherm was determined with the thermocouple temperatures at a certain depth.

J.1.2 Charring rates

Table 7.11 presents the charring rates obtained for the CLT walls in the 5 compartments. The values represent average charring rates for the corresponding layers of CLT, because thermocouples were spaced 10 mm over the depth of the material.

Table 7.11 charring rates CLT walls

Charring rate [mm/min]	Compartment 1		Compartment 2			Compartment 3		Compartment 4		Compartment 5	
	bw		bw	sw	swc	swr	swl	swr	swl	swr	swl
	0-20 mm	0,52	0,63	0,88	0,76	0,85	0,94	0,74	0,73	0,83	0,76
20-30 mm	-	2,4	1,29	0,4	1,76	0,6	0,56	-	-	-	
30-40 mm	-	0,36	1,01	0,32	0,26	0,27	0,24	-	-	-	
40-50 mm	-	0,31	0,71	0,49	0,49	0,63	-	-	-	-	
50-60 mm	-	1,08	0,33	-	0,17	0,39	-	-	-	-	
Average	0,52	0,96	0,84	0,49	0,71	0,57	0,51	0,73	0,83	0,76	

(bw = back wall, sw = side wall, swc = middle of side wall where it connects with the back wall, swr = side wall right-hand side, swl = side wall left-hand side)

Charring of the first 20 mm was fairly constant for all compartments, on average 0,76 mm/min, but values ranging from 0,52 to 0,94 mm/min were obtained. This average charring rate is higher than provided by Eurocode 5: 0,65 mm/min. This can be attributed to the relative severe propane fire compared to the standard fire in the beginning of the experiments and to the contribution of the CLT to the fire.

Charring of the deeper layers varied greatly. For the compartment that self-extinguished, charring rates are only obtained for the first couple of layers. In compartment 4 where some local flaming occurred, the charring rate for the right side wall decreased from 0,74 to 0,56 to 0,24 to 0 mm/min.

In the experiments where burn-through occurred a wide range of charring rates was obtained. For example the back wall in compartment 2 charred with 0,63 mm/min, then 2,4 mm/min, and then 0,36 mm/min subsequently. These subsequent rapid increases and decreases can be attributed to the wood being exposed suddenly due to delamination and fall-off, followed by periods of relative steady burning. It does not seem likely there were differences in material properties between the layers.

The average charring rate of the walls in the compartments that burned through (not taking into account the corner in compartment 2) was 0,77 mm/min. Similar to what was obtained for all compartments during charring of the first 20 mm. Again, this average charring rate is higher than provided by Eurocode 5: 0,65 mm/min. This can be attributed to the fact that delamination will increase the overall charring rate, as observed by Frangi *et al.* (2009).

J.1.3 Temperature profiles

The temperature profiles in the CLT showed temperatures kept increased to 700 – 800 °C, where they stabilized, when the compartment remained in flaming combustion (compartment 2). When fire alternated between smouldering and local flaming, temperatures stabilized in the range of 400 – 500 °C (compartments 3 and 4). When compartments extinguished (1, 4 and 5) temperatures dropped < 200 °C neat the end of the experiments.

CLT temperatures in most compartments experienced sudden increases or decreases to room temperatures when thermocouples became exposed to room conditions due to delamination and fall-off.

The smouldering zones that were clearly visible in the first series of experiments were not really observed in this second series of experiments. This can be explained by the fact that steady smouldering of the CLT did not occur in these compartments. The compartments either burned through in flaming combustion, or smouldered and extinguished. Burn-through by means of sustained smouldering, as was observed in the first series of experiments, did not occur.

Example assessment for self-extinguishment

K.1 Introduction

This appendix presents an example of an assessment method for self-extinguishment, based on compartment 5 with two CLT sidewalls opposite each other and a top lamella thickness of 40 mm, as used in the second series of experiments.

Two approaches are investigated; the original formulas from the work of Hadvig (1981) and confirmed by Olesen and Hansen (1992), Olesen and König (1992), and König and Walleij (1999), and the formulas offered by the Eurocode 1995-1-2 annex A.

K.2 Determination of critical lamella thickness

First the critical lamella thickness is determined. This thickness is based on the calculation of a finite charring depth for a parametric natural fire.

K.2.1 Input

The approach does not require the calculation of the exact parametric fire curve, but determines the charring behaviour directly from the input.

Opening factor

Independent of the approach, the parametric fire takes into account the opening factor O in the compartment, which represents the ventilation conditions.

$$O = \frac{A_v}{A_t} \cdot \sqrt{h_{eq}} \quad (\text{m}^{1/2}) \quad (\text{Eq. K.1})$$

Where

A_v	= total area of all openings in vertical boundaries (m ²)
A_t	= total area of floors, walls, and ceilings, including the openings (m ²)
h_{eq}	= weighted average of heights of all vertical openings (m)

The compartment dimensions and the openings factor are shown in the table on the next page.

Boundaries

Furthermore, the Eurocode approach requires information on the boundary conditions at ambient temperature, namely the absorptivity b for the total enclosure.

$$b = \sqrt{\rho \cdot c \cdot \lambda} \quad (\text{J/m}^2\text{s}^{1/2}\text{K}) \quad (\text{Eq. K.2})$$

Where

- ρ = the density of the boundary of the compartment (kg/m^3)
- c = specific heat of the boundary of the compartment (J/kgK)
- λ = thermal conductivity of the boundary of the compartment (W/mK)

Because various surfaces in the compartment are made from different materials, and average absorptivity is calculated, in accordance with Eurocode 1991-1-2 appendix A. Values are given in the table below.

compartment		
w	0.50 m	
d	0.50 m	
h	0.50 m	
CLT walls	2.00	
At	1.50 m ³	
opening		
w	0.18 m	
h	0.50 m	
Av	0.09 m ³	
heq	0.50 m	
O	0.042 m ^{1/2}	

boundary	CLT	PROMAT
rho	450	870
c	1530	1000
lambda	0.12	0.175
b	287.4369	390.1923
b*A	143.7185	355.075
b_avg	353.7542	

For the Eurocode approach, a “thermal properties factor” Γ needs to be determined.

$$\Gamma = \left(\frac{O}{b}\right)^2 / \left(\frac{0,04}{1160}\right)^2 \quad (\text{Eq. K.3})$$

Based on the input, this was found to be 12,10 for the compartment under consideration.

Fuel load

Independent of the approach, the parametric fire takes into account the total fuel load in the compartment. This should include the CLT contribution in addition to the “initial” fuel of the compartment contents.

In the experiment with compartment 5 the total heat release rate was measured and the propane flow was known. As a result, the CLT contribution and the initial fire can be calculated.

However, in reality, these are not known.

For the initial fuel load of the room contents, Eurocode 1991-1-2 appendix E offers values for various functions. A fuel load for the CLT needs to be assumed, which can be verified later, based on the total charring depth. This process was found to iterate quickly to a good estimation.

The fire load in the compartment is translated to the “design fire load density”, which is related to the total area of floor, walls and ceilings which encloses the compartment, in MJ/m². Values for the compartment are shown in the table below.

Fuel load			total	
compartment	252 MJ/m ²		63 MJ	
CLT assumption	142 MJ/m ²		71 MJ	
total			134 MJ	
q _{t;d}			89.33 MJ/m ²	

K.2.2 Charring behaviour

Both methods then calculate a parametric charring rate as it relates to the notional charring rate.

$$\beta_{par} = k_p \cdot \beta_n \quad (\text{Eq. K.4})$$

Where k_p = parametric char factor (-)
 β_n = notional charring rate (mm/min)

The char factor in the original research and in the Eurocode approach are calculated with the following formulas. Values for the compartment are shown in the table on the next page.

$$k_p = 1,5 \cdot (5 \cdot 0 - 0,04) / (4 \cdot 0 + 0,08) \quad (\text{Eq. K.5})$$

$$k_p = 1,5 \cdot (0,2 \cdot \sqrt{T} - 0,04) / (0,16 \cdot \sqrt{T} + 0,08) \quad (\text{EC}) \quad (\text{Eq. K.6})$$

notional charring rate		
beta n	0.70	mm/min
parametric charring rate		
EC	1.08	mm/min
original research	0.72	mm/min

Due to the decay phase of the parametric fire, the charring rate is assumed to slow down after an initial period t_0 and drop down to zero over a time of $2t_0$. For both methods, the initial char time t_0 is dependent on the design fire load density. However, the Eurocode applies an additional factor of 1,5.

$$t_0 = 0,006 \cdot \frac{q_{t;d}}{o} \quad (\text{Eq. K.7})$$

$$t_0 = 0,009 \cdot \frac{q_{t;d}}{o} \quad (\text{EC}) \quad (\text{Eq. K.8})$$

Where $q_{t;d}$ = design fire load density related to the total area of floor, walls and ceilings which encloses the compartment (MJ/m^2)

Because the charring rate decreases to zero, a finite charring depth can be determined.

$$d_{char} = 2 \cdot \beta_{par} \cdot t_0 \quad (\text{Eq. K.9})$$

Based on the charring depth, the total amount of burned CLT in kg can be estimated. This can be multiplied with the effective heat of combustion of $14,2 \text{ MJ}/\text{kg}$, as found as an average value for the CLT in the experiment series 1, and checked against the assumption of CLT contribution to the fuel load. After a couple of iterations, a final charring depth is achieved.

Values for compartment 5 are shown in the table on the next page. The charring depth according to the original formulas is slightly over 18 mm, while the Eurocode approach provides a total charring depth of 41 mm. The actual charring depth in the experiment was approximately 20 mm.

Furthermore in this example, the assumed value of the CLT contribution to the fuel load was found to be conservative when compared to value obtained with the charring depth and the effective heat of combustion; $142 > 116,86 \text{ MJ}/\text{m}^2$.

initial char time				
EC	18.95			
original research	12.63			
charring depth				
EC	40.99			
original research	18.29 mm			
check of fuel load				
Hu	14.20 MJ/kg			
Fuel load CLT	58.43 MJ		116.86 MJ/m ²	

K.2.3 Lamella thickness

In order to prevent delamination, the lamella thickness of the first layer of CLT should be larger than the calculated charring depth. It seems reasonable to add 5 mm additional thickness for safety and then round up to the nearest commercially available lamella thickness. However, it should be stressed, as was mentioned in the main report as well, that this approach is a first suggestion only.

Considering the limitations of this work, more research and validation would be required before this method could be applied in practice.

In this example, using the approach of the original research, a top lamella thickness of 25 – 30 mm would suffice. In compartment 5 the top lamella was 40 mm and indeed no delamination or fall-off were observed.

K.3 Check configuration for potential self-extinguishment

The second step in the design method is to ensure that the smouldering CLT can make the final transition to self-extinguishment. To achieve this, the heat flux on the CLT should be limited to $\leq 5 \text{ kW/m}^2$.

Based on the geometry and orientation of the compartment, the heat flux on the CLT during smouldering can be calculated. This flux will predominantly be (cross-) radiation between the smouldering CLT and other hot surfaces. The energy emitted by hot objects and surfaces to a receiver needs to be calculated.

$$E = \varphi \cdot \varepsilon \cdot \sigma \cdot T^4 \quad (\text{Eq. G.10})$$

Where

φ	= configuration factor (-)
ε	= emissivity (-)
σ	= Stefan-Boltzmann constant ($5,67 \times 10^{-8} \text{ W/m}^2\text{K}^4$)
T	= temperature (K)

In a real design situation all hot objects and surfaces have to be taken into account. By adding up the energy emitted by the various sources, the radiative heat flux on the CLT with the most unfavourable configuration can be calculated and compared to the threshold flux. In this example only the cross-radiation of the smouldering CLT is taken into account.

The energy emitted by the smouldering CLT can be based on the estimation of the CLT surface temperature of $400 \text{ }^\circ\text{C}$, as found in experiment series 1. The emissivity of char is taken as 0,8, as suggested by Eurocode 1995-1-2 for wood surfaces.

The most unfavourable position in this compartment (two CLT walls opposite each other) is in the middle of either wall. The walls are $0,5 \times 0,5$ meters and are spaced 0,5 meters apart. The resulting configuration factor is 0,24.

In other situations the configuration factor can be calculated as well. Drysdale (2012) and Eurocode 1991-1-2 appendix G provide calculation methods and also refer to values for common shapes and geometries from tables and charts in literature.

Based on these numbers, the energy received by the middle of the CLT wall in this compartment is estimated to be $2,2 \text{ kW/m}^2$. This flux is below the threshold flux of 5 to 6 kW/m^2 . As a result, the smouldering CLT can be expected to make the transformation from smouldering to self-extinguishment. Indeed, this was observed in the experiment.

Relation to previously conducted research

L.1 Introduction

This work partially relates to that of Longhi (2012), who performed a study on the fire safety of high rise timber buildings. Part of this was the parametric modelling of a complete burnout of a mass timber structure.

L.2 Potential for self-extinguishment

In the parametric investigation, room temperatures were determined based on an initial fire load for a natural fire using the simulation software Ozone. With these temperatures, the charring depth was estimated using the finite element software SAFIR. Based on this charring depth, an additional CLT fire load was determined. Different degrees of CLT contribution were investigated; varying in a 5 to 100 % contribution of the charred wood to the fire. This was added it to the initial fire load and the process was repeated.

The analysis showed that, depending on the initial fire load and the amount of timber that is taken into account, the charring depth can exceed that of a standard fire test or as calculated using the formulas of Eurocode 1991-1-2.

Furthermore, due to the contribution of the timber to the fire load, Longhi found it reasonable to assume that the fire could potentially not extinguish until the entire structure had been consumed. This would lead to a structural collapse. Unfortunately, due to limitations of the software, it was not possible to determine if the charred depth converged to a steady value for large percentages of additional fire load.

Longhi concluded that the decay phase of a fire is the main aspect that has to be considered in a fire model for timber compartments, as it will ensure that a fire will not consume the entire load bearing structure. He suggested it is important to evaluate if the fire has sufficient energy to heat up more of the timber section beyond ignition temperature. If not, a decay stage could start; otherwise the fire will continue burning.

Longhi suggested to further investigate if a fire could be self-extinguishing. When the initial fire load in the compartment has been consumed, it is unclear if the additional fire load of the CLT is sufficient to heat up the remaining timber section beyond ignition temperature and continuing burning.

L.3 Contribution of this work

This research relates to the work of Longhi and investigated the potential self-extinguishment. Longhi focussed on a parametric study with fire simulation and heat transfer software by calculating a charring depth based on compartment temperatures, which would depend in part on the fire load and the CLT contribution. He encountered issues with regards to modelling the fire behaviour and the contribution of the CLT to fire. The potential for self-extinguishment remained unclear.

This work took another approach. A model was formulated with steps that could lead to self-extinguishment. The conditions under which the transitions in this model take place were investigated in experiments. The experiments showed that the contribution of the CLT to the fire and the potential self-extinguishment depend on certain conditions, such as the heat flux, air flow, and the influence of delamination and fall-off.

L.4 Further research

Longhi investigated a range of initial fire loads and CLT contributions to the fire. He found in the model that self-extinguishment might depend on this fire load. It would be recommended to further investigate the influence of the fire load on self-extinguishment and tie this in the results of this work.

Furthermore, this work suggested an assessment method for self-extinguishment of CLT, which includes the calculation of a finite charring depth, based on existing guidance for natural parametric fire exposures. It would be recommended to compare the method used by Longhi to calculate the final charring depth (based on natural fire modelling and finite element heat transfer software) with the method proposed in this work (based on experiments and the Eurocode 1995-1-2 for charring in parametric fires). It would be recommended to further investigate the differences and similarities in both works and combine these.

SELF-EXTINGUISHMENT OF CROSS-LAMINATED TIMBER

Cross-laminated timber, or CLT, is currently receiving attention for its potential use in tall building structures. Timber being a combustible material, one of the main challenges for the construction of these buildings is the potential fire risk that results from its use in the structure.

In this research the effect of using the combustible material CLT as the main bearing structure is investigated. Unprotected CLT can burn along with the fuel load present in a compartment. Irrespective of its fire resistance rating, it is uncertain whether the structure will be totally consumed in the event of a fire. This can result in collapse of the structure.

However, there might be a potential for self-extinguishment, possibly in combination with active fire safety measures such as sprinkler activation or fire-brigade intervention. Self-extinguishment currently is not part of fire safety considerations for the structural design of tall timber buildings.

This master's thesis aims to increase insight into the fire behaviour of unprotected CLT structures in a compartment burnout, conservatively assuming no active measures. The main research question of this work is: "Under what conditions is there a potential for self-extinguishment of cross-laminated timber?"